

Louisiana State University LSU Digital Commons

LSU Doctoral Dissertations

Graduate School

2016

Riemann-Hilbert Formalism in the Study of Crack Propagation in Domains with a Boundary

Aleksandr Smirnov

Louisiana State University and Agricultural and Mechanical College, smirnov09al@gmail.com

Follow this and additional works at: https://digitalcommons.lsu.edu/gradschool_dissertations



Part of the [Applied Mathematics Commons](#)

Recommended Citation

Smirnov, Aleksandr, "Riemann-Hilbert Formalism in the Study of Crack Propagation in Domains with a Boundary" (2016). *LSU Doctoral Dissertations*. 2937.

https://digitalcommons.lsu.edu/gradschool_dissertations/2937

This Dissertation is brought to you for free and open access by the Graduate School at LSU Digital Commons. It has been accepted for inclusion in LSU Doctoral Dissertations by an authorized graduate school editor of LSU Digital Commons. For more information, please contact gradetd@lsu.edu.

RIEMANN–HILBERT FORMALISM IN THE STUDY OF CRACK PROPAGATION
IN DOMAINS WITH A BOUNDARY

A Dissertation

Submitted to the Graduate Faculty of the
Louisiana State University and
Agricultural and Mechanical College
in partial fulfillment of the
requirements for the degree of
Doctor of Philosophy

in

The Department of Mathematics

by

Aleksandr Smirnov

Candidate of Sciences, Chuvash State Pedagogical University, 2011

M.S., Louisiana State University, 2013

May 2016

Acknowledgments

I would like to express my sincere gratitude to my advisor Prof. Yuri Antipov for the continuous support of my Ph.D. study and related research, for his patience, motivation, and immense knowledge. His guidance helped me in all the time of research and writing of this thesis.

Besides my advisor, I would like to thank my thesis committee and especially Prof. Robert Lipton for his encouragement and insightful ideas, which helped me to widen my research from various perspectives.

I thank my fellow students for the stimulating discussions and for all the fun we have had in the last five years.

This dissertation is dedicated to Gaomin Wang for her support and encouragement.

Table of Contents

Acknowledgments	ii
List of Figures	v
Abstract	vi
Chapter 1: Introduction	1
1.1 A Brief History of Riemann–Hilbert Problem	1
1.2 An Application: Sommerfeld Half-Plane Diffraction Problem	3
1.3 Dynamic Fracture Mechanics	7
1.4 Overview	10
Chapter 2: Riemann–Hilbert Problem	16
2.1 Scalar Riemann–Hilbert Problem	17
2.2 Vector Riemann–Hilbert Problem	27
2.3 Solution of a Vector Riemann–Hilbert Problem	33
Chapter 3: Modeling of Crack Propagation	53
3.1 Suddenly Applied Crack Face Pressure	53
3.2 Crack Propagation at Constant Speed	64
3.3 Crack Propagation at Non-Uniform Speed	69
Chapter 4: Steady-State Crack Propagation in a Half-plane	77
4.1 Vector Riemann–Hilbert problem and Orthogonal Polynomials	77
4.2 Properties of the Solution	88
Chapter 5: Transient Crack Propagation in a Half-Plane	98
5.1 Crack Propagation at Constant Speed due to Time-Independent Loading	99
5.2 Approximate Solution of the Transient Problem for a Half-Plane	107
5.3 Crack Growth at Non-Uniform Speed	117
Chapter 6: Fracture in an Infinite Strip	126
6.1 Factorization of a Class of Wiener–Hopf Kernels	127
6.2 Symmetric Crack in an Infinite Strip	132
6.3 Lattice Model of a Fracture in a Composite Infinite Strip	138
Chapter 7: Summary and Conclusions	150
References	155
Vita	161

List of Figures

1.1	Sommerfeld half-plane diffraction problem.	5
1.2	Three modes of a crack deformation.	10
2.1	Limit of $\arg(z_2 - z_0) - \arg(z_1 - z_0)$ as $\rho \rightarrow 0$ when (a) z_0 is an inner point of L ; (b) z_0 is on the left from L , (c) z_0 is on the right from L	18
2.2	Connection between opposite edges of Γ_j , $j = 0, \dots, g$ on two copies of $\overline{\mathbb{C}} \setminus \Gamma$	37
2.3	Canonical homology basis $a_{1,2}$ and $b_{1,2}$ on the hyper-elliptic Riemann surface of genus 2. Dashed lines denote curves on the second sheet of the surface.	40
3.1	Suddenly applied crack pressure.	55
3.2	Functions k_I and k_{II} against v/c_R for $\nu = 0.3$	69
3.3	The piecewise linear curve $L(t)$ approximates the crack tip trajectory $l(t)$	71
4.1	Semi-infinite crack parallel to the boundary of a half-plane.	78
4.2	The stress intensity factors vs δ for $V/c_R = 0.5$: $K_I^{(1)}$ and $K_{II}^{(1)}$ are the factors for the case $\sigma_{22}^\circ(x) = 1$, $-1 < x < 0$, $\sigma_{22}^\circ(x) = 0$, $x < -1$, and $\sigma_{12}^\circ(x) = 0$, $x < 0$; $K_I^{(2)}$ and $K_{II}^{(2)}$ are the factors for the case $\sigma_{12}^\circ(x) = 1$, $-1 < x < 0$, $\sigma_{12}^\circ(x) = 0$, $x < -1$, and $\sigma_{22}^\circ(x) = 0$, $x < 0$	90
4.3	The stress intensity factors vs V/c_R for $\delta = 2$: $K_I^{(1)}$ and $K_{II}^{(1)}$ are the factors for the case $\sigma_{22}^\circ(x) = 1$, $-1 < x < 0$, $\sigma_{22}^\circ(x) = 0$, $x < -1$, and $\sigma_{12}^\circ(x) = 0$, $x < 0$; $K_I^{(2)}$ and $K_{II}^{(2)}$ are the factors for the case $\sigma_{12}^\circ(x) = 1$, $-1 < x < 0$, $\sigma_{12}^\circ(x) = 0$, $x < -1$, and $\sigma_{22}^\circ(x) = 0$, $x < 0$	91
4.4	The weight functions $W_{j,l}(x_0)$ ($j, l = I, II$) vs δ for $v/c_R = 0.5$, $x_0 = -1$	93
4.5	The weight functions $W_{j,l}(x_0)$ ($j, l = I, II$) vs v/c_R for $\delta = 1$, $x_0 = -1$	94
4.6	The function H vs δ for $v/c_R = 0.5$, $x_0 = -1$ and loading $\sigma_{22}^\circ = \delta(x - x_0)$, $\sigma_{12}^\circ = 0$: $H^{(1)}$; $\sigma_{22}^\circ = 0$, $\sigma_{12}^\circ = \delta(x - x_0)$: $H^{(2)}$; $\sigma_{22}^\circ = \delta(x - x_0)$, $\sigma_{12}^\circ = \delta(x - x_0)$: $H^{(3)}$	96
4.7	The function H vs v/c_R for $\delta = 2$, $x_0 = -1$ and loading $\sigma_{22}^\circ = \delta(x - x_0)$, $\sigma_{12}^\circ = 0$: $H^{(1)}$; $\sigma_{22}^\circ = 0$, $\sigma_{12}^\circ = \delta(x - x_0)$: $H^{(2)}$; $\sigma_{22}^\circ = \delta(x - x_0)$, $\sigma_{12}^\circ = \delta(x - x_0)$: $H^{(3)}$	97
4.8	Propagation speed v against the parameter σ_* corresponding to the loading $\sigma_{22}^\circ = \sigma_*\delta(x - x_0)$, $\sigma_{12}^\circ = 0$: $v^{(1)}$; $\sigma_{22}^\circ = 0$, $\sigma_{12}^\circ = \sigma_*\delta(x - x_0)$: $v^{(2)}$; $\sigma_{22}^\circ = \sigma_*\delta(x - x_0)$, $\sigma_{12}^\circ = \sigma_*\delta(x - x_0)$: $v^{(3)}$	97

5.1	Graphs of the functions $\text{Re } \tilde{K}_I(s)$, $\text{Re } \tilde{K}_{II}(s)$, $\text{Im } \tilde{K}_I(s)$, and $\text{Im } \tilde{K}_{II}(s)$ for $\text{Re } s = 0.5$	114
5.2	The functions $w_{i,j}(0, t) = \sqrt{\frac{1}{2}\pi vt} W_{i,j}(0, t)$ ($i, j = I, II$) versus time t when $\nu = 0.3$, $\delta = 1$ m, $v = 0.5c_R$ m/s, $c_l = 1$ m/s ($c_s \approx 0.5345$ m/s, $c_R \approx 0.4957$ m/s). . . .	115
5.3	The weight functions $W_{i,j}(0, t)$, ($i, j = I, II$) versus time t when $\nu = 0.3$, $\delta = 1$ m, $v = 0.5c_R$ m/s, $c_l = 1$ m/s ($c_s \approx 0.5345$ m/s, $c_R \approx 0.4957$ m/s).	116
5.4	Influence of the boundary of half-plane on the crack propagation.	117
5.5	The functions $w_{i,j}(0, t)$ ($i, j = I, II$) versus v/c_R when $\nu = 0.3$, $\delta = 1$ m, $t = 10$ s, $c_l = 1$ m/s ($c_s \approx 0.5345$ m/s, $c_R \approx 0.4957$ m/s).	118
5.6	The functions $w_{i,j}(0, t)$ ($i, j = I, II$) versus the distance δ from the crack to the half-plane boundary when $\nu = 0.3$, $v = 0.5c_R$ m/s, $c_l = 1$ m/s, $t = 10$ s ($c_s \approx 0.5345$ m/s, $c_R \approx 0.4957$ m/s).	118
6.1	Symmetric semi-infinite crack in a strip	127
6.2	The integration paths L and \mathcal{L} on the complex plane	128
6.3	The length l and the energy release rate G versus the half-width d of the strip for various speeds v of the crack propagation (for the case $\sigma_* = \sigma_c$ and $\nu = 1/3$)	138
6.4	The length l and the energy release rate G versus the ratio σ_*/σ_c for various speeds v of the crack propagation (for the case $d = x_0/2$ and $\nu = 1/3$)	139
6.5	Lattice model of a composite infinite strip	140
6.6	Anti-plane separation between the upper interface layer $n = 0_+$ and the lower interface layer $n = 0_-$ for parameters $U_2 = 1$, $c_2 = \frac{5}{6}c_1$, $v = \frac{4}{6}c_1$, $u_f \approx 0.2$, $N_1 = N_2 = 5$, $b_1 = b_2 = 0.01$, where $c_j = \sqrt{\frac{k_j}{m_j}}$, $j = 1, 2$, are the shear wave speeds for the upper and lower material.	147
6.7	Relation between the crack velocity v and the dimensionless parameter Δ for different numbers of the layers N_1 and N_2	149

Abstract

The Wiener–Hopf technique is a powerful tool for constructing analytic solutions for a wide range of problems in physics and engineering. The key step in its application is solution of the Riemann–Hilbert problem, which consists of finding a piece-wise analytic (vector-) function in the complex plane for a specified behavior of its discontinuities. In this dissertation, the applied theory of vector Riemann–Hilbert problems is reviewed. The analytical solution representing the problem on a Riemann surface, and a numerical solution that reduces the problem to singular integral equations, are considered, as well as a combination of the numerical and analytical techniques (partial Wiener–Hopf factorization) is proposed.

In this work, we begin with a brief survey of the Riemann–Hilbert problem: constructing solution of the scalar Riemann–Hilbert problem for a class of Hölder continuous functions; considering classes of matrices that admit the closed-form solution of the vector Riemann–Hilbert problem; discussing numerical and analytical techniques of constructing solutions of vector Riemann–Hilbert problems.

We continue with applications of the Wiener–Hopf technique to problems of Dynamic fracture mechanics: reviewing well-known solutions to problems on propagation of a semi-infinite crack in an unbounded plane in the cases of a stationary crack, a crack propagating at a constant speed, and a crack propagating at a non-uniform arbitrary speed. Based on those, we derive solutions to new problems on a semi-infinite crack propagation in a half-plane (steady-state and transient problems for subsonic speeds) as well as in a composite strip (for intersonic speeds). These latter results are new and were first derived by Y. Antipov and the author.

Chapter 1

Introduction

The Riemann–Hilbert problem and its application to solving partial differential equations is a powerful technique that is applied to a wide range of problems in physics and engineering. In more than half a century, since the first scalar Riemann–Hilbert problem was stated and solved, many studies were devoted to generalizing the problem and improving analytical and numerical techniques of its solution. Special attention was given to vector Riemann–Hilbert problems since they do not, in general, admit a closed-form analytical solution.

1.1 A Brief History of Riemann–Hilbert Problem

The Riemann–Hilbert boundary value problem was first introduced by B. Riemann in connection with the so-called “Riemann monodromy” problem that concerns the existence of a certain class of linear differential equations with specified singular points and monodromy group [7]. The Riemann monodromy problem was transformed to what we call a Riemann–Hilbert problem by D. Hilbert [44] and G.D. Birkhoff [21, 22]. J. Plemelj [67] used the results of Riemann–Hilbert problems to study the Riemann monodromy problem.

The Riemann–Hilbert problem is defined as follows: given a closed (for convenience) contour L , and functions $a(t)$ and $b(t)$ which are Hölder continuous on L and $a(t) \neq 0$ on L , find two functions $\phi^+(z)$ and $\phi^-(z)$, analytic respectively inside and outside of the contour L with a finite-degree growth at infinity, such that

$$\phi^+(t) = a(t)\phi^-(t) + b(t), \quad t \in L \quad (1.1)$$

This definition can be generalized with respect to the contour (e.g. open, infinite, non-simple contours) and to the functions $a(t)$, $b(t)$ (e.g. functions with finitely or countably many discontinuities on the contour L), as well as a system of several conditions of type (1.1) can be considered (vector Riemann–Hilbert problem).

The first solution of the homogeneous (i.e. for $b(t) = 0$ on L) scalar Riemann–Hilbert problem (1.1) was given by D. Hilbert [43] in terms of a Fredholm integral equation. J. Plemelj [65, 66] gave the first closed form solution of (1.1) in the case when $\arg a(t)$ has zero increment as t traverses along the contour L . T. Carleman [26] solved a related singular integral equations. F.D. Gakhov [40] gave the full solution of the scalar Riemann–Hilbert problem (1.1). Vector Riemann–Hilbert problems were considered by J. Plemelj [67], F.D. Gakhov [41], N.I. Muskhelishvili [61], and by I. Vekua [81].

We should also note that the work [83] of N. Wiener and E. Hopf is closely related to Riemann–Hilbert problems. They proposed a technique of solving the integral equation of the form

$$\int_0^\infty k(x-y)f(y)dy = g(x), \quad 0 < x < \infty \quad (1.2)$$

with respect to the function $f : \mathbb{R}_+ \rightarrow \mathbb{R}$, where $k : \mathbb{R} \rightarrow \mathbb{R}$ is a difference kernel and $g : \mathbb{R}_+ \rightarrow \mathbb{R}$ is a known function defined on the positive semi-axis. By introducing an auxiliary function $h : \mathbb{R}_- \rightarrow \mathbb{R}$ defined on the negative semi-axis so that

$$\int_0^\infty k(x-y)f(y)dy = \begin{cases} g(x), & 0 < x < \infty \\ h(x), & -\infty < x < 0 \end{cases}$$

and applying Fourier transform to the equation, it is reduced to the equality

$$\hat{g}^+(t) + \hat{h}^-(t) = \hat{f}^+(t)\hat{k}(t), \quad -\infty < t < \infty \quad (1.3)$$

where \hat{f}^+ and \hat{h}^- are half-range Fourier transforms (taken over the intervals $(0, \infty)$ and $(-\infty, 0)$ respectively), which are to be found. Moreover, the functions \hat{f}^+ and \hat{h}^- are analytic respectively in the upper \mathbb{C}^+ and the lower \mathbb{C}^- half-planes provided that f and h are integrable on the corresponding intervals. Thus, the equation (1.3) is a boundary condition of a Riemann–Hilbert problem in the form (1.1) with $a = 1/\hat{k}$ and $b = \hat{g}^+/\hat{k}$. For more details on the Wiener–Hopf method, see the monograph [62].

The Wiener–Hopf technique has been applied to many problems in Physics and Mechanics (see, for instance, works on diffraction [30], electromagnetic waves [27, 28], and sound waves

[55]). D.S. Jones [49] simplified the Wiener–Hopf method by demonstrating that the equation in form of a Riemann–Hilbert problem (1.1) can be derived immediately from a boundary value problem by applying Fourier transform to the partial differential equations and, thus, bypassing the integral equation (1.2).

There are two traditions to call the problems of determining analytic functions from the functional equation (1.1). One of them is to use the term “Riemann–Hilbert problem.” On the other hand, the term “Wiener–Hopf technique” refers to the method of reducing a boundary value problem to a functional equation of the form (1.1) and solving it. Thus, Riemann–Hilbert problem is an essential part of the Wiener–Hopf technique. On the other hand, a factorization of the function $a(t)$ in (1.1) is called the Wiener–Hopf factorization, which is a key part of the solution of the Riemann–Hilbert problem. Since the method of a Riemann–Hilbert problem and the Wiener–Hopf techniques refer to the same approach to solving boundary value problems, we will use these terms interchangeably in this work.

Along with the scalar case, vector Riemann–Hilbert problem arise in a variety of models in many areas, including mathematical physics, fluid and solid mechanics, and financial mathematics. However, exact solution of a vector Riemann–Hilbert problem can be derived only for few classes of matrices: the ones that allow for recasting a vector Riemann–Hilbert problem into uncoupled scalar Riemann–Hilbert problems [47, 68, 84]; commutative matrices of the Chebotarev–Khrapkov type [29, 52, 32]; matrices with special algebraic or group structure [9, 50, 51, 59, 82]. For the other matrices, a number of approximate techniques has been developed for solving Riemann–Hilbert problems or the corresponding singular integral equations (see, for instance, the collocation method [33, 34, 63] and Padè approximants [2, 3, 4]).

1.2 An Application: Sommerfeld Half-Plane Diffraction Problem

In order to illustrate the application of Riemann–Hilbert problems to solving partial differential equations, we begin with a discussion of the Sommerfeld half-plane diffraction problem

and its solution obtained by D. S. Jones [49]. While this application is short and simple, it demonstrates a routine procedure for the problems that will be solved later in the dissertation.

Consider waves propagating in two-dimensional space (x, y) . We do not specify the physical nature of the waves since the same technique is applied to the waves of any nature: sound waves, light waves, etc. The problem is restricted to the steady-state case, in which the wave oscillates in time with a constant angular velocity ω so that the solution has the form $\psi = \phi(x, y)e^{-i\omega t}$ where ϕ is the wave potential. Assume that a rigid boundary was placed along the negative x -axis and waves

$$\psi_i = e^{-i\omega t} \exp(-ik_1 x - ik_2 y) \quad (1.4)$$

where $k_1 = k \cos \theta$ and $k_2 = k \sin \theta$, are incident in the (x, y) -plane (see Figure 1.1). Let us represent the solution in the form $\psi_t = \psi_i + \psi$, where ψ_i is the incident waves defined by (1.4) and ψ is incident-free solution. The wave propagation with damping is governed by the partial differential equation

$$\frac{\partial^2 \psi}{\partial x^2} + \frac{\partial^2 \psi}{\partial y^2} - \frac{1}{c^2} \frac{\partial^2 \psi}{\partial t^2} - \frac{\varepsilon}{c^2} \frac{\partial \psi}{\partial t} = 0 \quad (1.5)$$

where x , y , and t are spacial and temporal coordinates, c a fixed constant denoting the wave speed, and ε a positive damping factor. The wave potential ϕ satisfies the Helmholtz equation

$$\frac{\partial^2 \phi}{\partial x^2} + \frac{\partial^2 \phi}{\partial y^2} + k^2 \phi = 0 \quad (1.6)$$

with the wave-number k such that $k^2 = (\omega^2 + i\varepsilon\omega)/c^2$. We choose k to have a positive imaginary part. The following conditions apply:

1. because of the boundary placed on the negative x -axis, the potentials ϕ_t and, therefore, ϕ are twice-differentiable everywhere in the (x, y) -plane except the boundary $-\infty < x \leq 0, y = 0$, where ϕ_t and ϕ may have jump discontinuities

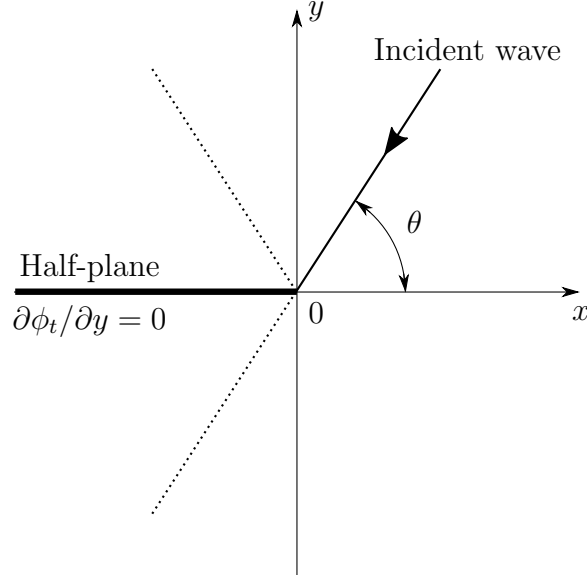


Figure 1.1: Sommerfeld half-plane diffraction problem.

2. the derivative $\partial\phi_t/\partial y$ vanishes on the boundary $y = 0$, $-\infty < x \leq 0$, implying the condition

$$\left. \frac{\partial\phi}{\partial y} \right|_{y=0} = ik_2 e^{-ik_1 x}, \quad x < 0 \quad (1.7)$$

3. the potentials ϕ_t and ϕ are bounded at infinity, while the derivatives $\partial\phi_t/\partial y$ and $\partial\phi/\partial y$ may have a power-type discontinuity at the origin $x = 0$, $y = 0$

In order to solve the Sommerfeld half-plane diffraction problem, introduce the Fourier transform

$$\Phi(z, y) = \underbrace{\int_{-\infty}^0 \phi(x, y) e^{izx} dx}_{\Phi^-(z, y)} + \underbrace{\int_0^{\infty} \phi(x, y) e^{izx} dx}_{\Phi^+(z, y)} \quad (1.8)$$

Let z be a complex variable. Notice that as long as $\text{Im } z > 0$, the integral $\Phi^+(z, y)$ is continuous and infinitely differentiable in z , thus $\Phi^+(z, y)$ is an analytic function in the upper half-plane $\mathbb{C}^+ = \{z : \text{Im } z > 0\}$. Similarly, $\Phi^-(z, y)$ is an analytic function in the lower half-plane $\mathbb{C}^- = \{z : \text{Im } z < 0\}$.

If we apply the Fourier transform to the differential equation (1.6), we find that

$$(k^2 - z^2)\Phi(z, y) + \frac{\partial^2 \Phi(z, y)}{\partial y^2} = 0, \quad -\infty < y < \infty \quad (1.9)$$

for all real values of z . Let $\gamma = (z^2 - k^2)^{1/2}$, where the branch of the square root is chosen so that the real part of γ is positive for all real values of z . Then the solution of the ordinary differential equation (1.9) that is bounded at infinity, is given by

$$\Phi(z, y) = \begin{cases} C_1(z) e^{-\gamma y}, & y \geq 0 \\ C_2(z) e^{\gamma y}, & y \leq 0 \end{cases}$$

where C_1 and C_2 are function of only one variable z . There are two forms of the function Φ since it is discontinuous across the line $y = 0$. Since $\partial\Phi/\partial y$ is continuous at $y = 0$, we have $C_1(z) = -C_2(z)$. Thus

$$\Phi(z, y) = \text{sgn}(y) C_1(z) e^{-\gamma|y|} \quad (1.10)$$

In order to find $C_1(z)$, we have to satisfy Φ to the boundary conditions. The equality (1.7), the representation (1.8), and the form (1.10) imply the identities

$$\begin{aligned} \Phi^+(z, 0) + \Phi^-(z, 0^+) &= C_1(z) \\ \Phi^+(z, 0) + \Phi^-(z, 0^-) &= -C_1(z) \\ \frac{\partial\Phi^+(z, y)}{\partial y} \Big|_{y=0} + \frac{k_2}{z - k_1} &= -\gamma C_1(z) \end{aligned} \quad (1.11)$$

for all real values of z . Eliminating $C_1(z)$ from (1.11), we derive a single equation

$$\Psi^+(z) = -\frac{\gamma}{2} \Psi^-(z, 0^+) - \frac{k_2}{z - k_1} \quad (1.12)$$

for all real values of z , where we introduced new functions

$$\Psi^+(z) = \frac{\partial\Phi^+(z, y)}{\partial y} \Big|_{y=0}, \quad \Psi^-(z) = \Phi^-(z, 0^+) - \Phi^-(z, 0^-)$$

in order to simplify the notation. Notice that the function Ψ^+ is analytic in the upper half-plane \mathbb{C}^+ , while Ψ^- is analytic in the lower half-plane \mathbb{C}^- . Thus, we derive a Riemann–Hilbert problem with the boudnary condition (1.12).

We will discuss existence and uniqueness of the solution of the Riemann–Hilbert problem later, assume here that there exists a unique solution satisfying the condition (1.12). This

solution (i.e. the functions $\Psi^+(z)$ and $\Psi^-(z)$) can be constructed explicitly. Given $\Psi^+(z)$ and $\Psi^-(z)$, the function $C_1(\alpha)$ can be found from the last identity in (1.11) and then Φ is explicitly determined by the formula (1.10) for all values of z and y .

Thus, the partial differential equation (1.6) with boundary condition (1.7) was reduced to the Riemann–Hilbert problem (1.12) with the help of Fourier transform. After solving the problem, we find the Fourier transform (1.10) and its inverse, that is the solution of the original partial differential equation (1.6). This procedure is common to the method of Riemann–Hilbert problem and will be applied to solve problems of Dynamic fracture mechanics in the following chapters.

1.3 Dynamic Fracture Mechanics

Later in the dissertation, we will consider applications of Riemann–Hilbert problem to several problems from Dynamic fracture mechanics. Here, we give necessary definitions and facts of the area. Although they can be found in any book on continuum fracture mechanics, we mostly follow the monograph [39].

Let us consider a three-dimensional Euclidean space and introduce a rectangular coordinate system with an orthonormal basis. Consider a deformable body occupying the region Ω of the three-dimensional space at time t . The two fields that describe deformation of the body are the *stress*- and *strain*-fields [54].

Stress is a physical quantity that expresses the internal forces that neighboring particles of a continuous material exert on each other. Stress at a point x of the material is completely determined by the second-order *Cauchy stress tensor* $\sigma(x, t)$ with components

$$\sigma_{ij}(x, t), \quad i, j = 1, 2, 3, \quad x = (x_1, x_2, x_3) \in \Omega$$

Suppose that a particular configuration of the body at time $t = t^\circ$ is identified as a reference configuration. Material particles are labeled by associating each with its position $x^\circ = x(t^\circ)$ in the reference configuration. We define the particle displacement at a time instance t as the vector $u(t) = x(t) - x^\circ$. The corresponding particle velocity and acceleration are given

by

$$v = \frac{\partial u}{\partial t} \Big|_{x^\circ}, \quad a = \frac{\partial v}{\partial t} \Big|_{x^\circ} = \frac{\partial v}{\partial t} \Big|_x + v \cdot \nabla v \quad (1.13)$$

In continuum mechanics, displacements of the material particles are assumed to be much smaller than any relevant dimension of the body. Under the assumption of small stress deformation, we introduce the strain tensor ϵ with components

$$\epsilon_{ij} = \frac{1}{2} \left(\frac{\partial u_i}{\partial x_j} + \frac{\partial u_j}{\partial x_i} \right), \quad i, j = 1, 2, 3 \quad (1.14)$$

Hereafter, we say that a body is *homogeneous* if its elastic parameters (density ρ , Lamé elastic constants λ and μ) are the same at every point. Likewise, we say that a body is *isotropic* if its elastic parameters are identical in all directions. The fundamental set of the equations governing the motion of a homogeneous and isotropic elastic body consists of the strain displacement relation (1.14), the linear stress-strain relation

$$\sigma_{ij} = \lambda \delta_{ij} (\epsilon_{11} + \epsilon_{22} + \epsilon_{33}) + 2\mu \epsilon_{ij}, \quad i, j = 1, 2, 3. \quad \text{in } \Omega \quad (1.15)$$

where δ_{ij} is the Kronecker delta function ($\delta_{ij} = 1$ if $i = j$, and $\delta_{ij} = 0$ if $i \neq j$), and the momentum balance equations

$$\sum_{i=1}^3 \frac{\partial \sigma_{ij}}{\partial x_i} + \rho f_j = \rho \ddot{u}_j, \quad j = 1, 2, 3, \quad \text{in } \Omega \quad (1.16)$$

where f_j are the components of a body force per unit mass f applied to the material, and \ddot{u}_j are the components of acceleration a defined in (1.13). After we plug the identities (1.14) and (1.15) into the balance equation (1.16), the latter, written in the vector form, reads

$$c_l^2 \nabla (\nabla \cdot u) - c_s^2 \nabla \times (\nabla \times u) + f = \ddot{u}, \quad c_l = \sqrt{\frac{\lambda + 2\mu}{\rho}}, \quad c_s = \sqrt{\frac{\mu}{\rho}} \quad (1.17)$$

where ∇ is the del operator defined by $(\partial/\partial x_1, \partial/\partial x_2, \partial/\partial x_3)^T$, the symbols “ \cdot ” and “ \times ” stand for the scalar and vector product respectively.

According to Helmholtz theorem [20], if the vector field u is twice continuously differentiable in Ω and vanishes faster than $1/||x||$ as $x \rightarrow \infty$, then the following decomposition

holds:

$$u = \nabla\phi + \nabla \times \psi$$

where $\phi : \Omega \rightarrow \mathbb{R}$ and $\psi : \Omega \rightarrow \mathbb{R}^3$ are scalar and vector fields on Ω . The first component of the decomposition is an irrotational (curl-free) field since $\nabla \times (\nabla\phi) = 0$, while the second component is a solenoidal (divergence-free) vector-field since $\nabla \cdot (\nabla \times \psi) = 0$. It follows from the equation (1.17), that the scalar ϕ and the vector ψ satisfy the wave equations

$$c_l^2 \nabla^2 \phi - \ddot{\phi} = 0, \quad c_s^2 \nabla^2 \psi - \ddot{\psi} = 0, \quad \text{in } \Omega \times \mathbb{R}_+ \quad (1.18)$$

provided $f = 0$ and $\nabla \cdot \psi = 0$. Hereafter, ϕ is called the longitudinal wave potential and ψ the shear wave potential.

In this work, we will consider only plane deformation, so that the stress and deformation fields are restricted to one of the planes in the reference configuration. If deformation is restricted to the plane (x_1, x_2) , then the shear wave potential ψ has only one non-zero component ψ_3 (hereafter, we will drop the index 3 and use ψ to denote the third component of the vector ψ). Then the wave equations (1.18) become

$$\frac{\partial^2 \phi}{\partial x_1^2} + \frac{\partial^2 \phi}{\partial x_2^2} - \frac{1}{c_l^2} \frac{\partial^2 \phi}{\partial t^2} = 0, \quad \frac{\partial^2 \psi}{\partial x_1^2} + \frac{\partial^2 \psi}{\partial x_2^2} - \frac{1}{c_l^2} \frac{\partial^2 \psi}{\partial t^2} = 0$$

In order to describe a crack propagation in an elastic body, we analyze the stress and displacement fields in the body surrounding the crack. Due to the fact that the stress field has a singularity at the tip of a crack, G. Irwin [48] introduced the *elastic stress intensity factors* K , which allow to state a crack propagation criterion: he proposed that a crack will begin to grow when K is increased to some values called the *fracture toughness*. For a tensile crack in a plane body, this criterion is equivalent to the Griffith energy criterion [39].

Let us consider (x_1, x_2) -plain deformation of the body that occupies whole space \mathbb{R}^3 and has a crack $\{(x_1, 0, x_3) : x_1 < 0, |x_3| < \infty\}$. Deformation of the faces of the crack can be described with three modes (see Figure 1.2):

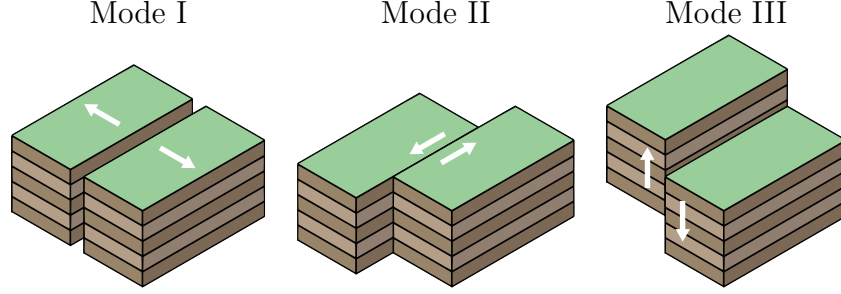


Figure 1.2: Three modes of a crack deformation.

- Mode I. In-plane opening deformation of the crack faces;
- Mode II. In-plane shear deformation of the crack faces;
- Mode III. Anti-plane shear deformation of the crack faces.

The corresponding stress intensity factors are defined by the relations

$$\sigma_{22} \sim \frac{K_I(v, t)}{\sqrt{2\pi(x_1 - l(t))}}, \quad \sigma_{12} \sim \frac{K_{II}(v, t)}{\sqrt{2\pi(x_1 - l(t))}}, \quad \sigma_{23} \sim \frac{K_{III}(v, t)}{\sqrt{2\pi(x_1 - l(t))}} \quad (1.19)$$

as $x_1 \rightarrow l(t)$, where $x_1 = l(t)$ is the position of the crack top on x_1 -axis. If the crack propagates in a homogeneous material, the stress field has a square root discontinuity (1.19) at the tip of the crack, where the stress intensity factors generally depend on the shape of a material, time t , and the propagation speed v . This dependence is the goal of many studies in Fracture mechanics, and one of the main results derived in the following chapters.

1.4 Overview

In this work, we will present several computational and analytical approaches to solving vector Riemann–Hilbert problem and consider their applications to problems of Dynamic fracture mechanics. We start with rather conventional techniques and then develop them farther to suit the particular set of problems under consideration.

The dissertation is laid out as follows. In Introduction, we briefly discussed the history of the Riemann–Hilbert problem, considered an example of its application to the Sommerfeld half-plane diffraction problem, and listed necessary facts from Fracture mechanics.

Chapter 2 contains an overview of the theory of Riemann–Hilbert problem. In the first section, which is based on the monograph [41], we provide some background information on Hölder continuous functions and Cauchy integrals, state the scalar Riemann–Hilbert problem, and construct its analytical solution in the closed form. Here, only necessary definitions and theorems are provided as well as the scalar Riemann–Hilbert problem is stated and solved only in the case when the functions $a(t)$ and $b(t)$ in the equation (1.1) are Hölder continuous everywhere on the contour L , the function $a(t)$ does not vanish on L , and the contour L is set to be the real axis \mathbb{R} of the complex plane. Other classes of functions will be considered later. In Section 2.1, we state the vector Riemann–Hilbert problem and discuss difficulties that arise when we try to apply the technique used in the scalar case to the vector problem. We list several classes of matrices, which allow for the closed-form solution of a vector Riemann–Hilbert problem. Those classes include diagonal and triangular matrices, functionally commutative matrices studied in [58, 29], and the Chebotarev–Khrapkov class of matrices [32, 52]. In Section 2.3, we describe techniques of solving vector Riemann–Hilbert problems. The first technique [13, 87] is applied to matrices of the Chebotarev–Khrapkov type and based on transforming the problem to a scalar Riemann–Hilbert problem on a Riemann surface, that can be solved in the closed form. The second technique is computational and can be applied to a much bigger class of matrices; it consists of transforming the problem to a system of singular integral equations, which is solved numerically [35]. In Section 2.3.3, we propose two variations on so-called partial Wiener–Hopf factorization, which the author and Y. Antipov successfully applied to some problems of Dynamic fracture mechanics (see Chapters 5, 6, and the work [18]). This new techniques combine broad applicability of numerical methods and reliability of analytical solutions.

In Chapter 3, we consider several well-known problems on a crack propagation in an unbounded plane, which are reduced to scalar Riemann–Hilbert problems and solved respectively. Although the solutions to those problems were already derived before (see, for

instance, [39]), they provide an insight on behavior of the solutions to the problems on a crack propagation in a half-plane, considered in the following chapters. The corresponding vector Riemann–Hilbert problems in Chapters 4 and 5 require more elaborate solution, but they are intrinsically similar to the scalar problems from Chapter 3, so we expect a similar behavior and properties of the solution. In Section 3.1, we consider a stationary crack in an unbounded plane, whose faces are subjected to uniform pressure; Section 3.2 contains a similar problem under assumption that the crack propagates at constant speed; finally, in Section 3.3, we build a solution of the problem for a non-uniform crack propagation when the crack speed is an arbitrary continuous function of time.

The following two chapters solve problems on crack propagation in a half-plane. Presence of the boundary of the half-plane results to vector Riemann–Hilbert problems that do not admit a closed-form solution, and require a development of new techniques. To the best of the author’s knowledge, these problems were first solved by Y. Antipov and the author and published in [17, 18].

In Chapter 4, we analyze a two-dimensional steady-state problem on propagation of a semi-infinite crack in a half-plane. The crack is subjected to normal and tangential loading applied to its faces, and propagates at speed v along the half-plane boundary, which is free of traction. The boundary of the half-plane violates the symmetry of the problem, and, in contrast to the problem on a plane, the modes I and II of the crack deformation are coupled. We derive an order-2 vector Riemann–Hilbert problem associated with the model. Since the coefficient of the problem is a Hermitian matrix, which cannot be factorized in a closed form, we reduce it to a system of two singular integral equations with respect to the derivatives of the displacement jumps. In order to solve the system, the unknown functions are expanded in terms of the orthonormal Jacobi polynomials, and the coefficients of the expansions are determined from an infinite system of linear algebraic equations of the second kind. Given the solution, we derive formulas for the stress intensity factors K_I , K_{II}

and the weight functions $W_{I,I}$, $W_{I,II}$, $W_{II,I}$, $W_{II,II}$. By determining the energy released as the crack extends to a small distance, we apply the Griffith criterion and establish a criterion of the crack propagation: $H(v, K_I, K_{II}) \geq \mu T$, where μ is the shear modulus and T is the Griffith material constant. We compute the stress intensity factors, the weight functions, and the Griffith criterion for different values of the speed v and the distance δ between the crack and the half-plane boundary. It is found that the value H grows to infinity when the distance δ between the crack and the half-plane boundary decreases while the crack speed does not vary. The function H monotonically decreases as δ grows. When the distance δ is fixed, H , as a function of v/c_R , attains its minimum in the interval $(0, 1)$ and grows as $v \rightarrow 0$ or $v \rightarrow c_R$.

In Chapter 5, we derive the fundamental solution and the weight functions of the transient two-dimensional problem on a semi-infinite crack propagating at constant speed in the direction parallel to the boundary of a half-plane. The boundary of the half-plane is free of traction, while the crack faces are subjected to general time-independent loading. As before, we reduce the boundary-value problem to a vector Riemann–Hilbert problem on the real axis. In the case when the crack is far away from the boundary of the half-plane, the problem is identical to the one considered in Section 3.2. We split the matrix coefficient into a discontinuous diagonal matrix and a continuous matrix, factorize the discontinuous part and rewrite the vector Riemann–Hilbert problem as a system of two convolution equations. We obtain numerical results for the stress intensity factors corresponding to concentrated loading applied (at time instance $t = 0$) to the crack faces. This model problem generates four weight functions $W_{i,j}$, $i, j = I, II$. It is discovered that during a certain initial period of time, $0 < t < 2t_l$, the off-diagonal weight functions $W_{i,j}$, $i \neq j$, vanish and the diagonal functions almost coincide with the ones derived in Section 3.2. For time $t > 2t_l$, the boundary effects play a significant role, and, in general, all the four weight functions do not vanish and are different from the corresponding functions associated with the unbounded plane plane.

Based on the Freund approximate algorithm [39] for the problem on a semi-infinite crack propagating at a nonuniform rate in an unbounded plane, we develop a procedure for the case when the crack propagates at prescribed variable sub-Rayleigh speed in a half-plane in the direction parallel to the boundary and when the boundary effects are significant. The implementation of the method requires solving a system of Volterra convolution equations whose kernels are the associated weight functions. We show that initially, before the longitudinal wave reflected from the boundary strikes the crack and when the weight functions coincide with those for an unbounded plane, the relatively simple Freund's algorithm works. At the same time, the solution is still different since it relies on the static solution on a cracked half-plane, instead of a plane with the crack. When the first longitudinal wave reflected from the half-plane boundary reaches the crack surface moving at speed $v(t) < c_R$, the boundary substantially affects the weight functions. In order to determine the stress intensity factors at the crack tip at some time $t \in (t_k, t_{k+1})$, one may use the procedure presented that requires solving the same transient problem for different constant speeds v_i ($i = 0, 1, \dots, k$) and a system of Volterra equations to determine at each step the loads need to be negated to make possible for the crack to advance. As for the speeds v_j ($j = 0, 1, \dots$) themselves, they are to be determined by applying the dynamic Griffith criterion and solving a certain transcendental equation associated with each step of the algorithm.

Chapter 6 contains the most recent problems. In Sections 6.1 and 6.2, we discuss Wiener–Hopf factorization of one class of functions, those with countably many singular points on the contour of a Riemann–Hilbert problem, which makes difficult an application of numerical techniques. In order to derive its solution, we deform contour so to bypass the singular points and show that the solution of the new Riemann–Hilbert problem can be used to find a closed-form solution of the original one. The main advantage of this approach is that, without recourse to the Cauchy integral, the solution is expressed in terms of integrals of exponentially vanishing functions, which are easy to compute. In the work [5], a similar

approach was applied to Wiener–Hopf factorization of a function that has two branch points on the contour, and the solution was expressed in terms of finite non-singular integrals. The technique described in Section 6.1 generalizes the approach to the case of countably many singularities. Its application to the problem on propagation of a symmetric crack in a strip is given in Section 6.2.

In Section 6.3, we consider a crack propagating in a strip along the interface between two elastic materials. In this case, we assume anti-plane deformation. The lattice model [37, 57] of the materials is accepted. Compared to the continuous mechanics, the lattice model allows for a better description of behavior of stress and deformation fields near the crack tip: specifically, for supersonic speeds of a crack propagation under anti-plane deformation, the continuum fracture mechanics results to a zero energy release rate around the crack tip, which yields to the conclusion that such propagation is impossible. However, some experiments register a crack propagation at intersonic and supersonic speeds [69]. In order to construct a feasible mathematical model of the phenomena, the cohesive zone model (see Section 6.2) and the lattice model (see, for instance, [74]) were proposed. It is interesting to note that even in the case of anti-plane deformation, the lattice model yields a vector Riemann–Hilbert problem. A similar situation is in the anti-plane strain problem of micropolar elasticity [10] when two out three modes are coupled, and the necessity of solving a vector Riemann–Hilbert problem arises. The solution of the Riemann–Hilbert problem was derived using the partial Wiener–Hopf factorization technique proposed in Section 2.3.3.

Chapter 2

Riemann–Hilbert Problem

In this chapter, we give a brief overview of the Riemann–Hilbert problem as well as classes of functions (and matrix-functions) for which the problem admits a solution, discuss its existence and uniqueness, and consider numerical methods of solving Riemann–Hilbert problems. Among all exemplar monographs and papers on the subject, let us highlight monographs by F.D. Gakhov [41] on Riemann–Hilbert problem, and by B. Noble [62] on Wiener–Hopf factorization, which plays a key part in solving the problem.

In Section 2.1, we introduce certain definitions and theorems from Complex Analysis, state the scalar Riemann–Hilbert problem, and derive its solution. This brief introduction to Riemann–Hilbert problem and the technique of its solution is mostly based on the monograph [41], where the reader can refer to for a more thorough information.

In Section 2.2, we state the vector Riemann–Hilbert problem and discuss difficulties that arise when we apply previous techniques to its solution. The classes of matrices that admit the Wiener–Hopf factorization (and analytical solution of the corresponding vector Riemann–Hilbert problems can be constructed) will be considered. We briefly discuss the method [13, 59] for the vector Riemann–Hilbert problem based on its transformation to a scalar Riemann–Hilbert problem on a Riemann surface [87].

Section 2.3 contains overview of several numerical techniques of solving vector Riemann–Hilbert problems, that will be used later in the next chapters. Main issue with most numerical methods for solving Riemann–Hilbert problem is an amount of work necessary for dealing with singularities of the solution, which grows exponentially (in general) with the number of singularities. In this section, we propose the method of a partial factorization that improves convergence and applicability of numerical techniques by utilizing some analytical tools.

2.1 Scalar Riemann–Hilbert Problem

In this section, we discuss the class of Hölder continuous functions, properties of the Cauchy integral of a Hölder continuous function, and its application in constructing Wiener–Hopf factorization of a Hölder continuous function. Then, we state and solve a scalar Riemann–Hilbert problem. This overview is mostly based on the study of Riemann–Hilbert problem by F.D. Gakhov [41].

2.1.1 Hölder theory of Cauchy integrals

The fundamental object of study in the method of Riemann–Hilbert problem is the Cauchy integral. Let L be a bounded smooth simple curve that lies in the complex plane \mathbb{C} and $f : L \rightarrow \mathbb{C}$ a continuous function on L . Then the singular integral

$$F(z) = \frac{1}{2\pi i} \int_L \frac{f(t)}{t - z} dt, \quad z \in \mathbb{C} \quad (2.1)$$

is called *the Cauchy integral*. Since $F(z)$ is infinitely differentiable at all points of the complex plane \mathbb{C} except the contour L , the function $F(z)$ is analytic in $\mathbb{C} \setminus L$. If the point z is large enough, the series representation of the kernel $1/(t - z)$ implies

$$F(z) = \sum_{n=1}^{\infty} \frac{c_n}{z^n}, \quad |z| > R, \quad c_n = -\frac{1}{2\pi i} \int_L t^{n-1} f(t) dt \quad (2.2)$$

where R is the radius of a disk around the origin, containing the curve L . Thus the function $F(z)$ vanishes as $z \rightarrow \infty$ since the series (2.2) does not contain the constant term.

The Cauchy integral is so important to solving Riemann–Hilbert problems due to its behavior on the contour L in the case when the integrand is a Hölder continuous function.

Definition 2.1. Let L be a bounded smooth curve. The function $f : L \rightarrow \mathbb{C}$ is said to be λ -Hölder continuous if there exists a positive constant A such that for any two points $t_1, t_2 \in L$,

$$|f(t_1) - f(t_2)| < A|t_1 - t_2|^\lambda \quad (2.3)$$

where A and λ are positive numbers.

Notice that if $\lambda > 1$ then the derivative of a λ -Hölder continuous function is always equal to zero and, therefore, such a function is just a constant. Hence, we consider only the values $\lambda \in (0, 1]$. If $\lambda = 1$, then f is Lipschitz continuous. Thus, the class of Hölder continuous functions contains the class of continuously differentiable functions.

Next, we introduce *the principal value* of the Cauchy integral.

Definition 2.2. Let L be a bounded smooth simple curve and z an arbitrary point on L . Denote $l_\rho = D_\rho \cap L$, where D_ρ is the disk of radius ρ centered at the point z . The integral defined by

$$P.V. \int_L \frac{f(t)}{t - z} dt = \lim_{\rho \rightarrow 0} \int_{L \setminus l_\rho} \frac{f(t)}{t - z} dt, \quad z \in L \quad (2.4)$$

is called the principal value of the Cauchy integral. In order to distinguish the principal value of an integral, we will write the letters “P.V.” in front of the integral.

It is helpful to consider the following example. Let us find the principal value of the integral

$$\int_L \frac{dt}{t - z_0}$$

where L is a smooth simple open curve with end points a and b (if L is closed, then $a = b$).

Fix $z_0 \in L$, then by definition

$$P.V. \int_L \frac{dt}{t - z_0} = \lim_{\rho \rightarrow 0} \int_{L \setminus l_\rho} \frac{dt}{t - z_0} = \ln \frac{b - z_0}{a - z_0} - \lim_{\rho \rightarrow 0} \ln \frac{z_2 - z_0}{z_1 - z_0} \quad (2.5)$$

where z_1 and z_2 are the points of intersection of the circle ∂D_ρ and the curve L (see Figure 2.1, a.). Assume that the complex plane \mathbb{C} has a cut along a curve connecting the points z_0

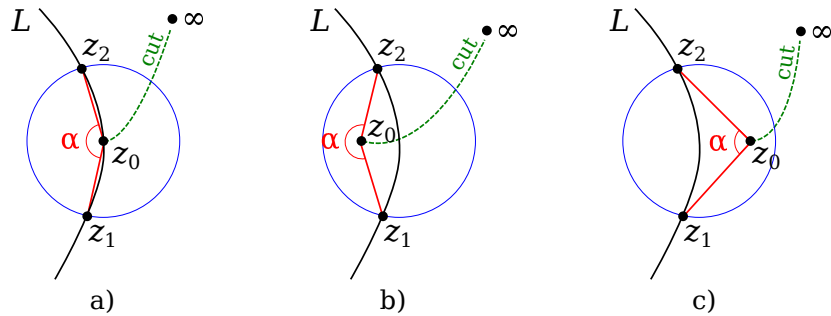


Figure 2.1: Limit of $\arg(z_2 - z_0) - \arg(z_1 - z_0)$ as $\rho \rightarrow 0$ when (a) z_0 is an inner point of L ; (b) z_0 is on the left from L , (c) z_0 is on the right from L .

and ∞ and lying on the right side from L . Fix the branch of the logarithm in the formula (2.5), then

$$\lim_{\rho \rightarrow 0} \ln \frac{z_2 - z_0}{z_1 - z_0} = i \lim_{\rho \rightarrow 0} \{\arg(z_2 - z_0) - \arg(z_1 - z_0)\} = -\pi i$$

since $|z_2 - z_0| = |z_1 - z_0|$ and the angle between the vectors $z_2 - z_0$ and $z_1 - z_0$ approaches $-\pi$ as ρ vanishes (Figure 2.1, a.). Thus

$$P.V. \int_L \frac{dt}{t - z_0} = \ln \frac{b - z_0}{a - z_0} + \pi i \quad (2.6)$$

where the logarithm in the right-hand side vanishes if the curve L is closed (i.e. $a = b$).

Now, we are ready to state the existence of the principal value.

Lemma 2.3. If L is a bounded smooth simple contour and $f : L \rightarrow \mathbb{C}$ is a Hölder continuous function, then the principal value of the integral

$$\int_L \frac{f(t)}{t - z} dt$$

exists for all inner points of the contour L .

Proof. Since L is a bounded contour, we can represent the principal value of the integral as follows

$$P.V. \int_L \frac{f(t)}{t - z} dt = P.V. \int_L \frac{f(t) - f(z)}{t - z} dt + f(z) P.V. \int_L \frac{dt}{t - z} \quad (2.7)$$

The last integral in the right-hand side exists and its value is given by the formula (2.6). The first integral in the right-hand side can be estimated using the condition (2.3) of a Hölder continuous function,

$$\left| \int_L \frac{f(t) - f(z)}{t - z} dt \right| \leq \int_L \frac{|f(t) - f(z)|}{|t - z|} dt < A \int_L |t - z|^{\lambda-1} dt$$

Since $\lambda > 0$, the integral $\int_L |t - z|^{\lambda-1} dt$ exists in the Riemann sense and so does the first integral in the right-hand side of (2.7). Then its principal value, that is the limit

$$\lim_{\rho \rightarrow 0} \int_{L \setminus l_\rho} \frac{f(t) - f(z)}{t - z} dt$$

exists and equals to the value of the Riemann integral over L . Thus, the right-hand side and, therefore, the left-hand side of the equality (2.7) exist. \square

Remark 2.4. If an integral exists in the Riemann sense, then its principal value exists and equals to the Riemann integral.

If L is a bounded smooth simple contour and $f : L \rightarrow \mathbb{C}$ is a Hölder function, then the Cauchy integral (2.1) is analytic in the region $\mathbb{C} \setminus L$, while there exists the principal value of the integral at all inner points of the contour L . Let us discuss the difference between the principal value of the integral (2.1) at the point $z_0 \in L$ and the limits of the same integral as $z \rightarrow z_0$ from the left and the right side of L . Hereafter, we use the following notation: $F^+(z_0)$ stands for the limit of $F(z)$ as $z \rightarrow z_0$ from the left side of L ; $F^-(z_0)$ stands for the limit of $F(z)$ as $z \rightarrow z_0$ from the right side of L ; and $F(z_0)$ stands for the principal value of $F(z)$. The relation between $F^\pm(z_0)$ and $F(z_0)$ for $z_0 \in L$ is given by the Sokhotski–Plemelj formulas as follows

Theorem 2.5. Let L be a bounded smooth simple contour, z_0 an inner point of L , and $f : L \rightarrow \mathbb{C}$ a Hölder function. The limit values $F^\pm(z_0)$ of the Cauchy integral

$$F(z) = \frac{1}{2\pi i} \int_L \frac{f(t)}{t - z} dt$$

satisfy the equations

$$F^\pm(z_0) = \pm \frac{1}{2} f(z_0) + \frac{1}{2\pi i} P.V. \int_L \frac{f(t)}{t - z_0} dt \quad (2.8)$$

Proof. In the proof of Lemma (2.3), we showed that the integral

$$\psi(z) = \int_L \frac{f(t) - f(z)}{t - z} dt$$

exists in the Riemann sense if f is a Hölder function. Since L is a bounded curve, the integral $\psi(z)$ is a continuous function of z -variable [41]. Therefore for any inner point z_0 of the curve

L , we have $\psi^+(z_0) = \psi^-(z_0) = \psi(z_0)$. On the other hand, if a and b are the end points of the curve L , then

$$\lim_{z \rightarrow z_0} \int_L \frac{dt}{t - z} = \begin{cases} \ln \frac{b - z_0}{a - z_0} + 2\pi i & \text{if } z \text{ is on the left from } L \\ \ln \frac{b - z_0}{a - z_0} + \pi i & \text{if } z \text{ is on } L \\ \ln \frac{b - z_0}{a - z_0} & \text{if } z \text{ is on the right from } L \end{cases}$$

since in the first case, the curve L intersects the cut joining z_0 and infinity so the value of the integral is increased by $2\pi i$ (see Figures 2.1, b. and 2.1, c.). The second case was already computed in (2.6).

Thus, we have the following representation

$$\begin{aligned} \psi^+(z_0) &= 2\pi i F^+(z_0) - f(z_0) \left\{ \ln \frac{b - z_0}{a - z_0} - 2\pi i \right\} \\ \psi(z_0) &= P.V. \int_L \frac{f(t)}{t - z_0} dt - f(z_0) \left\{ \ln \frac{b - z_0}{a - z_0} - \pi i \right\} \\ \psi^-(z_0) &= 2\pi i F^-(z_0) - f(z_0) \ln \frac{b - z_0}{a - z_0} \end{aligned}$$

Using the fact that the function ψ is continuous across L (i.e. $\psi^+(z_0) = \psi^-(z_0) = \psi(z_0)$), we immediately derive the identities (2.8). \square

Remark 2.6. If we take sum and difference of the equations (2.8), we derive formulas

$$\begin{aligned} F^+(z_0) - F^-(z_0) &= f(z_0) \\ F^+(z_0) + F^-(z_0) &= \frac{1}{\pi i} P.V. \int_L \frac{f(t)}{t - z_0} dt \end{aligned} \quad z_0 \in L \quad (2.9)$$

Remark 2.7. In the definition 2.2, we assume that L is a bounded curve. However, the principal value of the Cauchy integral (2.4) exists and the Sokhotski–Plemelj formulas (2.8) and (2.9) hold as well in the case when L is an unbounded curve [41] if the function $f : L \rightarrow \mathbb{C}$ satisfies an additional condition

$$|f(t) - f_\infty| < \frac{A}{|t|^\mu}, \quad \mu > 0, \quad A > 0 \quad (2.10)$$

for all $t \in L \setminus \{\infty\}$, where $f_\infty = \lim_{t \rightarrow \infty} f(t)$.

Now we can state the scalar Riemann–Hilbert problem and derive its solution, using the facts we just discussed.

2.1.2 Solution of a scalar Riemann–Hilbert problem

Hereafter, we assume that the curve L coincides with the real axis \mathbb{R} of the complex plane \mathbb{C} . Although, the described technique is applicable for any smooth simple curve, all the problems of the following chapters are reduced to Riemann–Hilbert problems on the real axis.

Let us introduce notation for the upper and lower half-plane, \mathbb{C}^+ and \mathbb{C}^- respectively:

$$\mathbb{C}^+ = \{z \in \mathbb{C} : \operatorname{Im} z > 0\}, \quad \mathbb{C}^- = \{z \in \mathbb{C} : \operatorname{Im} z < 0\}$$

Definition 2.8. Let $a : \mathbb{R} \rightarrow \mathbb{C}$ and $b : \mathbb{R} \rightarrow \mathbb{C}$ be Hölder continuous functions such that $a(t) \neq 0$ for all $t \in \overline{\mathbb{R}}$ (including the infinite point). The problem of determining two functions $F^\pm : \mathbb{C}^\pm \rightarrow \mathbb{C}$, which are analytic in \mathbb{C}^\pm respectively, continuous on the real axis \mathbb{R} , and may grow as a polynomial of degree n at infinity, such that they satisfy the condition

$$F^+(t) = a(t)F^-(t) + b(t), \quad t \in \mathbb{R} \tag{2.11}$$

is called the Riemann–Hilbert problem with coefficient $a(t)$ and inhomogeneous part $b(t)$.

We first outline the three main steps in construction of the solution of a scalar Riemann–Hilbert problem.

1. Find two functions that are analytic in \mathbb{C}^\pm as well as continuous on \mathbb{R} , such that

$$a(t) = \frac{a^+(t)}{a^-(t)}, \quad t \in \mathbb{R} \tag{2.12}$$

The representation (2.12) is crucial to the solution and is called the Wiener–Hopf factorization [62]. It can be achieved by using the first of the Sokhotski–Plemelj formulas (2.9). Notice that the functions a^\pm are defined in \mathbb{C}^\pm while the equality (2.12) holds only on \mathbb{R} . Hereafter, we define the values of the functions a^\pm on the real axis \mathbb{R} as the limits

$$a^\pm(t) = \lim_{z \rightarrow t, z \in \mathbb{C}^\pm} a^\pm(z), \quad t \in \mathbb{R} \tag{2.13}$$

That is, the value $a^+(t)$ for any $t \in \mathbb{R}$ is the limit of $a^+(z)$ as the variable z approaches t from the left (i.e. \mathbb{C}^-) of the real axis \mathbb{R} . Similarly, the value $a^-(t)$ for any $t \in \mathbb{R}$ is the limit of $a^-(z)$ as the variable z approaches t from the right (i.e. \mathbb{C}^+) of the real axis \mathbb{R} . We will use this convention (2.13) for any function with superscript “+” or “-”.

Given the representation (2.12) for the function a , we can rewrite the condition (2.11) as follows:

$$\frac{F^+(t)}{a^+(t)} = \frac{F^-(t)}{a^-(t)} + \frac{b(t)}{a^+(t)}, \quad t \in \mathbb{R}$$

2. Now we use a similar trick for the inhomogeneous part: represent it in the form

$$\frac{b(t)}{a^+(t)} = b^+(t) - b^-(t), \quad t \in \mathbb{R} \quad (2.14)$$

where the functions $b^\pm : \mathbb{C}^\pm \rightarrow \mathbb{C}$ are analytic in \mathbb{C}^\pm respectively, and rewrite the condition once again

$$\frac{F^+(t)}{a^+(t)} - b^+(t) = \frac{F^-(t)}{a^-(t)} - b^-(t), \quad t \in \mathbb{R} \quad (2.15)$$

3. Introduce an auxiliary function $P : \mathbb{C} \rightarrow \mathbb{C}$ by the formula

$$P(z) = \begin{cases} \frac{F^+(z)}{a^+(z)} - b^+(z) & \text{if } z \in \mathbb{C}^+ \\ \frac{F^-(z)}{a^-(z)} - b^-(z) & \text{if } z \in \mathbb{C}^- \end{cases} \quad (2.16)$$

Since all of the functions F^+ , a^+ , b^+ are analytic in \mathbb{C}^+ , the function P is analytic in \mathbb{C}^+ except the points where a^+ vanishes. Similarly, the function P is analytic in \mathbb{C}^- except the points where a^- vanishes. Finally, P is continuous on the real axis \mathbb{R} due to the equality (2.15). Therefore, uniqueness of an analytic function implies that P is a meromorphic function on \mathbb{C} and can be determined using Liouville’s theorem [41]. In the case when the functions a^\pm does not vanish in the half-planes \mathbb{C}^\pm , and due to the fact that the functions F^\pm may grow at infinity as a polynomial of degree n , while the functions a^\pm and b^\pm are bounded, we have

$$P(z) = C_0 + C_1 z + \dots + C_n z^n$$

where n is a degree of growth of the solution at infinity, defined in the statement of the Riemann–Hilbert problem; C_0, \dots, C_n are arbitrary complex-valued constants. Given P , a^\pm , and b^\pm , the solution of the Riemann–Hilbert problem can be derived from (2.16) as follows:

$$F^\pm(z) = a^\pm(z) [P(z) + b^\pm(z)], \quad z \in \mathbb{C}^\pm \quad (2.17)$$

Notice that if we seek solution of a Riemann–Hilbert problem, that vanishes at infinity, then $P(z) = 0$ for all $z \in \mathbb{C}$. Therefore, such a solution is unique (if exists). However in general, solution of a Riemann–Hilbert problem is not unique and determined up to $n + 1$ arbitrary complex constants.

Let us discuss now the first step of the technique above. Assume that there exist two functions a^\pm analytic in \mathbb{C}^\pm respectively, that satisfy the equation (2.12). Taking the logarithm of both sides of (2.12), we derive

$$\ln a(t) = \ln a^+(t) - \ln a^-(t), \quad t \in \mathbb{R}$$

Notice that the value $N^+ = [\ln a^+(t)]_{\mathbb{R}}$, the increment of $\ln a^+(t)$ when t changes from $-\infty$ to ∞ , is equal to the number of zeros of a^+ in the upper half-plane \mathbb{C}^+ , since a^+ has no poles in \mathbb{C}^+ . Similarly, $N^- = -[\ln a^-(t)]_{\mathbb{R}}$ is the number of zeros of a^- in the lower half-plane \mathbb{C}^- , where the sign “ $-$ ” indicates that the region \mathbb{C}^- lies on the right from the real axis \mathbb{R} . Thus

$$N^+ + N^- = \frac{1}{2\pi i} [\ln a(t)]_{\mathbb{R}} \quad (2.18)$$

Value $\kappa = [\ln a(t)]_{\mathbb{R}}/(2\pi i)$ is called *the index of the Riemman–Hilbert problem*. Notice that the index κ is an integer provided $a(t)$ is a continuous function on \mathbb{R} and has the same limit as $t \rightarrow \infty$ and $t \rightarrow -\infty$. Using the equality (2.18), we make the following conclusions:

1. The condition $\kappa \geq 0$ is necessary for existence of functions a^\pm satisfying (2.12) and analytic in \mathbb{C}^\pm respectively.
2. If $\kappa = 0$, then the functions a^\pm have no zeros in \mathbb{C}^\pm respectively.

3. If $\kappa > 0$, then the functions a^\pm together have κ zeros.

4. If $\kappa < 0$, then the functions a^\pm have a pole at infinity of order $-\kappa$.

Consider the case $\kappa = 0$. Let us show that the functions a^\pm defined by the formula

$$a^\pm(z) = \exp \left\{ \frac{1}{2\pi i} \int_{\mathbb{R}} \frac{\ln a(t)}{t - z} dt \right\}, \quad z \in \mathbb{C}^\pm \quad (2.19)$$

provide the Wiener–Hopf factorization (2.12) when the values of $a^\pm(t)$ on the real axis \mathbb{R} are considered to be limits of the functions $a^\pm(z)$ as z approaches the point $t \in \mathbb{R}$ from the half-spaces \mathbb{C}^\pm respectively.

Since the logarithm is a continuous and differentiable function on the positive or negative semi-axes of \mathbb{R} and the function $a(t)$ is Hölder continuous and does not vanish on \mathbb{R} , there exist positive constants A , C , and λ such that

$$|\ln a(t_1) - \ln a(t_2)| < C |a(t_1) - a(t_2)| < A \cdot C \cdot |t_1 - t_2|^\lambda$$

for any $t_1, t_2 \in \mathbb{R}$. Thus $\ln a(t)$ is a Hölder function on \mathbb{R} . Similarly, for any $t \in \mathbb{R}$, there exist positive constants A , C , and μ such that

$$|\ln a(t) - \ln a_\infty| < C |a(t) - a_\infty| < \frac{A \cdot C}{|t|^\mu}$$

where the value a_∞ , the limit of $a(t)$ as $t \rightarrow \infty$, exists since $\kappa = 0$ (i.e. the function $\ln a(t)$ is continuous at infinity).

Since $\ln a(t)$ satisfies the conditions (2.3) and (2.10), the functions $\ln a^\pm(z)$ exist and satisfy the Sokhotsky–Plemelj formulas (see Remark 2.6 and Theorem 2.5), that is

$$\ln a^+(t) - \ln a^-(t) = \ln a(t), \quad t \in \mathbb{R}$$

for any single-valued branch of the logarithm. From the identity above, we immediately derive the equality (2.12). Notice that analyticity of the functions $\ln a^\pm$ in the half-planes

\mathbb{C}^\pm implies that a^\pm are analytic and non-zero in \mathbb{C}^\pm respectively. Thus the functions a^\pm defined in (2.19), conclude the first step of the solution of the Riemann–Hilbert problem.

In the case $\kappa > 0$, choose and fix an arbitrary point $z_0 \in \mathbb{C}^+$. Then the function $(t - z_0)^{-\kappa}a(t)$ has zero index since

$$[\ln\{(t - z_0)^{-\kappa}a(t)\}]_{\mathbb{R}} = -\kappa[\ln(t - z_0)]_{\mathbb{R}} + [\ln a(t)]_{\mathbb{R}} = -\kappa + \kappa = 0$$

Let us define two auxiliary functions as follows

$$a_0^\pm(z) = \frac{1}{2\pi i} \int_{\mathbb{R}} \frac{\ln\{(t - z_0)^{-\kappa}a(t)\}}{t - z} dt, \quad z \in \mathbb{C}^\pm$$

Applying our derivations for the case of zero index, we conclude that

$$\frac{a_0^+(t)}{a_0^-(t)} = \frac{a(t)}{(t - z_0)^\kappa}, \quad t \in \mathbb{R}$$

After multiplying the equation above by the term $(t - z_0)^\kappa$, it immediately follows that the functions

$$a^+(z) = (z - z_0)^\kappa a_0^+(z), \quad a^-(z) = a_0^-(z)$$

satisfy the equation (2.12). Notice that in this case, the function a^+ analytic and have one zero of order κ in the half-plane \mathbb{C}^+ , while the function a^- is analytic and non-zero in \mathbb{C}^- .

Remark 2.9. In the case $\kappa > 0$, we can replace the factor $(t - z_0)^{-\kappa}$ by any other factor that has the index κ on \mathbb{R} . For instance, sometimes it is beneficial to choose arbitrary distinct points $z_1, \dots, z_\kappa \in \mathbb{C}$ and use the factor $\prod_{k=1}^\kappa (t - z_k)^{-1}$ instead of $(t - z_0)^{-\kappa}$.

In the case $\kappa < 0$, the solution exists only if the inhomogeneous part of the Riemann–Hilbert problem satisfies additional conditions

$$\int_{\mathbb{R}} \frac{b(t)}{a^+(t)} t^{k-1} dt = 0, \quad k = 1, 2, \dots, -\kappa - 1$$

which “kill” the growth of the function a^\pm at infinity in the formula (2.17).

The second step in the solution of the Riemann–Hilbert problem is fairly similar to the first one. In order to construct the functions $b^\pm : \mathbb{C}^\pm \rightarrow \mathbb{C}$ analytic in \mathbb{C}^\pm and satisfying

the equation (2.14), we use once again the Sokhotsky–Plemelj formulas (2.9) for the Cauchy integral

$$b^\pm(z) = \frac{1}{2\pi i} \int_{\mathbb{R}} \frac{b(t)}{a^+(t)} \frac{dt}{t - z} \quad (2.20)$$

Since $a^+(t)$ is a continuous function that does not vanish on \mathbb{R} and bounded at infinity, while the function $b(t)$ is Hölder continuous, the factor b/a^+ is Hölder continuous. Therefore, the Sokhotsky–Plemelj formulas (2.9) imply that the functions b^\pm defined by (2.20), satisfy the condition (2.14).

2.2 Vector Riemann–Hilbert Problem

In the previous section, we solved Riemann–Hilbert problem with respect to scalar functions F^\pm satisfying the boundary condition (2.11). Now we will consider $2N$ functions F_k^\pm , $k = 1, \dots, N$, that satisfy a system of the boundary conditions of the type (2.11). In the matrix form, such problem is formulated as follows

Definition 2.10. Let $A : \mathbb{R} \rightarrow \mathbb{C}^{N \times N}$ be an invertible matrix-function on the real axis \mathbb{R} with Hölder continuous non-zero components. Let $B : \mathbb{R} \rightarrow \mathbb{C}^N$ be a vector-function on the real axis \mathbb{R} with Hölder continuous components. The problem of determining two vector-functions $F^\pm : \mathbb{C}^\pm \rightarrow \mathbb{C}^N$ such that they satisfy the boundary condition

$$F^+(t) = A(t)F^-(t) + B(t), \quad t \in \mathbb{R} \quad (2.21)$$

while the components of F^\pm are analytic in \mathbb{C}^\pm respectively and may grow as a polynomial of degree n at infinity, is called the vector Riemann–Hilbert problem with matrix-coefficient A and inhomogeneous part B .

Hereafter, we assume that the matrix A is invertible and its components are Hölder continuous on the real axis \mathbb{R} . In order to construct solution of a vector Riemann–Hilbert problem in the closed form, we could follow the same steps 1, 2, and 3, described in the previous section. However, one difficulty arises due to the fact that matrices are non-commutative.

Consider the first step of the solution and define the matrices

$$A^\pm(z) = \exp \left\{ \frac{1}{2\pi i} \int_{\mathbb{R}} \frac{\ln A(t)}{t - z} dt \right\}$$

where the integral is understood as a component-wise operator. Assume that the components of $\ln A(t)$ are Hölder continuous on \mathbb{R} . The Sokhotsky–Plemelj formulas (2.8), applied to A^\pm , imply that

$$A^\pm(z_0) = \exp \left\{ \pm \frac{1}{2} \ln A(z_0) + \frac{1}{2\pi i} P.V. \int_{\mathbb{R}} \frac{\ln A(t)}{t - z_0} dt \right\}, \quad z_0 \in \mathbb{R}$$

In order to derive the equality $A^+[A^-]^{-1} = \exp\{\ln A\}$ on the real axis \mathbb{R} , the exponents of the matrices

$$g(z) = \ln A(z) \quad \text{and} \quad h(z) = P.V. \int_{\mathbb{R}} \frac{\ln A(t)}{t - z} dt \quad (2.22)$$

have to satisfy the equation $e^{g+h} = e^g e^h$ on the real axis \mathbb{R} . However, the equation $e^{g+h} = e^g e^h$ does not hold for arbitrary matrices g and h . Thus, we need to specify class of matrices A that admit the closed-form solution of the Riemann–Hilbert problem. Below, we consider some of such classes.

2.2.1 Diagonal and triangular matrix-coefficient

In the case of a diagonal matrix-coefficient A of the Riemann–Hilbert problem (2.21), it is easy to see that the problem is equivalent (except several special cases) to solving N separate scalar Riemann–Hilbert problems with the corresponding boundary conditions

$$f_j^+(t) = a_j(t) f_j^-(t) + b_j(t), \quad t \in L, \quad j = 1, \dots, N \quad (2.23)$$

where f_j^\pm , b_j are the components of the vectors F^\pm , B respectively, and a_j are the diagonal components of the matrix A . The question of existence and uniqueness of the solution is, therefore, reduced to existence and uniqueness of each of the separate scalar Riemann–Hilbert problems, which depend on their corresponding indices κ_j (called *partial indices* of a vector Riemann–Hilbert problem). In this case, the solution of (2.21) is given by the vector $F^\pm = (f_1^\pm, \dots, f_N^\pm)^T$. However, it is possible that a vector Riemann–Hilbert with a diagonal

coefficient has a solution, while each of the problems (2.23) do not: for instance, if A is 2×2 diagonal matrix and its components have partial indices $\kappa_1 = \infty$ and $\kappa_2 = -\infty$ [75].

In the case of a triangular matrix-coefficient A , the corresponding vector problem can be reduced to N separate scalar Riemann–Hilbert problems. Assume that A is a lower triangular matrix with components $a_{i,j}$, $j = 1, \dots, i$ and $i = 1, \dots, N$. Then the vector Riemann–Hilbert problem takes the form

$$\begin{aligned} f_1^+(t) &= a_{1,1}(t)f_1^-(t) + b_1(t) \\ f_2^+(t) &= a_{1,2}(t)f_1^-(t) + a_{2,2}(t)f_2^-(t) + b_2(t) \\ &\vdots \\ f_N^+(t) &= a_{N,1}(t)f_1^-(t) + \dots + a_{N,N}(t)f_N^-(t) + b_N(t) \end{aligned} \quad t \in L$$

From the first row of the equations, we can determine the functions f_1^\pm ; then, given f_1^\pm , we determine f_2^\pm from the second row, and so on. Once again, uniqueness and existence of the solution of the vector problem (2.21) will depend on uniqueness and existence of solution of each scalar Riemann–Hilbert problem with the corresponding boundary conditions.

Thus in both cases, the vector problem (2.21) can be reduced to N scalar Riemann–Hilbert problems. Next, we will consider several classes of matrices, that can be reduced to the diagonal or triangular form.

2.2.2 Functionally commutative matrix-coefficient

In this section, we follow the theory of functionally commutative matrices studied by V. Morozov [58] and applied to vector Riemann–Hilbert problems by G. Chebotarev [29].

Definition 2.11. Matrix $A(t)$ is called functionally commutative on contour L if for any $t_1, t_2 \in L$,

$$[A(t_1), A(t_2)] = 0$$

where $[\alpha, \beta] = \alpha\beta - \beta\alpha$ is the matrix commutator.

If $A(t)$ is functionally commutative, then so is the matrix $\ln A(t)$, which follows from the series representation of the logarithm. Therefore, for the matrices g and h defined in (2.22), we have the equality

$$[g(z_0), h(z_0)] = P.V. \int_L \frac{[g(z_0), g(t)]}{t - z_0} dt = 0$$

for all $z_0 \in L$. Thus, using the series representation of the matrix exponential, we can conclude that e^g and e^h commute,

$$[e^{g(z_0)}, e^{h(z_0)}] = \sum_{k=0}^{\infty} \frac{1}{k!} \sum_{l=0}^{\infty} \frac{1}{l!} [g^k(z_0), h^l(z_0)] = 0$$

where commutativity of g^k and g^l can be shown for any $j, k \in \mathbb{N}$ by the induction starting with $j = k = 1$.

Theorem 2.12. Matrix $A(t)$ is functionally commutative on contour L if and only if there exist M linear independent functions $\tilde{a}_1(t), \dots, \tilde{a}_M(t)$ and M constant pairwise commutative matrices A_1, \dots, A_M such that

$$A(t) = \sum_{j=1}^M \tilde{a}_j(t) A_j, \quad \forall t \in L \quad (2.24)$$

Proof of the theorem can be found in [58]. One property of functionally commutative matrices is of special importance for us: if $A(t)$ is functionally commutative, then there exists a constant matrix T such that $TA(t)T^{-1}$ is a triangular matrix-function. This property is based on the fact that if the matrices A_j , $j = 1, \dots, M$ in the representation (2.24) are pairwise commutative, then they are simultaneously triangularisable [58].

Corollary 2.13. Eigenvalues of a functionally commutative matrix in the form

$$A(t) = \sum_{j=1}^M \tilde{a}_j(t) A_j, \quad \forall t \in L$$

are linear combinations of functions $\tilde{a}_j(t)$ with constant coefficients:

$$\lambda_k(t) = \sum_{j=1}^M \tilde{a}_j(t) \tilde{\lambda}_{jk}, \quad k = 1, \dots, N \quad (2.25)$$

Indeed, there exists a constant matrix T such that the matrices $TA(t)T^{-1}$ and TA_jT^{-1} , $j = 1, \dots, M$, are triangular. Since the diagonal components of triangular matrices contain their eigenvalues, we derive the equations (2.25) from component-wise comparison of the elements on the matrix diagonals.

Since the functionally commutative matrix $A(t)$ in (2.21) is triangularizable by a constant matrix T , condition of the Riemann–Hilbert problem can be transformed to the form

$$TF^+(t) = \underbrace{TA(t)T^{-1}}_{\text{triangular}} TF^-(t) + TB(t), \quad t \in L$$

where the components of the vectors TF^\pm are analytic in \mathbb{C}^\pm respectively. In order to construct the vectors TF^\pm , we proceed as in the case of a triangular matrix-coefficient (see section 2.2.1).

2.2.3 Chebotarev–Khrapkov class of matrices

The following derivation is based on the results [29]. Let A be 2×2 matrix-function with Hölder continuous components. Find the class of matrices A such that the matrices g and h defined in (2.22), commute. Notice that the condition $[g, h] = 0$ is equivalent to the following three equations:

$$\begin{aligned} g_{12}h_{21} &= h_{12}g_{21} \\ g_{11}h_{12} + g_{12}h_{22} &= h_{11}g_{12} + h_{12}g_{22} \\ g_{21}h_{11} + g_{22}h_{21} &= h_{21}g_{11} + h_{22}g_{21} \end{aligned} \tag{2.26}$$

with respect to components g_{ij} and h_{ij} , $i, j \in \{1, 2\}$, of the matrices g and h respectively. In order to solve the system (2.26), we introduce the Cauchy integrals

$$G_{ij}(z) = \frac{1}{2\pi i} \int_{\mathbb{R}} \frac{g_{ij}(t)}{t - z} dt, \quad i, j \in \{1, 2\}$$

Using the Sokhotsky–Plemelj formulas (2.9), we can write $g_{ij} = G_{ij}^+ - G_{ij}^-$ and $h_{ij} = \pi i(G_{ij}^+ + G_{ij}^-)$. Then the equations (2.26) take the form

$$\frac{G_{12}^+}{G_{21}^+} = \frac{G_{12}^-}{G_{21}^-}, \quad \frac{G_{11}^+ - G_{22}^+}{G_{12}^+} = \frac{G_{11}^- - G_{22}^-}{G_{12}^-}, \quad \frac{G_{11}^+ - G_{22}^+}{G_{21}^+} = \frac{G_{11}^- - G_{22}^-}{G_{21}^-} \tag{2.27}$$

where the third equation is redundant. The first equation implies that the function $G_{12}(z)/G_{21}(z)$ is continuous across the real axis \mathbb{R} and meromorphic in the complex plane \mathbb{C} . The second equation implies that the function $[G_{11}(z) - G_{22}(z)]/G_{12}(z)$ is continuous across \mathbb{R} and meromorphic in \mathbb{C} . Since the zeroes of G_{12}/G_{21} coincide with the poles of $(G_{11} - G_{22})/G_{12}$, there exist three entire functions $l, m, n : \mathbb{C} \rightarrow \mathbb{C}$ such that

$$\frac{G_{12}}{G_{21}} = \frac{m}{n}, \quad \frac{G_{11} - G_{22}}{G_{12}} = 2 \frac{l}{m}$$

where the factor 2 is chosen for convenience. Using the Sokhotsky–Plemelj formulas (2.9), we find that $ng_{12} = n(G_{12}^+ - G_{12}^-) = m(G_{21}^+ - G_{21}^-) = mg_{21}$ on the real axis \mathbb{R} and, similarly, $m(g_{11} - g_{22}) = 2lg_{12}$. Finally, we rewrite the matrix g in the form

$$g = g_1 I + g_2 J, \quad \text{where} \quad g_1 = g_{11} - \frac{l}{m} g_{12}, \quad g_2 = \frac{g_{12}}{m}, \quad J = \begin{pmatrix} l & m \\ n & -l \end{pmatrix}$$

and I is the identity matrix. Notice that g_1 and g_2 are Hölder continuous functions on the real axis \mathbb{R} and $J^2 = \Delta^2 I$, where $\Delta^2 = l^2 + mn$. Therefore,

$$\begin{aligned} A = e^g &= \sum_{n=0}^{\infty} \frac{g^n}{n!} = \sum_{n=0}^{\infty} \frac{1}{n!} \sum_{k=0}^n \binom{n}{k} g_1^{n-k} g_2^k J^k \\ &= \left(\sum_{k=0}^{\infty} \sum_{\substack{k=0 \\ k \text{ is even}}}^n \binom{n}{k} \frac{g_1^{n-k} g_2^k \Delta^k}{n!} \right) I + \left(\sum_{k=0}^{\infty} \sum_{\substack{k=0 \\ k \text{ is odd}}}^n \binom{n}{k} \frac{g_1^{n-k} g_2^k \Delta^{k-1}}{n!} \right) J \end{aligned}$$

Thus if the matrix-functions g and h defined in (2.22) commute, then $A = \alpha I + \beta J$, where α and β are Hölder continuous on the real axis \mathbb{R} , $J^2 = \Delta^2 I$, and Δ^2 is an entire function on \mathbb{C} . Such matrices A were first introduced and used in several works by G.N. Chebotarev [29], A.A. Khrapkov [52, 53], and V.G. Daniele [32].

In the case of the matrix-coefficient A of size $N \times N$ for $N > 2$, D.S. Jones showed [50, 51] that if matrix A has representation

$$A(t) = \sum_{k=0}^{m-1} \alpha_k(t) J^k(t), \quad J^m = \Delta^m I \quad (2.28)$$

where m is a positive integer, α_k are Hölder continuous functions on the contour L , components of the matrix J are entire functions in the complex plane \mathbb{C} , and $\text{tr} J^k = 0$ for $k = 1, \dots, m-1$, then the matrix A admits Wiener–Hopf factorization (the latter condition is not necessary, as was shown by N.G. Moiseev [59]). Moreover, if A admits Wiener–Hopf representation

$$A(t) = A^+(t)[A^-(t)]^{-1}, \quad t \in L$$

where A^\pm are analytic in D^\pm respectively, and A^\pm have distinct eigenvalues, then the matrix A can be represented in the form (2.28).

2.3 Solution of a Vector Riemann–Hilbert Problem

Due to the difficulty of deriving the Wiener–Hopf factorization for a matrix, that we discussed in the previous section, there are many analytical and numerical methods for solving vector Riemann–Hilbert problems, which depend on a class of the matrix-coefficient A in the equation (2.21). In this section, we will discuss some of those methods.

As an example of deriving an analytical solution of a vector Riemann–Hilbert problem in the closed form, we will consider the technique that allows for transformation of a vector Riemann–Hilbert problem with a matrix-coefficient A of the Chebotarev–Khrapkov class to a scalar Riemann–Hilbert problem on a Riemann surface. This technique is based on the theory of the scalar Riemann–Hilbert problem on a Riemann surface [87], it was proposed in [59] and developed and applied in [9, 11, 13, 14, 15, 70]. Another technique of matrix factorization that is arising in fluid mechanics and built on the theory [87], was worked out in [16].

In the case when Wiener–Hopf factorization for the matrix-coefficient A in (2.21) cannot be found analytically in the closed form, various numerical techniques can be applied, which take advantage of the intrinsic relation between vector Riemann–Hilbert problems and singular integral equations. There exist numerous techniques for obtaining numerical solution of the latter. Convenience and suitability of applying those techniques mostly depends on a class

of the matrix-coefficient A and a shape of the contour L of a Riemann–Hilbert problem. In this section, we will consider a technique of solving singular integral equations, that is based on expanding the solution into the series over orthogonal polynomials on the contour L , since this technique is actively used in the following chapters. At the end of this section, we will also discuss the method of partial Wiener–Hopf factorization, which may significantly improve convergence of the numerical methods.

Speaking of numerical solutions of matrix Riemann–Hilbert problems, it would be unfair not to mention some other works. In the case when the contour L has a complex shape consisting of several arcs, lines, and rays joined together, an effective numerical Wiener–Hopf factorization can be achieved by special versions of the collocation method [33], [34], [63]. On another hand, an approximate Wiener–Hopf factorization of the matrix-coefficient A can be achieved by using Padè approximants, which was successfully employed for solving various Riemann–Hilbert problems [2], [3], [4].

2.3.1 Scalar Riemann–Hilbert problem on Riemann surface

Let us consider a Riemann–Hilbert problem (2.21) with 2×2 matrix-coefficient $A : \mathbb{R} \rightarrow \mathbb{C}^{2 \times 2}$ of the Chebotarev–Khrapkov class. Although it can be generalized for matrix-coefficients of size $N \times N$, $N > 2$, we will focus on the former case to demonstrate the technique.

In order to transform (2.21) into a scalar Riemann–Hilbert problem on a Riemann surface, we perform the spectral decomposition $A = VDV^{-1}$ of the Chebotarev–Khrapkov matrix-coefficient A . Since the matrix A is of the Chebotarev–Khrapkov class, it can be represented in the form

$$A = \alpha I + \beta J, \quad J = \begin{pmatrix} l & m \\ n & -l \end{pmatrix}$$

where α, β are Hölder continuous function on the real axis \mathbb{R} and l, m, n are entire functions in the complex plane \mathbb{C} . Let us assume that the components of the matrix J are polynomials (otherwise, the matrix J can be approximated; see, for instance, Padè approximants and Abrahams’ technique [3]). The eigenvalues of the matrix A have the form $\alpha \pm \beta w$, where

$w = \sqrt{l^2 + mn}$. In order to fix a single-valued branch of the square root, we cut the complex plane \mathbb{C} along the union Γ of curves connecting pairs of the branch points of the function w , such that $\Gamma \cap \mathbb{R} = \emptyset$. After computing the corresponding eigenvectors, we derive $A = VDV^{-1}$, where

$$D = \begin{pmatrix} \alpha + \beta w & 0 \\ 0 & \alpha - \beta w \end{pmatrix}, \quad V = \begin{pmatrix} 1 & 1 \\ \frac{w-l}{m} & \frac{n}{l-w} \end{pmatrix} \quad (2.29)$$

Notice that $\det V = -2w/m$. Therefore, if the function w is not identically zero on the real axis \mathbb{R} , then the eigenvectors of the matrix A are linearly independent and the spectral decomposition $A = VDV^{-1}$ exists with

$$V^{-1} = \frac{1}{2w} \begin{pmatrix} w+l & m \\ w-l & -m \end{pmatrix} \quad (2.30)$$

Consider now the vector Riemann–Hilbert problem with the condition (2.21). Replacing the matrix A by its spectral decomposition and multiplying the equation by V^{-1} on the left, we have

$$\Phi^+(t) = D(t)\Phi^-(t) + V^{-1}(t)B(t), \quad t \in \mathbb{R}$$

where $\Phi^\pm = V^{-1}F^\pm$. Since D is a diagonal matrix, the condition above is equivalent to two separate equations

$$\phi_j^+(t) = \lambda_j(t)\phi_j^-(t) + \mu(t), \quad j = 1, 2, \quad t \in \mathbb{R} \quad (2.31)$$

where the functions $\phi_{1,2}^\pm$ and $\mu_{1,2}$ are components of the vectors Φ^\pm and $V^{-1}B$ respectively, $\lambda_{1,2}$ are the diagonal elements of the matrix D . However, unlike F^\pm , components of the vectors Φ^\pm are not necessarily analytic in the half-planes \mathbb{C}^\pm . Moreover, they are multi-valued functions on the complex plane \mathbb{C} due to the presence of the function w in the matrix V^{-1} .

Above, we defined Γ to be the union of curves on the complex plane \mathbb{C} such that the function w is single-valued on $\mathbb{C} \setminus \Gamma$ and Γ does not intersect the contour L . Since components

of the vectors F^\pm are to be continuous across Γ , the vectors Φ^\pm have to satisfy the equations

$$V(t^+)\Phi(t^+) = V(t^-)\Phi(t^-), \quad t \in \Gamma \quad (2.32)$$

where t^+ stands for a limit of the corresponding function as $z \in \mathbb{C}$ approaches the point $t \in \Gamma$ while being on the left from Γ , and t^- stands for the limit as $z \rightarrow t$ while being on the right from Γ . Due to the property $\Delta(t^+) = -\Delta(t^-)$, and continuity of the functions l , m , and n across Γ , we compute

$$V^{-1}(t^+)V(t^-) = \begin{pmatrix} 0 & 1 \\ 1 & 0 \end{pmatrix}, \quad t \in \Gamma$$

After multiplying (2.32) by $V^{-1}(t^+)$ on the left and using the identity above, we conclude that the condition (2.32) is equivalent to

$$\phi_1(t^+) = \phi_2(t^-), \quad \phi_2(t^+) = \phi_1(t^-), \quad t \in \Gamma \quad (2.33)$$

Thus, the vector Riemann–Hilbert problem can be reduced to determining four functions $\phi_{1,2}^\pm : \mathbb{C}^\pm \setminus \Gamma \rightarrow \mathbb{C}$ that are analytic in $\mathbb{C}^\pm \setminus \Gamma$ respectively and satisfy the conditions (2.31) and (2.33).

The Riemann–Hilbert problem with the boundary conditions (2.31) and (2.33) can be transformed to a scalar Riemann–Hilbert problem on a Riemann surface. In order to do that, let us recall that w is an algebraic function since it satisfies the equation

$$w^2 = (z - z_1) \times \dots \times (z - z_n) \quad (2.34)$$

where z_1, \dots, z_n are the branch points of the function $w(z)$ (without loss of generality, we assume that w^2 is a monic polynomial). Let

$$g = \begin{cases} \frac{n}{2} - 1 & \text{if } n \text{ is even} \\ \frac{n-1}{2} & \text{if } n \text{ is odd} \end{cases}$$

and define the union $\Gamma = \Gamma_0 \cup \dots \cup \Gamma_g$ of open oriented smooth curves Γ_j connecting the points z_{2j+1} and z_{2j+2} respectively (if n is odd, Γ_g connects the point z_{2g+1} and infinity), such that $\Gamma_j \cap \Gamma_k = \emptyset$ for all $j \neq k$. It can be shown [36] that there are two branches of function $w(z)$ that are single-valued on $\overline{\mathbb{C}} \setminus \Gamma$, where $\overline{\mathbb{C}}$ is the extended complex plane (the Riemann sphere).

In order to construct a Riemann surface for the algebraic function w (such surface is called *hyperelliptic Riemann surface*), we consider two copies $(\overline{\mathbb{C}} \setminus \Gamma)_1$ and $(\overline{\mathbb{C}} \setminus \Gamma)_2$ of the extended complex plane $\overline{\mathbb{C}}$ with cuts along Γ , and then topologically identify the edges $\Gamma^\pm \in (\overline{\mathbb{C}} \setminus \Gamma)_1$ with the edges $\Gamma^\pm \in (\overline{\mathbb{C}} \setminus \Gamma)_2$ of the cuts on the first and second copies (see Figure 2.2). Assume w_1 and w_2 are the two different branches of the function w on $(\overline{\mathbb{C}} \setminus \Gamma)_1$ and $(\overline{\mathbb{C}} \setminus \Gamma)_2$, and define the point (z, w) of the Riemann surface \mathcal{R} as follows:

$$(z, w) = \begin{cases} (z, w_1) & \text{on } (\overline{\mathbb{C}} \setminus \Gamma)_1 \\ (z, w_2) & \text{on } (\overline{\mathbb{C}} \setminus \Gamma)_2 \end{cases}$$

Then the function $w : \mathbb{R} \rightarrow \overline{\mathbb{C}}$ defined by

$$w = \begin{cases} w_1(z) & \text{on } (\overline{\mathbb{C}} \setminus \Gamma)_1 \\ w_2(z) & \text{on } (\overline{\mathbb{C}} \setminus \Gamma)_2 \end{cases}$$

is analytic and single-valued on the constructed Riemann surface \mathcal{R} due to uniqueness of analytical continuation, since $w = w_1$ is analytic on $(\overline{\mathbb{C}} \setminus \Gamma)_1$, $w = w_2$ is analytic on $(\overline{\mathbb{C}} \setminus \Gamma)_2$, and w is continuous on Γ . The Riemann surface \mathbb{R} is of genus g and topologically equivalent to a sphere with g handles.

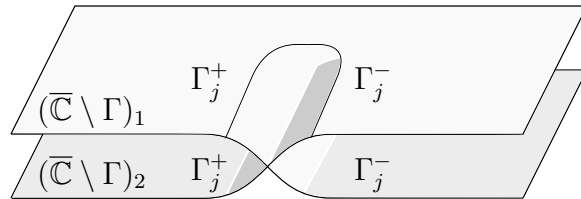


Figure 2.2: Connection between opposite edges of Γ_j , $j = 0, \dots, g$ on two copies of $\overline{\mathbb{C}} \setminus \Gamma$.

Let us derive a scalar Riemann–Hilbert problem on \mathbb{R} . On the Riemann surface \mathcal{R} , we define the following functions:

$$\phi^\pm(z, w) = \begin{cases} \phi_1^\pm(z) & \text{on } (\overline{\mathbb{C}} \setminus \Gamma)_1 \\ \phi_2^\pm(z) & \text{on } (\overline{\mathbb{C}} \setminus \Gamma)_2 \end{cases}, \quad \lambda(z, w) = \begin{cases} \lambda_1(z) & \text{on } (\overline{\mathbb{C}} \setminus \Gamma)_1 \\ \lambda_2(z) & \text{on } (\overline{\mathbb{C}} \setminus \Gamma)_2 \end{cases}$$

$$\mu(z, w) = \begin{cases} \mu_1(z) & \text{on } (\overline{\mathbb{C}} \setminus \Gamma)_1 \\ \mu_2(z) & \text{on } (\overline{\mathbb{C}} \setminus \Gamma)_2 \end{cases}$$

The functions $\phi^\pm : \mathcal{R} \rightarrow \overline{\mathbb{C}}$ are analytic and single-valued in the regions $\mathcal{D}^\pm = (\mathbb{C}^\pm \setminus \Gamma)_1 \cup (\mathbb{C}^\pm \setminus \Gamma)_2$ respectively, while they satisfy the boundary condition

$$\phi^+(t, w(t)) = \lambda(t, w(t))\phi^-(t, w(t)) + \mu(t, w(t)), \quad (t, w(t)) \in \mathcal{L} \quad (2.35)$$

due to (2.31), where \mathcal{L} is the union of two copies of the contour L on $(\overline{\mathbb{C}} \setminus \Gamma)_1$ and $(\overline{\mathbb{C}} \setminus \Gamma)_2$. Notice that the condition (2.32) is satisfied for any functions ϕ^\pm analytic in \mathcal{D}^\pm due to the identities

$$\phi_{1,2}(t^+) = \phi(t, w_{1,2}(t^+)) = \phi(t, w_{2,1}(t^-)) = \phi_{2,1}(t^-), \quad t \in \Gamma$$

Thus, the vector Riemann–Hilbert problem is reduced to a scalar Riemann–Hilbert problem on the Riemann surface \mathcal{R} of determining two functions $\phi^\pm : \mathcal{D}^\pm \rightarrow \mathbb{C}$ analytic in \mathcal{D}^\pm and satisfying the boundary condition (2.35) on the contour $\mathcal{L} \subset \mathcal{R}$.

A thorough study of the Riemann–Hilbert problem on a compact Riemann surface was given by È.I. Zverovič in his work [87]. Here, we highlight the major differences between the problems on the complex plane and a Riemann surface.

The key element in constructing the solution of a Riemann–Hilbert problem on the complex plane \mathbb{C} , is the Cauchy integral with kernel

$$\frac{dt}{t - z}$$

In the framework of the theory of Riemann surfaces [36], this kernel has the following properties: (i) as a function of z , the kernel is holomorphic everywhere on $\overline{\mathbb{C}}$ except a single pole

at $z = t$ and a single zero at $z = \infty$; (ii) as a function of t , the kernel is an abelian differential (meromorphic one-form) of the third kind [36] with two poles $t = z$ and $t = \infty$ with the corresponding residues 1 and -1 .

Unfortunately, the kernel with the properties (i) and (ii) does not exist on a Riemann surface of genus $g > 1$, which follows from the Riemann-Roch theorem [36]. More specifically, there is no way to satisfy the property (i). Instead, let us find an analogue of the Cauchy integral with the property (ii) only. An algorithm for constructing such a kernel was given by Karl Weierstrass. The result of that algorithm applied in the hyper-elliptic case (that is, when an algebraic function $w(z)$ of the Riemann surface \mathcal{R} is the square root of a polynomial) is the differential

$$d\mathcal{W} = \frac{w(z) + w(t)}{2w(t)} \cdot \frac{dt}{t - z} \quad (2.36)$$

Properties of the kernel $d\mathcal{W}$:

1. As a function of $(t, w(t))$, the differential $d\mathcal{W}$ is an abelian differential of the third kind with three poles at the points $(z, w(z))$, $(\infty, w_1(\infty))$, and $(\infty, \Delta_2(\infty))$, where $w_{1,2}$ are two different single-valued branches of the algebraic function w . Indeed,

$$\begin{aligned} d\mathcal{W} &= \frac{dt}{t - z} + \text{regular terms}, & \text{as } (t, w(t)) \rightarrow (z, w(z)) \\ d\mathcal{W} &\sim \frac{1}{2} \frac{d\tau}{\tau}, \quad \tau = \frac{1}{t}, & \text{as } (t, w(t)) \rightarrow (\infty, w_{1,2}(\infty)) \end{aligned} \quad (2.37)$$

2. As a function of $(z, w(z))$, the differential $d\mathcal{W}$ is a meromorphic function on \mathcal{R} with a simple pole at $(t, w(t))$ and two poles at the points $(\infty, w_{1,2}(\infty))$:

$$\begin{aligned} d\mathcal{W} &= \frac{dt}{t - z} + \text{regular terms}, & \text{as } (z, \Delta(z)) \rightarrow (t, \Delta(t)) \\ d\mathcal{W} &\sim O(z^g) \frac{dt}{w(t)}, & \text{as } (z, \Delta(z)) \rightarrow (\infty, \Delta_{1,2}(\infty)) \end{aligned} \quad (2.38)$$

Let us show that using the kernel $d\mathcal{W}$, we can construct solution of the Riemann–Hilbert problem (2.35). As on the complex plane \mathbb{C} , the first step is to derive Wiener–Hopf decom-

position of the coefficient of the problem,

$$\lambda(t, w(t)) = \frac{\lambda^+(t, w(t))}{\lambda^-(t, w(t))}, \quad t \in \mathcal{L} \quad (2.39)$$

where $\lambda^\pm : \mathcal{D}^\pm \rightarrow \mathbb{C}$ are analytic functions in \mathcal{D}^\pm that are bounded at infinity $(\infty, w_{1,2}(\infty))$.

Theorem 2.14. If \mathcal{R} is a compact hyper-elliptic Riemann surface glued of two sheets of the complex plane, and the function $\lambda : \mathcal{L} \rightarrow \mathbb{C}$ is Hölder continuous on the contour $\mathcal{L} \subset \mathcal{R}$, then there exist g points $(z_j, w(z_j)) \in \mathcal{R}$ and integers $m_j, n_j \in \mathbb{Z}$, $j = 1, \dots, g$, such that the equation (2.39) holds on the contour \mathcal{L} for the functions $\lambda^\pm : \mathcal{D}^\pm \rightarrow \mathbb{C}$ bounded at infinity $(\infty, w_{1,2}(\infty))$, that are defined by

$$\begin{aligned} \lambda^\pm(z, w(z)) &= \exp\{\chi^\pm(z, w(z))\}, \quad (z, w(z)) \in \mathcal{D}^\pm, \\ \chi^\pm(z, w(z)) &= \frac{1}{2\pi i} \int_{\mathcal{L}} \ln \lambda(t, w(t)) d\mathcal{W} \\ &\quad + \sum_{j=1}^g \left(\int_{(z_0, w(z_0))}^{(z_j, w(z_j))} + m_j \int_{a_j} + n_j \int_{b_j} \right) d\mathcal{W} \end{aligned} \quad (2.40)$$

where $d\mathcal{W}$ is the Weierstrass kernel (2.36), a_j and b_j are the canonical homology basis (see Figure 2.3) of \mathcal{R} , that does not intersect the contour \mathcal{L} .

Proof. First, let us show that the function $\lambda^\pm : \mathcal{D}^\pm \rightarrow \mathbb{C}$ defined in (2.40) satisfy the equation (2.39). Due to the first property in (2.37), the differential $d\mathcal{W}$ behaves like $dt/(t - z)$ as $(t, w(t)) \rightarrow (z, w(z))$. Therefore the Sokhotsky–Plemelj formulas are applicable to the integral over \mathcal{L} in (2.40) if we replace $dt/(t - z)$ by $d\mathcal{W}$ in the identities (2.9). Since the curves Γ_j ,

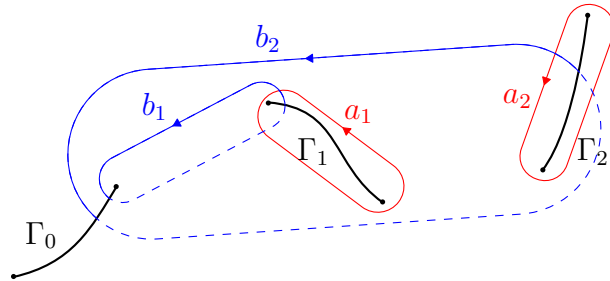


Figure 2.3: Canonical homology basis $a_{1,2}$ and $b_{1,2}$ on the hyper-elliptic Riemann surface of genus 2. Dashed lines denote curves on the second sheet of the surface.

a_j , and b_j have no common points with the contour \mathcal{L} , the integrals over these curves are continuous across \mathcal{L} . Thus

$$\chi^+(z, w(z)) - \chi^-(z, w(z)) = \ln \lambda(z, w(z)), \quad z_0 \in \mathcal{L}$$

which implies the formula (2.39).

We also need to show that the functions λ^\pm are bounded at infinity points $(\infty, w_{1,2}(\infty))$. Due to the second property in (2.38), the differential $d\mathcal{W}$ may grow at infinity points as $O(z^g)$. However, it is possible to choose the integers m_j and n_j in the formula (2.40) so that to cancel the growth. Let us analyze the behavior of the differential $d\mathcal{W}$ at infinity. Since for any t and z , we have

$$\frac{1}{t-z} = -\frac{1}{z} - \frac{t}{z^2} - \dots - \frac{t^{g-1}}{z^g} + \frac{t^g}{z^g(t-z)}$$

we can rewrite $d\mathcal{W}$ in the form

$$d\mathcal{W} = -\frac{1}{2} \sum_{j=1}^g \frac{\Delta(z)}{z^j} \frac{t^{j-1} dt}{\Delta(t)} + \frac{1}{2} \left(\frac{\Delta(z)}{z^g} \frac{t^g}{\Delta(t)} + 1 \right) \frac{dt}{t-z}$$

Notice that the last term in the right-hand side is bounded at the infinite points $(\infty, w_{1,2}(\infty))$ since the function $w(z)$ may grow at most like z^g . Hence, in order to make the function $\chi^\pm(z, w(z))$ bounded at infinity, we have to satisfy the following g equations

$$\frac{1}{2\pi i} \int_{\mathcal{L}} \ln \lambda(t, w(t)) \frac{t^{k-1} dt}{w(t)} + \sum_{j=1}^g \left(\int_{(z_0, w(z_0))}^{(z_j, w(z_j))} + m_j \int_{a_j} + n_j \int_{b_j} \right) \frac{t^{k-1} dt}{w(t)} = 0$$

$$k = 1, \dots, g$$

Given the values of the first inetgral, the homology basis a_j , b_j , and the point $(z_0, w(z_0))$, these equations uniquely determine the points $(z_j, w(z_j)) \in \mathcal{R}$ and the integers m_j , n_j ($j = 1, \dots, g$), which can be found by solving the Jacobi inverse problem [87].

Finally, the functions λ^\pm are continuous on the contours of integration of the integrals

$$\int_{(z_0, w(z_0))}^{(z_j, w(z_j))} d\mathcal{W}, \quad \int_{a_j} d\mathcal{W}, \quad \text{and} \quad \int_{b_j} d\mathcal{W} \quad (2.41)$$

since the Sokhotsky–Plemelj formulas and the definition (2.36) imply that the integrals, as functions of $(z, w(z))$, have jumps on the contours of integration, which are equal to $2\pi i$. Therefore the functions λ^\pm containing exponents of the integrals (2.41) is continuous on the contours of integration. \square

The second and third steps of constructing solution of a Riemann–Hilbert problem on a Riemann surface \mathcal{R} is similar to the one on the complex plane \mathbb{C} . On the second step, we define the function

$$\psi^\pm(z, w(z)) = \int_{\mathcal{L}} \frac{\mu(t, w(t))}{\lambda^\pm(t, w(t))} dW, \quad (z, w(z)) \in \mathcal{D}^\pm \quad (2.42)$$

which satisfies the equation $\psi^+ - \psi^- = \mu/\lambda^+$ on the contour \mathcal{L} . After multiplying the equation (2.35) by $1/\lambda^+$ and using the representations (2.39) and (2.42), we derive the equation

$$\frac{\phi^+(t, w(t))}{\lambda^+(t, w(t))} - \psi^+(t, w(t)) = \frac{\phi^-(t, w(t))}{\lambda^-(t, w(t))} - \psi^-(t, w(t)), \quad (t, w(t)) \in \mathcal{L}$$

On the third step, we define the function $P : \mathcal{R} \rightarrow \mathbb{C}$ by the formula

$$P(z, w(z)) = \begin{cases} \frac{\phi^+(z, w(z))}{\lambda^+(z, w(z))} - \psi^+(z, w(z)), & (z, w(z)) \in \mathcal{D}^+ \\ \frac{\phi^-(z, w(z))}{\lambda^-(z, w(z))} - \psi^-(z, w(z)), & (z, w(z)) \in \mathcal{D}^- \end{cases}$$

The function $P(z, w(z))$ is meromorphic on the Riemann surface \mathcal{R} and can be determined by Liouville's theorem.

Thus, the solution of the Riemann–Hilbert problem (2.35) is given by

$$\phi^\pm(z, w(z)) = \lambda^\pm(z, w(z)) [P(z, w(z)) + \psi^\pm(z, w(z))], \quad (z, w(z)) \in \mathcal{D}^\pm \quad (2.43)$$

From (2.43), we can recover the solution of the vector Riemann–Hilbert problem (2.21):

$$F^\pm(z) = V(z, w_1(z)) \cdot \begin{pmatrix} \phi_1^\pm(z) \\ \phi_2^\pm(z) \end{pmatrix}$$

$$\phi_j^\pm(z) = \lambda^\pm(z, w_j(z)) [P(z, w_j(z)) + \psi^\pm(z, w_j(z))], \quad j = 1, 2$$

where $w_1(z)$ and $w_2(z)$ are the two branches of the function $w(z)$, and the matrix $V(z, w_1(z))$ is defined in (2.29) with w replaces by $w_1(z)$.

2.3.2 Gauss–Jacobi quadrature rule

In order to transform a vector Riemann–Hilbert problem into a system of singular integral equations, we apply the inverse Fourier transform to the equation (2.21). Let us define the inverse Fourier transform by the formula

$$\mathcal{F}(x) = \frac{1}{2\pi} \int_{\mathbb{R}} F(t) e^{-itx} dt, \quad x \in \mathbb{R}$$

as a component-wise operator on vectors F^{\pm} , B and matrix A in (2.21) with the corresponding transforms denoted by \mathcal{F}^{\pm} , \mathcal{B} and \mathcal{A} . After applying the transform to (2.21) and using the convolution theorem, we derive the equation

$$\mathcal{F}^+(x) = \int_{\mathbb{R}} \mathcal{A}(x - \xi) \mathcal{F}^-(\xi) d\xi + \mathcal{B}(x), \quad x \in \mathbb{R} \quad (2.44)$$

Since the components of the vector F^+ are to be analytic in the upper half-plane \mathbb{C}^+ , it immediately follows from the Cauchy integral theorem that $\mathcal{F}^+(x) = 0$ for all $x < 0$. Similarly, since components of F^- are to be analytic in the lower half-plane \mathbb{C}^- , we have $\mathcal{F}^-(x) = 0$ for all $x > 0$. Thus, considering the equation (2.44) for negative values of x , we derive the integral equation with respect to the vector \mathcal{F}^- ,

$$0 = \int_{-\infty}^0 \mathcal{A}(x - \xi) \mathcal{F}^-(\xi) d\xi + \mathcal{B}(x), \quad x < 0 \quad (2.45)$$

Then, given \mathcal{F}^- , we can determine \mathcal{F}^+ from the equation (2.44) considered for positive values of x .

Let us notice that if the matrix $A(t)$ takes different limits as $t \rightarrow \infty$ and $t \rightarrow -\infty$ (i.e. $\lim_{t \rightarrow -\infty} A(t) \neq \lim_{t \rightarrow \infty} A(t)$), its inverse Fourier transform $\mathcal{A}(x)$ contains the term $1/x$. Thus, (2.45) is a system of singular integral equation with the Cauchy kernel $1/(x - \xi)$.

Thus, we transformed a vector Riemann–Hilbert problem (2.21) to a system of singular integral equations (2.45) with the Cauchy kernel. Let us consider a method of solving those singular integral equations. Notice that the interval $(-\infty, 0)$ of the equation (2.45) is homeomorphic to a finite interval $(-1, 1)$. We will make two changes to the equation (2.45): (i)

replace the interval $(-\infty, 0)$ by the interval $(-1, 1)$ and (ii) consider a scalar case (however, the method can be easily generalized to a system of singular integral equations; see Chapter 4). Thus, we consider the scalar equation

$$af(x) + \frac{b}{\pi} P.V. \int_{-1}^1 \frac{f(t)}{t-x} dt + \int_{-1}^1 k(x, t) f(t) dt = g(x), \quad -1 < x < 1 \quad (2.46)$$

where a, b are constants, g is a Hölder continuous function on the interval $[-1, 1]$.

Let us find numerical approximation of the solution f that is Hölder continuous on $(-1, 1)$, and at the end of the interval it behaves as follows:

$$f(x) = O(|1-x|^\alpha) \quad \text{as } x \rightarrow 1, \quad f(x) = O(|1+x|^\beta) \quad \text{as } x \rightarrow -1 \quad (2.47)$$

Existence and uniqueness of the Hölder continuous solution of (2.46) were proved in the monograph [61] by studying existence and uniqueness of the solution of a scalar Riemann–Hilbert problem that is equivalent to the dominant part of (2.46). The result of the study is that there exists solution of the singular integral equation (2.46) in one of the following classes of Hölder continuous functions on $(-1, 1)$:

1. Class of functions bounded at the end points of the interval $(-1, 1)$ satisfying (2.47) with $0 < \alpha < 1$ and $\beta = 1 - \alpha$;
2. Class of functions having an integrable discontinuity only at the point $x = 1$ and satisfying (2.47) with $-1 < \alpha < 0$ and $\beta = -\alpha$;
3. Class of functions having an integrable discontinuity only at the point $x = -1$ and satisfying (2.47) with $0 < \alpha < 1$ and $\beta = -\alpha$;
4. Class of functions having integrable discontinuities at both end-points and satisfying (2.47) with $-1 < \alpha < 0$ and $\beta = -1 - \alpha$.

Erdogan and Gupta [35] have shown that the integral equation (2.46) can be solved using the Gauss–Jacobi quadrature rule. By using the orthogonality property of the Jacobi

polynomials $P_j^{(\alpha, \beta)}$ on the interval $[-1, 1]$, we represent solution of the equation (2.46) in the form

$$f(x) = w(x) \sum_{j=0}^{\infty} f_j P_j^{(\alpha, \beta)}(x) \quad (2.48)$$

where $w(x) = (1-x)^\alpha(1+x)^\beta$. From the classes of the solution listed above, it follows that the sum $\alpha + \beta$ always takes one of the values $-1, 0$, or 1 . In either case, the Jacobi polynomials satisfy the following relations [76], [78] on the interval $(-1, 1)$:

$$\begin{aligned} \frac{1}{\pi} P.V. \int_{-1}^1 \frac{P_n^{(\alpha, \beta)}(t)}{t-x} w(t) dt &= -\frac{a}{b} w(x) P_n^{(\alpha, \beta)}(x) - \frac{2^{\alpha+\beta}}{\sin(\pi\alpha)} P_{n+\alpha+\beta}^{(-\alpha, -\beta)}(x) \\ \int_{-1}^1 P_n^{(\alpha, \beta)}(t) P_m^{(\alpha, \beta)}(t) w(t) dt &= \begin{cases} 0 & \text{if } n \neq m \\ \theta_n & \text{if } n = m \end{cases} \\ \theta_n &= \frac{2^{1+\alpha+\beta}}{2n+1+\alpha+\beta} \frac{\Gamma(n+\alpha+1)\Gamma(n+\beta+1)}{n!\Gamma(n+1+\alpha+\beta)} \end{aligned} \quad (2.49)$$

where Γ is the Gamma-function. Thus, after substituting the representation (2.48) into the equation (2.46) and applying the first relation in (2.49), we derive the equation for $x \in (-1, 1)$

$$\sum_{j=0}^{\infty} f_j \left(-b \frac{2^{\alpha+\beta}}{\sin(\pi\alpha)} P_{j+\alpha+\beta}^{(-\alpha, -\beta)}(x) + \int_{-1}^1 k(x, t) P_j^{\alpha, \beta}(t) w(t) dt \right) = g(x) \quad (2.50)$$

In order to make use of the second relation in (2.49), we multiply the equation by $P_k^{(-\alpha, -\beta)}(x) w(x)$ for $k = 0, 1, \dots$ and integrate in x -variable over the interval $(-1, 1)$. Then the integral of the first term in the parenthesis in (2.50) vanishes for all $j \neq k$. The truncated version of the system takes the form

$$\begin{aligned} -b \frac{2^{\alpha+\beta}}{\sin(\pi\alpha)} \theta_k f_{k-\alpha-\beta} + \sum_{j=0}^M d_{jk} f_j &= g_k, \quad k = 0, \dots, M \\ d_{jk} &= \int_{-1}^1 \int_{-1}^1 k(x, t) P_j^{(\alpha, \beta)}(t) P_{k+\alpha+\beta}^{(-\alpha, -\beta)}(x) w(t) w^{-1}(x) dt dx \\ g_k &= \int_{-1}^1 g(x) P_{k+\alpha+\beta}^{(-\alpha, -\beta)}(x) w^{-1}(x) dx \end{aligned} \quad (2.51)$$

In the case $\alpha + \beta = 0$, the equations of the system (2.51) give unique solution for $M+1$ unknown variables f_0, \dots, f_M . If $\alpha + \beta = 1$, then the first term in (2.51) for $k = 0$, should

vanish because of the orthogonality of $P_0^{(-\alpha, -\beta)}$ and $P_{j+1}^{(-\alpha, -\beta)}$, $j = 0, 1, \dots$; thus, in the case $\alpha + \beta = 1$, we solve the system (2.51) for $M + 1$ unknown variables f_0, \dots, f_M provided $f_{-1} = 0$. If $\alpha + \beta = -1$, then there are $M + 2$ unknown variables f_0, \dots, f_{M+2} but only $M + 1$ equations given by (2.51); thus, the solution is not unique. In this case, we use one more equation that is provided by the compatibility condition

$$\int_{-1}^1 f(t) dt = f_c$$

which, after substitution of the representation (2.48) and using orthogonality of $P_j^{(\alpha, \beta)}$, takes the form $f_0 \theta_0 = f_c$.

Notice that if we seek the solution bounded at the end-points, we can choose $\alpha = \beta = 0$, then the Jacobi polynomials become Legendre polynomials. If we seek the solution vanishing at the end-points, we can choose $\alpha = \beta = 1/2$, then the Jacobi polynomials becomes Chebyshev polynomials. In Chapter 4, we will consider the case $\alpha = -\beta = 1/2$.

2.3.3 Partial Wiener–Hopf Factorization

In this section, we will consider two applications of partial Wiener–Hopf factorization. In the first application, the partial factorization will be used in order to derive a vector Riemann–Hilbert problem suitable for numerical algorithms and ensure a good convergence. In the second application, a new algorithm of constructing an approximate solution of a vector Riemann–Hilbert problem with the matrix-coefficient that is not of the Chebotarev–Khrapkov class, will be discussed. That algorithm finds a numerical approximation to the solution of the Riemann–Hilbert problem by reducing it to a system of linear equations.

Application I. Although the technique described in the previous section can be applied to any invertible matrix A and any vector B whose components are Hölder continuous functions on the real axis \mathbb{R} and satisfy the condition bounded at infinity, the convergence rate of the series (2.48) and the truncated system (2.51) may not be satisfactory for numerical estimation of the solution of a Riemann–Hilbert problem.

In Chapter 5, we will consider a problem with the matrix $\mathcal{A}(x)$, the inverse Fourier transform of the matrix $A(t)$, can be represented as follows:

$$\mathcal{A}(x) = \gamma \cdot \coth x + \mathcal{A}^\circ(x), \quad x \in \mathbb{R}$$

where γ is a constant diagonal matrix and $\mathcal{A}^\circ(x)$ is a matrix-function with components that vanish as $x \rightarrow \pm\infty$ and diagonal elements that have a logarithmic singularity at the point $x = 0$. Since the singular kernel $\coth x$ does not vanish at infinity and \mathcal{A}° has a logarithmic singularity, straightforward application of the technique from Section 2.3.2 was found extremely time-consuming. In Chapter 5, the partial Wiener–Hopf factorization was used. Since only the diagonal elements contribute to the “bad” behavior of the matrix \mathcal{A} , constructing Wiener–Hopf factorization for the diagonal elements of the matrix-coefficient A before transforming the Riemann–Hilbert problem to a system of singular integral equations leads to significant improvements in the rate of convergence of numerical solution.

A thorough description of this method will be given in Chapter 5. Here, let us highlight its key parts. Consider the Riemann–Hilbert problem (2.21) with 2×2 matrix-coefficient $A(t)$ with Hölder continuous components $a_{jk}(t)$, $i, j = 1, 2$, that have the following behavior:

1. At infinity, the diagonal components $a_{11}(t)$ and $a_{22}(t)$ converge to non-zero values, while the off-diagonal elements exponentially vanish as $t \rightarrow \pm\infty$;
2. At the origin, the diagonal components $a_{11}(t)$ and $a_{22}(t)$ have simple poles $t = 0$, while the off-diagonal elements are continuous in its neighborhood.

We seek the vector-functions $F^\pm : \mathbb{C}^\pm \rightarrow \mathbb{C}^2$ whose components are analytic in \mathbb{C}^\pm , bounded at infinity, and satisfy the equation (2.21) on the real axis \mathbb{R} .

First, let us find Wiener–Hopf decomposition for the diagonal elements of the matrix A ,

$$a_{jj}(t) = \frac{a_{jj}^+(t)}{a_{jj}^-(t)}, \quad t \in \mathbb{R}, \quad j = 1, 2$$

This can be done analytically, using the Cauchy integral and Sokhotski–Plemelj formulas (see Section 2.1.2). Then the Riemann–Hilbert problem (2.21) can be represented in the form

$$\begin{pmatrix} f_1^+/a_{11}^+ \\ f_2^+/a_{22}^+ \end{pmatrix} = \begin{pmatrix} 1 & a_{12}a_{22}^-/a_{11}^+ \\ a_{21}a_{11}^-/a_{22}^+ & 1 \end{pmatrix} \begin{pmatrix} f_1^-/a_{11}^- \\ f_2^-/a_{22}^- \end{pmatrix} + \begin{pmatrix} b_1/a_{11}^+ \\ b_2/a_{22}^+ \end{pmatrix} \quad \text{on } \mathbb{R}$$

Notice that the new matrix-coefficient has no singular points on the real axis \mathbb{R} and equal to the unitary matrix I at infinity, while the new unknown vectors are analytic in \mathbb{C}^+ and \mathbb{C}^- respectively and bounded at infinity since the elements of the Wiener–Hopf decomposition $a_{11}^\pm(z)$ and $a_{22}^\pm(z)$ does not vanish as $z \rightarrow \infty$. In this form, the Riemann–Hilbert problem can be easily transformed to non-singular integral equation and solved numerically. See Chapter 5 for more detailed analysis of this technique.

Application II. Let us consider a Riemann–Hilbert problem (2.21) with 2×2 matrix-coefficient A that is not of the form (2.28). If we construct LDU-decomposition of the matrix A , then the equation (2.21) can be rewritten as follows:

$$L^{-1}F^+ = DUF^- + L^{-1}B, \quad \text{on } \mathbb{R} \quad (2.52)$$

Here, L is the lower triangular matrix, D is the diagonal matrix, and U is the upper triangular matrix given by

$$L = \begin{pmatrix} 1 & 0 \\ a_{21}/a_{11} & 1 \end{pmatrix}, \quad D = \begin{pmatrix} a_{11} & 0 \\ 0 & a_{22} - a_{12}a_{21}/a_{11} \end{pmatrix}, \quad U = \begin{pmatrix} 1 & a_{12}/a_{11} \\ 0 & 1 \end{pmatrix}$$

Since the matrix D is diagonal it can be easily factorized, $D = D^+[D^-]$ on the real axis \mathbb{R} , where

$$D^\pm(z) = \begin{pmatrix} d_1^\pm(z) & 0 \\ 0 & d_2^\pm(z) \end{pmatrix}, \quad z \in \mathbb{C}^\pm$$

and d_1^\pm, d_2^\pm are the elements of the Wiener–Hopf factorization of each diagonal component of the matrix D ; that is, $a_{11} = d_1^+/d_1^-$ on \mathbb{R} , and $a_{22} - a_{12}a_{21}/a_{11} = d_2^+/d_2^-$ on \mathbb{R} . Such

factorization is always exists provided the functions a_{11} and $a_{22} - a_{12}a_{21}/a_{11}$ are Hölder continuous on the real axis \mathbb{R} . After substituting the Wiener–Hopf factorization, the equation (2.52) takes the form

$$[D^+]^{-1}L^{-1}F^+ = D^-UF^- + [D^+]^{-1}L^{-1}B \quad \text{on } \mathbb{R} \quad (2.53)$$

After introducing the vector

$$\Psi^\pm(z) = \frac{1}{2\pi i} \int_{\mathbb{R}} [D^+(t)]^{-1}L^{-1}(t)B(t) \frac{dt}{t-z}, \quad z \in \mathbb{C}^\pm$$

that satisfies the equation $\Psi^+ - \Psi^- = [D^+]^{-1}L^{-1}B$ on \mathbb{R} , the condition (2.53) becomes

$$[D^+]^{-1}L^{-1}F^+ - \Psi^+ = D^-UF^- - \Psi^- \quad \text{on } \mathbb{R} \quad (2.54)$$

Finally, we consider the vector $P : \mathbb{C} \rightarrow \mathbb{C}^2$ defined as follows:

$$P(z) = \begin{cases} [D^+(z)]^{-1}L^{-1}(z)F^+(z) - \Psi^+(z), & z \in \mathbb{C}^+ \\ [D^-(z)]^{-1}U(z)F^-(z) - \Psi^-(z), & z \in \mathbb{C}^- \end{cases} \quad (2.55)$$

Let us analyze singularities of the vector in order to determine its form. First, vector P is continuous across the real axis \mathbb{R} due to the equation (2.54). After substituting definitions of the matrices in (2.55), the components of the vector P in the upper half-plane \mathbb{C}^+ are defined as follows:

$$\begin{pmatrix} p_1 \\ p_2 \end{pmatrix} = \begin{pmatrix} 1/d_1^+ & 0 \\ 0 & 1/d_2^+ \end{pmatrix} \begin{pmatrix} 1 & 0 \\ -a_{21}/a_{11} & 1 \end{pmatrix} \begin{pmatrix} f_1^+ \\ f_2^+ \end{pmatrix} - \begin{pmatrix} b_1^+ \\ b_2^+ \end{pmatrix} \quad (2.56)$$

which implies that the components p_1 is analytic in \mathbb{C}^+ , while the component p_2 has singularities in \mathbb{C}^- due to the factor a_{21}/a_{11} . In the lower half-plane, the components of the vector P are defined by

$$\begin{pmatrix} p_1 \\ p_2 \end{pmatrix} = \begin{pmatrix} 1/d_1^- & 0 \\ 0 & 1/d_2^- \end{pmatrix} \begin{pmatrix} 1 & a_{12}/a_{11} \\ 0 & 1 \end{pmatrix} \begin{pmatrix} f_1^- \\ f_2^- \end{pmatrix} - \begin{pmatrix} b_1^- \\ b_2^- \end{pmatrix} \quad (2.57)$$

Thus, the component p_1 has singularities in \mathbb{C}^- due to the factor a_{12}/a_{11} , while the component p_2 is analytic in \mathbb{C}^- . For simplicity, assume that the vector P is bounded at infinity, and the factors a_{21}/a_{11} and a_{12}/a_{11} are meromorphic functions on the complex plane \mathbb{C} with only simple poles. In this case, Liouville's theorem [41] implies that

$$\begin{aligned} p_1(z) &= \sum_{\zeta' \in \mathcal{Z}^-} \frac{1}{z - \zeta'} \frac{f_2^-(\zeta')}{d_1^-(\zeta')} \operatorname{res}_{\zeta'} \frac{a_{12}}{a_{11}} \\ p_2(z) &= \sum_{\zeta'' \in \mathcal{Z}^+} \frac{1}{\zeta'' - z} \frac{f_1^+(\zeta'')}{d_2^+(\zeta'')} \operatorname{res}_{\zeta''} \frac{a_{21}}{a_{11}} \end{aligned} \quad (2.58)$$

where \mathcal{Z}^- are the set of poles of the function a_{12}/a_{11} in the lower half-plane \mathbb{C}^- , and \mathcal{Z}^+ is the set of poles of the function a_{21}/a_{11} in the upper half-plane \mathbb{C}^+ . If at least one of \mathcal{Z}^\pm is an infinite set, then the only possible limit point for the elements of those sets is infinity $\zeta = \infty$ (otherwise, components of the matrix A are not meromorphic functions). Thus, the corresponding series in (2.58) is absolutely convergent if

$$\left\{ \frac{f_2^-(\zeta')}{d_1^-(\zeta')} \operatorname{res}_{\zeta'} \frac{a_{12}}{a_{11}} \right\}_{\zeta' \in \mathcal{Z}^-} \quad \text{and} \quad \left\{ \frac{f_1^+(\zeta'')}{d_2^+(\zeta'')} \operatorname{res}_{\zeta''} \frac{a_{21}}{a_{11}} \right\}_{\zeta'' \in \mathcal{Z}^+}$$

are l_p -sequences for $0 \leq p < \infty$, which can be provided, for instance, by requiring the components of the vector-functions F^\pm to vanish at infinity and the off-diagonal components of the matrix-function A to grow slower at infinity than its diagonal components.

In order to find the values $f_1^+(\zeta'')$ and $f_2^-(\zeta')$ in the series (2.58), we use the formulas (2.56) and (2.57) once again. It follows from the identities (2.56) and (2.58) that

$$p_1(\zeta'') = \frac{f_1^+(\zeta'')}{d_1^+(\zeta'')} - b_1^+(\zeta'') = \sum_{\zeta' \in \mathcal{Z}^-} \frac{1}{\zeta'' - \zeta'} \frac{f_2^-(\zeta')}{d_1^-(\zeta')} \operatorname{res}_{\zeta'} \frac{a_{12}}{a_{11}}, \quad \zeta'' \in \mathcal{Z}^+$$

Similarly, from the identities (2.57) and (2.58), we derive

$$p_2(\zeta') = \frac{f_2^-(\zeta')}{d_2^-(\zeta')} - b_2^-(\zeta') = \sum_{\zeta'' \in \mathcal{Z}^+} \frac{1}{\zeta'' - \zeta'} \frac{f_1^+(\zeta'')}{d_2^+(\zeta'')} \operatorname{res}_{\zeta''} \frac{a_{21}}{a_{11}}, \quad \zeta' \in \mathcal{Z}^-$$

The last two equations can be written in the vector form $\mathbf{f} + \mathfrak{A} \cdot \mathbf{f} = \mathbf{b}$, where \mathbf{f} and \mathbf{b} are the infinite sequences and \mathfrak{A} is the operator defined by

$$\mathbf{f} = \begin{pmatrix} f_1^+(\zeta_1'') \\ f_2^-(\zeta_1') \\ f_1^+(\zeta_2'') \\ f_2^-(\zeta_2') \\ \vdots \end{pmatrix}, \quad \mathfrak{A} = \begin{pmatrix} 0 & \mathfrak{a}_{11}^1 & 0 & \mathfrak{a}_{12}^1 & \cdots \\ \mathfrak{a}_{11}^2 & 0 & \mathfrak{a}_{12}^2 & 0 & \cdots \\ 0 & \mathfrak{a}_{21}^1 & 0 & \mathfrak{a}_{22}^1 & \cdots \\ \mathfrak{a}_{21}^2 & 0 & \mathfrak{a}_{22}^2 & 0 & \cdots \\ \vdots & \vdots & \vdots & \vdots & \ddots \end{pmatrix}, \quad \mathbf{b} = \begin{pmatrix} d_1^+(\zeta_1'')b_1^+(\zeta_1'') \\ d_2^-(\zeta_1')b_2^-(\zeta_1') \\ d_1^+(\zeta_2'')b_1^+(\zeta_2'') \\ d_2^-(\zeta_2')b_2^-(\zeta_2') \\ \vdots \end{pmatrix}$$

$$\mathfrak{a}_{jk}^1 = \frac{1}{\zeta_j' - \zeta_k''} \frac{d_1^+(\zeta_k'')}{d_1^-(\zeta_j')} \operatorname{res}_{\zeta_j'} \frac{a_{12}}{a_{11}}, \quad \mathfrak{a}_{jk}^2 = \frac{1}{\zeta_j' - \zeta_k''} \frac{d_2^-(\zeta_j')}{d_2^+(\zeta_k'')} \operatorname{res}_{\zeta_k''} \frac{a_{21}}{a_{11}}$$

$$\zeta_j' \in \mathcal{Z}^-, \quad \zeta_k'' \in \mathcal{Z}^+, \quad j, k = 1, 2, 3, \dots$$

Denote l_∞ the space of bounded sequences. Recall [72] that the equation $T \cdot x = v$ has a unique l_∞ solution if $v \in l_\infty$ and the operator $T = \{t_{jk}\}$ satisfies the conditions

1. There exists a $\eta > 0$ such that

$$|t_{jj}| \geq \eta \quad \forall j = 1, 2, 3, \dots \quad (2.59)$$

2. There exists a $\sigma \in [0, 1)$ such that

$$\sum_{k=1, k \neq j}^{\infty} |t_{jk}| = \sigma_j |t_{jj}| \quad (2.60)$$

where $0 \leq \sigma_j \leq \sigma < 1$ for all $j = 1, 2, 3, \dots$

Moreover, the solution x satisfies the inequality $\|x\| \leq [\eta(1 - \sigma)]^{-1} \|v\|$.

Let us consider existence and uniqueness of the solution of the system $\mathbf{f} + \mathfrak{A} \cdot \mathbf{f} = \mathbf{b}$ with the operator \mathfrak{A} defined above. Notice that the operator $\mathfrak{I} + \mathfrak{A}$, where \mathfrak{I} is the identity operator, contains only the value 1 on its main diagonal; thus the first condition (2.59) is satisfied with $\eta = 1$. In order to satisfy the condition (2.60), the following identities have to hold

$$\sum_{k=1}^{\infty} \left| \frac{1}{\zeta_j' - \zeta_k''} \frac{d_1^+(\zeta_k'')}{d_1^-(\zeta_j')} \operatorname{res}_{\zeta_j'} \frac{a_{12}}{a_{11}} \right| = \sigma_j^1, \quad \sum_{k=1}^{\infty} \left| \frac{1}{\zeta_j' - \zeta_k''} \frac{d_2^-(\zeta_j')}{d_2^+(\zeta_k'')} \operatorname{res}_{\zeta_k''} \frac{a_{21}}{a_{11}} \right| = \sigma_j^2$$

where $j = 1, 2, 3, \dots$ and σ_j^1, σ_j^2 do not exceed some value $\sigma \in [0, 1)$. Then the solution of the system exists and is unique [72].

If we allow the sequences \mathbf{f} and \mathbf{b} to be from l_2 -space, then there exists a unique l_2 solution of the equation $\mathbf{f} + \mathfrak{A} \cdot \mathbf{f} = \mathbf{b}$, provided [79]

$$\sum_{j,k=1}^{\infty} \left| \frac{1}{\zeta'_j - \zeta''_k} \frac{d_1^+(\zeta''_k)}{d_1^-(\zeta'_j)} \operatorname{res}_{\zeta'_j} \frac{a_{12}}{a_{11}} \right|^2 < \infty, \quad \sum_{j,k=1}^{\infty} \left| \frac{1}{\zeta'_j - \zeta''_k} \frac{d_2^-(\zeta'_j)}{d_2^+(\zeta''_k)} \operatorname{res}_{\zeta''_k} \frac{a_{21}}{a_{11}} \right|^2 < \infty$$

Given the values $f_1^+(\zeta''_j)$ and $f_2^-(\zeta'_j)$, $j = 1, 2, 3, \dots$, the solution of the Riemann–Hilbert problem is derived from (2.55) as follows:

$$F^+(z) = L(z)D^+(z) [P(z) + \Psi^+(z)], \quad z \in \mathbb{C}^+$$

$$F^-(z) = U^{-1}(z)D^-(z) [P(z) + \Psi^-(z)], \quad z \in \mathbb{C}^+$$

where the components of the vector P are defined in (2.58).

Chapter 3

Modeling of Crack Propagation

The field of fracture mechanics is concerned with quantitative description of deformation in materials containing cracks. Describing the deformation of a particular system is provided by building a mathematical model of the system and applying methods of mathematical analysis. Dynamic fracture mechanics considers fracture phenomena that significantly change in time due to, for instance, rapidly applied loading on a cracked solid or rapid crack propagation. There are several reasons for the study of the asymptotic crack tip field for dynamic growth of a crack in a material: (i) The influence of material inertia on the distribution of stress and deformation near the crack edge in order to understand mechanisms of crack propagation; (ii) Numerical methods are often the only means for obtaining full field solutions within this problem class, however for points very close to the crack edge where stresses are most severe the accuracy of numerical solutions is difficult to assess. The ability to match computed fields to asymptotic fields valid in this region establishes confidence in the numerical results.

In this chapter, we will consider three typical problems on the crack propagation: stationary crack problem (i.e. the crack does not propagate), the crack propagation at constant speed v , and the crack propagation at a non-uniform speed $v(t)$. These are well known problems and their solutions can be found, for instance, in [39]. However, this consideration will be helpful in the study of more complex cases in the following chapters.

3.1 Suddenly Applied Crack Face Pressure

The following problem and its solution can be found in [39]. Consider an elastic unbounded body that contains a half-plane crack. It is assumed that the crack has no thickness; that is, when no loading is applied to the body, the two faces of the crack form the same surface

in space. Introduce a rectangular coordinate system so that x_3 -axis lies along the crack edge, and x_2 -axis is normal to the plane of the crack. The crack occupies the half-plane $\{(x_1, 0, x_3) : -\infty < x_1 \leq 0, |x_3| < \infty\}$ (see Figure 3.1).

Assume that the crack faces are subjected to uniform pressure of magnitude σ^* suddenly applied at time $t = 0$. We seek the solution of the wave equations (1.18) with the boundary conditions

$$\begin{aligned}\sigma_{21}(x_1, 0^\pm, x_3, t) &= 0 \\ \sigma_{22}(x_1, 0^\pm, x_3, t) &= \mp \sigma^* H(t) \\ \sigma_{23}(x_1, 0^\pm, x_3, t) &= 0 \\ -\infty < x_1 < 0, \quad -\infty < x_3 < \infty, \quad -\infty < t < \infty\end{aligned}\tag{3.1}$$

In the case of (x_1, x_2) -plane deformations, the component u_3 of the displacement vector u is equal to zero, while u_1 and u_2 do not depend on x_3 -variable and satisfy the symmetry relations [39] $u_1(x_1, -x_2, t) = u_1(x_1, x_2, t)$ and $u_2(x_1, -x_2, t) = -u_2(x_1, x_2, t)$ for all values of x_1, x_2 , and t .

Let Ω be an unbounded plane (x_1, x_2) with the crack $\{(x_1, 0) : -\infty < x_1 < 0\}$ on the negative part of x_1 -axis. For the plane strain deformation that is independent of x_3 , the vector potential ψ has only one non-zero component. Thus, we need to find functions $\phi, \psi : \mathbb{R}^2 \times \mathbb{R}_+ \rightarrow \mathbb{R}$ that satisfy the wave equations

$$c_l^2 \left(\frac{\partial^2 \phi}{\partial x_1^2} + \frac{\partial^2 \phi}{\partial x_2^2} \right) - \ddot{\phi} = 0, \quad c_s^2 \left(\frac{\partial^2 \psi}{\partial x_1^2} + \frac{\partial^2 \psi}{\partial x_2^2} \right) - \ddot{\psi} = 0 \quad \text{in } \Omega \times \mathbb{R}_+\tag{3.2}$$

with the initial conditions

$$\phi(x_1, x_2, 0) = \frac{\partial \phi}{\partial t}(x_1, x_2, 0) = \psi(x_1, x_2, 0) = \frac{\partial \psi}{\partial t}(x_1, x_2, 0) = 0, \quad x_1, x_2 \in \mathbb{R}\tag{3.3}$$

and, through the relations (1.14) and (1.15), the boundary conditions (3.1).

3.1.1 Solution of the partial differential equations

In order to solve the problem (3.1), (3.2), (3.3), we apply Laplace and Fourier transform to transform it to the Riemann–Hilbert problem. Assume that the functions ϕ and ψ are

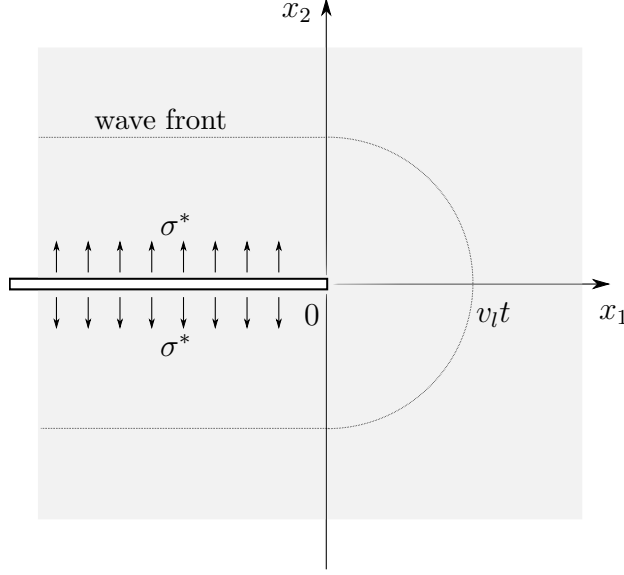


Figure 3.1: Suddenly applied crack pressure.

continuous in t -variable on the interval $(0, \infty)$ and absolute integrable in x_1 -variable on the interval $(-\infty, \infty)$ provided $x_2 \neq 0$. First, we take Laplace transform with respect to the temporal variable,

$$\tilde{\phi}(x_1, x_2, s) = \int_0^\infty \phi(x_1, x_2, t) e^{-st} dt, \quad \tilde{\psi}(x_1, x_2, s) = \int_0^\infty \psi(x_1, x_2, t) e^{-st} dt$$

which are valid for $\text{Re } s > 0$. Using integration by parts and the initial conditions (3.3), we find that $(\ddot{\phi})^\sim = s^2 \tilde{\phi}$ and $(\ddot{\psi})^\sim = s^2 \tilde{\psi}$. Thus, Laplace transform applied to the wave equations (3.2), gives

$$c_l^2 \left(\frac{\partial^2 \tilde{\phi}}{\partial x_1^2} + \frac{\partial^2 \tilde{\phi}}{\partial x_2^2} \right) - s^2 \tilde{\phi} = 0, \quad c_s^2 \left(\frac{\partial^2 \tilde{\psi}}{\partial x_1^2} + \frac{\partial^2 \tilde{\psi}}{\partial x_2^2} \right) - s^2 \tilde{\psi} = 0 \quad \text{in } \Omega \times \mathbb{R}_+$$

where we assume that the variable s is positive. Next, we apply Fourier transform

$$\begin{aligned} \hat{\phi}(z, x_2, s) &= \int_{-\infty}^{\infty} \tilde{\phi}(x_1, x_2, s) e^{iszx_1} dx_1 \\ \hat{\psi}(z, x_2, s) &= \int_{-\infty}^{\infty} \tilde{\psi}(x_1, x_2, s) e^{iszx_1} dx_1 \end{aligned} \quad z \in \mathbb{R} \quad (3.4)$$

where the exponent factor s is introduced for convenience. Since $(\partial^2 \tilde{\phi} / \partial x_1^2)^\wedge = -s^2 z^2 \hat{\phi}$ and $(\partial^2 \tilde{\psi} / \partial x_1^2)^\wedge = -s^2 z^2 \hat{\psi}$, the partial differential equations above become the ordinary

differential equations

$$\frac{\partial^2 \hat{\phi}}{\partial x_2^2} - s^2(z^2 + c_l^{-2})\hat{\phi} = 0, \quad \frac{\partial^2 \hat{\psi}}{\partial x_2^2} - s^2(z^2 + c_s^{-2})\hat{\psi} = 0 \quad \text{in } \Omega \times \mathbb{R}_+$$

Because of the symmetry conditions, it is sufficient to find solutions for only positive values of x_2 . Assuming $x_2 > 0$, the bounded at infinity solutions of the ordinary differential equations are given by

$$\begin{aligned} \hat{\phi}(z, x_2, s) &= P(z, s)e^{-s\alpha(z)x_2} \\ \hat{\psi}(z, x_2, s) &= Q(z, s)e^{-s\beta(z)x_2} \end{aligned} \quad z \in \mathbb{R}, \quad x_2, s \in \mathbb{R}_+ \quad (3.5)$$

where $\alpha(z) = \sqrt{z^2 + c_l^{-2}}$ and $\beta(z) = \sqrt{z^2 + c_s^{-2}}$ are branches of the square roots such that $\alpha(z) > 0$ and $\beta(z) > 0$ for all $z \in \mathbb{R}$.

The functions $P(z, s)$ and $Q(z, s)$ are to be determined from the boundary conditions (3.1). In terms of the functions ϕ , ψ and wave velocities c_l , c_s , components of the stress tensor σ and displacement vector u take the form

$$\begin{aligned} \frac{1}{\mu}\sigma_{11} &= \frac{c_l^2}{c_s^2} \frac{\partial^2 \phi}{\partial x_1^2} + \left(\frac{c_l^2}{c_s^2} - 2 \right) \frac{\partial^2 \phi}{\partial x_2^2} + 2 \frac{\partial^2 \psi}{\partial x_1 \partial x_2} \\ \frac{1}{\mu}\sigma_{22} &= \left(\frac{c_l^2}{c_s^2} - 2 \right) \frac{\partial^2 \phi}{\partial x_1^2} + \frac{c_l^2}{c_s^2} \frac{\partial^2 \phi}{\partial x_2^2} - 2 \frac{\partial^2 \psi}{\partial x_1 \partial x_2} \\ \frac{1}{\mu}\sigma_{12} &= 2 \frac{\partial^2 \phi}{\partial x_1 \partial x_2} - \frac{\partial^2 \psi}{\partial x_1^2} + \frac{\partial^2 \psi}{\partial x_2^2} \end{aligned} \quad \begin{aligned} u_1 &= \frac{\partial \phi}{\partial x_1} + \frac{\partial \psi}{\partial x_2} \\ u_2 &= \frac{\partial \phi}{\partial x_2} - \frac{\partial \psi}{\partial x_1} \end{aligned} \quad (3.6)$$

After applying Laplace and Fourier transforms and plugging the solution (3.5) into the equations (3.6), we have the identities

$$\begin{aligned} \frac{1}{\mu s^2} \hat{\sigma}_{11}(z, x_2, s) &= (c_s^{-2} - 2\alpha^2(z)) P(z, s)e^{-s\alpha(z)x_2} + 2iz\beta(z)Q(z, s)e^{-s\beta(z)x_2} \\ \frac{1}{\mu s^2} \hat{\sigma}_{22}(z, x_2, s) &= (z^2 + \beta^2(z)) P(z, s)e^{-s\alpha(z)x_2} - 2iz\beta(z)Q(z, s)e^{-s\beta(z)x_2} \\ \frac{1}{\mu s^2} \hat{\sigma}_{12}(z, x_2, s) &= 2iz\alpha(z)P(z, s)e^{-s\alpha(z)x_2} + (z^2 + \beta^2(z)) Q(z, s)e^{-s\beta(z)x_2} \\ \frac{1}{s} \hat{u}_1(z, x_2, s) &= -izP(z, s)e^{-s\alpha(z)x_2} - \beta(z)Q(z, s)e^{-s\beta(z)x_2} \\ \frac{1}{s} \hat{u}_2(z, x_2, s) &= -\alpha(z)P(z, s)e^{-s\alpha(z)x_2} + izQ(z, s)e^{-s\beta(z)x_2} \end{aligned} \quad (3.7)$$

On the other hand, the transforms applied to the boundary conditions (3.1) imply

$$\begin{aligned}\hat{\sigma}_{12}(x, 0^\pm, s) &= \hat{\sigma}_{12}^+(z, 0^\pm, s) \\ \hat{\sigma}_{22}(z, 0^\pm, s) &= \hat{\sigma}_{22}^+(z, 0^\pm, s) \mp \frac{\sigma^*}{is^2z}\end{aligned}\quad z \in \mathbb{R}, s \in \mathbb{R}_+ \quad (3.8)$$

where $\hat{\sigma}_{12}^+$ and $\hat{\sigma}_{22}^+$ are defined as Fourier transforms of the products $H(x_1)\sigma_{j2}(x_1, x_2, s)$ of the stress components σ_{j2} and the step function $H(x_1)$ that is equal to 1 for $x_1 > 0$ and to 0 for $x_1 < 0$.

As we consider only positive values of x_2 -variable, combining the equations (3.7) and (3.8) for $x_2 = 0^+$ gives

$$\begin{aligned}\frac{1}{\mu s^2} \hat{\sigma}_{12}^+(z, 0^+, s) &= 2iz\alpha(z)P(z, s) + (z^2 + \beta^2(z))Q(z, s) \\ \frac{1}{\mu s^2} \hat{\sigma}_{22}^+(z, 0^+, s) - \frac{\sigma^*}{i\mu s^4 z} &= (z^2 + \beta^2(z))P(z, s) - 2iz\beta(z)Q(z, s)\end{aligned}\quad (3.9)$$

By solving the system above with respect to the functions $P(z, s)$ and $Q(z, s)$, we derive

$$\begin{aligned}P(z, s) &= \frac{2iz\beta(z)}{\mu s^2 R(z)} \hat{\sigma}_{12}^+(z, 0^+, s) + \frac{z^2 + \beta^2(z)}{\mu s^2 R(z)} \left(\hat{\sigma}_{22}^+(z, 0^+, s) - \frac{\sigma^*}{is^2 z} \right) \\ Q(z, s) &= \frac{z^2 + \beta^2(z)}{\mu s^2 R(z)} \hat{\sigma}_{12}^+(z, 0^+, s) - \frac{2iz\alpha(z)}{\mu s^2 R(z)} \left(\hat{\sigma}_{22}^+(z, 0^+, s) - \frac{\sigma^*}{is^2 z} \right) \\ R(z) &= (z^2 + \beta^2(z))^2 - 4z^2\alpha(z)\beta(z)\end{aligned}\quad (3.10)$$

The solution of the system (3.9) exists whenever the function $R(z)$, which is proportional to the determinant of the system (3.9), does not equal zero. In fact, $R(z)$ is called the *Rayleigh function*, it is a multi-valued function with branch points $\pm i/c_l$ and $\pm i/c_s$ and, for a fixed choice of its single-valued branch, has two zeros $\pm i/c_R$, where c_R is the Rayleigh wave speed [39]. Thus, the function $R(z)$ does not vanish on the real axis \mathbb{R} .

The Fourier transforms $\hat{\phi}$ and $\hat{\psi}$ of the wave potentials are defined by the formulas (3.5) and (3.10). However, the values of the Fourier transforms $\hat{\sigma}_{12}^+$ and $\hat{\sigma}_{22}^+$ for $x_2 = 0^+$ in the right-hand side of the equations (3.10), are not known yet. In order to find $\hat{\sigma}_{12}^+(z, 0^+, s)$ and $\hat{\sigma}_{22}^+(z, 0^+, s)$, we formulate and solve a Riemann–Hilbert problem.

Notice that the condition $u_1(x_1, -x_2, t) = u_1(x_1, x_2, t)$ implies that the line $x_2 = 0$ is a symmetry axis of the displacement component u_2 . Therefore, $\partial u_1 / \partial x_2 = 0$ if $x_2 = 0$. The condition $u_2(x_1, -x_2, t) = -u_2(x_1, x_2, t)$ implies that the component u_2 is zero if $x_2 = 0$. Hence, in front of the crack, we have

$$u_2(x_1, 0, t) = 0, \quad \sigma_{12}(x_1, 0, t) = \mu \left(\frac{\partial u_1}{\partial x_2} + \frac{\partial u_2}{\partial x_1} \right) \Big|_{x_2=0} = 0, \quad x_1 > 0$$

for any time instance t . Since $\sigma_{12}(x_1, 0, t) = 0$ for all $x_1 < 0$ due to the boundary condition (3.1), the formula (3.10) for $P(z, s)$ and $Q(z, s)$ can be simplified by setting $\hat{\sigma}_{12}^+$ to zero. Moreover, since the displacement component u_2 is equal to zero for $x_1 > 0$, $x_2 = 0$, the last equation in (3.7) reads

$$\begin{aligned} \frac{1}{s} \hat{u}_2^-(z, 0^+, s) &= -\alpha(z)P(z, s) + izQ(z, s) \\ &= -\frac{1}{\mu s^4 c_s^2} \frac{\alpha(z)}{R(z)} \left(s^2 \hat{\sigma}_{22}^+(z, 0^+, s) - \frac{\sigma^*}{iz} \right), \quad z \in \mathbb{R}, \quad s \in \mathbb{R}_+ \end{aligned} \quad (3.11)$$

Introduce two new functions

$$\begin{aligned} \Sigma^+(z) &= s^2 \hat{\sigma}_{22}^+(z, 0^+, s) = s^2 \int_0^\infty \tilde{\sigma}_{22}(x_1, 0^+, s) e^{iszx_1} dx_1 \\ U^-(z) &= s^3 \hat{u}_2^-(z, 0^+, s) = s^3 \int_{-\infty}^0 \tilde{u}_2(x_1, 0^+, s) e^{iszx_1} dx_1 \end{aligned} \quad (3.12)$$

then they satisfy the condition

$$\Sigma^+(z) = a(z)U^-(z) + b(z), \quad z \in \mathbb{R} \quad (3.13)$$

$$a(z) = -\mu c_s^2 \frac{R(z)}{\alpha(z)}, \quad b(z) = \frac{\sigma^*}{iz}$$

which follows from (3.11). Since all of the known terms in the equation (3.13) do not depend on s -variable, the functions Σ^+ and U^- do not depend on s either. Moreover, the first and second integrals in the right-hand sides of the identities (3.12) exist and infinitely differentiable whenever $\text{Im } z > 0$ and $\text{Im } z < 0$ respectively, provided that $\tilde{\sigma}_{22}$ and \tilde{u}_2 are absolute integrable in x_1 -variable. Thus, the function $\Sigma^+ : \mathbb{C}^+ \rightarrow \mathbb{C}$ is analytic in the upper half-plane

$\mathbb{C}^+ = \{z : \text{Im } z > 0\}$ and continuous on the real axis $\mathbb{R} = \{z : \text{Im } z = 0\}$. Similarly, the function $U^- : \mathbb{C}^- \rightarrow \mathbb{C}$ is analytic in the lower half-plane $\mathbb{C}^- = \{z : \text{Im } z < 0\}$ and continuous on the real axis \mathbb{R} . The problem of determining such functions that satisfy the condition (3.13) is the Riemann-Hilbert problem discussed in the previous chapter.

3.1.2 Solution of the Riemann-Hilbert problem

In order to solve the Riemann-Hilbert problem (3.13), let us first determine index κ of the problem. Both functions $\alpha(z)$ and $R(z)$ in the equation (3.13) take only real values for $z \in \mathbb{R}$, while $\alpha(z)$ is continuous and $R(z)$ does not vanish on the real axis \mathbb{R} . Thus, $\arg\{R(z)/\alpha(z)\}$ does not change on \mathbb{R} and

$$\kappa = \arg\{a(z)\}_{|z=-\infty}^{z=\infty} = 0$$

Since the problem has zero index, there exists a unique solution of the Riemann-Hilbert problem (3.13) that vanishes at infinity.

Now, we will follow the general algorithm of solving a scalar Riemann-Hilbert problem described in the previous chapter. However, due to the behavior of the coefficient $a(z)$ of the problem (3.13), we will need to make several changes in the algorithm.

Notice that the function $a(z)$ is Hölder continuous on the real axis \mathbb{R} since it is continuously differentiable there. But it has a simple pole at infinity since $R(z) = O(|z|^2)$ and $\alpha(z) = O(|z|)$ as $z \rightarrow \pm\infty$. Therefore, the integral in the formula (2.19) would not exist. In order to construct the Wiener-Hopf factorization of $a(z)$, we represent it in the form

$$a(z) = -\mu c_s^2 a_*(z) a_{**}(z), \quad a_*(z) = \frac{z^2 + c_R^{-2}}{\alpha(z)}, \quad a_{**}(z) = \frac{R(z)}{z^2 + c_R^{-2}}$$

where c_R is the Rayleigh wave speed. The factor $a_{**}(z)$ is Hölder continuous on the real axis \mathbb{R} , takes a finite non-zero value as $z \rightarrow \pm\infty$ and, hence, can be factorized by the formula (2.19). The factor $a_*(z)$ is relatively simple and can be factorized as follows

$$a_*(z) = \frac{a_*^+(z)}{a_*^-(z)}, \quad z \in \mathbb{R}, \quad a_*^+(z) = \frac{z + i/c_R}{\sqrt{z + i/c_l}}, \quad a_*^-(z) = \frac{\sqrt{z - i/c_l}}{z - i/c_R}$$

for a specific choice of branches of the square roots. It is clear that the functions a_*^\pm are analytic and non-zero in the half-planes \mathbb{C}^\pm respectively.

In order to factorize a_{**} on the real axis \mathbb{R} , we define the functions

$$a_{**}^\pm(z) = \exp \left\{ \frac{1}{2\pi i} \int_{-\infty}^{\infty} \frac{\ln a_{**}(t)}{t - z} dt \right\}, \quad z \in \mathbb{C}^\pm$$

Since a_{**} is Hölder continuous on the real axis \mathbb{R} and takes a finite non-zero value as $z \rightarrow \pm\infty$, we have the equality $a_{**}(z) = a_{**}^+(z)/a_{**}^-(z)$ for all $z \in \mathbb{R}$ due to the Sokhotski–Plemelj formulas (2.9). Thus, $a(z) = a^+(z)/a^-(z)$, $z \in \mathbb{R}$, for

$$a^+(z) = -\mu c_s^2 a_*^+(z) a_{**}^+(z), \quad z \in \mathbb{C}^+, \quad a^-(z) = a_*^-(z) a_{**}^-(z), \quad z \in \mathbb{C}^- \quad (3.14)$$

The functions $a^\pm(z)$ are continuous on the real axis \mathbb{R} , and $a^+(z) = O(|z|^{1/2})$, $a^-(z) = O(|z|^{-1/2})$ as $z \rightarrow \infty$.

According to the algorithm of solving a scalar Riemann–Hilbert problem, replace the function a in (3.13) by the fraction a^+/a^- and divide the equation (3.13) by a^+ , then

$$\frac{\Sigma^+(z)}{a^+(z)} = \frac{U^-(z)}{a^-(z)} + \frac{b(z)}{a^+(z)}, \quad z \in \mathbb{R} \quad (3.15)$$

The next step is to take the Cauchy integral of the term b/a^+ . At infinity, the fraction $b(z)/a^+(z)$ vanishes as $|z|^{-3/2}$ and has a simple pole at the origin,

$$\frac{b(z)}{a^+(z)} \sim \frac{\sigma^*}{ia^+(0)} \frac{1}{z} \quad \text{as } z \rightarrow 0$$

In order to deal with the pole, we transform the contour \mathbb{R} to pass around the point $z = 0$. So far, we considered the functions Σ^+ and U_- to be analytical in the upper \mathbb{C}^+ and the lower \mathbb{C}^- half-planes respectively. However, a thorough analysis allows for expansion of those regions of analyticity.

Consider behavior of the functions $\sigma_{22}(x_1, 0, t)$ and $u_2(x_1, 0, t)$ in front of the crack. Fix an arbitrary point $(x_1^\circ, 0)$ such that $x_1^\circ > 0$. Since the body is initially stress-free, the stress

component $\sigma_{22}(x_1^\circ, 0, t)$ is equal to zero until the wave of deformation reaches this point (see Figure 3.1), that is for all $t < x_1^\circ/c_l$. Thus

$$\begin{aligned}\tilde{\sigma}_{22}(x_1^\circ, 0, s) &= \int_{x_1^\circ/c_l}^{\infty} \sigma_{22}(x_1^\circ, 0, t) e^{-st} dt \\ &= e^{-s \frac{x_1^\circ}{c_l}} \int_0^{\infty} \sigma_{22}(x_1^\circ, 0, t + x_1^\circ/c_l) e^{-st} dt\end{aligned}\tag{3.16}$$

The function $\tilde{\sigma}_{22}$ exponentially vanishes as $x_1^\circ \rightarrow \infty$ since the integral in the right-hand side of the last equality in (3.16) is bounded. From properties of the Fourier integral, it follows [77] that in this case, the function Σ^+ is analytic in the region $\{z : \text{Im } z > -1/c_l\}$. As for the displacement component $u_2(x_1, 0, t)$, it is non-zero for all $t > 0$ since the loading σ^* is applied uniformly to the faces of the crack ($x_1 < 0$). Analysis of the regions of analyticity of the functions Σ^+ and U^- implies that in the equation (3.15) the contour \mathbb{R} can be changed to the contour

$$\mathbb{R}_{-\varepsilon} = \{z : \text{Im } z = -\varepsilon\}$$

for some $\varepsilon \in (0, 1/c_l)$. Let us introduce the half-planes $\mathbb{C}_{-\varepsilon}^+ = \{z : \text{Im } z > -\varepsilon\}$ and $\mathbb{C}_{-\varepsilon}^- = \{z : \text{Im } z < -\varepsilon\}$ and consider the functions Σ^+ and U^- on them. According to the third step in the solution of a scalar Riemann–Hilbert problem, we define

$$P(z) = \begin{cases} \frac{\Sigma^+(z) - b(z)}{a^+(z)} & z \in \mathbb{C}_{-\varepsilon}^+ \\ \frac{U^-(z)}{a^-(z)} & z \in \mathbb{C}_{-\varepsilon}^- \end{cases}\tag{3.17}$$

Notice that the function $P(z)$ is continuous across the boundary between $\mathbb{C}_{-\varepsilon}^-$ and $\mathbb{C}_{-\varepsilon}^+$ due to the condition (3.15) with the contour \mathbb{R} replaced by $\mathbb{R}_{-\varepsilon}$. Moreover, $P(z)$ is analytic in $\mathbb{C}_{-\varepsilon}^-$ and has a single simple pole $z = 0$ in $\mathbb{C}_{-\varepsilon}^+$. At infinity, $P(z)$ vanishes since

$$\frac{\Sigma^+(z) - b(z)}{a^+(z)} = O(|z|^{-1/2}) \quad \text{and} \quad \frac{U^-(z)}{a^-(z)} = O(|z|^{1/2}) \quad \text{as } z \rightarrow \infty$$

Thus, by Liouville's theorem [41]

$$P(z) = \frac{C}{z}$$

where C is an arbitrary constant. From the formula (3.17), we conclude that

$$\Sigma^+(z) = \frac{C}{z}a^+(z) + b(z), \quad z \in \mathbb{C}_{-\varepsilon}^+, \quad U^-(z) = \frac{C}{z}a^-(z), \quad z \in \mathbb{C}_{-\varepsilon}^-$$

Since the function Σ^+ is required to be analytic in $\mathbb{C}_{-\varepsilon}^+$, we set $C = i\sigma^*/a^+(0)$ in order to eliminate the pole at $z = 0$. Finally, the solution of the Riemann–Hilbert problem (3.13) takes the form

$$\Sigma^+(z) = \left(1 - \frac{a^+(z)}{a^+(0)}\right)b(z), \quad U^-(z) = -\frac{a^-(z)}{a^+(0)}b(z) \quad (3.18)$$

After plugging values $\hat{\sigma}_{22}^+(z, 0^+, s) = \Sigma^+(z)/s^2$ into the formulas (3.10) and (3.5) and applying inverse Fourier transform and inverse Laplace transform to $\hat{\phi}$ and $\hat{\phi}$, we derive the explicit formulas for the wave potentials ϕ and ψ in $\Omega \times \mathbb{R}_+$. Using the identities (3.6), we can find all displacement and stress components in the body.

3.1.3 Derivation of stress intensity factor K_I

One of the advantages of explicit solutions is that they allow for describing behavior of the stress and displacement components near the tip of a crack. In order to do that, we derive useful relations between behavior of a function and its Fourier transforms at singular points. Assume that $f_+ : \mathbb{R} \rightarrow \mathbb{C}$ is L^1 -function such that $f_+(x) = 0$ for all $x < 0$, and $f_+(x) \sim f_+^\circ/x^\lambda$ as $x \rightarrow 0^+$, $\lambda \in (0, 1)$. Then its Fourier transform $\hat{f}^+ : \mathbb{C}^+ \rightarrow \mathbb{C}$ is analytic in \mathbb{C}^+ and

$$\begin{aligned} \hat{f}^+(iy) &= \int_0^\infty f_+(x)e^{-yx}dx = \frac{1}{y} \int_0^\infty f_+(\xi/y)e^{-\xi}d\xi \\ &\sim f_+^\circ y^{\lambda-1} \int_0^\infty \xi^{-\lambda}e^{i\xi}d\xi = f_+^\circ y^{\lambda-1}\Gamma(1-\lambda), \quad y \rightarrow \infty \end{aligned}$$

where Γ is Gamma-function and $x = \xi/y$. A similar identity holds for $f_- : \mathbb{R} \rightarrow \mathbb{C}$ such that $f_-(x) = 0$ for all $x > 0$ and $f_-(x) \sim f_-^\circ/x^\lambda$ as $x \rightarrow 0^-$. Therefore,

$$\begin{aligned} \lim_{x \rightarrow 0^+} (x^\lambda f_+(x)) &= \frac{1}{\Gamma(1-\lambda)} \lim_{y \rightarrow \infty} (y^{1-\lambda} \hat{f}^+(iy)) \\ \lim_{x \rightarrow 0^-} (x^\lambda f_-(x)) &= \frac{1}{\Gamma(1-\lambda)} \lim_{y \rightarrow \infty} (y^{1-\lambda} \hat{f}^-(-iy)) \end{aligned} \quad 0 < \lambda < 1 \quad (3.19)$$

From the identities (3.19), it follows that in order to determine behavior of $\sigma_{22}^+(x_1, 0, t)$ and $u_2^-(x_1, 0, t)$ as $x_1 \rightarrow 0$, we need to consider behavior of the functions $\Sigma^+(z)$ and $U^-(z)$

as $z \rightarrow \infty$. We can easily find that $a_*^\pm(z) = O(|z|^{\pm 1/2})$ as $\text{Im } z \rightarrow \pm\infty$ and

$$\lim_{z \rightarrow \infty} a_{**}^\pm(z) = \left(\lim_{z \rightarrow \infty} a_{**}(z) \right)^{\pm 1/2} = \left(\frac{2}{c_s^2} - \frac{2}{c_l^2} \right)^{\pm 1/2}$$

Thus,

$$\begin{aligned} a^+(iy) &\sim -\sqrt{2i}\mu \frac{c_s}{c_l} \sqrt{c_l^2 - c_s^2} y^{1/2} \\ a^-(-iy) &\sim \frac{1}{\sqrt{-2i}} \frac{c_l c_s}{\sqrt{c_l^2 - c_s^2}} y^{-1/2} \end{aligned} \quad y \rightarrow \infty$$

Substituting $b(z) = -i\sigma^*/z$ into the solution (3.18), we find that as $y \rightarrow \infty$

$$\Sigma^+(iy) \sim -\sqrt{2i}\mu \frac{c_s}{c_l} \sqrt{c_l^2 - c_s^2} \frac{\sigma^*}{a^+(0)} y^{-1/2}$$

Using the first identity in (3.19) for $\lambda = 1/2$, we derive

$$\begin{aligned} \tilde{\sigma}_{22}(x_1, 0, s) &\sim -\sqrt{2i}\mu \frac{c_s}{c_l} \sqrt{c_l^2 - c_s^2} \frac{\sigma^*}{a^+(0)} \frac{1}{s^{3/2}} \frac{1}{\sqrt{\pi x_1}} \quad \text{as } x_1 \rightarrow 0^+ \\ \sigma_{22}(x_1, 0, t) &\sim -\frac{2\sqrt{2i}}{\pi} \mu \frac{c_s}{c_l} \sqrt{c_l^2 - c_s^2} \frac{\sigma^*}{a^+(0)} \sqrt{\frac{t}{x_1}} \quad \text{as } x_1 \rightarrow 0, \quad t > 0 \end{aligned} \quad (3.20)$$

By comparing the expression (3.20) and the definition of the stress intensity factors (1.19), we derive the formula for the stress intensity factor K_I ,

$$K_I(t) = -4\mu \sqrt{\frac{i}{\pi}} \frac{c_s}{c_l} \sqrt{c_l^2 - c_s^2} \frac{\sigma^*}{a^+(0)} \sqrt{t}, \quad t > 0$$

In order to find the value $a^+(0)$, we notice that due to symmetry of the function a_{**} on the real axis \mathbb{R} , we have

$$a_{**}^+(iy) = \exp \left\{ \frac{1}{2\pi i} \int_{-\infty}^{\infty} \frac{\ln a_{**}(t)}{t - iy} dt \right\} = \exp \left\{ -\frac{1}{2\pi i} \int_{-\infty}^{\infty} \frac{\ln a_{**}(t)}{t + iy} dt \right\} = \frac{1}{a_{**}^-(-iy)}$$

for all $y > 0$. Taking the limit as $y \rightarrow 0^+$, we derive the identity $a_{**}^+(0) = 1/a_{**}^-(0)$. Together with the factorization $a_{**} = a_{**}^+/a_{**}^-$ on the real axis \mathbb{R} , the latter gives $a_{**}^+(0) = \sqrt{a_{**}(0)}$. After finding values $a_*^+(0)$ and $a_{**}^+(0)$ and plugging them into the formula (3.14), we derive the value $a^+(0) = -\mu\sqrt{ic_l}$. Hence

$$K_I(t) = \sigma^* \frac{4}{\sqrt{\pi}} \frac{c_s}{\sqrt{c_l}} \sqrt{1 - \frac{c_s^2}{c_l^2}} \sqrt{t}, \quad t > 0$$

3.2 Crack Propagation at Constant Speed

Let us consider the problem on suddenly applied crack face loading from Section 3.1, but assume that the crack propagates at a constant subsonic speed ($v < c_R$) along x_1 -axis (see Figure 3.1). Although the solution to this problem is known [39], the solution derived here has a different form, which will be used as a building block for the approximate procedure proposed later for the solution of the problem on a crack in a half-plane (see Chapter 5). Derivation of the solution for the problem is identical to the one described in Section 3.1 except the choice of a moving coordinate system (x, y) such that the crack tip coincides with the origin at any time instance t . Thus, in the wave equations 3.2, we make the substitution $x_1 = x + vt$ and $x_2 = y$:

$$\begin{aligned} (c_l^2 - v^2) \frac{\partial^2 \phi}{\partial x^2} + c_l^2 \frac{\partial^2 \phi}{\partial y^2} + 2v \frac{\partial^2 \phi}{\partial x \partial t} - \frac{\partial^2 \phi}{\partial t^2} &= 0 \\ (c_s^2 - v^2) \frac{\partial^2 \psi}{\partial x^2} + c_s^2 \frac{\partial^2 \psi}{\partial y^2} + 2v \frac{\partial^2 \psi}{\partial x \partial t} - \frac{\partial^2 \psi}{\partial t^2} &= 0 \end{aligned} \quad \text{in } \Omega \times \mathbb{R}_+ \quad (3.21)$$

where Ω is the unbounded plane with the cut $\{(x, 0) : -\infty < x < 0\}$, the functions $\phi(x, y, t)$ and $\psi(x, y, t)$ are the wave potentials in the moving coordinate system (x, y) (i.e. they are different from ϕ and ψ used in Section 3.1).

We assume the stress-free state for $t < 0$ as an initial condition, while the boundary conditions have the form

$$\sigma_{j2}(x + vt, 0^\pm, t) = -\sigma_j^\circ(x + vt)H(t), \quad -\infty < x < 0, \quad j = 1, 2 \quad (3.22)$$

which expresses the fact that the shear σ_1° and normal σ_2° loading is time-independent in (x_1, x_2) -coordinate system so that the crack tip moves away from the loading.

3.2.1 General solution of the problem

This solution follows the works [18, 19]. As in Section 3.1, we apply the Laplace transform with respect to the temporal variable t and Fourier transform with respect to the spacial variable x , defined by

$$\tilde{f}(x, s) = \int_0^\infty f(x, t) e^{-st} dt, \quad \hat{f}(z, s) = \int_{-\infty}^\infty f(x, s) e^{izx} dx$$

for all values $z \in \mathbb{R}$ and $\operatorname{Re} s > 0$, provided the function $f : \mathbb{R} \times \mathbb{R}_+ \rightarrow \mathbb{C}$ is integrable on the interval $(0, \infty)$ in t -variable and on the interval $(-\infty, \infty)$ in x -variable. Notice that the Fourier transform is different from the one used in (3.4) and (3.12) since the exponent e^{izz} does not contain the factor s .

After solving partial differential equations (3.21) with the boundary conditions (3.22), the problem is reduced to two separate Riemann–Hilbert problems with the conditions

$$\hat{\sigma}_j^+(z, s) = \mu i a_j(z, s) \hat{\chi}_j^-(z, s) + b_j(z, s), \quad z \in \mathbb{R}, \quad j = 1, 2. \quad (3.23)$$

where $\hat{\sigma}_j^+$, b_j , $\hat{\chi}_j^-$ are the Fourier and Laplace transforms of the stress components $\sigma_{j2}(x + vt, 0, t)$ in front of the crack tip ($x > 0$), the loading $\sigma_j^o(x + vt)$ behind the crack tip ($x < 0$), and the jumps of displacement rate of change

$$\chi_j(x, t) = \frac{\partial u_j}{\partial x}(x + vt, 0^+, t) - \frac{\partial u_j}{\partial x}(x + vt, 0^-, t)$$

behind the crack tip ($x < 0$) respectively. The coefficients a_j of the Riemann–Hilbert problems are defined as follows:

$$a_1(z, s) = \frac{R_s(z)}{2\beta_s(z)(z^2 - \beta_s^2(z))z}, \quad a_2(z, s) = \frac{R_s(z)}{2\alpha_s(z)(z^2 - \beta_s^2(z))z} \quad (3.24)$$

$$R_s(z) = (z^2 + \beta_s^2(z))^2 - 4z^2\alpha_s(z)\beta_s(z)$$

$$\alpha_s^2(z) = \left(1 - \frac{v^2}{c_l^2}\right)z^2 + 2iz\frac{sv}{c_l^2} + \frac{s^2}{c_l^2}, \quad \beta_s^2(z) = \left(1 - \frac{v^2}{c_s^2}\right)z^2 + 2iz\frac{sv}{c_s^2} + \frac{s^2}{c_s^2}$$

Notice that the functions $R_s(zs)$, $\alpha_s(zs)$, and $\beta_s(zs)$ are identical to $R(z)$, $\alpha(z)$, and $\beta(z)$ defined in Section 3.1 if we set $v = 0$. Moreover, using the identities $\alpha_s(zs) = s\alpha_1(z)$, $\beta_s(zs) = s\beta_1(z)$, and $R_s(zs) = s^4R_1(z)$, where single-valued branches of the functions α_1 , β_1 are chosen so that $\alpha_1(z) > 0$ and $\beta_1(z) > 0$, we can rewrite the equation (3.23) in the form

$$\hat{\sigma}_j^+(zs, s) = \mu i a_j(z, 1) \hat{\chi}_j^-(zs, s) + b_j(zs, s), \quad z \in \mathbb{R}, \quad j = 1, 2, \quad (3.25)$$

The functions $a_j(z, 1)$ take non-zero values $\pm\gamma_j$ as $z \rightarrow \pm\infty$ and have simple poles at the origin $z = 0$. once again, the integral of $\ln a_j(z, 1)$ in the formula (2.19) would not exist. In

order to deal with these singularities, let us represent the coefficients of the Riemann–Hilbert problems as

$$a_j(z, 1) = -\gamma_j \coth(\pi z) a_j^*(z). \quad (3.26)$$

Since the coefficients of the Riemann-Hilbert problems, \tilde{a}_1 and \tilde{a}_2 , have a simple pole at the point $z = 0$, we deform the contour \mathbb{R} to bypass this point. Following the argument conducted for the case of stationary crack in the paragraph below the formula (3.16), we conclude that the contour \mathbb{R} in the equation (3.25) can be replaced by the line $\mathbb{R}_{-\varepsilon} = \{z : \text{Im } z = -\varepsilon\}$ for some value $\varepsilon \in (0, 1/c_l)$, which splits the z -plane into two domains: $\mathbb{C}_{-\varepsilon}^+$ containing the origin $z = 0$, and $\mathbb{C}_{-\varepsilon}^-$. On the contour $\mathbb{R}_{-\varepsilon}$, the functions a_j° can be easily factorized in terms of the Cauchy integrals

$$a_j^\pm(z) = \exp \left\{ \frac{1}{2\pi i} \int_{\mathbb{R}_{-\varepsilon}} \frac{\ln a_j^\circ(\tau)}{\tau - z} d\tau \right\}, \quad z \in \mathbb{C}_{-\varepsilon}^\pm, \quad (3.27)$$

due to the fact that the functions $\ln a_j^\circ$ are Hölder continuous on the contour $\mathbb{R}_{-\varepsilon}$, vanish at infinity, and have zero-increment of the argument of $a_j^\circ(\tau)$ as τ traverses the contour $\mathbb{R}_{-\varepsilon}$ (i.e. index κ of the problem is equal to zero).

After factorizing the function $\coth(\pi z)$ in terms of the Gamma-functions

$$\coth(\pi z) = \frac{iK^+(z)}{K^-(z)}, \quad K^+(z) = \frac{\Gamma(1-iz)}{\Gamma(1/2-iz)}, \quad K^-(z) = \frac{\Gamma(1/2+iz)}{\Gamma(iz)}, \quad (3.28)$$

and using the identity $a_j^\circ = a_j^+/a_j^-$ on $\mathbb{R}_{-\varepsilon}$, it is possible to transform the boundary condition (3.25) of the Riemann–Hilbert problem to the form

$$\frac{\hat{\sigma}_j^+(zs, s)}{K^+(z)a_j^+(z)} - \Psi_j^+(z, s) = \frac{\mu\gamma_j\hat{\chi}_j^-(zs, s)}{K^-(z)a_j^-(z)} - \Psi_j^-(z, s), \quad z \in \mathbb{R}_{-\varepsilon}, \quad (3.29)$$

where

$$\Psi_j(z, s) = \frac{1}{2\pi i} \int_{\mathbb{R}_{-\varepsilon}} \frac{b_j(\tau s, s)}{K^+(\tau)a_j^+(\tau)} \frac{d\tau}{\tau - z}, \quad z \in \mathbb{C}_{-\varepsilon}^\pm \quad (3.30)$$

Analysis of behavior of the functions in (3.29) shows that

$$K^\pm(z) \sim (\mp iz)^{1/2}, \quad a_j^\pm(z) \sim 1, \quad \Psi_j^\pm(z, s) = O(|z|^{-1}), \quad z \rightarrow \infty \quad (3.31)$$

while $\hat{\sigma}_j^+$ and $\hat{\chi}_j^-$ are assumed to be bounded at infinity. By applying the continuity principle and the Liouville theorem, we derive the unique solution of the Riemann–Hilbert problem (3.25):

$$\begin{aligned}\hat{\sigma}_j^+(zs, s) &= K^+(z)a_j^+(z)\Psi_j^+(z, s), & z \in \mathbb{C}_{-\epsilon}^+, \\ \hat{\chi}_j^-(zs, s) &= (\mu\gamma_j)^{-1}K^-(z)a_j^-(z)\Psi_j^-(z, s), & z \in \mathbb{C}_{-\epsilon}^-. \end{aligned} \quad (3.32)$$

Passing to the limit $\varepsilon \rightarrow 0^+$ shows that the functions $\hat{\chi}_j^-(-i\varepsilon s, s) \rightarrow 0$, which is consistent with the fact that the difference between the displacement components on the faces of the crack vanishes at infinity (i.e. as $x \rightarrow -\infty$).

3.2.2 Fundamental solutions of the problem

In this section, we will consider the stress intensity factors $K_I(t)$ and $K_{II}(t)$ introduced in (1.19). In the moving coordinate system (x, y) , we define the stress intensity factors by the relations

$$\sigma_{12}(x + vt, 0, t) \sim \frac{K_{II}(t)}{\sqrt{2\pi}}x^{-1/2}, \quad \sigma_{22}(x + vt, 0, t) \sim \frac{K_I(t)}{\sqrt{2\pi}}x^{-1/2}, \quad x \rightarrow 0^+.$$

After applying Laplace transform, the relations above become

$$\tilde{\sigma}_{12}(x, s) \sim \frac{\tilde{K}_{II}(s)}{\sqrt{2\pi}}x^{-1/2}, \quad \tilde{\sigma}_{22}(x, s) \sim \frac{\tilde{K}_I(s)}{\sqrt{2\pi}}x^{-1/2}, \quad x \rightarrow 0^+ \quad (3.33)$$

On the other hand, behavior of the functions $\tilde{\sigma}_{12}$ and $\tilde{\sigma}_{22}$ near the point $x = 0$ can be determined from the first identity in (3.19) if we know behavior of their Fourier transforms at infinity. Combining the formulas (3.32) and (3.31), we derive

$$\hat{\sigma}_j^+(z, s) \sim i \left(-i \frac{z}{s} \right)^{-1/2} \Psi_j^\infty(s), \quad \text{Im } z \rightarrow \infty$$

where

$$\Psi_j^\infty(s) = \frac{1}{2\pi i} \int_{\mathbb{R}_{-\epsilon}} \frac{b_j(\tau s, s)}{K^+(\tau)a_j^+(\tau)} d\tau \quad (3.34)$$

Thus, the first identity in (3.19) with $\lambda = 1/2$ and the relations (3.33) imply

$$\tilde{K}_{II}(s) = i\sqrt{2s}\Psi_1^\infty(s), \quad \tilde{K}_I(s) = i\sqrt{2s}\Psi_2^\infty(s), \quad \text{Re } s > 0$$

Let us consider fundamental solutions of the problem, which corresponds to the loading $\sigma_j^\circ(x_1) = \delta(x_1)$. After taking Laplace and Fourier transforms of $\sigma_j^\circ(x+vt)$, we derive $b_j(z, s) = 1/(s + izv)$ provided $\text{Im } z < 0$. After plugging these values into the formula (3.34), the functions Ψ_1^∞ and Ψ_2^∞ take the form

$$\Psi_j^\infty(s) = -\frac{1}{2\pi s v} \int_{\mathbb{R}_{-\varepsilon}} \frac{d\tau}{(\tau - i/v)K^+(\tau)a_j^+(\tau)}$$

Since the integrand has only one simple pole $z = i/v$ and vanishes as $O(|z|^{-3/2})$ at infinity in the upper half-plane $\mathbb{C}_{-\varepsilon}^+$, the residue theorem implies that

$$\Psi_j^\infty(s) = -i \frac{1}{s v K^+(i/v) a_j^+(i/v)}, \quad j = 1, 2, \quad \text{Re } s > 0$$

The corresponding Laplace transforms \tilde{K}_{II} and \tilde{K}_I of the stress intensity factors, are given by

$$\tilde{K}_{II}(s) = \sqrt{\frac{2}{s}} \frac{1}{v K^+(i/v) a_1^+(i/v)}, \quad \tilde{K}_I(s) = \sqrt{\frac{2}{s}} \frac{1}{v K^+(i/v) a_2^+(i/v)} \quad (3.35)$$

As in the case of a stationary crack, we can explicitly determine the inverse Laplace transforms of (3.35) due to the fact that the inverse Laplace transform of $1/\sqrt{s}$ is $1/\sqrt{\pi t}$,

$$\begin{aligned} K_{II}(t) &= \sqrt{\frac{2}{\pi v t}} k_{II}(v), \quad k_{II}(v) = \frac{\Gamma(1 + 1/v)}{\sqrt{v} \Gamma(1/2 + 1/v) a_1^+(i/v)} \\ K_I(t) &= \sqrt{\frac{2}{\pi v t}} k_I(v), \quad k_I(v) = \frac{\Gamma(1 + 1/v)}{\sqrt{v} \Gamma(1/2 + 1/v) a_2^+(i/v)} \end{aligned} \quad (3.36)$$

Thus, the temporal variable t contributes to the stress intensity factors K_I and K_{II} only through the term $1/\sqrt{\pi v t}$, while the factors k_I and k_{II} depend only on the velocity v . Graphs of the dimensionless functions k_I and k_{II} versus the dimensionless speed v/c_R for $\nu = 0.3$ is shown in Figure 3.2. The graph of the function k_I is in good agreement with the one presented in [39], p. 349.

If $\sigma_1^\circ(x_1)$ and $\sigma_2^\circ(x_1)$ is arbitrary shear and normal loading applied to the crack faces ($x_1 < 0$), then the corresponding stress intensity factors are given by the integrals

$$K_{II}(t) = \int_{-\infty}^0 \sigma_1(x_1) K_{II}(x_1; t) dx_1, \quad K_I(t) = \int_{-\infty}^0 \sigma_2(x_1) K_I(x_1; t) dx_1$$

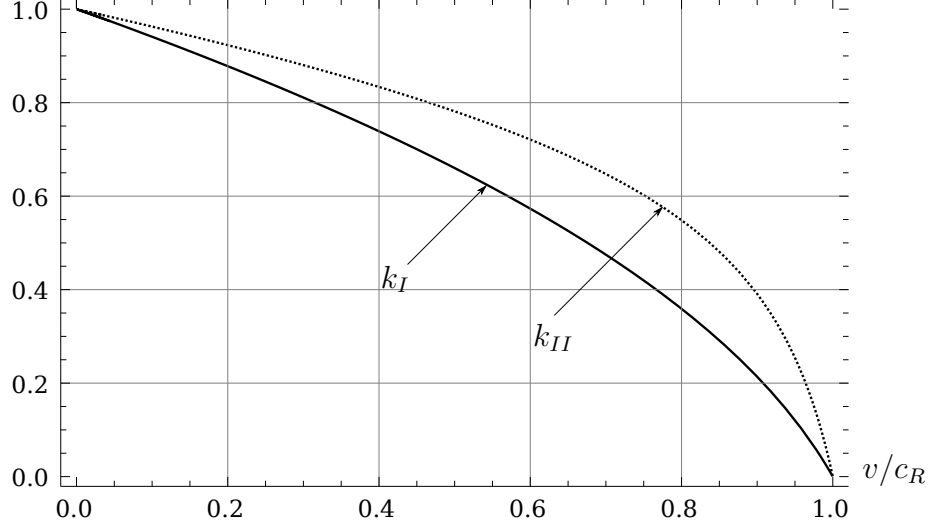


Figure 3.2: Functions k_I and k_{II} against v/c_R for $\nu = 0.3$.

where $K_I(x_1; t)$ and $K_{II}(x_1; t)$ are given by the formula (3.36) with vt replaced by $vt - x_1$. After substituting them into the integrals, we derive the stress intensity factors for arbitrary loading

$$\begin{aligned} K_{II}(t) &= k_{II}(v) \sqrt{\frac{2}{\pi}} \int_{-\infty}^0 \frac{\sigma_1^\circ(x_1)}{\sqrt{vt - x_1}} dx_1 \\ K_I(t) &= k_I(v) \sqrt{\frac{2}{\pi}} \int_{-\infty}^0 \frac{\sigma_2^\circ(x_1)}{\sqrt{vt - x_1}} dx_1 \end{aligned} \quad (3.37)$$

provided the integrals above exist.

3.3 Crack Propagation at Non-Uniform Speed

In the previous two sections, we discussed behavior of the stress field near the tip of a stationary crack and of a crack growing at constant speed. However, the more natural assumption is that a crack grows at speed $v(t)$ that changes in time t . Following [39], we will construct an approximate solution of such problem as the superposition of solutions for the problem on a suddenly stopped crack.

3.3.1 Piecewise model of a crack propagation

Consider an unbounded plane \mathbb{R}^2 with a semi-infinite crack $\{(x_1, 0) : -\infty < x_1 < 0\}$ subjected to the external in-plane loading $\sigma^{ext}(x_1)$ (Figure 3.1). Assume that at the time instance $t = 0$, the crack begins growing in x_1 -direction and then stops at the time instance

T , so that the position of the crack tip is described by the law $x_1 = l(t)$, $t \in [0, T]$, where $l(t)$ is a continuous increasing function of time t .

In order to determine the stress distribution $\sigma(x_1, x_2, t)$ in the body, we replace the function $l(t)$ by its piecewise linear approximation $L(t)$. Let $\{t_n\}_{n=0}^N$ be a partition of the time-interval $[0, T]$ such that $0 = t_0 < t_1 < t_2 < \dots < t_N = T$. Let us assume that on the time-interval $[t_{n-1}, t_n]$, the crack tip is moving at constant speed

$$v_n = \frac{l_n - l_{n-1}}{t_n - t_{n-1}}, \quad l_n = l(t_n), \quad n = 1, 2, \dots, N$$

according to the law $x_1 = l_{n-1} + v_n(t - t_{n-1})$. Thus, the function $l(t)$ is approximated by the piecewise linear continuous function (see Figure 3.3)

$$L(t) = \begin{cases} v_1 t, & 0 < t < t_1 \\ l_1 + v_2(t - t_1), & t_1 < t < t_2 \\ \dots, & \dots \\ l_{N-1} + v_N(t - t_{N-1}), & t_{N-1} < t < t_N \end{cases}$$

We seek the stress field σ in the unbounded plane with the crack $\{(x_1, 0) : -\infty < x_1 < L(t)\}$, that satisfies the boundary condition

$$\sigma(x_1, 0^\pm, t) = \sigma^{ext}(x_1)H(-x_1), \quad -\infty < x_1 < L(t) \quad (3.38)$$

The stress tensor σ is represented in the form

$$\sigma(x_1, x_2, t) = \sum_{n=0}^N \sigma^n(x_1, x_2, t) \quad (3.39)$$

The term $\sigma^0(x_1, x_2, t)$ is the stress distribution corresponding to the stationary crack $\{(x_1, 0) : -\infty < x_1 < 0\}$ in the plane \mathbb{R}^2 with the boundary condition

$$\sigma^0(x_1, 0, t) = \sigma^{ext}(x_1), \quad -\infty < x_1 < 0, \quad t > 0 \quad (3.40)$$

This problem in the case of uniform pressure on the crack faces was solved in Section 3.1.

Since for an arbitrary loading σ^{ext} the solution is similar, σ^0 is assumed to be known.

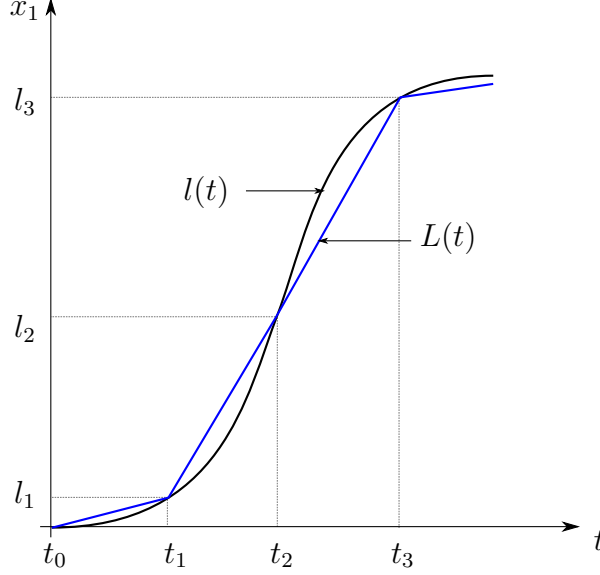


Figure 3.3: The piecewise linear curve $L(t)$ approximates the crack tip trajectory $l(t)$.

The term $\sigma^n(x_1, x_2, t)$ for $n = 1, 2, \dots, N$ is the stress distribution corresponding to the dynamic problem on propagation of a semi-infinite crack in a stress-free plane when the preexisting crack $\{(x_1, 0) : -\infty < x_1 < l_{n-1}\}$ starts to grow at the time instance $t = t_{n-1}$ with the constant velocity v_n , and suddenly stops at the time instance $t = t_n$ at the point $x_1 = l_n$. In this case, the crack faces are subjected to the loads $p^n(x_1)$ on the interval $[l_{n-1}, L(t)]$:

$$\sigma^n(x_1, 0, t) = p^n(x_1)H(x_1 - l_{n-1}), \quad -\infty < x_1 < L(t) \quad (3.41)$$

where

$$p^n(x_1) = - \sum_{j=0}^{n-1} \sigma^j(x_1, 0, t_j) \quad (3.42)$$

Let us show that the stress field $\sigma(x_1, x_2, t)$ defined in (3.39) satisfies the boundary condition (3.38). For the time $t \leq 0$, all the terms except σ^0 in (3.39) are identically zero. Since σ^0 is the solution of the corresponding problem on a stationary crack, $\sigma(x_1, x_2, t)$ satisfies the boundary conditions for $t \leq 0$.

Fix the time instance $t \in (0, T)$. If $x_1 \leq 0$, then $\sigma(x_1, 0, t) = \sigma^{ext}(x_1)$ since all but the first term σ^0 in the sum (3.39) vanish due to the boundary condition (3.41), and $\sigma^0 = \sigma^{ext}$ due (3.40). If $0 < x_1 < L(t)$, then there exists an integer m such that $x_1 \in [l_{m-1}, l_m)$. Notice that

$\sigma^n(x_1, 0, t) = 0$ for all $n > m$ due to the boundary condition (3.41) and the fact that since $x_1 < l_m \leq l_{n-1}$. Thus

$$\sigma(x_1, 0, t) = \sum_{n=0}^m \sigma^n(x_1, 0, t) = \sum_{n=0}^{m-1} \sigma^n(x_1, 0, t_n) + p^m(x_1) = 0$$

where t was replaced by t_n for $n = 0, 1, \dots, m-1$ since $\sigma^n(x_1, x_2, t)$ do not change on the time-interval $[t_n, \infty)$, and the last equality holds due to the definition (3.42) of the loading $p^m(x_1)$. Hence

$$\sigma(x_1, 0, t) = \begin{cases} \sigma^{ext}(x_1), & x_1 < 0 \\ 0, & 0 < x_1 < L(t) \end{cases} \quad 0 < t < T$$

For any time instance $t \geq T$, the stress fields σ^n do not depend on time t and their sum (3.39) satisfies the boundary condition (3.38) due to the same argument as for the case $t \in (0, T)$.

Thus, the formula (3.39) gives an approximate solution of the problem on a crack that start propagating at time $t = 0$ and stops at time $t = T$ with the crack tip position described by the law $x_1 = l(t)$, $t \in [0, T]$.

3.3.2 Problem of a suddenly stopped crack

In order to find the stress field σ^n , we need to solve the problem of a suddenly stopped crack: a semi-infinite crack $\{(x_1, 0) - \infty < x_1 < l_{n-1}\}$ in the stress-free unbounded plane, begins to grow in x_1 -direction at the time $t = t_{n-1}$ with the constant speed v_n and suddenly stops at the time $t = t_n$ at the point $x_1 = x_n$, while the crack faces are subjected to the loading

$$\sigma^n(x_1, 0, t) = p^n(x_1)H(x_1 - l_{n-1}), \quad x_1 < L(t)$$

Assume that the cracks keeps propagating for $t > t_n$ at the same velocity v_n , while its faces are subjected to auxiliary loads $q^n(x_1)$ for $l_n < x_1 < L_n(t)$, where $L_n(t) = l_n + v_n(t - t_n)$.

Then the stress intensity factors $K_I(t)$ and $K_{II}(t)$ are determined by

$$\begin{pmatrix} K_I(t) \\ K_{II}(t) \end{pmatrix} = \int_{l_{n-1}}^{l_n} W(x_1, t) \cdot p^n(x_1) dx_1 + \int_{l_n}^{L_n(t)} W(x_1, t) \cdot q^n(x_1) dx_1, \quad t > t_{n-1}$$

where W is the matrix of stress intensity factors for the fundamental solutions of the problem on propagation of semi-infinite crack at constant speed in a plane. To model a suddenly stopped crack, set $K_I(t) = K_{II}(t) = 0$ for $t > t_n$ (according to [39], zero stress intensity factors for $t > t_n$ implies that the displacement field $u(x_1, 0, t)$ is continuous for $x_1 > l_n$).

Then the vector q^n is to be determined from the system of integral equations

$$\begin{aligned} 0 &= \int_{l_{n-1}}^{l_n} W(x_1, t) \cdot p^n(x_1) dx_1 \\ &+ \int_{l_n}^{L_n(t)} W(x_1, t) \cdot q^n(x_1) dx_1, \quad t > t_n \end{aligned} \quad (3.43)$$

Notice that

$$\sigma^n(x_1, 0, t) = q^n(x_1), \quad x_1 > l_n$$

is the stress distribution ahead of the crack after the crack has stopped. For future references, we write the values $\sigma^n(x_1, 0, t_n)$ as they are used in (3.42):

$$\sigma^n(x_1, 0, t_n) = \begin{cases} 0, & -\infty < x_1 < l_{n-1} \\ p^n(x_1), & l_{n-1} < x_1 < l_n \\ q^n(x_1), & l_n < x_1 < \infty \end{cases} \quad (3.44)$$

where p^n is defined in (3.42) and q^n is the solution of the system of integral equations (3.43).

In the case of a crack propagation in a plane (see Section 3.2), the matrix W is a diagonal matrix with the stress intensity factors K_I and K_{II} determined by (3.36) for the fundamental solutions. Thus, the system (3.43) is split into two separate equations. Let us consider one of them,

$$0 = \int_{l_{n-1}}^{l_n} \frac{p_{22}^n(x_1) dx_1}{\sqrt{v_n t - x_1}} + \int_{l_n}^{L_n(t)} \frac{q_{22}^n(x_1) dx_1}{\sqrt{v_n t - x_1}}, \quad t > t_n$$

By making the substitution $x_1 = v_n \tau' + l_n$ and $t = \tau + t_n$, we derive Volterra integral equation

$$0 = \int_{t_{n-1}-t_n}^0 \frac{p_{22}^n(v_n \tau' + l_n)}{\sqrt{\tau - \tau'}} d\tau' + \int_0^\tau \frac{q_{22}^n(v_n \tau' + l_n)}{\sqrt{\tau - \tau'}} d\tau', \quad \tau > 0 \quad (3.45)$$

which can be solved by applying Laplace transform. The solution of (3.45) is given by

$$\begin{aligned} q_{22}^n(v_n \tau + l_n) = & \frac{1}{2\pi} \int_0^\tau \int_{t_{n-1}-t_n}^0 \frac{p_{22}^n(v_n \xi + l_n)}{\sqrt{(\tau - \tau')(\tau' - \xi)^3}} d\tau' d\xi \\ & - \frac{1}{\pi\sqrt{\tau}} \int_{t_{n-1}-t_n}^0 \frac{p_{22}^n(v_n \tau' + l_n)}{\sqrt{-\tau'}} d\tau', \quad \tau > 0 \end{aligned}$$

3.3.3 Inverse problem of a crack propagation

So far, we assumed the function $l(t)$ (and the function $L(t)$ respectively) is known. However, in most cases the motion of the crack tip is what needs to be found. Let the crack tip motion be described by the law $x_1 = L(t)$, where $L(t)$ is an unknown piecewise linear continuous function with vertexes at the points (t_n, l_n) , $n = 0, 1, \dots$, and $L(t) = 0$ for $t < 0$. Given the time instances t_n , we need to determine the corresponding positions l_n of the crack tip.

Let us adopt one of the crack propagation criteria. For instance, assume that the crack propagates when its energy release rate G near the crack tip equals to some constant, say Γ . Typically, the energy release rate G depends on the speed v of the crack, stress intensity factors $K_I(t, v)$ and $K_{II}(t, v)$, and the material parameters. Thus

$$G(v(t), K_I(t, v(t)), K_{II}(t, v(t))) = \Gamma, \quad t > 0$$

Now we are able to construct the function $L(t)$. Assume that for some positive integer n , we know the values l_j for $j = 0, 1, \dots, n$ and v_j for $j = 1, 2, \dots, n$. That is, the function $L(t)$ is known on the time-interval $(0, t_n]$. In order to construct $L(t)$ for $t_n < t < t_{n+1}$, we have to determine velocity v_{n+1} . It can be found from the propagation criterion, specifically we will solve the equation

$$G(v_{n+1}, K_I(t_n, v_{n+1}), K_{II}(t_n, v_{n+1})) = \Gamma \quad (3.46)$$

with respect to the unknown v_{n+1} .

The only terms in the sum (3.39) that have discontinuities at the point $x_1 = l_n$ are the stress fields σ^n and σ^{n+1} since the tensor σ^n corresponds to the crack that stops propagation at the point $x_1 = l_n$ while σ^{n+1} corresponds to the crack that starts propagation at $x_1 = l_n$. Thus

$$K_{I,II}(t_n, v_{n+1}) = K_{I,II}^n(t_n) + K_{I,II}^{n+1}(t_n, v_{n+1}) \quad (3.47)$$

The values $K_{I,II}^n(t_n)$ are the stress intensity factors of σ^n , which do not depend on velocity v_{n+1} and can be determined from (3.44) for $n = 1, 2, \dots$,

$$\begin{pmatrix} K_I^n(l_n) \\ K_{II}^n(l_n) \end{pmatrix} = \sqrt{2\pi} \lim_{x_1 \rightarrow l_n^+} \left[\sqrt{x_1 - l_n} q^n(x_1) \right] \quad (3.48)$$

In the case $n = 0$,

$$\begin{pmatrix} K_I^0(l_0) \\ K_{II}^0(l_0) \end{pmatrix} = \sqrt{2\pi} \lim_{x_1 \rightarrow 0^+} \left[\sqrt{x_1} \sigma^0(x_1, 0, t_0) \right] \quad (3.49)$$

The values $K_{I,II}^{n+1}(t_n, v_{n+1})$ can be determined by the formula

$$\begin{pmatrix} K_I^{n+1}(t, v_{n+1}) \\ K_{II}^{n+1}(t, v_{n+1}) \end{pmatrix} = \int_{l_n}^{l_n + v_{n+1}(t - t_n)} W(x_1 - l_n, t, v_{n+1}) \cdot p^{n+1}(x_1) dx_1$$

by taking the limit $t \rightarrow t_n$. Since $W(x_1 - l_n, t, v_{n+1})$ has a square-root discontinuity at $x_1 = l_n + v_{n+1}(t - t_n)$ and p^{n+1} has a square-root discontinuity at $x_1 = l_n$, the limit of $K_{I,II}^{n+1}$ as $t \rightarrow t_n^+$ is equal to

$$\begin{pmatrix} K_I^{n+1}(t_n, v_{n+1}) \\ K_{II}^{n+1}(t_n, v_{n+1}) \end{pmatrix} = -w(0, t_n^+, v_{n+1}) \cdot \begin{pmatrix} K_I^n(l_n) \\ K_{II}^n(l_n) \end{pmatrix} \quad (3.50)$$

where

$$w(x, t, v) = \sqrt{\frac{\pi}{2}(vt - x)} W(x, t, v)$$

The formulas (3.48), (3.49), and (3.50), and the identity (3.47) imply

$$\begin{pmatrix} K_I(l_n, v_{n+1}) \\ K_{II}(l_n, v_{n+1}) \end{pmatrix} = [I - w(0, t_n^+, v_{n+1})] \cdot \begin{pmatrix} K_I^n(l_n) \\ K_{II}^n(l_n) \end{pmatrix} \quad (3.51)$$

where I is the identity matrix. By plugging the stress intensity factors $K_{I,II}(l_n, v_{n+1})$ into the equation (3.46) and solving it, we determine the velocity v_{n+1} .

Now describe how a piece-wise linear continuous function $L(t)$ can be constructed. On the first step, we choose the partition $\{t_n\}_{n=0}^{\infty}$ of the time interval $[0, \infty)$ with $t_0 = 0$. Assume that for $t < 0$, the crack lies on the negative semi-axis $\{-\infty < x_1 < 0, x_2 = 0\}$, that is $l_0 = 0$ is the position of the crack tip at the time $t = 0$. Let $\sigma^0(x_1, x_2)$ be the stress distribution of the corresponding static problem. Then the stress intensity factors $K_{I,II}(0, v_1)$ of $\sigma(x_1, x_2, t_0)$ as $x_1 \rightarrow 0$ are determined from (3.51), where $n = 0$ and $K_{I,II}^0(0)$ are the stress intensity factors of $\sigma^0(x_1, x_2)$. Notice that $K_{I,II}(0, v_1)$ depend on unknown velocity v_1 through the matrix $w(0, 0^+, v_1)$. It is interesting to notice that the off-diagonal components of $w(0, 0^+, v_1)$ are equal to zero; thus, for $n = 0$ the formula (3.51) is analogous to its counterpart for a crack propagation in a plane [39]. Given the stress intensity factors $K_{I,II}(0, v_1)$, we determine the velocity v_1 from the equation (3.46) for $n = 0$ and calculate the next position of the crack as $l_1 = v_1 t_1$.

On the second step, we know the position of the crack l_1 at the time instance t_1 and the stress intensity factors $K_{I,II}^1(l_1)$ determined by the formula (3.48) for $n = 1$, where $q^1(x_1)$ is the solution of the system of integral equations (3.43). In order to find velocity v_2 , we solve the equation (3.46) for $n = 1$ with respect to v_2 , where the stress intensity factors $K_{I,II}(t_1, v_2)$ are defined by (3.51). Then we calculate the next position of the crack: $l_2 = l_1 + v_2(t_2 - t_1)$.

On the third step, given l_2 and $K_{I,II}^2(l_2)$, we determine v_3 and l_3 , and thus continue iteratively.

Chapter 4

Steady-State Crack Propagation in a Half-plane

In this chapter, we will study the boundary effects on a crack propagating with constant subsonic speed in the direction parallel to the boundary of a solid. The static problem for a semi-infinite crack parallel to the boundary of a half-plane was analyzed by A.N. Zlatin and A.A. Khrapkov [86]. They reduced the problem to a vector Riemann–Hilbert problem of the second order and derived a closed-form solution, by explicitly constructing the Wiener–Hopf factorization of the matrix coefficient. The steady-state problem for a plane with a semi-infinite crack $\{(x_1, 0) : -\infty < x_1 < 0\}$ driven by moving normal and tangential forces applied to the crack faces, was considered by J.W. Craggs [31]. Because of the symmetry, Craggs’ problem admits decoupling and can be solved in closed form by a variety of methods including the factorization method for a scalar Riemann–Hilbert problem, the Mellin transform method which bypasses the Riemann–Hilbert problem, and the method of orthogonal polynomials. Many researchers analyzed different aspects of the Craggs model problem and considered its generalizations. Surveys of the results were given by L.B. Freund [39] and K.B. Broberg [24]. The problem considered in this chapter, was first solved by Y. Antipov and the author in [17].

4.1 Vector Riemann–Hilbert problem and Orthogonal Polynomials

Let us start with describing the model problem for a half-plane $\{(x_1, x_2) : -\infty < x_1 < \infty, -\infty < x_2 < \delta\}$, $\delta > 0$, containing a crack $\{(x_1, 0) : -\infty < x_1 < vt\}$ driven by normal and tangential traction loading applied to the crack faces (see Figure 4.1). It is assumed that the loading moves with the crack at the same speed v . By employing the method of integral transformations, we map the boundary value problem for the governing system of partial differential equations to a vector Riemann–Hilbert problem with the matrix coefficient

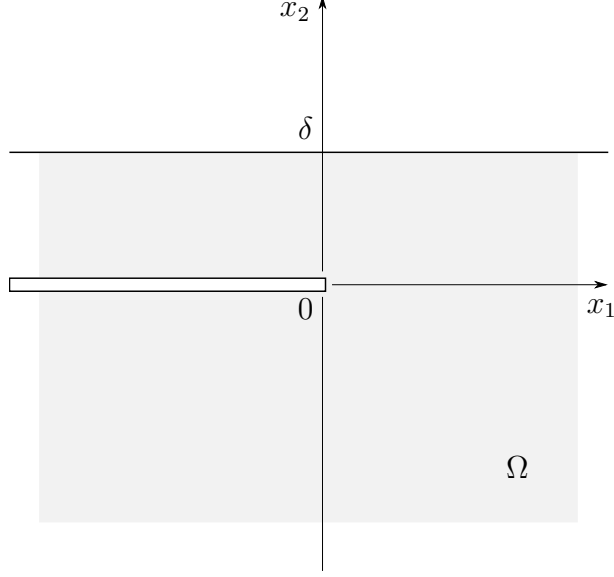


Figure 4.1: Semi-infinite crack parallel to the boundary of a half-plane.

$A(z) = a(z)I + b(z)J(z)$, where $a(z)$, $b(z)$ are Hölder continuous functions on the real axis \mathbb{R} , I is the identity matrix, and

$$J(z) = \begin{pmatrix} 1 & -i\alpha_1 \tanh(\alpha_0 z) \\ i\alpha_2 \tanh(\alpha_0 z) & -1 \end{pmatrix}, \quad (4.1)$$

with real nonzero constants α_1 , α_2 .

Next, we transform the Riemann–Hilbert problem into a system of two singular integral equations on the finite interval $(-1, 1)$. We seek its solution in the Hilbert space $L_{2,\rho}(-1, 1)$ of square integrable functions with the weight $\rho(z) = (1+z)^{1/2}(1-z)^{-1/2}$. By representing the unknown functions as a series over elements of an orthonormal basis on $L_{2,\rho}(-1, 1)$, we reduce the system of integral equations to an infinite system of linear algebraic equations that is solved numerically.

Finally, we derive the stress intensity factors K_I , K_{II} for the fundamental problem. In addition, we determine the energy released as the crack extends from x_1 to $x_1 + \delta x_1$, and δx_1 is small. Then, we apply the Griffith criterion of propagation and derive a Willis-type formula for a mode-I,II semi-infinite crack propagating along the boundary of a half-plane, similar to the criterion of steady-state propagation of a semi-infinite crack in a plane, derived

by Willis [85]. We also discuss some numerical results obtained for the stress intensity factors and the Griffith criterion.

4.1.1 Derivation of the vector Riemann–Hilbert problem

A semi-infinite crack that occupies the region $\{(x_1, 0, x_3) : -\infty < x_1 < vt, |x_3| < \infty\}$ propagates in the direction parallel to the boundary of an elastic half-space $\mathbb{R}_+^3 = \{(x_1, x_2, x_3) : |x_1| < \infty, -\infty < x_2 < \delta, |x_3| < \infty\}$ where $\delta > 0$. The boundary of the half-space is assumed to be free of traction. The speed v is constant and does not exceed the Rayleigh wave speed c_R for the elastic isotropic homogeneous solid whose density and the Lamé constants are ρ , λ , and μ respectively. The faces of the crack are subjected to plane-strain loading

$$\sigma_{j2}(x_1, x_2, t) = \sigma_{j2}^\circ(x_1 - vt), \quad -\infty < x_1 < vt, \quad x_2 = 0^\pm, \quad j = 1, 2. \quad (4.2)$$

In the case of the plain-strain deformation that does not change in x_3 -direction, the displacement vector and stress tensor are expressed (see Chapter 3) in terms of the dynamic potentials ϕ and ψ that satisfy the system of equations identical to (3.2) in the spacial region $\Omega = \mathbb{R}_+^2 \setminus S(t)$, where $\mathbb{R}_+^2 = \{(x_1, x_2) : |x_1| < \infty, -\infty < x_2 < \delta\}$ is a half-plane and $S(t) = \{(x_1, 0) : -\infty < x_1 < vt\}$ a semi-infinite crack growing at constant speed v (see Figure 4.1).

We introduce the coordinate system (x, y) moving with the crack so that $x = x_1 - vt$ and $y = x_2$. Since both the configuration of the body and the traction distribution are time invariant in the new coordinate system, we seek the *steady state solution* of the problem, which does not depend on time t in (x, y) -coordinate system. The latter permits to “drop” the temporal variable t from all equations. In this case, the governing equations (3.2) are simplified to

$$\alpha^2 \frac{\partial^2 \phi}{\partial x^2} + \frac{\partial^2 \phi}{\partial y^2} = 0, \quad \beta^2 \frac{\partial^2 \psi}{\partial x^2} + \frac{\partial^2 \psi}{\partial y^2} = 0 \quad (4.3)$$

where $\alpha = \sqrt{1 - v^2/c_l^2}$, $\beta = \sqrt{1 - v^2/c_s^2}$. After applying Fourier transform

$$\hat{\phi}(z, y) = \int_{-\infty}^{\infty} \phi(x, y) e^{izx} dx, \quad \hat{\psi}(z, y) = \int_{-\infty}^{\infty} \psi(x, y) e^{izx} dx \quad (4.4)$$

to the differential equations (4.3), we find the solution of the corresponding ordinary differential equation with respect to y -variable. The bounded solution on the semi-axis $-\infty < y < 0$ is given by

$$\hat{\phi}(z, y) = C_0(z)e^{\alpha|z|y}, \quad \hat{\psi}(z, y) = D_0(z)e^{\beta|z|y}, \quad z \in \mathbb{R} \quad (4.5)$$

where C_0 and D_0 are two arbitrary functions independent of y . On the interval $0 < y < \delta$, the bounded solution takes the form

$$\begin{aligned} \hat{\phi}(z, y) &= C_1(z) \cosh(\alpha zy) + C_2(z) \sinh(\alpha zy) \\ \hat{\psi}(z, y) &= D_1(z) \cosh(\beta zy) + D_2(z) \sinh(\beta zy) \end{aligned} \quad z \in \mathbb{R} \quad (4.6)$$

The functions $C_j : \mathbb{R} \rightarrow \mathbb{C}$ and $D_j : \mathbb{R} \rightarrow \mathbb{C}$ ($j = 0, 1, 2$) are to be determined from the boundary conditions

$$\begin{aligned} \sigma_{12}(x, \delta) &= \sigma_{22}(x, \delta) = 0, & -\infty < x < \infty \\ \sigma_{12}(x, 0^\pm) &= \sigma_{12}^\circ(x), \quad \sigma_{22}(x, 0^\pm) = \sigma_{22}^\circ(x), & x < 0 \end{aligned} \quad (4.7)$$

where the first line expresses the fact that the body is free of tension on the boundary $y = \delta$, while the second line is derived from (4.2). Recall that the stress components are related to the potentials ϕ and ψ through the identities (3.6). After applying Fourier transform to the corresponding equations in (3.6) and to the boundary conditions (4.7), we derive the equations

$$\begin{aligned} \frac{d^2 \hat{\psi}}{dy^2} + z^2 \hat{\psi} - 2iz \frac{d\hat{\phi}}{dy} &= 0 & y = \delta \\ \frac{c_l^2}{c_s^2} \frac{d^2 \hat{\phi}}{dy^2} + z^2 \left(2 - \frac{c_l^2}{c_s^2} \right) \hat{\phi} + 2iz \frac{d\hat{\psi}}{dy} &= 0, & y = \delta \\ \frac{d^2 \hat{\psi}}{dy^2} + z^2 \hat{\psi} - 2iz \frac{d\hat{\phi}}{dy} &= \Sigma_1^+(z) + \Sigma_1^-(z), & y = 0^\pm \\ \frac{c_l^2}{c_s^2} \frac{d^2 \hat{\phi}}{dy^2} + z^2 \left(2 - \frac{c_l^2}{c_s^2} \right) \hat{\phi} + 2iz \frac{d\hat{\psi}}{dy} &= \Sigma_2^+(z) + \Sigma_2^-(z), & y = 0^\pm \end{aligned} \quad (4.8)$$

where the Fourier transforms

$$\Sigma_j^+(z) = \frac{1}{\mu} \int_0^\infty \sigma_{j2}(x, 0) e^{izx} dx, \quad \Sigma_j^-(z) = \frac{1}{\mu} \int_{-\infty}^0 \sigma_{j2}^\circ(x) e^{izx} dx, \quad j = 1, 2$$

considered as functions of complex variable z , are analytic in the upper half-plane $\mathbb{C}^+ = \{z : \text{Im } z > 0\}$ and in the lower half-plane $\mathbb{C}^- = \{z : \text{Im } z < 0\}$ respectively, provided that $\sigma_{j2}(\cdot, 0)$ and σ_{j2}° are integrable on the corresponding intervals $(0, \infty)$ and $(-\infty, 0)$. Notice that the functions Σ_1^+ and Σ_2^+ are unknown since the stress components $\sigma_{12}(x, 0)$ and $\sigma_{22}(x, 0)$ in front of the crack tip ($x > 0$) are not determined yet. These functions Σ_1^+ and Σ_2^+ will be found later from a Riemann–Hilbert problem.

Plugging the functions $\hat{\phi}$ and $\hat{\psi}$ defined by (4.5) and (4.6), into the boundary conditions (4.8), we find the unknown functions C_j and D_j , $j = 0, 1, 2$:

$$\begin{aligned} C_0(z) &= \frac{1 + \beta^2}{z^2 R_1} \Sigma_2^+(z) - \frac{2i\beta \operatorname{sgn}\{z\}}{z^2 R_1} \Sigma_1^+(z) \\ D_0(z) &= \frac{1 + \beta^2}{z^2 R_1} \Sigma_1^+(z) + \frac{2i\alpha \operatorname{sgn}\{z\}}{z^2 R_1} \Sigma_2^+(z) \end{aligned}$$

$$\begin{aligned} C_1(z) &= - \left\{ 2\alpha\beta(1 + \beta^2)(3 + \beta^2) [\cosh(\beta\delta z) \cosh(\alpha\delta z) - 1] \right. \\ &\quad \left. + [(1 + \beta^2)^3 + 8\alpha^2\beta^2] \sinh(\alpha\delta z) \sinh(\beta\delta z) \right\} \frac{\Sigma_1^+(z)}{z^2 \Delta(z)} \end{aligned}$$

$$\begin{aligned} C_2(z) &= - (1 - \beta^2) \left\{ 4\alpha\beta \cosh(\beta\delta z) \sinh(\alpha\delta z) \right. \\ &\quad \left. - (1 + \beta^2)^2 \cosh(\alpha\delta z) \sinh(\beta\delta z) \right\} \frac{\Sigma_2^+(z)}{z^2 \Delta(z)} \end{aligned}$$

$$\begin{aligned} D_1(z) &= \left\{ -2\alpha\beta(1 + \beta^2)(3 + \beta^2) [\cosh(\beta\delta z) \cosh(\alpha\delta z) - 1] \right. \\ &\quad \left. + [(1 + \beta^2)^3 + 8\alpha^2\beta^2] \sinh(\alpha\delta z) \sinh(\beta\delta z) \right\} \frac{\Sigma_1^+(z)}{z^2 \Delta(z)} \end{aligned}$$

$$\begin{aligned} D_2(z) &= - (1 - \beta^2) \left\{ 4\alpha\beta \cosh(\alpha\delta z) \sinh(\beta\delta z) \right. \\ &\quad \left. - (1 + \beta^2)^2 \cosh(\beta\delta z) \sinh(\alpha\delta z) \right\} \frac{\Sigma_2^+(z)}{z^2 \Delta(z)} \end{aligned}$$

where

$$\begin{aligned} \Delta(z) &= R_1^2 \sinh^2 \left(\frac{\alpha + \beta}{2} \delta z \right) - R_2^2 \sinh^2 \left(\frac{\alpha - \beta}{2} \delta z \right) \\ R_1 &= (1 + \beta^2)^2 - 4\alpha\beta, \quad R_2 = (1 + \beta^2)^2 + 4\alpha\beta \end{aligned}$$

Thus, the Fourier transforms $\hat{\phi}$ and $\hat{\psi}$ of wave potentials are given by the formulas (4.5), (4.6), (4.7). In order to determine the unknown functions Σ_1^+ and Σ_2^+ in the identities above,

let us consider discontinuities of the derivative ∂_x of the displacement components u_1 and u_2 across x -axis. Define the auxiliary functions

$$\chi_j(x) = \frac{\partial u_j}{\partial x}(x, 0^+) - \frac{\partial u_j}{\partial x}(x, 0^-), \quad j = 1, 2, \quad -\infty < x < \infty, \quad (4.9)$$

Since the displacement components are continuous in front of the crack tip ($x > 0$), the functions χ_1 and χ_2 vanish for positive values of the argument. Therefore, their Fourier transforms

$$X_j^-(z) = i \int_{-\infty}^0 \chi_j(x) e^{izx} dx, \quad j = 1, 2$$

are analytic in the lower half-plane \mathbb{C}^- . Applying the Fourier transforms to the identities (4.9) and using the formulas (3.6), we derive equations

$$\begin{aligned} \left(\frac{d\hat{\psi}}{dy} - iz\hat{\phi} \right)_{y=0^+} - \left(\frac{d\hat{\psi}}{dy} - iz\hat{\phi} \right)_{y=0^-} &= \frac{X_1^-(z)}{z} \\ \left(\frac{d\hat{\phi}}{dy} + iz\hat{\psi} \right)_{y=0^+} - \left(\frac{d\hat{\phi}}{dy} + iz\hat{\psi} \right)_{y=0^-} &= \frac{X_2^-(z)}{z} \end{aligned} \quad z \in \mathbb{R}$$

which, after using the formulas (4.5), (4.6) for $\hat{\phi}$, $\hat{\psi}$, and the expressions for C_j , D_j ($j = 0, 1, 2$), take the form of a vector Riemann–Hilbert problem:

$$\begin{pmatrix} \Sigma_1^+(z) \\ \Sigma_2^+(z) \end{pmatrix} = A(z) \begin{pmatrix} \beta^{-1} X_1^-(z) \\ \alpha^{-1} X_2^-(z) \end{pmatrix} - \begin{pmatrix} \Sigma_1^-(z) \\ \Sigma_2^-(z) \end{pmatrix}, \quad -\infty < z < +\infty, \quad (4.10)$$

where $\Sigma_{1,2}^+$ are functions analytic in the upper half-plane \mathbb{C}^+ , while $X_{1,2}^-$ and $\Sigma_{1,2}^-$ are analytic in the lower half-plane \mathbb{C}^- . At the infinite point, all the functions $\Sigma_{1,2}^\pm$ and $X_{1,2}^-$ are assumed to be bounded. The matrix coefficient A has the structure $A = aI + bJ$, where

$$\begin{aligned} a(z) &= \frac{e^{-(\alpha+\beta)\delta|z|}}{2(1-\beta^2)} \left[R_1 \sinh(\alpha+\beta)\delta z + \frac{2\Delta(z) \operatorname{sgn} z}{R_1} \right] \\ b(z) &= -\frac{R_2}{1-\beta^2} e^{-(\alpha+\beta)\delta|z|} \sinh \frac{1}{2}(\alpha-\beta)\delta z \\ J(z) &= \begin{pmatrix} \cosh \frac{1}{2}(\alpha-\beta)\delta z & -\frac{4i\alpha}{R_1}(1+\beta^2) \sinh \frac{1}{2}(\alpha-\beta)\delta z \\ \frac{4i\beta}{R_1}(1+\beta^2) \sinh \frac{1}{2}(\alpha-\beta)\delta z & -\cosh \frac{1}{2}(\alpha-\beta)\delta z \end{pmatrix} \end{aligned} \quad (4.11)$$

and I is the unit 2×2 matrix. The matrix A does not admit a Wiener-Hopf factorization by the methods currently available in the literature. Although it can be represented in the form (2.28) and it is possible to transform the vector problem (4.10) to a scalar Riemann–Hilbert problem on a Riemann surface, the corresponding Riemann surface would have infinitely many branch points and the problem can be solved only approximately (see Section 2.3.1).

Evaluating of the total index κ of the Riemann–Hilbert problem (4.10), shows that $\kappa = 2$ if the real axis \mathbb{R} is transformed to pass under the origin $x = 0$ (see the contour $\mathbb{R}_{-\varepsilon}$ introduces in Section 3.1.2). Since the problem does not admit the closed-form solution, evaluating of the partial indexes currently presents a certain difficulty. However, the fact that in the case $\delta \rightarrow \infty$, the matrix $A(z)$ converges to a diagonal piece-wise constant matrix

$$A(z) = \operatorname{sgn} z \frac{R_1}{2(1 - \beta^2)} I$$

and the corresponding two partial indexes κ_1 and κ_2 are equal to 1, makes us to suggest that $\kappa_1 = \kappa_2 = 1$ for finite values of δ as well (however, justification of this suggestion is a separate and challenging problem on its own, so it is left beyond the scope of the dissertation). In the case $\kappa_1 = \kappa_2 = 1$, the solution of the Riemann–Hilbert problem is stable [42], meaning the an approximate solution is expected to converge to the exact solution of the problem, and depends on two arbitrary constants that can be determined from the condition $X_1^-(0) = X_2^-(0) = 0$ (see the paragraph after formula (3.32)). Notice that in the next section, this condition is satisfied due to the choice of a class of the solution (4.16).

4.1.2 System of integral equations

Since there are no known method that would allow for explicit construction of a Wiener–Hopf factorization of the matrix coefficient A in the closed form, we will find an approximate solution of the Riemann–Hilbert problem (4.10) based on the method described in Section 2.3.2. Let us transform the equation (4.10) to a system of singular integral equations on a semi-infinite interval and develop an efficient numerical scheme for its solution.

By applying the inverse Fourier transform to the equation (4.10) and using the convolution theorem, we find the following expressions valid for $-\infty < x < \infty$:

$$\begin{aligned} -\frac{\pi\beta}{\gamma}\sigma_{12}(x, 0) &= \int_{-\infty}^0 \left[\frac{1}{\xi - x} + k_{11}(\xi - x) \right] \chi_1(\xi) d\xi + \int_{-\infty}^0 k_{12}(\xi - x) \chi_2(\xi) d\xi \\ -\frac{\pi\alpha}{\gamma}\sigma_{22}(x, 0) &= \int_{-\infty}^0 k_{21}(\xi - x) \chi_1(\xi) d\xi + \int_{-\infty}^0 \left[\frac{1}{\xi - x} + k_{22}(\xi - x) \right] \chi_2(\xi) d\xi \end{aligned} \quad (4.12)$$

where

$$\begin{aligned} k_{11}(x) &= \frac{R(1-R)x}{2[x^2 + 4\alpha^2\delta^2]} - \frac{R(1+R)x}{2[x^2 + 4\beta^2\delta^2]} + \frac{(R^2-1)x}{x^2 + (\alpha + \beta)^2\delta^2} \\ k_{22}(x) &= -\frac{R(1+R)x}{2[x^2 + 4\alpha^2\delta^2]} + \frac{R(1-R)x}{2[x^2 + 4\beta^2\delta^2]} + \frac{(R^2-1)x}{x^2 + (\alpha + \beta)^2\delta^2} \\ k_{12}(x) &= \frac{4R(1+\beta^2)\beta}{R_1} \left(\frac{\alpha}{x^2 + 4\alpha^2\delta^2} + \frac{\beta}{x^2 + 4\beta^2\delta^2} - \frac{\alpha + \beta}{x^2 + (\alpha + \beta)^2\delta^2} \right) \\ k_{21}(x) &= -\frac{\alpha}{\beta}k_{12}(x), \quad R = \frac{R_2}{R_1}, \quad \gamma = \frac{\mu R_1}{2(1-\beta^2)} \end{aligned}$$

Due to the fact that the stress components $\sigma_{12}(x, 0)$ and $\sigma_{22}(x, 0)$ are prescribed for the values x on the negative semi-axis $(-\infty, 0)$ (see the boundary conditions (4.7)), the equations (4.12) yield the system of singular integral equations with respect to the functions χ_1 and χ_2 on the interval $(-\infty, 0)$:

$$\begin{aligned} \int_{-\infty}^0 \left[\frac{1}{\xi - x} + k_{11}(\xi - x) \right] \chi_1(\xi) d\xi + \int_{-\infty}^0 k_{12}(\xi - x) \chi_2(\xi) d\xi &= -\pi f_1(x) \\ \int_{-\infty}^0 k_{21}(\xi - x) \chi_1(\xi) d\xi + \int_{-\infty}^0 \left[\frac{1}{\xi - x} + k_{22}(\xi - x) \right] \chi_2(\xi) d\xi &= -\pi f_2(x) \end{aligned} \quad (4.13)$$

where $f_1(x) = \sigma_{12}^o(x)\beta/\gamma$ and $f_2(x) = \sigma_{22}^o(x)\alpha/\gamma$.

As $\delta \rightarrow \infty$ (the half-plane becomes an unbounded plane), the kernels k_{12} and k_{21} vanish so the system (4.13) decouples. Then, its closed form solution is given by

$$\chi_j(x) = \frac{1}{\pi\sqrt{-x}} \int_{-\infty}^0 \frac{\sqrt{-\xi} f_j(\xi) d\xi}{\xi - x}, \quad -\infty < x < 0, \quad j = 1, 2 \quad (4.14)$$

In the case of a finite value δ , the system can be solved numerically by an approximate scheme based on the method of orthogonal polynomials (see Section 2.3.2).

First, let us transform the interval $(-\infty, 0)$ into the interval $(-1, 1)$ by making substitutions $\xi = (\xi' + 1)/(\xi' - 1)$, $x = (x' + 1)/(x' - 1)$, and introducing new functions $\tilde{\chi}_j$ and \tilde{f}_j as

follows:

$$(1 - x')\tilde{\chi}_j(x') = \chi_j(x), \quad (1 - x')\tilde{f}_j(x') = f_j(x), \quad j = 1, 2. \quad (4.15)$$

Since in the problem on a semi-infinite crack in an unbounded plane [31], the displacement components vanish as $O(|x|^{1/2})$ at the origin $x = 0$ and as $O(|x|^{-1/2})$ as $x \rightarrow -\infty$, the same behavior is assumed the displacement components in a half-plane. The latter results to the following behavior of the functions χ_1 and χ_2 on the negative semi-axis $(-\infty, 0)$:

$$\chi_j(x) = O(|x|^{-1/2}), \quad x \rightarrow 0^-; \quad \chi_j(x) = O(|x|^{-3/2}), \quad x \rightarrow -\infty \quad (4.16)$$

When written for the new functions $\tilde{\chi}_1$ and $\tilde{\chi}_2$ defined in (4.15), this yield the identities

$$\tilde{\chi}_j(x') = O(|1 + x'|^{-1/2}), \quad x' \rightarrow -1; \quad \tilde{\chi}_j(x') = O(|1 - x'|^{1/2}), \quad x' \rightarrow 1 \quad (4.17)$$

Let $\tilde{P}_n^{1/2, -1/2}$ be Jacobi polynomials scaled so that they form an orthonormal basis in the space of square integrable functions on the interval $(-1, 1)$. We represent the functions $\tilde{\chi}_1$ and $\tilde{\chi}_2$ in the form

$$\tilde{\chi}_j(x') = \sqrt{\frac{1 - x'}{1 + x'}} \sum_{m=0}^{\infty} a_m^{(j)} \tilde{P}_m^{1/2, -1/2}(x'), \quad j = 1, 2, \quad x' \in (-1, 1) \quad (4.18)$$

where the coefficients $a_n^{(j)}$ are to be determined. The original functions $\chi_1(x)$ and $\chi_2(x)$ may be put into the form

$$\chi_j(x) = \frac{2}{(1 - x)\sqrt{-x}} \sum_{m=0}^{\infty} a_m^{(j)} \hat{P}_m^{1/2, -1/2} \left(\frac{x + 1}{x - 1} \right), \quad j = 1, 2, \quad x \in (-\infty, 0) \quad (4.19)$$

By employing the spectral relation

$$\int_{-1}^1 \sqrt{\frac{1 - \xi'}{1 + \xi'}} \frac{\tilde{P}_m^{1/2, -1/2}(\xi') d\xi'}{\xi' - x'} = -\pi \hat{P}_m^{-1/2, 1/2}(x'), \quad x' \in (-1, 1) \quad (4.20)$$

and the orthogonality of the polynomials,

$$\int_{-1}^1 \sqrt{\frac{1 + x'}{1 - x'}} \tilde{P}_m^{-1/2, 1/2}(x') \tilde{P}_n^{-1/2, 1/2}(x') dx' = \delta_{mn}, \quad n, m = 0, 1, \dots \quad (4.21)$$

(δ_{mn} is the Kronecker symbol), we transform the system of integral equations into an infinite algebraic system

$$a_n^{(j)} + \sum_{m=0}^{\infty} [c_{nm}^{(j,j)} a_m^{(j)} + c_{nm}^{(j,3-j)} a_m^{(3-j)}] = b_n^{(j)}, \quad n = 0, 1, \dots; j = 1, 2. \quad (4.22)$$

Here,

$$c_{nm}^{(j,l)} = \frac{2}{\pi} \int_{-1}^1 \int_{-1}^1 \sqrt{\frac{1+x'}{(1-x')^3}} \frac{\tilde{P}_n^{-1/2,1/2}(x') \tilde{P}_m^{1/2,-1/2}(\xi')}{\sqrt{1-\xi'^2}} k_{jl}(\xi-x) d\xi' dx',$$

$$b_n^{(j)} = - \int_{-1}^1 \sqrt{\frac{1+x'}{(1-x')^3}} \tilde{P}_n^{-1/2,1/2}(x') f_j(x) dx' \quad (4.23)$$

In order to compute the coefficients $c_{nm}^{(j,l)}$, we rearrange the integrands as

$$\sqrt{\frac{1+x'}{(1-x')^3}} \frac{k_{jj}(\xi-x)}{\sqrt{1-\xi'^2}} = \sqrt{\frac{1+x'}{1-x'}} \sqrt{\frac{1-\xi'}{1+\xi'}} \hat{k}_{jj}(\xi', x'), \quad j = 1, 2,$$

$$\sqrt{\frac{1+x'}{(1-x')^3}} \frac{k_{12}(\xi-x)}{\sqrt{1-\xi'^2}} = \sqrt{1-x'^2} \sqrt{\frac{1-\xi'}{1+\xi'}} \hat{k}_{12}(\xi', x'), \quad (4.24)$$

where

$$\hat{k}_{jj}(\xi', x') = (R^2 - 1) \Sigma_1(\xi', x'; \alpha + \beta) + (-1)^j [r_j \Sigma_1(\xi', x'; 2\beta) - r_{3-j} \Sigma_1(\xi', x'; 2\alpha)], \quad j = 1, 2,$$

$$\hat{k}_{12}(\xi', x') = \frac{2R(1+\beta^2)\beta}{R_1} [\Sigma_0(\xi', x'; 2\alpha) + \Sigma_0(\xi', x'; 2\beta) - 2\Sigma_0(\xi', x'; \alpha + \beta)],$$

$$\hat{k}_{21}(\xi', x') = -\frac{\alpha}{\beta} \hat{k}_{12}(\xi', x'),$$

$$r_1 = \frac{R}{2}(1+R), \quad r_2 = \frac{R}{2}(1-R), \quad \Sigma_0(\xi', x'; \varepsilon) = \frac{\varepsilon(1-\xi')}{4(\xi'-x')^2 + [\varepsilon\delta(1-\xi')(1-x')]^2},$$

$$\Sigma_1(\xi', x'; \varepsilon) = \frac{2(x'-\xi')}{4(\xi'-x')^2 + [\varepsilon\delta(1-\xi')(1-x')]^2}, \quad (4.25)$$

and apply the Gaussian type quadrature formulas [6]

$$\int_{-1}^1 \sqrt{\frac{1+x'}{1-x'}} f(x') dx' = \frac{4\pi}{2M+1} \sum_{j=1}^M \cos^2 \phi_j f(\cos 2\phi_j),$$

$$\int_{-1}^1 \sqrt{1-x'^2} f(x') dx' = \frac{\pi}{M+1} \sum_{j=1}^M \sin^2 2\psi_j f(\cos 2\psi_j), \quad (4.26)$$

where

$$\phi_j = \frac{(2j-1)\pi}{2(2M+1)}, \quad \psi_j = \frac{j\pi}{2(M+1)}, \quad (4.27)$$

and M is the number of abscissas. Using the connection between the Chebyshev and the orthonormal Jacobi polynomials

$$\begin{aligned} \tilde{P}_n^{-1/2,1/2}(x') &= \sqrt{\frac{2}{\pi(x'+1)}} T_{2n+1} \left(\sqrt{\frac{x'+1}{2}} \right), \\ \tilde{P}_n^{1/2,-1/2}(x') &= \frac{1}{\sqrt{\pi}} U_{2n} \left(\sqrt{\frac{x'+1}{2}} \right), \end{aligned} \quad (4.28)$$

we derive

$$\begin{aligned} c_{nm}^{(j,j)} &= \frac{32(-1)^m}{(2M+1)^2} \sum_{j=1}^M \cos \phi_j \cos(2n+1)\phi_j \sum_{s=1}^M \cos \phi_s \cos(2m+1)\phi_s \hat{k}_{jj}(-\cos 2\phi_s, \cos 2\phi_j), \\ c_{nm}^{(1,2)} &= \frac{32(-1)^m}{(2M+1)(M+1)} \sum_{j=1}^M \sin^2 \psi_j \cos \psi_j \cos(2n+1)\psi_j \\ &\quad \times \sum_{s=1}^M \cos \phi_s \cos(2m+1)\phi_s \hat{k}_{12}(-\cos 2\phi_s, \cos 2\psi_j). \quad c_{nm}^{(2,1)} = -\frac{\alpha}{\beta} c_{nm}^{(1,2)}. \end{aligned} \quad (4.29)$$

The integrals $b_n^{(j)}$ can be written in the form

$$b_n^{(j)} = -\frac{1}{\sqrt{\pi}} \int_{-\infty}^0 \frac{1}{\sqrt{1-x}} T_{2n+1} \left(\sqrt{\frac{-x}{1-x}} \right) f_j(x) dx. \quad (4.30)$$

Their convergence is guaranteed if $f_j(x) \in L_1(-A, 0)$ for any finite $A > 0$, and $f_j(x) = o(|x|^{-1/2})$, $x \rightarrow -\infty$.

Show finally that if $\delta \rightarrow \infty$, then the solution of the infinite system tends to the closed-form solution (4.14) for the whole plane. When $\delta \rightarrow \infty$, then $c_{nm}^{(j,l)} \rightarrow 0$ and $a_m^{(j)} \rightarrow b_m^{(j)}$, that is if $\delta = \infty$, then

$$\tilde{\chi}_j(x') = -\sqrt{\frac{1-x'}{1+x'}} \int_{-1}^1 f_j(\xi) \sqrt{\frac{1+\xi'}{(1-\xi')^3}} \Lambda(\xi', x') d\xi', \quad (4.31)$$

where

$$\Lambda(\xi', x') = \sum_{m=0}^{\infty} \tilde{P}_m^{-1/2,1/2}(\xi') \tilde{P}_m^{1/2,-1/2}(x'). \quad (4.32)$$

To summarize this series, we employ the relations (4.28) and also the formula

$$\lim_{q \rightarrow 1^-} \sum_{m=0}^{\infty} q^{2m+1} \sin(2m+1)x = \frac{1}{2 \sin x}. \quad (4.33)$$

This gives us

$$\Lambda(\xi', x') = \frac{1}{\pi(\xi' - x')}, \quad (4.34)$$

and therefore,

$$\chi_j(x) = -\frac{1}{\pi} \sqrt{\frac{(1-x')^3}{1+x'}} \int_{-1}^1 f_j(\xi) \sqrt{\frac{1+\xi'}{(1-\xi')^3}} \frac{d\xi'}{\xi' - x'}, \quad (4.35)$$

where $x = (x' + 1)/(x' - 1)$, $\xi = (\xi' + 1)/(\xi' - 1)$. This formula, when rearranged, coincides with (4.14).

4.2 Properties of the Solution

In this section, we will discuss the stress intensity factors for the problem, its dependence on elastic parameters of the problem and construct Griffith criterion of the crack propagation.

4.2.1 Stress field near the tip of the crack

In order to evaluate the stress intensity factors, we analyze behavior of the stress components $\sigma_{12}(x + vt, 0)$, $\sigma_{22}(x + vt, 0)$ as $x \rightarrow 0^+$. From the integral equations (4.12), we have

$$\sigma_{22}(x + vt, 0) \sim -\frac{\gamma}{\pi\alpha} \int_{-\infty}^0 \frac{\chi_2(\xi) d\xi}{\xi - x}, \quad x \rightarrow 0^+. \quad (4.36)$$

since the kernels k_{ij} , $i, j = 1, 2$, are continuous on the real axis \mathbb{R} . After replacing the functions χ_j with $\tilde{\chi}_j$ according to the identities (4.15), and using the representation (4.18), the formula (4.36) becomes

$$\sigma_{22}(x + vt, 0) \sim \frac{\gamma(1-x')}{\pi\alpha} \sum_{m=0}^{\infty} a_m^{(2)} \int_{-1}^1 \sqrt{\frac{1-\xi'}{1+\xi'}} \hat{P}_m^{1/2, -1/2}(\xi') \frac{d\xi'}{\xi' - x'}. \quad (4.37)$$

The integrals in the right-hand side can be evaluated using the following relation for the Jacobi polynomials:

$$\begin{aligned} \int_0^1 \sqrt{\frac{\tau}{1-\tau}} P_n^{1/2, -1/2}(1-2\tau) \frac{d\tau}{\tau-t} &= \frac{\sqrt{\pi} \Gamma(1/2+n)}{\Gamma(1+n)} F(1+n, -n, 1/2; t) \\ &- \frac{2\sqrt{\pi} \Gamma(3/2+n)}{n!} (-t)^{1/2} F(3/2+n, 1/2-n, 3/2; t), \quad t \notin (0, 1) \end{aligned}$$

For the orthonormal Jacobi polynomials $\hat{P}_n^{1/2, -1/2}(\xi')$, this relation can be simplified, and we obtain

$$\sigma_{22}(x + vt, 0) \sim \frac{2\gamma x^{-1/2}}{\sqrt{\pi}\alpha} \sum_{m=0}^{\infty} (-1)^m a_m^{(2)}, \quad x \rightarrow 0^+.$$

After comparing this asymptotic relation with the definition of the stress intensity factor K_I , we derive the final formula for K_I ,

$$K_I = \frac{2\sqrt{2}\gamma}{\alpha} \sum_{m=0}^{\infty} (-1)^m a_m^{(2)}. \quad (4.38)$$

Similarly,

$$K_{II} = \frac{2\sqrt{2}\gamma}{\beta} \sum_{m=0}^{\infty} (-1)^m a_m^{(1)}. \quad (4.39)$$

For computations, we take the Poisson ratio $\nu = 0.3$. The Rayleigh speed c_R is defined explicitly [8] as

$$c_R = c_s \sqrt{s_*}, \quad s_* = \frac{1}{3}(8 - R_+ - R_-), \quad R_{\pm} = \left(\frac{45\kappa_0}{2} - 404 \pm \frac{3\sqrt{3R_*}}{2} \right)^{1/3},$$

$$R_* = -14656 + 2768\kappa_0 - 181\kappa_0^2 + 4\kappa_0^3, \quad \kappa_0 = 8(2 - \nu)/(1 - \nu) \in (16, 24).$$

The way in which the stress intensity factors approach their asymptotic values as $\delta \rightarrow \infty$ is seen in Figure 4.2: the factors $K_I^{(1)}$ and $K_{II}^{(2)}$ tend to K_I° and K_{II}° , respectively, while the other two factors, $K_I^{(2)}$ and $K_{II}^{(1)}$ tend to zero. Here,

$$K_I^\circ = \frac{2\sqrt{2}\gamma}{\alpha} \sum_{m=0}^{\infty} (-1)^m b_m^{(2)}, \quad K_{II}^\circ = \frac{2\sqrt{2}\gamma}{\beta} \sum_{m=0}^{\infty} (-1)^m b_m^{(1)}. \quad (4.40)$$

In Figure 4.2, the crack propagation speed v is chosen to be the half of the Rayleigh speed, $v = 0.5c_R$. The factors $K_I^{(1)}$ and $K_{II}^{(1)}$ denote the stress intensity factors for the case when $\sigma_{22}^\circ(x) = 1$ for $-1 < x < 0$, and $\sigma_{22}^\circ(x) = 0$ otherwise, and $\sigma_{12}^\circ(x) = 0$ for all $x < 0$. The factors $K_I^{(2)}$ and $K_{II}^{(2)}$ are the SIFs for the case $\sigma_{12}^\circ(x) = 1$ for $-1 < x < 0$, and $\sigma_{12}^\circ(x) = 0$, $x < -1$, and $\sigma_{22}^\circ(x) = 0$ for all $x < 0$. As $\delta \rightarrow 0$, the absolute values of all the factors except for $K_{II}^{(2)}$ are growing. The factor $K_{II}^{(2)}$ approaches zero as the distance between the crack and the boundary of the half-plane tends to zero.

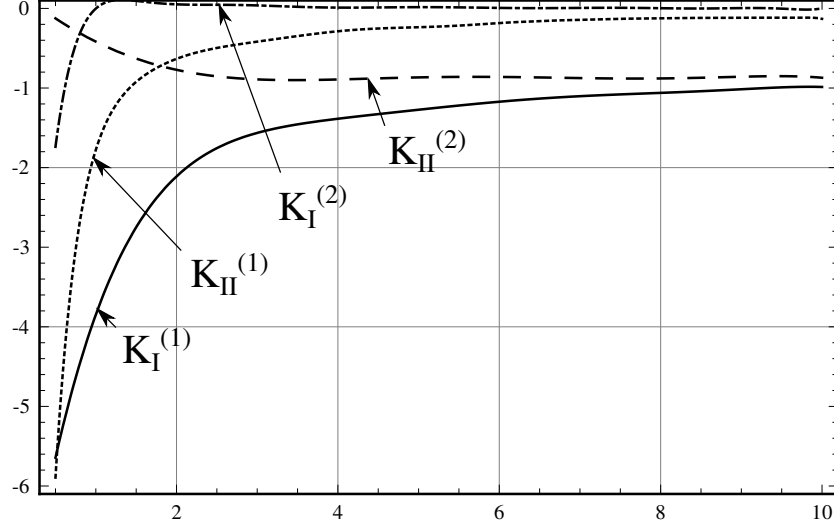


Figure 4.2: The stress intensity factors vs δ for $V/c_R = 0.5$: $K_I^{(1)}$ and $K_{II}^{(1)}$ are the factors for the case $\sigma_{22}^\circ(x) = 1$, $-1 < x < 0$, $\sigma_{22}^\circ(x) = 0$, $x < -1$, and $\sigma_{12}^\circ(x) = 0$, $x < 0$; $K_I^{(2)}$ and $K_{II}^{(2)}$ are the factors for the case $\sigma_{12}^\circ(x) = 1$, $-1 < x < 0$, $\sigma_{12}^\circ(x) = 0$, $x < -1$, and $\sigma_{22}^\circ(x) = 0$, $x < 0$.

When the crack is close to the surface ($\delta = 2$) and the crack propagation speed v is growing toward the Rayleigh speed c_R , the magnitudes of all the stress intensity factors apart from $K_I^{(1)}$ are growing. The factor $K_I^{(1)}$ is decreasing as $v \rightarrow c_R$. This is seen plotted in Figure 4.3.

4.2.2 Weight functions

In the problem on a crack in an unbounded plane, propagating at a constant speed (see Section 3.2), we used two fundamental solutions in order to express stress intensity factors for an arbitrary loading. In the case of a half-plane, a similar approach can be taken so that

$$K_I = \int_{-\infty}^0 W_{I,I}(\xi) \sigma_{22}^\circ(\xi) d\xi + \int_{-\infty}^0 W_{I,II}(\xi) \sigma_{12}^\circ(\xi) d\xi$$

$$K_{II} = \int_{-\infty}^0 W_{II,I}(\xi) \sigma_{22}^\circ(\xi) d\xi + \int_{-\infty}^0 W_{II,II}(\xi) \sigma_{12}^\circ(\xi) d\xi$$

where σ_{12}° and σ_{22}° are time-independent tangential and normal loading applied to the faces of the crack. The weight functions $W_{I,I}$, $W_{I,II}$, $W_{II,I}$, and $W_{II,II}$ are defined as the stress intensity factors corresponding to two fundamental solutions. Let us notice that we have two stress intensity factors for each fundamental solution since the equations for tangential and normal components are coupled because of presence of the boundary of a half-plane.

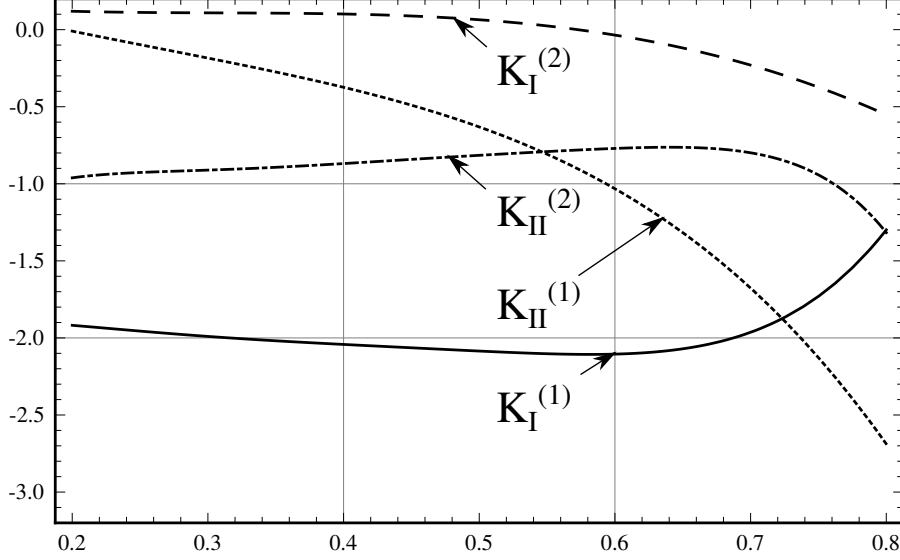


Figure 4.3: The stress intensity factors vs V/c_R for $\delta = 2$: $K_I^{(1)}$ and $K_{II}^{(1)}$ are the factors for the case $\sigma_{22}^\circ(x) = 1$, $-1 < x < 0$, $\sigma_{22}^\circ(x) = 0$, $x < -1$, and $\sigma_{12}^\circ(x) = 0$, $x < 0$; $K_I^{(2)}$ and $K_{II}^{(2)}$ are the factors for the case $\sigma_{12}^\circ(x) = 1$, $-1 < x < 0$, $\sigma_{12}^\circ(x) = 0$, $x < -1$, and $\sigma_{22}^\circ(x) = 0$, $x < 0$.

In order to determine the weight functions, we use the method introduced in [10]. The values $W_{I,I}(x_0)$ and $W_{II,I}(x_0)$ are equal to the stress intensity factors K_I and K_{II} for the fundamental solution of the problem (4.3), (4.7) with the loading

$$\sigma_{12}(x + vt, 0) = 0, \quad \sigma_{22}(x + vt, 0) = \delta(x - x_0), \quad -\infty < x < 0, \quad (4.41)$$

where $-\infty < x < 0$ and $\delta(x)$ is the Dirac delta function. In this case, the right-hand side of the system of equations (4.22), i.e. the coefficients $b_n^{(1)}$ and $b_n^{(2)}$, can be computed explicitly by the formula (4.30), where we take $f_1(x) = 0$ and $f_2(x) = \delta(x - x_0)\alpha/\gamma$:

$$b_n^{(1)} = 0, \quad b_n^{(2)} = -\frac{\alpha}{\gamma\sqrt{\pi(1-x_0)}} T_{2n+1} \left(\sqrt{\frac{x_0}{x_0-1}} \right) \quad (4.42)$$

For improving convergence of the method used to solve the system (4.22), we represent the coefficients $a_n^{(j)}$ as the sum $a_n^{(j)} = b_n^{(j)} + \tilde{a}_n^{(j)}$, $j = 1, 2$. After using the formulas (4.38) and (4.39) for the stress intensity factors, we derive

$$W_{I,I}(x_0) = W_{I,I}^\circ(x_0) + \tilde{W}_{I,I}(x_0), \quad W_{II,I}(x_0) = W_{II,I}^\circ(x_0) + \tilde{W}_{II,I}(x_0)$$

where

$$\begin{aligned}
W_{I,I}^\circ(x_0) &= \frac{2\sqrt{2}\gamma}{\alpha} \sum_{m=0}^{\infty} (-1)^m b_m^{(2)} \\
W_{II,I}^\circ(x_0) &= \frac{2\sqrt{2}\gamma}{\alpha} \sum_{m=0}^{\infty} (-1)^m b_m^{(1)} \\
\tilde{W}_{I,I}(x_0) &= \frac{2\sqrt{2}\gamma}{\alpha} \sum_{m=0}^{\infty} (-1)^m \tilde{a}_m^{(2)} \\
\tilde{W}_{II,I}(x_0) &= \frac{2\sqrt{2}\gamma}{\beta} \sum_{m=0}^{\infty} (-1)^m \tilde{a}_m^{(1)}
\end{aligned}$$

Notice that $W_{II,I}^\circ(x_0) = 0$ since $b_m^{(1)} = 0$ for all $m = 0, 1, 2, \dots$ due to (4.42). The value $W_{I,I}^\circ(x_0)$ can be computed explicitly by plugging $b_m^{(2)}$ defined in (4.42) and using the identity $T_n(x) = \frac{1}{2}(x - \sqrt{x^2 - 1})^n + \frac{1}{2}(x + \sqrt{x^2 - 1})^n$ for Chebyshev polynomials; then, $W_{I,I}^\circ(x_0) = -\sqrt{2}/\sqrt{-\pi x_0}$. The coefficients $\tilde{a}_m^{(1)}, \tilde{a}_m^{(2)}$ (and the values $\tilde{W}_{I,I}(x_0)$ and $\tilde{W}_{II,I}(x_0)$ respectively) are to be determined from the system of linear equations

$$\tilde{a}_n^{(j)} + \sum_{m=0}^{\infty} [c_{nm}^{(j,j)} \tilde{a}_m^{(j)} + c_{nm}^{(j,3-j)} \tilde{a}_m^{(3-j)}] = \tilde{b}_n^{(j)}, \quad n = 0, 1, \dots; \quad j = 1, 2, \quad (4.43)$$

where

$$\tilde{b}_n^{(1)} = 0, \quad \tilde{b}_n^{(2)} = - \sum_{m=0}^{\infty} c_{nm}^{(2,2)} b_m^{(2)}. \quad (4.44)$$

The values $W_{I,II}(x_0)$ and $W_{II,II}(x_0)$ are the stress intensity factors K_I and K_{II} for the fundamental solution of the problem (4.3), (4.7) with $\sigma_{12}(x + vt, 0) = \delta(x - x_0)$ and $\sigma_{22}(x + vt, 0) = 0$. They can be represented as

$$\begin{aligned}
W_{I,II}(x_0) &= \frac{2\sqrt{2}\gamma}{\alpha} \sum_{m=0}^{\infty} (-1)^m \tilde{a}_m^{(2)} \\
W_{II,II}(x_0) &= -\sqrt{\frac{2}{-\pi x_0}} + \frac{2\sqrt{2}\gamma}{\beta} \sum_{m=0}^{\infty} (-1)^m \tilde{a}_m^{(1)}
\end{aligned}$$

where the coefficients $\tilde{a}_m^{(1)}, \tilde{a}_m^{(2)}$ form the solution of the infinite system (4.43) with the right-hand side defined by

$$\tilde{b}_n^{(1)} = - \sum_{m=0}^{\infty} c_{nm}^{(1,1)} b_m^{(1)}, \quad b_m^{(1)} = - \frac{\beta}{\gamma \sqrt{\pi(1-x_0)}} T_{2n+1} \left(\sqrt{\frac{x_0}{x_0-1}} \right), \quad \tilde{b}_n^{(2)} = 0$$

For numerical computations of the weight functions, we choose $\nu = 0.3$ and $x_0 = -1$. When the velocity v is fixed ($v < c_R$) and $\delta \rightarrow \infty$, the weight functions $W_{I,I}$ and $W_{II,II}$ tend to the value $-\sqrt{2/\pi}$, which correspond to the problem on an unbounded plane. The other two functions, $W_{I,II}$ and $W_{II,I}$, vanish so that the problem for tangential and normal stress components decouples (see Figure 4.4). The magnitudes of all of the weight functions grow as $\delta \rightarrow 0$, while v is fixed ($v = 0.5c_R$ in Figure 4.4).

The weight function curves on Figure 4.5 for $\delta = 1$, $\nu = 0.3$, $x_0 = -1$ show that the weight function $W_{I,I}$ decreases as $v \rightarrow c_R$. The other functions may also decrease when the normalized speed v/c_R is close to 1. Our numerical scheme becomes less reliable when v approaches the critical speed c_R .

4.2.3 Griffith criterion

In order to construct Griffith crack propagation criteria [85], let us consider the potential energy δU released when the crack $S(t) = \{(x_1, 0) : -\infty < x_1 < vt\}$ extends by a small value r to the crack $S(t) + \delta S(t) = \{(x_1, 0) : -\infty < x_1 < vt + r\}$. The energy δU may be expressed as

$$\delta U = \frac{1}{2} \int_{vt}^{vt+r} \{\sigma_{12}(x_1, 0)[u_1](x_1) + \sigma_{22}(x_1, 0)[u_2](x_1)\} dx_1 \quad (4.45)$$

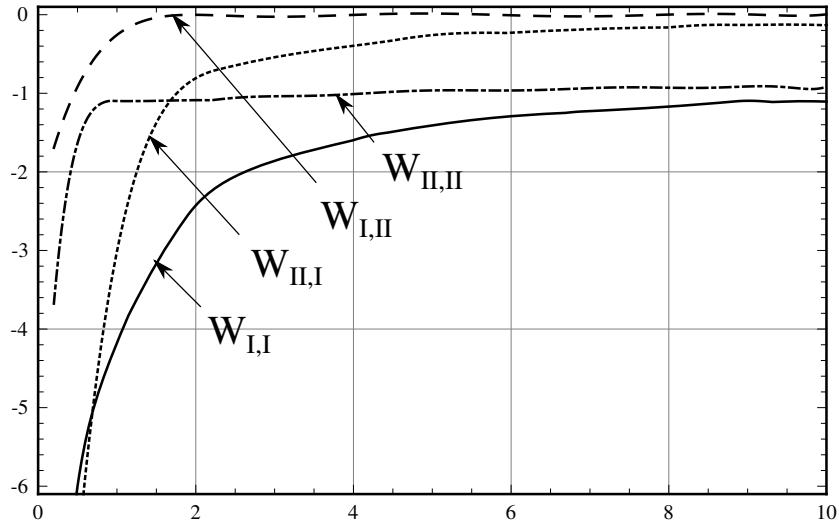


Figure 4.4: The weight functions $W_{j,l}(x_0)$ ($j, l = I, II$) vs δ for $v/c_R = 0.5$, $x_0 = -1$.

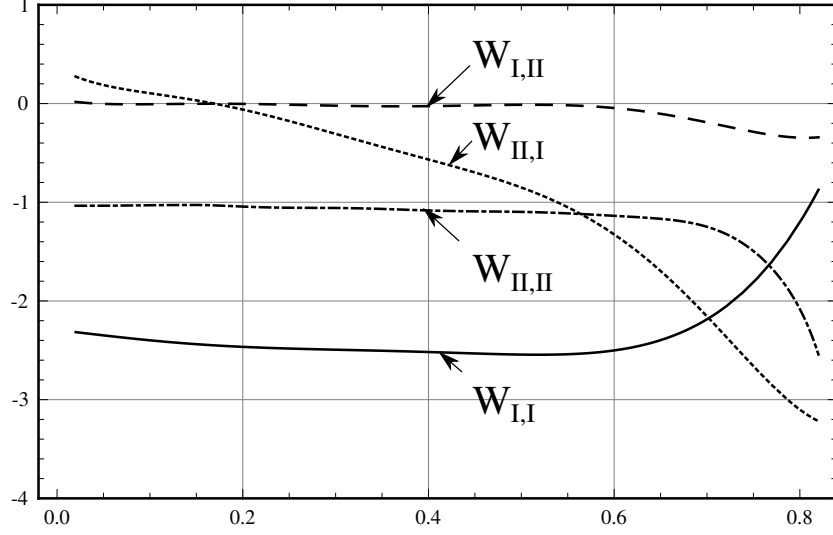


Figure 4.5: The weight functions $W_{j,l}(x_0)$ ($j, l = I, II$) vs v/c_R for $\delta = 1$, $x_0 = -1$.

where $[u_1]$, $[u_2]$ are the displacement jumps related to the extended crack in the horizontal and vertical direction respectively.

Recall that the stress field has the following asymptotic behavior near the tip of the crack:

$$\sigma_{12}(x + vt, 0) \sim \frac{K_{II}}{\sqrt{2\pi x}}, \quad \sigma_{22}(x + vt, 0) \sim \frac{K_I}{\sqrt{2\pi x}}, \quad x \rightarrow 0^+ \quad (4.46)$$

In order to find asymptotic expansions for $\delta[u_1]$, $\delta[u_2]$, we integrate the identities (4.19) and fix the constant of integration so that the displacement jumps vanish at the crack tip. For the displacement jumps $[u_1]$ and $[u_2]$, we derive

$$\begin{pmatrix} [u_1](x + vt) \\ [u_2](x + vt) \end{pmatrix} = 2 \sum_{m=0}^{\infty} \begin{pmatrix} a_m^{(1)} \\ a_m^{(2)} \end{pmatrix} \int_0^x \hat{P}_m^{1/2, -1/2} \left(\frac{\xi + 1}{\xi - 1} \right) \frac{d\xi}{(1 - \xi)\sqrt{-\xi}}, \quad x < 0. \quad (4.47)$$

The displacement jumps vanish at the point $x = 0$ and tend to finite and, in general, non-zero values as $x \rightarrow -\infty$. Since $\hat{P}_m^{1/2, -1/2}(-1) = \pi^{-1/2}(-1)^m$, the formula (4.31) implies

$$[u_2](x + vt) = -4\sqrt{\frac{-x}{\pi}} \sum_{m=0}^{\infty} (-1)^m a_m^{(2)} + O(|x|^{3/2}), \quad x \rightarrow 0^-. \quad (4.48)$$

By comparing the formula (4.48) to (4.38) and (4.39), we can express the jumps $[u_1](x + vt)$ and $[u_2](x + vt)$ through the stress intensity factor K_I and K_{II} as follows

$$[u_1](x + vt) \sim -\sqrt{\frac{-2x}{\pi}} \frac{\beta K_{II}}{\gamma}, \quad [u_2](x + vt) \sim -\sqrt{\frac{-2x}{\pi}} \frac{\alpha K_I}{\gamma}, \quad x \rightarrow 0^- \quad (4.49)$$

After plugging the identities (4.46) and (4.49) in the integral in (4.45) and noticing that the products $\sigma_{12}[u_1]$ and $\sigma_{22}[u_2]$ are bounded on the interval $[vt, vt + r]$, we derive the formula

$$\delta U \sim -\frac{1}{4\gamma}(\alpha K_I^2 + \beta K_{II}^2)r, \quad r \rightarrow 0^+. \quad (4.50)$$

This formula can be written in terms of the Rayleigh function

$$R(v) = 4\sqrt{\left(1 - \frac{v^2}{c_l^2}\right)\left(1 - \frac{v^2}{c_s^2}\right) - \left(2 - \frac{v^2}{c_s^2}\right)^2} \quad (4.51)$$

as

$$\delta U \sim \frac{v^2 r}{2c_s \mu R(v)}(\alpha K_I^2 + \beta K_{II}^2), \quad r \rightarrow 0^+. \quad (4.52)$$

According to the Griffith criterion, the crack starts propagating if the energy δU equals or greater than the increase in the surface energy $2Tr$, $\delta U \geq 2Tr$, where T is the Griffith material constant. This criterion may be represented in terms of the stress intensity factors in the form

$$\sqrt{1 - \frac{v^2}{c_l^2}} K_I^2 + \sqrt{1 - \frac{v^2}{c_s^2}} K_{II}^2 \geq \frac{4T c_s^2 \mu R(v)}{v^2}. \quad (4.53)$$

Notice, that if $\delta = \infty$, and $\sigma_{12}^\circ(x) = 0$ for all $x < 0$, then the inequality (4.53) coincides with the criterion

$$K_I^2 \geq \frac{4T c_s^2 \mu R(v)}{v^2 \sqrt{1 - v^2/c_l^2}} \quad (4.54)$$

obtained by Willis [85]. For finite values of δ , even when the tangential component of loading vanishes, the stress intensity factor K_{II} does not equal to zero, and both factors, K_I and K_{II} , are involved in the Griffith crack propagation criterion.

Another way to represent the crack propagation criterion is to rewrite inequality (4.53) as

$$H(K_I, K_{II}, v/c_s, v/c_l) \geq \mu T, \quad (4.55)$$

where

$$H = \frac{\alpha K_I^2 + \beta K_{II}^2}{4(c_s/v)^2 R(v)}. \quad (4.56)$$

Figure 4.6 shows the results of calculations of the function H versus δ for $v/c_R = 0.5$ and some loads. It is seen that H rapidly advances as the distance between the crack and the half-plane boundary decreases. The dependence of H on the normalized crack speed v/c_R when $\delta = 2$ is plotted in Figure 4.7. The function $H \rightarrow \infty$ as $v/c_R \rightarrow 0$ and it grows as the crack speed v approaches the Rayleigh speed. The curves in Figure 4.7 are reminiscent of the graph of modulus of cohesion $k_c(v)$ versus v/c_s in the Barenblatt-type criterion for intersonic shear crack propagation [12].

Let us notice that the solution of the steady-state problem, considered in this chapter, holds for propagation of the crack at any speed v in the range $0 < v < c_R$. However, one important question that arises in the problems on crack propagation is how to determine the propagation speed v for a specified loading and a shape of the domain containing the crack. In order to answer that question, we apply the Griffith propagation criterion (4.55) and find speed v from the equation $H = \mu T$. On Figure 4.8, we demonstrate values of the propagation speed v for some loading (here, $x_0 = -1$, $\nu = 0.3$, $T = 100$). It is clear from Figure 4.7 that the equation $H = \mu T$ may have no solutions, one solution, or two different solutions, say v_1 and v_2 . We can assume the following two scenarios: (i) the crack starts propagating and its speed slowly increases until it reaches value v_1 at which the speed becomes stable and

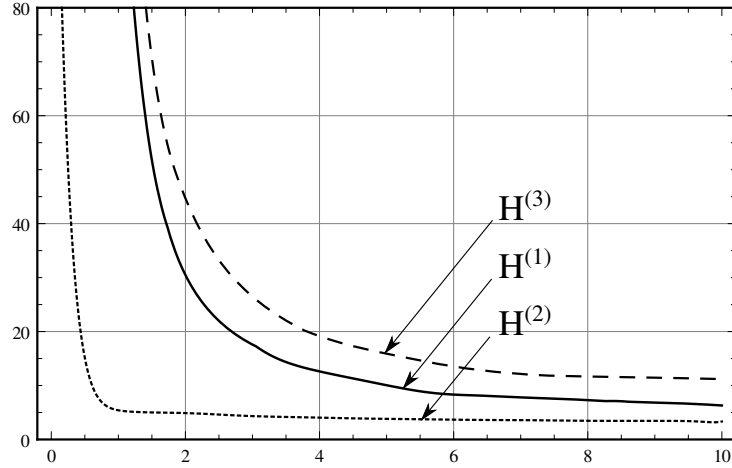


Figure 4.6: The function H vs δ for $v/c_R = 0.5$, $x_0 = -1$ and loading $\sigma_{22}^\circ = \delta(x - x_0)$, $\sigma_{12}^\circ = 0$: $H^{(1)}$; $\sigma_{22}^\circ = 0$, $\sigma_{12}^\circ = \delta(x - x_0)$: $H^{(2)}$; $\sigma_{22}^\circ = \delta(x - x_0)$, $\sigma_{12}^\circ = \delta(x - x_0)$: $H^{(3)}$.

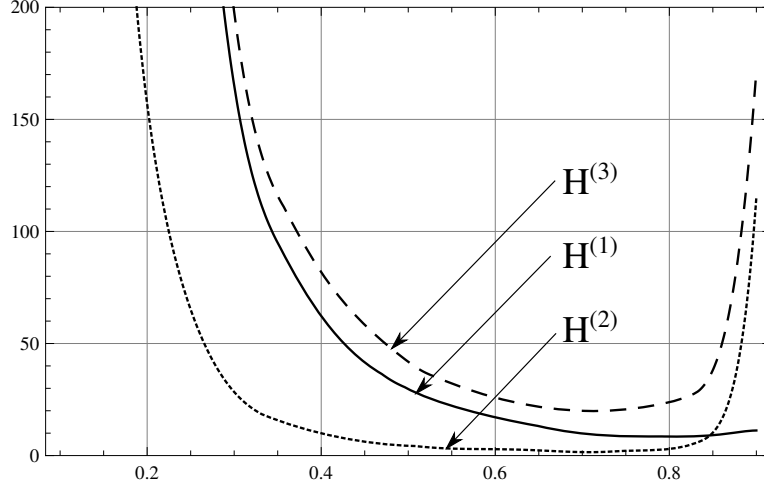


Figure 4.7: The function H vs v/c_R for $\delta = 2$, $x_0 = -1$ and loading $\sigma_{22}^\circ = \delta(x - x_0)$, $\sigma_{12}^\circ = 0$: $H^{(1)}$; $\sigma_{22}^\circ = 0$, $\sigma_{12}^\circ = \delta(x - x_0)$: $H^{(2)}$; $\sigma_{22}^\circ = \delta(x - x_0)$, $\sigma_{12}^\circ = \delta(x - x_0)$: $H^{(3)}$.

the crack approaches the steady-state regime; (ii) the crack starts propagating and its speed quickly jumps up to the Rayleigh speed limit c_R and then stabilizes at value v_2 . Notice that if the loading has high enough amplitude, then the equation $H = \mu T$ has no solution (take, for instance, parameter $\sigma_* = 25$ and speed $v^{(3)}$ on Figure 4.8). In this case, the function H exceeds the value μT resulting to the crack propagation, but its speed becomes unstable and, thus, such propagation cannot be described by the model considered in this chapter.

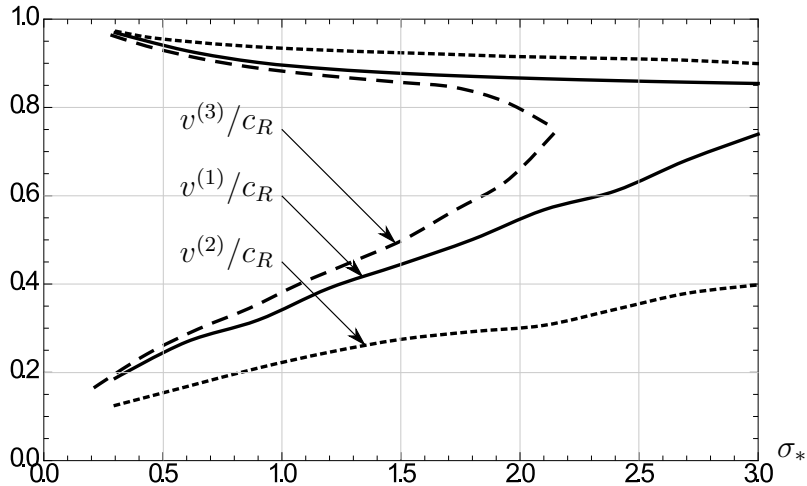


Figure 4.8: Propagation speed v against the parameter σ_* corresponding to the loading $\sigma_{22}^\circ = \sigma_* \delta(x - x_0)$, $\sigma_{12}^\circ = 0$: $v^{(1)}$; $\sigma_{22}^\circ = 0$, $\sigma_{12}^\circ = \sigma_* \delta(x - x_0)$: $v^{(2)}$; $\sigma_{22}^\circ = \sigma_* \delta(x - x_0)$, $\sigma_{12}^\circ = \sigma_* \delta(x - x_0)$: $v^{(3)}$.

Chapter 5

Transient Crack Propagation in a Half-Plane

In this chapter we will propose a new method of partial Wiener–Hopf factorization for analyzing plane dynamic transient problems in the case when the two deformation modes are coupled, and the standard Wiener-Hopf method does not work. In addition to factorization of two scalar functions it employs derivation and solution of a certain system of two integral equations. The method is illustrated by the study of a crack propagating at sub-Rayleigh speed parallel to the boundary of a solid when loading is time independent. The model problem admits formulation as a vector Riemann–Hilbert problem.

First, we will describe the transient model and apply the Fourier and Laplace transforms in a standard manner [39, 73, 19] in order to reduce the governing boundary-value problem to a second order vector Riemann–Hilbert problem.

Next, we will propose an approximate solution for the vector Riemann–Hilbert problem associated with the transient problem on a half-plane. The solution takes advantage of a partial Wiener–Hopf factorization. First, we split the matrix coefficient into a diagonal matrix that is discontinuous at infinity and a matrix that is continuous. After factorizing the discontinuous part and recasting the vector Riemann–Hilbert problem, we derive a new problem that is equivalent to a system of two integral equations on the interval $(-\infty, 0)$. The diagonal elements of the matrix kernel are constants, while the off-diagonal elements are continuous functions which have a second order zero at infinity. We will show that in order to determine the Laplace transforms of the stress intensity factors and the weight functions, it is sufficient to know the solution to the system of integral equations at one point only. We will describe the numerical procedure and the inversion method of the Laplace transform we applied and discuss the numerical results for the weight functions.

5.1 Crack Propagation at Constant Speed due to Time-Independent Loading

In this section, we will describe the problem on a semi-infinite crack propagation in the direction parallel to the boundary of a half-plane, compare it to similar problems considered in Chapter 3 and Chapter 4, and transform the problem to a vector Riemann–Hilbert problem.

5.1.1 Comparison to the previous problems

When the crack is far away from the boundary of an elastic material, the problem can be described as propagation of a semi-infinite crack along the interface between two weakly bonded, identical and isotropic half-planes. The problem on a crack growth in a plane at a constant sub-Rayleigh speed due to general time-independent loading (including the case of concentrated forces applied to the crack faces) was solved explicitly in [38, 39] by applying the Wiener–Hopf method. The intersonic regime corresponding to a speed propagation from the range between the shear wave speed c_s and the longitudinal wave speed c_l , was analyzed in [45, 46]. The case of concentrated forces (the fundamental solution problem) and the model problem on a suddenly stopping crack were considered.

In the case of an unbounded plane, the problem was solved in Section 3.2. The vector Riemann–Hilbert problem is decoupled and solved by quadratures. We derived explicit formulas for the stress intensity factors (3.36) and the weight functions (3.37).

If the crack is close to the boundary of the body, the boundary effects cannot be ignored, and the problem on a crack propagating parallel to the half-plane boundary can be considered as an adequate model. In the static case, the matrix coefficient of the corresponding Riemann–Hilbert problem admits a closed-form factorization [86]. The steady-state case, when the faces of a propagating crack are subjected to the loading moving with the crack at the same constant speed, was analyzed in Chapter 4. By applying Fourier transform, the problem was reduced to a vector Riemann–Hilbert problem whose matrix coefficient does not allow for an explicit factorization. The problem was transformed to a system of singular integral equations, and an approximate method of orthogonal polynomials for its solution

was proposed. To the best of my knowledge, no analytical solution to the transient problem on a semi-infinite crack propagating along the boundary of a half-plane is available in the literature.

Although the matrix coefficient for the transient problem in a half-plane has the same structure (4.11) as in the steady-state case (see Chapter 4), the solution of the transient problem is more elaborate since the parameters α and β are functions of the variables introduced by Laplace and Fourier transforms, involved. As in the steady-state case, the Wiener–Hopf factorization cannot be constructed explicitly using standard techniques (for instance, the one described in Section 2.3.1) due to infinitely many branch points of the matrix J^2 in (4.11).

The partial indices [81] play an essential part in solvability theory of a vector Riemann–Hilbert problem and in the theory of approximate Wiener-Hopf matrix factorization. According to the stability criterion for partial indices [23, 42, 81] applied to a 2×2 matrix, an approximate matrix factorization is stable if and only if $|\kappa_1 - \kappa_2| \leq 1$ for partial indices κ_1 and κ_2 of the corresponding Riemann–Hilbert problem. If they do not satisfy this criterion, then approximate canonical Wiener-Hopf factors may not converge to the exact ones. At the same time, without knowledge of exact factorization, in general, there is no way to determine the partial indices. An example (not inspired by an applied physical problem) of unstable partial indices is given in [56]. However, the partial indices associated with contact, fracture, and diffraction models available in the literature [60, 11, 13] are stable. Due to this fact, we will eliminate the problem of determination of the partial indices and bypass the approximate matrix Wiener–Hopf factorization. Instead, we will propose a method of partial factorization that comprises factorization of some scalar functions and numerical solution of a certain system of integral equations.

After deriving solution for the problem on a semi-infinite crack propagating at a constant speed, it is possible to construct solution to the problem in the case of an arbitrary non-

uniform speed (see Section 3.3). For an unbounded plane such an algorithm based on the fundamental solution and the solution of the model problem on a suddenly stopped crack is known [39]. In this chapter, we will generalize this procedure to the case of a half-plane. The key feature here is the fact that the Mode I and Mode II weight functions after the longitudinal wave reflects from the boundary and strikes the crack do not act alone anymore and the off-diagonal weight functions play a substantial part in the solution. In order to determine the stress field radiated out by a suddenly stopped crack, one needs to solve a system of two Volterra convolution equations, a generalization of the single Abel equation appeared in the Freund method in the case of an unbounded plane. By solving this system explicitly, we determine the stress values the crack needs to negate on the prospective fracture plane to proceed further. This procedure allows for the possibility of finding the stress intensity factors at the tip of a crack propagating at a piecewise constant speed below the boundary and, in conjunction with the dynamic Griffith criterion, describing the actual nonuniform speed of crack propagation.

5.1.2 Transient problem for a half-plane as a vector Riemann–Hilbert problem

The statement of the transient problem on a semi-infinite crack in a half-plane is similar to the one considered in Chapter 4 except the loading is assumed to be time-independent. The elastic medium $\{(x_1, x_2) : |x_1| < \infty, -\infty < x_2 < \delta\}$ through which the crack propagates, consists of an infinite strip $\{(x_1, x_2) : |x_1| < \infty, 0 < x_2 < \delta\}$ and a half-plane $\{(x_1, x_2) : |x_1| < \infty, -\infty < x_2 < 0\}$ bonded together. The bonding is not perfect, and a semi-infinite crack is assumed to lie along the interface. The boundary of the body is free of traction, while the faces of the crack are subjected to plane strain loading that forces the crack to propagate at a constant sub-Rayleigh speed v :

$$\begin{aligned} \sigma_{j2}(x_1, 0^\pm, t) &= -\sigma_{j2}^\circ(x_1)H(t), & -\infty < x_1 < vt \\ \sigma_{j2}(x_1, \delta, t) &= 0, & -\infty < x_1 < \infty \end{aligned} \quad j = 1, 2 \quad (5.1)$$

where σ_{12}° , σ_{22}° are prescribed functions and $H(t)$ is the unit step function. The presence of the weak interface encourages the crack to propagate parallel to the boundary of the half-plane rather than deviate towards it (see Figure 4.2). The Lamé constants λ and μ and the density ρ of the strip and the half-plane are assumed to be the same.

It is helpful to change variables from the material coordinates x_1, x_2 to the local crack tip coordinates $x = x_1 - vt$, $y = x_2$. In these coordinates, displacement potentials φ and ψ of the medium satisfy the wave equations

$$\begin{aligned} c_l^2 \hat{\alpha}^2 \frac{\partial^2 \varphi}{\partial x^2} + c_l^2 \frac{\partial^2 \varphi}{\partial y^2} + 2v \frac{\partial^2 \varphi}{\partial x \partial t} - \frac{\partial^2 \varphi}{\partial t^2} &= 0, \\ c_s^2 \hat{\beta}^2 \frac{\partial^2 \psi}{\partial x^2} + c_s^2 \frac{\partial^2 \psi}{\partial y^2} + 2v \frac{\partial^2 \psi}{\partial x \partial t} - \frac{\partial^2 \psi}{\partial t^2} &= 0, \end{aligned} \quad (x, y) \in \Omega, \quad t > 0, \quad (5.2)$$

where $\Omega = \{(x, y) : |x| < \infty, y < \delta\} \setminus \{(x, 0) : x < 0\}$ is the shape of the material. The potentials ϕ and ψ are to satisfy the zero initial conditions

$$\varphi = \psi = 0, \quad \frac{\partial \varphi}{\partial t} = \frac{\partial \psi}{\partial t} = 0, \quad (x, y) \in \Omega, \quad t < 0. \quad (5.3)$$

Here, c_l and c_s are the longitudinal and shear wave speeds defined in (1.17) and $\hat{\alpha} = \sqrt{1 - v_l^2}$, $\hat{\beta} = \sqrt{1 - v_s^2}$, $v_l = v/c_l$, $v_s = v/c_s$.

Let us transform the boundary value problem (5.1), (5.2), (5.3) to a vector Riemann–Hilbert problem. By applying first Laplace transform with respect to temporal variable t

$$\begin{pmatrix} \tilde{\varphi} \\ \tilde{\psi} \end{pmatrix} (x, y, s) = \int_0^\infty \begin{pmatrix} \varphi \\ \psi \end{pmatrix} (x, y, t) e^{-st} dt, \quad \text{Re } s = \sigma > 0,$$

and then Fourier transform with respect to spacial variable x

$$\begin{pmatrix} \hat{\varphi} \\ \hat{\psi} \end{pmatrix} (z, y, s) = \int_{-\infty}^\infty \begin{pmatrix} \tilde{\varphi} \\ \tilde{\psi} \end{pmatrix} (x, y, s) e^{izx} dx, \quad p \in \mathbb{R},$$

we can write the governing equations (5.2) in the form

$$\frac{\partial^2 \hat{\varphi}}{\partial y^2} - \alpha^2 \hat{\varphi} = 0, \quad \frac{\partial^2 \hat{\psi}}{\partial y^2} - \beta^2 \hat{\psi} = 0, \quad y \in \{-\infty, \delta\} \setminus \{0\}, \quad (5.4)$$

where

$$\alpha^2(z) = \hat{\alpha}^2 z^2 + 2izsv_l/c_l + s^2/c_l^2, \quad \beta^2(z) = \hat{\beta}^2 z^2 + 2izsv_s/c_s + s^2/c_s^2. \quad (5.5)$$

The coefficients α and β of the ordinary differential equations (5.4), are multi-valued functions of z -variable with the branch points $a_{\pm} = is/(v \pm c_l) \in \mathbb{C}^{\pm}$ and $b_{\pm} = is/(v \pm c_s) \in \mathbb{C}^{\pm}$ respectively. In order to fix single branches of $\alpha(z)$ and $\beta(z)$, we cut the z -plane along lines that pass through the infinite point and join the branch points a_{\pm} of the function α and β_{\pm} of the function β . Let us choose the single branches

$$\alpha(z) = \hat{\alpha}(z - a_-)^{1/2}(z - a_+)^{1/2}, \quad \beta(z) = \hat{\beta}(z - b_-)^{1/2}(z - b_+)^{1/2}, \quad (5.6)$$

so that $\text{Re } \alpha(z) > 0$ and $\text{Re } \beta(z) > 0$ for all $z \in \mathbb{R}$.

For the values $y \in (-\infty, 0)$ and $z \in \mathbb{R}$, the differential equations (5.4) admit the solution that is bounded as $y \rightarrow -\infty$, in the form

$$\hat{\varphi}(z, y, s) = C_0(z, s)e^{\alpha y}, \quad \hat{\psi}(z, y, s) = D_0(z, s)e^{\beta y}, \quad -\infty < y < 0, \quad (5.7)$$

since $\alpha > 0$ and $\beta > 0$ (hereafter, we drop the argument z of the functions α, β in the case when it does not cause a confusion). For the values $y \in (0, \delta)$, $z \in \mathbb{R}$, the solution of (5.4) is given by

$$\begin{aligned} \hat{\varphi}(z, y, s) &= C_1(z, s) \cosh(\alpha y) + C_2(z, s) \sinh(\alpha y), \\ \hat{\psi}(z, y, s) &= D_1(z, s) \cosh(\beta y) + D_2(z, s) \sinh(\beta y), \end{aligned} \quad 0 < y < \delta. \quad (5.8)$$

As in the steady-state case, we introduce auxiliary functions representing the jumps of the tangential derivatives of the displacement components u_1, u_2 on the crack faces,

$$\begin{aligned} \chi_1(x, t) &= \frac{\partial u_1}{\partial x}(x + vt, 0^+, t) - \frac{\partial u_1}{\partial x}(x + vt, 0^-, t) \\ \chi_2(x, t) &= \frac{\partial u_2}{\partial x}(x + vt, 0^+, t) - \frac{\partial u_2}{\partial x}(x + vt, 0^-, t) \end{aligned} \quad (5.9)$$

defined for $x \in (-\infty, 0)$ and $t \in (0, \infty)$. Then, we define the Laplace transforms with respect to time t ,

$$\begin{aligned}\tilde{\chi}_j(x, s) &= \int_0^\infty \chi_j(x, t) e^{-st} dt \\ b_j(x, s) &= \int_0^\infty \sigma_j^\circ(x + vt) e^{-st} dt \quad \text{Re } s > 0, \quad j = 1, 2 \\ \tilde{\sigma}_j(x, s) &= \int_0^\infty \sigma_{j2}(x + vt, 0, t) e^{-st} dt\end{aligned}$$

and the one-sided Fourier transforms with respect to x -variable

$$\begin{aligned}\hat{\chi}_j^-(z, s) &= \int_{-\infty}^0 \tilde{\chi}_j(x, s) e^{izx} dx \\ \hat{b}_j^-(z, s) &= \int_{-\infty}^0 b_j(x, s) e^{izx} dx \quad j = 1, 2 \\ \hat{\sigma}_j^+(z, s) &= \int_0^\infty \tilde{\sigma}_j(x, s) e^{izx} dx\end{aligned} \tag{5.10}$$

For a fixed values of s , if z is treated as a complex variable, then the functions $\hat{\sigma}_j^+(\cdot, s)$ are analytic in the upper half-plane \mathbb{C}^+ , while the functions $\hat{\chi}_j^-$, \hat{b}_j^- are analytic in the lower half-plane \mathbb{C}^- provided $\tilde{\sigma}_j$, $\tilde{\chi}_j$, and b_j are integrable in x on the corresponding intervals.

In order to derive a vector Riemann–Hilbert problem, we apply the Laplace and Fourier transforms to the six boundary conditions (5.1) and identities (5.9), plug the solutions (5.7) and (5.8), and eliminate the functions $C_j(z, s)$ and $D_j(z, s)$ ($j = 0, 1, 2$) (here, we follow the pattern described in Section 3.2). The two equations left comprise a vector Riemann–Hilbert problem with the condition

$$\begin{pmatrix} \hat{\sigma}_1^+(z, s) \\ \hat{\sigma}_2^+(z, s) \end{pmatrix} = \mu i A(z, s) \begin{pmatrix} \hat{\chi}_1^-(z, s) \\ \hat{\chi}_2^-(z, s) \end{pmatrix} + \begin{pmatrix} \hat{b}_1^-(z, s) \\ \hat{b}_2^-(z, s) \end{pmatrix}, \quad z \in \mathbb{R} \tag{5.11}$$

Assume that the value s is fixed so that $\text{Re } s > 0$. We seek two functions $\hat{\sigma}_j^+(z, s)$ that are analytic in the upper half-plane \mathbb{C}^+ and bounded at infinity, and two functions $\hat{\chi}_j^-(z, s)$ that are analytic in the lower half-plane \mathbb{C}^- and also vanish at infinity. On the real axis \mathbb{R} , they satisfy the condition (5.11). The matrix coefficient A of the problem is defined by

$$A(z, s) = \begin{pmatrix} a_{11}(z, s) & ia_{12}(z, s) \\ -ia_{12}(z, s) & a_{22}(z, s) \end{pmatrix} \tag{5.12}$$

$$\begin{aligned}
a_{11}(z, s) &= \frac{e^{-(\alpha+\beta)\delta}}{2\beta(z^2 - \beta^2)z} \left[R_1 \sinh\{(\alpha + \beta)\delta\} - R_2 \sinh\{(\alpha - \beta)\delta\} + \frac{2\Delta}{R_1} \right], \\
a_{12}(z, s) &= \frac{4R_2(z^2 + \beta^2)}{R_1(z^2 - \beta^2)} e^{-(\alpha+\beta)\delta} \sinh^2 \frac{(\alpha - \beta)\delta}{2}, \\
a_{22}(z, s) &= \frac{e^{-(\alpha+\beta)\delta}}{2\alpha(z^2 - \beta^2)z} \left[R_1 \sinh\{(\alpha + \beta)\delta\} + R_2 \sinh\{(\alpha - \beta)\delta\} + \frac{2\Delta}{R_1} \right], \\
\Delta &= R_1^2 \sinh^2 \frac{(\alpha + \beta)\delta}{2} - R_2^2 \sinh^2 \frac{(\alpha - \beta)\delta}{2}, \\
R_1 &= (z^2 + \beta^2)^2 - 4\alpha\beta z^2, \quad R_2 = (z^2 + \beta^2)^2 + 4\alpha\beta z^2.
\end{aligned} \tag{5.13}$$

The matrix $A(p, s)$ resembles its analogue in the steady-state case (4.11). However, although we drop the argument z of the parameters Δ , R_1 , R_2 , α , and β , let us highlight that all of them are functions of z -variable and depend on s as well.

5.1.3 Kernel of the integral equations

We show first that the direct use of the convolution theorem reduces the boundary condition of the vector Riemann–Hilbert problem (5.11) to a system of integral equations that is not convenient for numerical method of its solution due to a singular kernel.

Applying the inverse Fourier transform to the equation (5.11) and using the convolution theorem and the fact that $\tilde{\sigma}_1, \tilde{\sigma}_2$ vanish for negative x -values, we derive a system of integral equations

$$\int_{-\infty}^0 K(x - \xi, s) \begin{pmatrix} \tilde{\chi}_1(\xi, s) \\ \tilde{\chi}_2(\xi, s) \end{pmatrix} d\xi = -\frac{1}{\mu} \begin{pmatrix} b_1(x, s) \\ b_2(x, s) \end{pmatrix}, \quad -\infty < x < 0 \tag{5.14}$$

with the kernel

$$K(\xi, s) = \frac{i}{2\pi} \int_{-\infty}^{\infty} A(z, s) e^{-iz\xi} dz$$

By analyzing asymptotic behavior of the elements of the matrix function $A(z, s)$ as $z \rightarrow 0$ and $z \rightarrow \infty$, we discover that the diagonal elements of A have a jump discontinuity at infinity, while the off-diagonal elements exponentially vanish at infinity:

$$\begin{aligned}
a_{jj}(z, s) &\sim -\gamma_j \operatorname{sgn} z \left[1 + \frac{r_j}{z} + O\left(\frac{1}{z^2}\right) \right], \quad j = 1, 2, \\
a_{12}(z, s) &\sim r_0 e^{-2\hat{\beta}\delta|z|}, \quad z \rightarrow \pm\infty,
\end{aligned} \tag{5.15}$$

where r_j ($j = 0, 1, 2$) are nonzero constants, and γ_j are positive constants. Near the origin, the diagonal elements have simple poles and the off-diagonal elements are continuous: $a_{jj}(z, s) \sim -\tilde{\gamma}_j z^{-1}$ and $a_{12}(z, s) \sim -\tilde{\gamma}_0$ as $z \rightarrow 0$ ($\tilde{\gamma}_j$ are positive constants).

In order to clarify the structure of the diagonal elements of the kernel K , we represent the functions $a_{jj}(z, s)$ as the sum $a_{jj}(z, s) = -\gamma_j[\coth(\pi z) + a_{jj}^\circ(z, s)]$. From the behavior of $\coth(\pi z)$ on the real axis \mathbb{R} and the described above properties of a_{jj} at the origin and infinity, it immediately follows that

$$a_{jj}^\circ(z, s) = \frac{r_j}{|z|} + O\left(\frac{1}{z^2}\right), \quad z \rightarrow \pm\infty, \quad a_{jj}^\circ(z, s) \sim \frac{\hat{\gamma}_j}{z}, \quad z \rightarrow 0, \quad (5.16)$$

where $\hat{\gamma}_j$ are constants. Thus, a_{jj}° have simple zeros at infinity and simple poles at the origin.

Due to the identity

$$\int_{-\infty}^{\infty} \coth(\pi z) e^{-izx} dz = -i \coth \frac{x}{2}, \quad x \in \mathbb{R}$$

the equation (5.14) takes the form of a system of singular integral equations

$$\begin{aligned} \int_{-\infty}^0 \left[\coth \frac{\xi - x}{2} + k_{jj}(x - \xi, s) \right] \tilde{\chi}_j(\xi, s) d\xi \\ + \int_{-\infty}^0 k_{j3-j}(x - \xi, s) \tilde{\chi}_{3-j}(\xi, s) d\xi = -\frac{2\pi}{\mu\gamma_j} b_j(x, s) \end{aligned} \quad j = 1, 2 \quad (5.17)$$

on the negative semi-axis $(-\infty, 0)$, where the kernels k_{ij} are defined by the identities

$$\begin{aligned} k_{jj}(\xi, s) &= \frac{i}{2\pi} \int_{-\infty}^{\infty} a_{jj}^\circ(z, s) e^{-ix\xi} d\xi, \quad j = 1, 2 \\ k_{12}(\xi, s) &= -\frac{1}{2\pi} \int_{-\infty}^{\infty} a_{12}(z, s) e^{-ix\xi} d\xi, \quad k_{21}(\xi, s) = -k_{12}(\xi, s) \end{aligned}$$

Due to the behavior (5.16), the functions $k_{jj}(\xi, s)$ have a logarithmic singularity at the origin $\xi = 0$, while the functions $k_{j3-j}(\xi, x)$ are bounded at $\xi = 0$. As $\xi \rightarrow \pm\infty$, all of the kernels decay, $k_{ij} = O(|\xi|^{-1})$. Thus, the numerical method for solving the system of integral equations (5.17) has to take into account simple poles and the logarithmic discontinuity at $\xi = 0$ of the diagonal elements of the kernel K , as well as their jump discontinuity at infinity. That is, an application of the technique described in Section 2.3.2 or similar ones would not work or would work poorly.

5.2 Approximate Solution of the Transient Problem for a Half-Plane

Since the structure of the matrix $A(z, s)$ given by (5.12), (5.13) does not allow for its explicit factorization by the methods currently available in the literature, let us propose a method of partial Wiener–Hopf factorization. This technique eventually leads to a system of two integral equations convenient for the determination of the stress intensity factors and numerical implementation.

5.2.1 Partial Wiener–Hopf factorization

In order to avoid dealing with the kernel K described in Section 5.1.3, let us take another approach. Before transforming the system (5.14) to a system of singular integral equations, we rewrite it in a different form.

As in the case of an unbounded plane (see Section 3.2), we construct a Wiener–Hopf factorization of the diagonal elements of the matrix A . Represent the elements in the form

$$a_{jj}(z, s) = -\gamma_j \coth(\pi z) \check{a}_{jj}(z, s), \quad j = 1, 2, \quad (5.18)$$

Wiener–Hopf factorization for the function $\coth(\pi z)$ is given in (3.28), while the functions $\check{a}_{jj}(z, s)$ admit the factorization as follows:

$$\check{a}_{jj}(z, s) = \frac{\check{a}_{jj}^+(z, s)}{\check{a}_{jj}^-(z, s)}, \quad z \in \mathbb{R}_{-\varepsilon} \quad (5.19)$$

$$\check{a}_{jj}(z, s) = \exp \left\{ \frac{1}{2\pi i} \int_{\mathbb{R}_{-\varepsilon}} \frac{\ln \check{a}_{jj}(\tau, s) d\tau}{\tau - z} \right\}, \quad z \in \mathbb{C}_{-\varepsilon}^{\pm}.$$

where, as in Section 3.2, $\mathbb{C}_{-\varepsilon}^+$ is the upper half-plane $\{z : \operatorname{Im} z > -\varepsilon\}$, $\mathbb{C}_{-\varepsilon}^-$ is the lower half-plane $\{z : \operatorname{Im} z < -\varepsilon\}$, and $\mathbb{R}_{-\varepsilon}$ is the line $\{z : \operatorname{Im} z = -\varepsilon\}$, for some small parameter $\varepsilon \in (0, 1/c_l)$. The reason and justification for taking $\mathbb{C}_{-\varepsilon}^{\pm}$, $\mathbb{R}_{-\varepsilon}$ instead of \mathbb{C}^{\pm} , \mathbb{R} is given in Section 3.2; in short, the functions a_{jj} have simple poles at the origin $z = 0$, so we choose the contour $\mathbb{R}_{-\varepsilon}$ to pass around under the singular point.

Introduce new functions

$$\begin{aligned}\check{\sigma}_j^+(z, s) &= \frac{\hat{\sigma}_j^+(z, s)}{K^+(z)\check{a}_{jj}^+(z, s)}, & \check{\chi}_j^-(p, s) &= \frac{\mu\hat{\chi}_j^-(z, s)}{K^-(z)\check{a}_{jj}^-(z, s)}, \\ \check{b}_j(z, s) &= \frac{\hat{b}_j^-(z, s)}{K^+(z)\check{a}_{jj}^+(z, s)}, & j &= 1, 2.\end{aligned}\tag{5.20}$$

After the representations (5.18), (5.19), and (3.28) are substituted in the matrix A in (5.12), and the rows of A are divided by the terms $K^+\check{a}_{11}^+$ and $K^+a_{22}^+$, while the terms $1/(K^-\check{a}_{11}^-)$ and $1/(K^-\check{a}_{22}^-)$ are factored out from the columns of A , the equation (5.11) of the original vector Riemann–Hilbert problem takes the form

$$\begin{pmatrix} \check{\sigma}_1^+(z, s) \\ \check{\sigma}_2^+(z, s) \end{pmatrix} = \begin{pmatrix} \gamma_1 & \check{a}_1(z, s) \\ \check{a}_2(z, s) & \gamma_2 \end{pmatrix} \begin{pmatrix} \check{\chi}_1^-(z, s) \\ \check{\chi}_2^-(z, s) \end{pmatrix} + \begin{pmatrix} \check{b}_1(z, s) \\ \check{b}_2(z, s) \end{pmatrix}\tag{5.21}$$

on the contour $\mathbb{R}_{-\epsilon}$, where

$$\check{a}_1(z, s) = -\frac{ia_{12}(z, s)\check{a}_{22}^-(z, s)}{\coth(\pi z)\check{a}_{11}^+(z, s)}, \quad \check{a}_2(z, s) = \frac{ia_{12}(z, s)\check{a}_{11}^-(z, s)}{\coth(\pi z)\check{a}_{22}^+(z, s)},\tag{5.22}$$

and values of the functions $\check{a}_{jj}^\pm(z, s)$ on $\mathbb{R}_{-\epsilon}$ are determined by the Sokhotski–Plemelj formulas (2.8).

Assume that the value x is negative. By applying the inverse Fourier transform and the convolution theorem to the equation (5.21), we conclude that the vector Riemann–Hilbert problem (5.21) yields the system of integral equations

$$\begin{aligned}\gamma_1\chi_1^*(x, s) + \int_{-\infty}^0 k_1^*(x - \xi, s)\chi_2^*(\xi, s)d\xi &= -b_1^*(x, s) \\ \gamma_2\chi_2^*(x, s) + \int_{-\infty}^0 k_2^*(x - \xi, s)\chi_1^*(\xi, s)d\xi &= -b_2^*(x, s)\end{aligned}\quad -\infty < x < 0\tag{5.23}$$

where

$$\begin{aligned}\chi_j^*(x, s) &= \frac{1}{2\pi} \int_{\mathbb{R}_{-\epsilon}} \check{\chi}_j^-(z, s)e^{-izx}dz, & k_j^*(x, s) &= \frac{1}{2\pi} \int_{\mathbb{R}_{-\epsilon}} \check{a}_j(z, s)e^{-izx}dz, \\ b_j^*(x, s) &= \frac{1}{2\pi} \int_{\mathbb{R}_{-\epsilon}} \check{b}_j(z, s)e^{-izx}dz, & j &= 1, 2.\end{aligned}\tag{5.24}$$

Due to the behavior (5.15) of the off-diagonal element a_{12} at infinity, the functions $\check{a}_j(z, s)$ decay exponentially as $z \rightarrow \pm\infty$. Moreover, it follows from the definitions (5.22) that the

functions $\check{a}_j(z, s)$ are continuously differentiable on the contour \mathbb{R} including the point $z = 0$, where they vanish. Therefore, $k_j^*(x, s) = O(|x|^{-2})$ as $x \rightarrow \pm\infty$ (for fixed values of s). By the Riemann-Lebesgue lemma [], the functions $\chi_j^*(x, s)$ vanish as $x \rightarrow -\infty$.

5.2.2 Weight functions

Since the mode-I and mode-II are coupled in the case of a crack in a half-plane, we use four weight functions $W_{I,I}$, $W_{I,II}$, $W_{II,I}$, and $W_{II,II}$ such that the stress intensity factors for arbitrary loading σ_{12}° and σ_{22}° , are given by

$$\begin{aligned} K_I(t) &= \int_{-\infty}^{vt} W_{I,I}(x_1, t) \sigma_{22}^\circ(x_1, 0) dx_1 + \int_{-\infty}^{vt} W_{I,II}(x_1, t) \sigma_{12}^\circ(x_1, 0) dx_1 \\ K_{II}(t) &= \int_{-\infty}^{vt} W_{II,I}(x_1, t) \sigma_{22}^\circ(x_1, 0) dx_1 + \int_{-\infty}^{vt} W_{II,II}(x_1, t) \sigma_{12}^\circ(x_1, 0) dx_1 \end{aligned} \quad (5.25)$$

The weight functions $W_{I,I}$ and $W_{II,I}$ for a fixed value $x_1 = x_0$ are defined as the stress intensity factors K_I and K_{II} respectively, derived for the fundamental solution of the problem with the boundary conditions $\sigma_{22}^\circ(x_1, 0) = \delta(x_1 - x_0)$ and $\sigma_{12}^\circ(x_1, 0) = 0$. Similarly, the weight functions $W_{I,II}$ and $W_{II,II}$ are equal to the stress intensity factors K_I and K_{II} corresponding to the fundamental solution with the boundary conditions $\sigma_{22}^\circ(x_1, 0) = 0$ and $\sigma_{12}^\circ(x_1, 0) = \delta(x_1 - x_0)$. As in the case of a plane, the transforms of the traction components, $\hat{\sigma}_1^+$ and $\hat{\sigma}_2^+$, have the following behavior at infinity:

$$\hat{\sigma}_1^+(z, s) \sim \frac{\tilde{K}_{II}(s)}{\sqrt{-2iz}}, \quad \hat{\sigma}_2^+(z, s) \sim \frac{\tilde{K}_I(s)}{\sqrt{-2iz}}, \quad \text{Im } z \rightarrow \infty \quad (5.26)$$

Let χ_1^* and χ_2^* be the solution of the system (5.23). Since the convolution theorem applied to the equation (5.21) gives the identities

$$\begin{aligned} \int_{-\infty}^0 k_1^*(x - \xi, s) \chi_2^*(\xi, s) d\xi &= \sigma_1^*(x, s) - b_1^*(x, s) \\ \int_{-\infty}^0 k_2^*(x - \xi, s) \chi_1^*(\xi, s) d\xi &= \sigma_2^*(x, s) - b_2^*(x, s) \end{aligned} \quad (5.27)$$

for positive values of x -variable, where

$$\sigma_j^*(x, s) = \frac{1}{2\pi} \int_{\mathbb{R}_{-\epsilon}} \check{\sigma}_j^+(z, s) e^{-izx} dz, \quad j = 1, 2. \quad (5.28)$$

taking the limit $x \rightarrow 0^+$ yields the equations $(k_j^* * \chi_{3-j}^*)(0^+) = \sigma_j^*(0^+, s) - b_j^*(0^+, s)$, $j = 1, 2$. On the other hand, the identities (5.23) as $x \rightarrow 0^-$ imply the equations $\gamma_j \chi^*(0^-) + (k_j^* * \chi_{3-j}^*)(0^-) = -b_j^*(0^-, s)$, $j = 1, 2$. Due to the fact that the kernels k_1^* and k_2^* are continuous on the real axis \mathbb{R} , we derive the equality

$$\gamma_j \chi_j^*(0^-, s) = -\sigma_j^*(0^+, s) + b_j^*(0^+, s) - b_j^*(0^-, s), \quad j = 1, 2, \quad (5.29)$$

which will be used to express behavior of the stress field near the crack tip through the solution χ_1^* , χ_2^* of the system (5.23).

Next, we will show that $b_j^*(0^+) = b_j^*(0^-, s)$ for the fundamental solutions. Let us fix s -value so that $s > 0$. The functions \check{b}_j are defined as follows

$$\check{b}_1(x, s) = 0, \quad \check{b}_2(z, s) = \frac{e^{izx_0}}{s + ivz} \frac{1}{K^+(z) \check{a}_{22}^+(z, s)} \quad (5.30)$$

for the weight functions $W_{I,I}$, $W_{II,I}$, and as

$$\check{b}_1(z, s) = \frac{e^{izx_0}}{s + ivz} \frac{1}{K^+(z) \check{a}_{11}^+(z, s)}, \quad \check{b}_2(z, s) = 0 \quad (5.31)$$

for the weight functions $W_{I,II}$, $W_{II,II}$. Let us consider the formula (5.30). By plugging the identities (5.30) into the definition (5.23) of the functions b_j^* , we derive

$$b_1^*(x, s) = 0, \quad b_2^*(x, s) = \frac{1}{2\pi} \int_{\mathbb{R}_{-\varepsilon}} \frac{e^{iz(x_0-x)}}{(s + ivz) K^+(z) \check{a}_{22}^+(z, s)} dz \quad (5.32)$$

If $x < x_0$, then the integrand in (5.32) has only one simple pole $z = is/v$ in the upper half-plane \mathbb{C}^+ and exponentially vanishes as $\text{Im } z \rightarrow \infty$. Thus, the residue theorem implies

$$b_2^*(x, s) = \frac{e^{s(x-x_0)/v}}{v K^+(is/v) \check{a}_{22}^+(is/v, s)}, \quad x < x_0$$

Assume that $x > x_0$. Due to the identities (3.28), (5.18), (5.19), we replace the terms $K^+ \check{a}_{22}^+$ by the terms $-a_{22} K^- \check{a}_{22}^- / \gamma_2$ in the integral in (5.30). Then the integrand is analytic in the lower half-plane $\mathbb{C}_{-\varepsilon}^-$ except the imaginary semi-axis $\{z : \text{Re } z = 0, -\infty < \text{Im } z \leq s/(v - c_l)\}$ where the function a_{22} has branch points a_- and b_- due to the functions $\alpha(z)$ and $\beta(z)$.

Since the integrand exponentially vanishes as $\text{Im } z \rightarrow -\infty$, we transform the contour $\mathbb{R}_{-\varepsilon}$ into the imaginary semi-axis and make a substitution $z = -iy$:

$$b_2^*(x, s) = \frac{\gamma_2}{2\pi i} \int_{\frac{s}{c_l - v}}^{\infty} \frac{e^{y(x_0 - x)}}{(s + vy)K^-(-iy)\check{a}_{22}^-(-iy, s)} \left[\frac{1}{a_{22}} \right] (y) dy \quad (5.33)$$

where

$$\left[\frac{1}{a_{22}} \right] (y) = \frac{1}{a_{22}(-0 - iy)} - \frac{1}{a_{22}(0 - iy)}$$

is the difference between the values $a_{22}(-0 - iy)$ of the functions a_{22} on the left side of the semi-axis and the values $a_{22}(0 - iy)$ of the function a_{22} on the right side of the semi-axis. Thus, near the point $x = 0$, the function $b_2^*(x, s)$ is defined by the formula (5.33) and is continuous on the interval (x_0, ∞) . The continuity of b_2^* and the fact that b_1^* is equal to 0 imply $b_j^*(0^+) = b_j^*(0^-, s)$, $j = 1, 2$. Similar analysis holds for the functions (5.31), which yield the right-hand side b_1^* , b_2^* of the system (5.23) defined as follows:

$$b_1^*(x, s) = \begin{cases} \frac{e^{s(x-x_0)/v}}{vK^+(is/v)\check{a}_{11}^+(is/v, s)}, & x < x_0 \\ \frac{\gamma_1}{2\pi i} \int_{\frac{s}{c_l - v}}^{\infty} \frac{e^{y(x_0 - x)}}{(s + vy)K^-(-iy)\check{a}_{11}^-(-iy, s)} \left[\frac{1}{a_{11}} \right] (y) dy, & x > x_0 \end{cases}$$

$$b_2^*(x, s) = 0, \quad -\infty < x < \infty$$

$$\left[\frac{1}{a_{11}} \right] (y) = \frac{1}{a_{11}(-0 - iy)} - \frac{1}{a_{11}(0 - iy)}$$

Since $b_j^*(0^+) = b_j^*(0^-, s)$ ($j = 1, 2$) in the case of the fundamental solutions, the identity (5.29) reduces to the form

$$\gamma_j \chi_j^*(0^-, s) = -\sigma_j^*(0^+, s), \quad j = 1, 2 \quad (5.34)$$

The formula (5.28) and the identities (3.19) and (5.34) imply that

$$\check{\sigma}_j^+(z, s) \sim \frac{\sigma_j^*(0^+, s)}{-iz} = \frac{\gamma_j \chi_j^*(0^-, s)}{iz}, \quad \text{Im } z \rightarrow \infty \quad (5.35)$$

From the definition (5.20) of the function $\check{\sigma}_j^+$ and the asymptotic behavior (5.35) and (3.31) of the functions in (5.20), we derive the formula

$$\hat{\sigma}_j^+(z, s) \sim -\frac{\gamma_j \chi_j^*(0^-, s)}{\sqrt{-iz}}, \quad \text{Im } z \rightarrow \infty$$

Comparing the latter identity with (5.26), we conclude that the Laplace transforms of the stress intensity factors are given by

$$\tilde{K}_I(s) = -\sqrt{2}\gamma_2\chi_2^*(0^-, s), \quad \tilde{K}_{II}(s) = -\sqrt{2}\gamma_1\chi_1^*(0^-, s). \quad (5.36)$$

The stress intensity factors are recovered from their Laplace transform by the inversion formula. The inversion can be implemented by computing one of the real integrals

$$\begin{aligned} K_j(t) &= \frac{2e^{\sigma t}}{\pi} \int_0^\infty \operatorname{Re}\{\hat{K}_j(\sigma + i\tau)\} \cos \tau t \, d\tau \\ K_j(t) &= -\frac{2e^{\sigma t}}{\pi} \int_0^\infty \operatorname{Im}\{\hat{K}_j(\sigma + i\tau)\} \sin \tau t \, d\tau \end{aligned} \quad j = I, II \quad (5.37)$$

where the preference is made to the one with a better rate of convergence.

5.2.3 Solution of the system of integral equations

Let us now describe the numerical procedure for evaluation of the weight functions. Recall that the weight functions coincide with the stress intensity factors of the fundamental solutions. Due to the formulas (5.36), the Laplace transforms of the stress intensity factors require the knowledge of the solution of the system of integral equations (5.23) at the point $x = 0$, that is $\chi_j^*(0^-, s)$, $j = 1, 2$. It is convenient to map the system (5.23) on the semi-infinite interval into a system on the finite interval $(-1, 1)$, which is achieved by introducing the variables

$$\xi = \frac{\xi' - 1}{\xi' + 1}, \quad -1 < \xi' < 1, \quad x = \frac{x' - 1}{x' + 1}, \quad -1 < x' < 1.$$

In the new variables, the system (5.26) of integral equations takes the form

$$\gamma_j \mathcal{X}_j(x', s) + \int_{-1}^1 \mathcal{K}_{3-j}(x', \xi', s) \mathcal{X}_j(\xi', s) d\xi' = -\mathcal{B}_j(x', s), \quad j = 1, 2 \quad (5.38)$$

on the interval $(-1, 1)$, where

$$\mathcal{X}_j(x', s) = \chi_j^*(x, s), \quad \mathcal{K}_j(x', \xi', s) = \frac{2k_j^*(x - \xi, s)}{(\xi' + 1)^2}, \quad \mathcal{B}_j(x', s) = q_j^*(x, s).$$

Due to the behavior of the original kernels, $k_j^*(x, s) = O(|x|^{-2})$ as $x \rightarrow \pm\infty$, the new kernels $\mathcal{K}_j(x', \xi', s)$ are bounded as the end point $\xi' = -1$ and $\xi' = 1$. Hence, the kernels \mathcal{K}_j are

non-singular on the interval $(-1, 1)$, and the system (5.38) can be approximately solved, for instance, by using the collocation method with the collocation points ξ_k ($k = 1, 2, \dots, N$) chosen to be the zeros of the degree- N Legendre polynomial $P_N(x)$. The system of $2N$ linear algebraic equations associated with the system (5.38) has the form

$$\begin{aligned} \gamma_j \mathcal{X}_j(x_n, s) + \sum_{k=1}^N v_k \mathcal{K}_{3-j}(x_n, x_k, s) \mathcal{X}_{3-j}(x_k, s) &= -\mathcal{Q}_j(x_n, s), \\ n = 1, 2, \dots, N, \quad j = 1, 2, \end{aligned} \quad (5.39)$$

where v_k are the Gauss-Legendre weights given by $v_k = 2(1 - x_k^2)^{-1} [P'_N(x_k)]^{-2}$.

The chief difficulty in the implementation of this procedure is the evaluation of the principal value of the Cauchy integrals. It is helpful to rewrite them as integrals over the arc $l = \{|z'| = 1, \arg z' \in (-\pi/2, \pi/2)\}$

$$\check{a}_{jj}^{\pm}(z, s) = \exp \left\{ \frac{1 + z'}{2\pi i} P.V. \int_l \frac{\Gamma_j(\tau', s) d\tau'}{\tau' - z'} \right\}, \quad z \in \mathbb{C}^{\pm} \quad (5.40)$$

where

$$\Gamma_j(\tau', s) = \frac{\ln \check{a}_{jj}(\tau, s)}{1 + \tau'}, \quad \tau' = \frac{1 + i\tau}{1 - i\tau}, \quad z' = \frac{1 + iz}{1 - iz}. \quad (5.41)$$

Among numerous approximate formulas for the principal value of the Cauchy integral over a circle we choose [64], p.116

$$\begin{aligned} \Omega_{jj}(z, s) = \exp \left\{ \frac{1 + z'}{2M + 1} \sum_{j=-M}^M \Gamma_j(e^{i\theta_j}, s) \right. \\ \left. \times \left[\frac{1}{2} + \frac{i \sin \frac{M}{2}(\theta - \theta_j) \sin \frac{M+1}{2}(\theta - \theta_j)}{\sin \frac{1}{2}(\theta - \theta_j)} \right] \right\} \end{aligned}$$

as the one proving a good accuracy. Here, $\theta = -i \ln z'$, $\theta_j = 2\pi j/(2M + 1)$.

The final step in the evaluation of the weight functions or, equivalently, the stress intensity factors K_I and K_{II} with the special loads applied, is the inversion of the Laplace transform. This can be done by applying one of the formulas in (5.37). For computations, we employ

the uniform grid trapezoidal rule with $m + 1$ grid points

$$K_j(t) \approx \frac{he^{s_0 t}}{\pi} \left[\operatorname{Re} \tilde{K}_j(\sigma) + \operatorname{Re} \tilde{K}_j(\sigma + iT) \cos Tt + 2 \sum_{n=1}^{m-1} \operatorname{Re} \tilde{K}_j(\sigma + inh) \cos nht \right] \quad (5.42)$$

where h is the grid spacing. The numerical estimation of the functions $\tilde{K}_I(s)$ and $\tilde{K}_{II}(s)$ show (see Figure 5.1) that both their real and imaginary parts vanish slow as $\operatorname{Im} s \rightarrow \pm\infty$. To accelerate the convergence of the series in (5.42), we apply the Euler summation method [71] for alternating series. In order to transform (5.42) into an alternating sum, we put $h = \pi/(2t)$, $\sigma = A/(2t)$ and $T = \pi m/(2t)$, where A is a fixed real positive constant. Then [1]

$$K_j(t) \approx \frac{e^{A/2}}{2t} \left[\operatorname{Re} \tilde{K}_j \left(\frac{A}{2t} \right) + \operatorname{Re} \tilde{K}_j \left(\frac{A + i\pi m}{2t} \right) \cos \frac{\pi m}{2} + 2 \sum_{n=1}^{m-1} (-1)^n \frac{\Delta_n}{2^{n+1}} \right],$$

where

$$\Delta_n = \sum_{k=0}^n (-1)^k \binom{n}{k} \operatorname{Re} \left\{ \tilde{K}_j \left(\frac{A + 2(n-k)\pi i}{2t} \right) \right\}.$$

Following [1], we take $A = 8 \ln 10$.

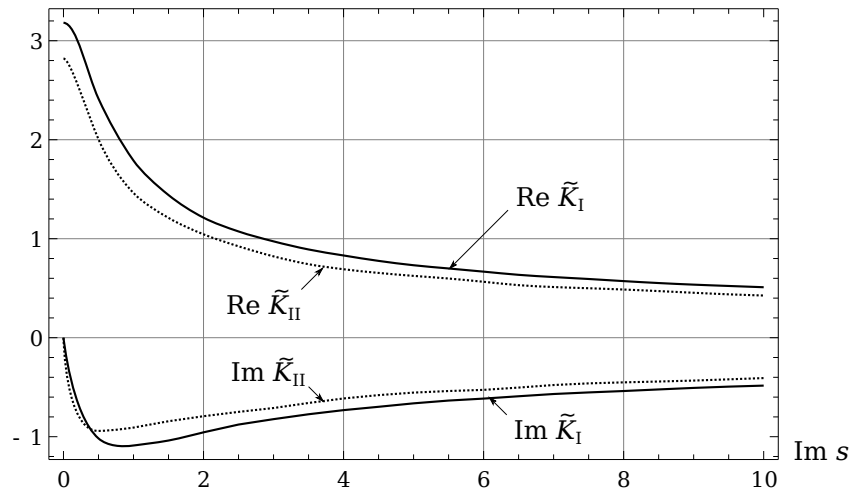


Figure 5.1: Graphs of the functions $\operatorname{Re} \tilde{K}_I(s)$, $\operatorname{Re} \tilde{K}_{II}(s)$, $\operatorname{Im} \tilde{K}_I(s)$, and $\operatorname{Im} \tilde{K}_{II}(s)$ for $\operatorname{Re} s = 0.5$.

Figures 5.2 and 5.3 show how the functions $w_{i,j}(x_0, t) = \sqrt{\frac{1}{2}\pi(vt - x_0)}W_{i,j}(x_0, t)$ and the weight functions $W_{i,j}(x_0, t)$ evolve in time. For computations, we assume x_0 to be zero, that is the time independent concentrated loads are applied at the origin $(0, 0)$ of the (x_1, x_2) -plane, which coincides with the tip of the crack at the initial time instance $t = 0$. Since the material is stress-free for $t < 0$, it is expected that, when the crack starts propagating at constant speed v , the elastic medium remains stress-free outside the disc of radius $c_l t$ centered at the point $x_1 = x_2 = 0$.

On the Figures 5.2 and 5.3, we can see the zero values of the functions $w_{I,II}$, $w_{II,I}$ and $W_{I,II}$, $W_{II,I}$ during some time interval at the beginning of the crack propagation. Then, those values start growing. This happens at the time instance when the longitudinal and shear waves, reflected from the boundary of the half-plane, come back to the crack tip, so the crack propagation gets affected by the presence of the boundary. At time $t'_l = \delta/c_l$, the first longitudinal wave strikes the boundary of the half-plane at the right angle, and at time $t = 2t'_0$, it returns to the origin $x_1 = x_2 = 0$. By that time, the crack tip has covered the distance $2vt'_l$ away from the origin, and the distortion caused by the reflected wave reaches the crack tip at time $t_l^* > 2t'_l$ (for $\delta \gg 1$, we have $t_l^* \sim 4t'_l$). The shear waves propagate

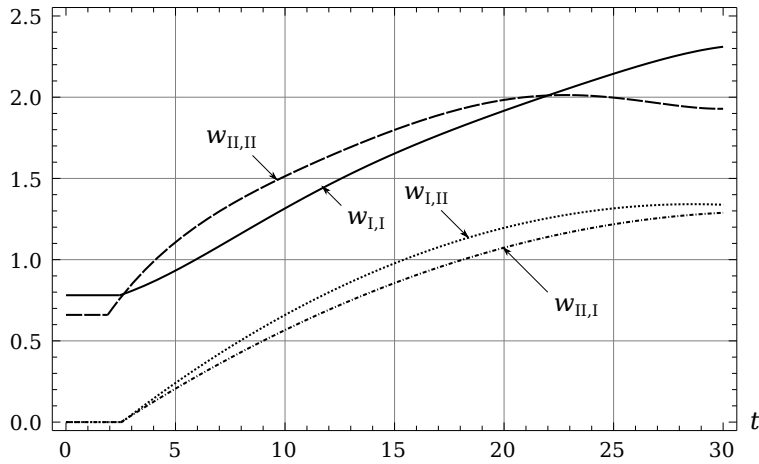


Figure 5.2: The functions $w_{i,j}(0, t) = \sqrt{\frac{1}{2}\pi vt}W_{i,j}(0, t)$ ($i, j = I, II$) versus time t when $\nu = 0.3$, $\delta = 1$ m, $v = 0.5c_R$ m/s, $c_l = 1$ m/s ($c_s \approx 0.5345$ m/s, $c_R \approx 0.4957$ m/s).

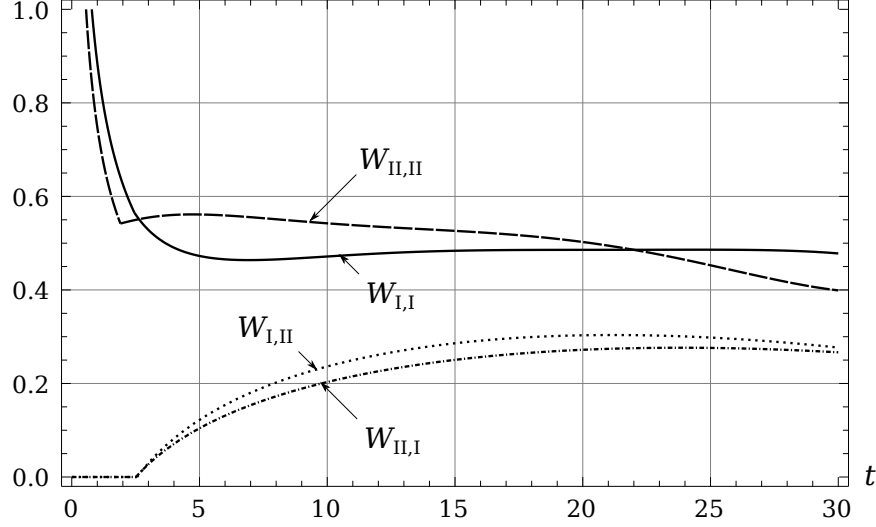


Figure 5.3: The weight functions $W_{i,j}(0, t)$, $(i, j = I, II)$ versus time t when $\nu = 0.3$, $\delta = 1$ m, $v = 0.5c_R$ m/s, $c_l = 1$ m/s ($c_s \approx 0.5345$ m/s, $c_R \approx 0.4957$ m/s).

slower, and the corresponding time, when the shear wave incident normally alters the stress intensity factors, is greater than $2\delta/c_s > t_l^*$. Due to other longitudinal waves reflected from the boundary at acute angles, the actual time when the boundary affects the stress intensity factors lies in the range between $2t_l'$ and t_l^* . The time when the reflected longitudinal wave strikes the crack at its tip can be quickly evaluated. Let this wave hit the boundary of the half-plane at time $t = t_l$ at angle θ ($\theta \in (\pi/2, \pi)$) is measured from the incident wave direction to the boundary of the half-plane) (see Figure 5.4). Then the reflected wave strikes the crack tip at time $t = 2t_l$. By that time, the crack has covered the distance $2vt_l$, and therefore, $\sqrt{c_l^2 t_l^2 - \delta^2} = vt_l$. This implies

$$t_l = \frac{\delta}{\sqrt{c_l^2 - v^2}}, \quad \theta = \frac{\pi}{2} + \tan^{-1} \frac{1}{\sqrt{1/v_l^2 - 1}}. \quad (5.43)$$

In the example used on Figures 5.2 and 5.3, we take the following values $\delta = 1$ m, $v = 0.5c_R$, and $c_R \approx 0.4957$ m/s. Simple calculations show that $2t_l \approx 2.0644$ s and $\theta = 1.8213$. This time is consistent with the time $2t_l \approx 2$ s discovered from the approximate solution. The numerical calculations (Figure 5.2 and 5.3) show that for time $0 < t < 2t_l$, the functions $w_{ii}(0, t)$ ($i = I, II$) are constant and practically coincide with the parameters k_i associated

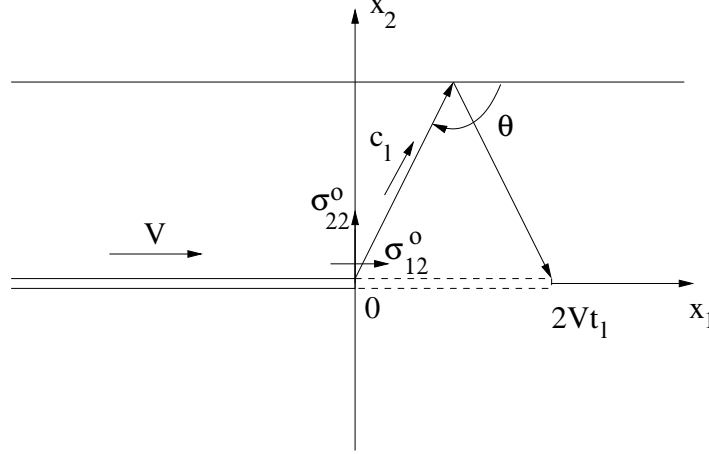


Figure 5.4: Influence of the boundary of half-plane on the crack propagation.

with the mode-I and II weight functions for the whole plane, which are given by (3.36). The mixed mode functions $w_{I,II}(0,t)$ and $w_{II,I}(0,t)$ are very close to zero when $0 < t < 2t_l$. The weight functions $W_{ij}(t,0)$ approximately equal the corresponding weight functions of the problem on the whole plane for $0 < t < 2t_l$. At time $t = 2t_l$, the graphs of the weight functions associated with the half-plane and the plane start to diverge.

The functions $w_{i,j}(0,t)$ versus the dimensionless speed v/c_R are plotted in Figure 5.5. As in the case of the whole plane, the functions $w_{I,I}$ and $w_{II,II}$ tend to 1 and to 0 when $v/c_R \rightarrow 0$ and $v/c_R \rightarrow 1$ respectively, while the off-diagonal functions, $w_{I,II}$ and $w_{II,I}$ tend to zero not only when $v/c_R \rightarrow 1$, but also when $v/c_R \rightarrow 0$. In the case of the whole plane, the functions w_I and w_{II} are monotonic, while in the case of the half-plane, they are not.

When the distance δ from the crack to the boundary of the half-plane decreases, all the four functions $w_{i,j}(0,t)$ grow (see Figure 5.6). As it is expected, when $\delta \rightarrow \infty$, the functions $w_{i,j}$ approach their limits, the corresponding functions for the whole plane, $w_{I,II} \rightarrow 0$, $w_{II,I} \rightarrow 0$, and when $\nu = 0.3$, $w_{I,I} \rightarrow k_I = 0.781473$, $w_{II,II} \rightarrow k_{II} = 0.659882$.

5.3 Crack Growth at Non-Uniform Speed

With the fundamental solution and weight functions at hand, derived and computed in the previous sections, we come to the problem on nonuniform motion of a semi-infinite crack in the direction parallel to the boundary of a half-plane. In order to do this, first we describe

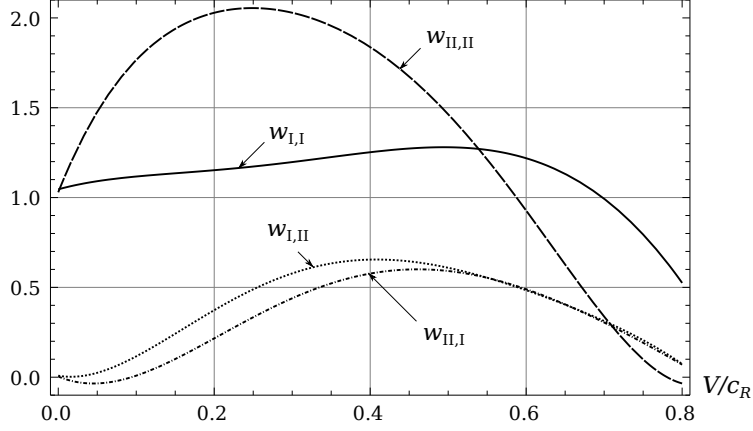


Figure 5.5: The functions $w_{i,j}(0, t)$ ($i, j = I, II$) versus v/c_R when $\nu = 0.3$, $\delta = 1$ m, $t = 10$ s, $c_l = 1$ m/s ($c_s \approx 0.5345$ m/s, $c_R \approx 0.4957$ m/s).

the motion of the crack when speed, $v(t)$, is a prescribed smooth function of time $t > 0$. Then we solve the inverse problem of determining the speed by employing one of the propagation criteria. For elaborate on the approximate method proposed in [39] and described in Section 3.3 for a semi-infinite crack moving at non-uniform speed in an unbounded body.

5.3.1 Problem on a suddenly stopped crack

Suppose at time $t = 0$ the crack starts moving, and its position at time t is described by $l(t)$, a continuously differentiable non-decreasing function such that $v(t) = l'(t) < c_R$ for all $t > 0$.

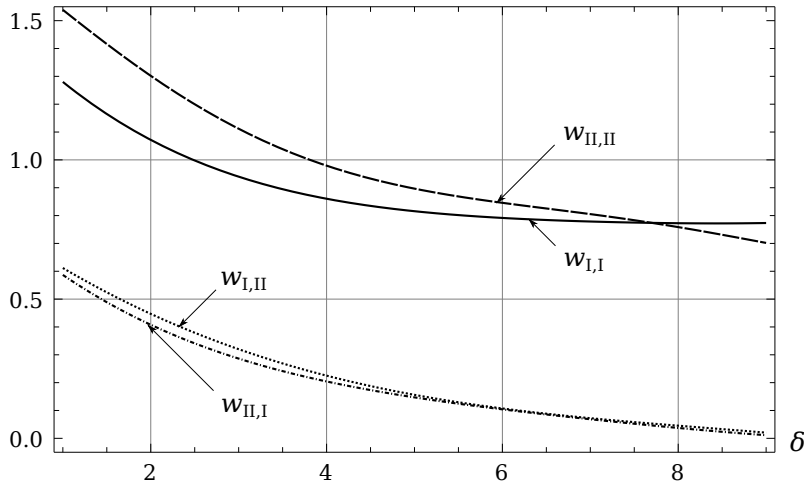


Figure 5.6: The functions $w_{i,j}(0, t)$ ($i, j = I, II$) versus the distance δ from the crack to the half-plane boundary when $\nu = 0.3$, $v = 0.5c_R$ m/s, $c_l = 1$ m/s, $t = 10$ s ($c_s \approx 0.5345$ m/s, $c_R \approx 0.4957$ m/s).

We approximate the curve $l(t)$ by a polygonal line with the vertices (t_k, l_k) , $l_k = l(t_k)$, $t_0 = 0$, $l_0 = 0$. Thus, we assume that during the time-interval $t_k < t < t_{k+1}$, the crack propagates at constant speed $v_k = (l_{k+1} - l_k)/(t_{k+1} - t_k)$.

As in Section 3.3, let us represent the stress field corresponding to the crack propagation $x_1 = l(t)$ as the superposition of the stress fields derived as the solution of the problems on a suddenly stopped crack. We will refer to those problems as P_0 -problem, P_1 -problems, etc. We also denote the problem on a stationary crack as P_{-1} -problem.

On the time-interval $0 < t < t_1$, the crack extends at constant speed v_0 by negating the stresses $\sigma_{12}^0(x_1, 0)$ and $\sigma_{22}^0(x_1, 0)$ in front of the crack tip ($x_1 > 0$), which are determined from the solution of P_{-1} -problem on a stationary semi-infinite crack parallel to the boundary of a half-plane. This problem provides the starting point for a complete description of the non-uniform motion of the crack. An exact method of matrix Wiener-Hopf factorization for this problem was presented in [86] for the case when the forces were applied to the strip at infinity, and the boundary was free of traction. The problem was reduced to a homogeneous second-order vector Riemann–Hilbert problem, that was solved, and the corresponding stress intensity factors were found. Hereafter, we assume that the solution to P_{-1} -problem is already known.

Before, we continue with the solution of P_0 -problem, let us show the following remarkable property of the weight functions:

$$W_{i,j}(x_0, t; v) = W_{i,j}(0, t - x_0/v; v), \quad i, j = I, II. \quad (5.44)$$

Recall that the Laplace transforms of the loading for the weight functions are given by $b_j(x, s) = e^{-sx_0/v} \frac{e^{sx/v}}{v}$, $j = 1, 2$. From the identities (5.10), (5.20), and (5.24), it follows that the relations

$$\begin{aligned} \hat{b}_j^-(z, s; x_0) &= e^{-sx_0/v} \hat{b}_j^-(z, s; 0), & \check{b}_j(z, s; x_0) &= e^{-sx_0/v} \check{b}_j^-(z, s; 0), \\ \check{\chi}_j^-(z, s; x_0) &= e^{-sx_0/v} \check{\chi}_j^-(z, s; 0), & \chi_j^*(x, s; x_0) &= e^{-sx_0/v} \chi_j^*(x, s; 0), \end{aligned}$$

which, together with (5.36), imply that the Laplace transforms of the weight functions satisfy the equation

$$\tilde{W}_{i,j}(x_0, s; v) = e^{-sx_0/v} \tilde{W}_{i,j}(0, s; v), \quad i, j = I, II. \quad (5.45)$$

The relation (5.44) immediately follows from (5.45).

Assume that the crack suddenly stops at time $t = t_1$ at the point $(l_1, 0)$ of the half-plane. The stress field with components $\tilde{\sigma}_{12}^1(x_1, 0)$ and $\tilde{\sigma}_{22}^1(x_1, 0)$ is radiated away along the line $x_2 = 0$, $x_1 > l_1$. In order to describe a crack that suddenly stops at time t and at the point $(l_1, 0)$, we require the stress intensity factors to vanish for all $x_1 = v_0 t > l_1$:

$$K_I(t; v_0) = 0, \quad K_{II}(t; v_0) = 0, \quad v_0 t > l_1, \quad (5.46)$$

where $K_I(t; v_0)$ and $K_{II}(t; v_0)$ are the stress intensity factors corresponding to the problem on propagation of a semi-infinite crack in a half-plane with constant speed v_0 . The statement of P_0 -problem coincides with that given in the previous section with the exception that $v = v_0$ and the boundary conditions (5.1) on the faces of the crack takes the form

$$\sigma_{j2}(x_1, 0, t) = \begin{cases} 0, & -\infty < x_1 < 0 \\ -\sigma_{j2}^0(x_1, 0), & 0 < x_1 < l_1 \quad t > t_1 \\ \tilde{\sigma}_{j2}^1(x_1, 0), & l_1 < x_1 < v_0 t \end{cases} \quad (5.47)$$

with $\tilde{\sigma}_{j2}^1(x_1, 0)$ to be determined from the condition (5.46) that expresses the fact that the crack stops propagating at time instance $t_1 = l_1/v_0$.

Combining these results, we can write down formulas (5.25) for the stress intensity factors in the form

$$\begin{aligned} K_I(t; v_0) &= -K'(t; v_0) + \int_{l_1}^{v_0 t} [W_{I,I}(0, t - x_1/v_0; v_0) \tilde{\sigma}_{22}^1(x_1, 0) \\ &\quad + W_{I,II}(0, t - x_1/v_0; v_0) \tilde{\sigma}_{12}^1(x_1, 0)] dx_1 \\ K_{II}(t; v_0) &= -K''(t; v_0) + \int_{l_1}^{v_0 t} [W_{II,I}(0, t - x_1/v_0; v_0) \tilde{\sigma}_{22}^1(x_1, 0) \\ &\quad + W_{II,II}(0, t - x_1/v_0; v_0) \tilde{\sigma}_{12}^1(x_1, 0)] dx_1 \end{aligned} \quad (5.48)$$

where the functions $K'(t; v_0)$ and $K''(t; v_0)$ are defined by

$$\begin{aligned} K'(t; v_0) &= \int_0^{l_1} [W_{I,I}(0, t - x_1/v_0; v_0)\sigma_{22}^0(x_1, 0) \\ &\quad + W_{I,II}(0, t - x_1/v_0; v_0)\sigma_{12}^0(x_1, 0)] dx_1 \\ K''(t; v_0) &= \int_0^{l_1} [W_{II,I}(0, t - x_1/v_0; v_0)\sigma_{22}^0(x_1, 0) \\ &\quad + W_{II,II}(0, t - x_1/v_0; v_0)\sigma_{12}^0(x_1, 0)] dx_1 \end{aligned}$$

The left-hand side of the equations (5.48) vanishes for $t > t_1$ due to the condition (5.46), while the terms $K'(y, v_0)$ and $k''(t, v_0)$ are known functions containing σ_{22}^0 and σ_{12}^0 determined from the solution of P_{-1} -problem. Thus, we solve the system (5.25) on the time-interval (t_1, ∞) with respect to the functions $\tilde{\sigma}_{12}^1(x_1, 0)$ and $\tilde{\sigma}_{12}^1(x_1, 0)$.

The system (5.25) can be transformed to a system of two Volterra convolution equations, which admits the solution by applying Laplace transform. Indeed, after the substitution

$$x_1 = v_0\tau' + l_1, \quad t = \tau + l_1/v_0, \quad (5.49)$$

the system (5.46) takes the form

$$\sum_{j=I}^{II} \int_0^\tau W_{i,j}(0, \tau - \tau'; v_0) \pi_i(\tau') d\tau' = \omega_i(\tau), \quad \tau > 0, \quad i = I, II, \quad (5.50)$$

where

$$\pi_I(\tau') = \tilde{\sigma}_{22}^1(v_0\tau' + l_1, 0), \quad \pi_{II}(\tau') = \tilde{\sigma}_{12}^1(v_0\tau' + l_1, 0)$$

$$\omega_I(\tau) = v_0^{-1} K'(\tau + l_1/v_0; v_0), \quad \omega_{II}(\tau) = v_0^{-1} K''(\tau + l_1/v_0; v_0)$$

The Laplace images $\tilde{\pi}_i(s)$ of the unknown functions $\pi_i(\tau')$ can be determined from the system of linear algebraic equations

$$\sum_{j=I}^{II} \tilde{W}_{i,j}(0, s; v_0) \tilde{\pi}_i(s) = \tilde{\omega}_i(s), \quad i = I, II.$$

By performing the Laplace inversion, we derive

$$\begin{aligned} \pi_I(\tau') &= \frac{1}{2\pi i} \int_{\sigma-i\infty}^{\sigma+i\infty} \frac{\tilde{W}_{II,II}(0, s; v_0) \tilde{\omega}_I(s) - \tilde{W}_{I,II}(0, s; v_0) \tilde{\omega}_{II}(s)}{\tilde{W}(s; v_0)} e^{s\tau'} ds \\ \pi_{II}(\tau') &= \frac{1}{2\pi i} \int_{\sigma-i\infty}^{\sigma+i\infty} \frac{\tilde{W}_{I,I}(0, s; v_0) \tilde{\omega}_{II}(s) - \tilde{W}_{II,I}(0, s; v_0) \tilde{\omega}_I(s)}{\tilde{W}(s; v_0)} e^{s\tau'} ds, \end{aligned}$$

where $\sigma > 0$ and

$$\tilde{W}(s; v_0) = \tilde{W}_{I,I}(0, s; v_0) \tilde{W}_{II,II}(0, s; v_0) - \tilde{W}_{I,II}(0, s; v_0) \tilde{W}_{II,I}(0, s; v_0)$$

Thus, the stress components in front of the suddenly stopped crack, corresponding to P_0 -problem can be found from

$$\tilde{\sigma}_{22}^1(x_1, 0) = \pi_I \left(\frac{x_1 - l_1}{v_0} \right), \quad \tilde{\sigma}_{12}^1(x_1, 0) = \pi_{II} \left(\frac{x_1 - l_1}{v_0} \right), \quad x_1 > l_1. \quad (5.51)$$

Let us note that the Laplace transforms $\tilde{W}_{i,j}(0, s; v_0)$ have already been determined. They are expressed through the solution at the point 0 of the system of integral equations (5.27) by the formula (5.36) for $v = v_0$ with the loading $\sigma_{22}^0(x_1, 0) = \delta(x_1)$ and $\sigma_{12}^0(x_1, 0) = 0$ for the weight functions $W_{I,I}(0, t; v_0)$ and $W_{II,I}(0, t; v_0)$, and with the loading $\sigma_{22}^0(x_1, 0) = 0$ and $\sigma_{12}^0(x_1, 0) = \delta(x_1)$ for the functions $W_{I,II}(0, t; v_0)$ and $W_{II,II}(0, t; v_0)$.

In addition to vanishing stress intensity factors in front of a suddenly stopped crack, the solution $\tilde{\sigma}_{12}^1$ and $\tilde{\sigma}_{22}^1$ has to generate zero displacement jumps through the line $x_2 = 0$ on the segment $l_1 < x_1 < v_0 t$. In contrast to the problem in an unbounded plane, when this is possible to verify analytically [39] for the sub-Rayleigh speeds and [46] for the transonic regime), it is not visible how it can be done without deploying computer based computations. That is why this condition needs to be tested numerically when the algorithm is applied.

By employing this procedure for the next period of time, $t_1 < t < t_2$, and determining the weight functions associated with speed $v = v_1$, we can find the loads $\tilde{\sigma}_{i2}^2(x_1, 0)$ ($i = 1, 2$) needed to negate the stresses generated by the crack when it suddenly stops at the point $x_1 = l_2$. In this case, we replace the boundary conditions (5.47) by

$$\sigma_{j2}(x_1, 0, t) = \begin{cases} 0, & -\infty < x_1 < l_1 \\ -\sigma_{j2}^1(x_1, 0), & l_1 < x_1 < l_2 \\ \tilde{\sigma}_{j2}^2(x_1, 0), & l_2 < x_1 < l_1 + v_1 t \end{cases} \quad t > t_2$$

where the traction components $\sigma_{j2}^1(x_1, 0)$ are known

$$\sigma_{j2}^1(x_1, 0) = \sigma_{j2}^0(x_1, 0) + \tilde{\sigma}_{j2}^1(x_1, 0),$$

while the components $\tilde{\sigma}_{j2}^2(x_1, 0)$ have to be recovered from the system of two equations $K_I(t; v_1) = 0$, $K_{II}(t; v_1) = 0$, $v_1 t > l_2$, that is equivalent to the corresponding system of two Volterra equations solvable by the Laplace transform as in the previous step.

Following the pattern established above, this procedure can be continued further up to any period of time (t_k, t_{k+1}) . It gives an approximate solution of the problem on motion of a semi-infinite crack beneath the boundary at piecewise constant speed $v = v_i$, $t \in (t_i, t_{i+1})$, $i = 0, 1, \dots, k$, that approximates the original smooth function $v(t)$. The solution of this model problem is obtained by the superposition of the solutions of all Problems P_i ($i = -1, 0, 1, 2, \dots, k$), where P_{-1} is the problem for a stationary semi-infinite crack, Problems P_i ($i = 0, 1, \dots, k-1$) are the transient problems with the boundary conditions chosen accordingly. As it was shown in Section 3.3, for the total problem P , the homogeneous boundary conditions on the crack faces $\{(x_1, 0^\pm) : 0 < x_1 < l(t)\}$ are satisfied. As for the stress intensity factors at the tip of the crack at time $t \in (t_k, t_{k+1})$, when the crack moves at speed v_k , (in general, they do not vanish) they are defined by the stress intensity factors generated by Problem P_k .

A feature of Problem P is in the presence of the boundary. As it was pointed out in the previous section, initially, when $t < 2t_l$ (t_l is given by (5.43)), and when the longitudinal wave reflected from the half-plane boundary has not reached the crack, the off-diagonal weight functions $W_{I,II}$ and $W_{II,I}$ vanish, and the diagonal functions $W_{I,I}$ and $W_{II,II}$ coincide with those associated with the problem on an unbounded plane with a crack. Therefore, for this short period of time, the algorithm proposed in [39] can be repeated without any changes. However, this does not mean that the actual motion of the crack in a half-plane will be the same as in the case of an unbounded plane even for time $t < 2t_l$. To make this conclusion, we need to recall that the boundary conditions of Problems P_k depend on the stresses $\sigma_{i2}^0(x_1, 0)$ ($i = 1, 2$) generated by the static crack in the half-plane which are apparently not the same as the ones associated for an unbounded plane. When time exceeds $2t_l$, then, in general, all

the weight functions $W_{i,j}$ are nonzero and different from those associated with the case of an unbounded plane. Thus, the boundary of the half-plane affects the stress field near the crack tip. In this case, in order to describe a non-uniform propagation of the semi-infinite crack parallel to the boundary of a half-plane, the algorithm introduced in this section needs to be applied.

5.3.2 Determination of propagation speed

In the previous section, prescribed piece-wise constant speed $v(t)$ was considered. Assume now that the speed is an unknown function of time t and determine it by employing the Griffith dynamic criterion [85, 17]. Let $\delta U(t)$ be the potential energy released when the crack $S(t) = \{(x_1, 0) : -\infty < x_1 < v_0 t\}$ extends to $S(t) + \delta S(t) = \{(x_1, 0) : -\infty < x_1 < v_0 t + r\}$, where r is small. The energy $\delta U(t)$ may be expressed as

$$\delta U(t) = \frac{1}{2} \int_0^r \{\sigma_{xy}(x, 0, t) \delta[u](x, t) + \sigma_{yy}(x, 0, t) \delta[v](x, t)\} dx. \quad (5.52)$$

Here, $[u] + \delta[u]$, $[v] + \delta[v]$ are the displacement jumps related to the extended crack, and

$$\sigma_{12} \sim \frac{K_{II}(t)}{\sqrt{2\pi x}}, \quad \sigma_{22} \sim \frac{K_I(t)}{\sqrt{2\pi x}}, \quad x \in (0, r), \quad r \rightarrow 0^+. \quad (5.53)$$

To find asymptotic expansions for $\delta[u]$, $\delta[v]$, we employ the relations (5.20), take into account that

$$\tilde{\chi}_j^-(z, s) \sim \frac{1}{iz} \chi_j^*(0^-, s), \quad \text{Im } z \rightarrow \infty \quad (5.54)$$

and also formulas (5.36). This and the Tauberian theorem eventually bring us to

$$\tilde{\chi}_1(x, s) \sim -\frac{\tilde{K}_{II}(s)}{\mu\gamma_1\sqrt{-2\pi x}}, \quad \tilde{\chi}_2(x, s) \sim -\frac{\tilde{K}_I(s)}{\mu\gamma_2\sqrt{-2\pi x}}, \quad x \rightarrow 0^-. \quad (5.55)$$

On integrating these relations with respect to x and fixing the constant of integration by assuring that the displacement jumps vanish at the crack tip we obtain the displacement jumps $[u]$ and $[v]$ for small negative x . When the crack extends to $x = r$, these formulas give

$$[v](x, t) \sim \sqrt{\frac{2(r-x)}{\pi}} \frac{K_I(t)}{\mu\gamma_2}, \quad [u](x, t) \sim \sqrt{\frac{2(r-x)}{\pi}} \frac{K_{II}(t)}{\mu\gamma_1}, \quad x \rightarrow r^-. \quad (5.56)$$

Finally, by substituting the asymptotic relations (5.53) and (5.56) into (5.52) we find the potential energy increment when the crack extends to $S(t) + \delta S(t)$

$$\delta U(t) \sim \frac{r}{4\mu} \left(\frac{K_I^2(t)}{\gamma_2} + \frac{K_{II}^2(t)}{\gamma_1} \right), \quad r \rightarrow 0^+. \quad (5.57)$$

According to the Griffith criterion, the crack starts propagating if the energy $\delta U(t)$ equals or greater than the increase in the surface energy $2Tr$, $\delta U \geq 2Tr$, where T is the Griffith material constant. This criterion may be represented in terms of the stress intensity factors in the form

$$\frac{K_I^2(t)}{\gamma_2} + \frac{K_{II}^2(t)}{\gamma_1} \geq 8\mu T. \quad (5.58)$$

On applying this criterion, that is on solving the transcendental equation

$$\gamma_1 K_I^2(t) + \gamma_2 K_{II}^2(t) = 8\mu\gamma_1\gamma_2 T, \quad (5.59)$$

one may predict v_0 , the initial speed of crack propagation. Following the successive algorithm described above and solving the associated equation (5.59) it is possible to determine all the speeds v_j $j = 1, 2, \dots$

Chapter 6

Fracture in an Infinite Strip

In this chapter, we will consider two problems on propagation of a crack in an infinite strip, which use the cohesive zone and the lattice models of a crack propagation.

For intersonic propagation speed ($c_s < v < c_l$), the continuous model of a crack propagation results to the zero release energy rate near the crack tip, which yields the fact that such propagation is impossible. However, it has been observed experimentally [69]. In order to describe propagation at intersonic speed, the cohesive zone model is employed, by assuming the cohesive zone interval of unknown length l in front of the crack (see Figure 6.1) where the constant stress components are prescribed. This problem gives rise to a scalar Riemann–Hilbert problem with the coefficient-function that has infinitely many simple poles on the contour of the problem, which was not solved in the closed form before (to the best of my knowledge). Although its solution can be constructed using the standard technique described in Section 2.1, it is expressed through Cauchy integrals of functions with infinitely many singular points on the contour, which are not easy to compute. The natural approach in this case is the contour transformation (see, for instance, [4]). Here, we will describe a technique of constructing Wiener–Hopf factorization of such a function.

Another approach that is used to deal with intersonic propagation speeds is to apply the lattice model of crack propagation, where the material is described as a lattice of atoms connected by massless bonds, while the crack propagation is modeled as breaking bonds when their length exceeds certain critical value. Even in the case of anti-plane deformation, this problem is equivalent to a vector Riemann–Hilbert problem with 2×2 matrix coefficient, which does not admit a closed-form solution. This vector Riemann–Hilbert problem is solved by employing a partial Wiener–Hopf factorization described earlier in Section 2.3.3.

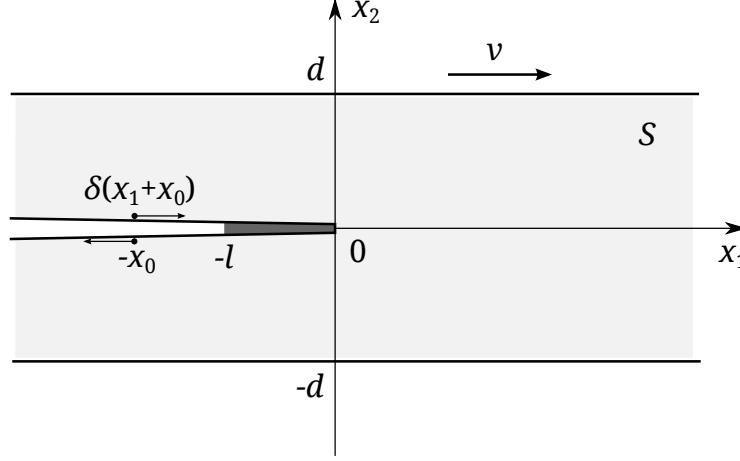


Figure 6.1: Symmetric semi-infinite crack in a strip

6.1 Factorization of a Class of Wiener–Hopf Kernels

Consider a function $a(\xi)$ meromorphic in the complex plane \mathbb{C} with infinitely many discrete poles and zeros on the real and imaginary axes and at most finitely many poles and zeros elsewhere (on example of such a function is $a(\xi) = \tan(\xi) \tanh(\xi)$). Let L be a curve in \mathbb{C} , which mostly coincides with the real axis \mathbb{R} but passes around under the poles and zeros of the function $a(\xi)$ (see Figure 6.2), so that L contains neither poles nor zeros of $a(\xi)$. The radius of the semi-circular parts of L is considered to be infinitely small so that the curve L coincides with the real axis \mathbb{R} almost everywhere. Notice that the curve L splits the complex plane \mathbb{C} into two parts \mathbb{C}^+ and \mathbb{C}^- , above and below of L respectively.

The paper’s objective is to construct the Wiener–Hopf factorization

$$a(\xi) = a^+(\xi)/a^-(\xi), \quad \xi \in L \quad (6.1)$$

such that the function $a^\pm(\xi)$ is analytic in \mathbb{C}^\pm . Obtaining the Wiener–Hopf factorization on the curve L is problematic since the function $a(\xi)$ have no limits as $\xi \rightarrow \infty$ along the line L and the poles and zeros of $a(\xi)$ are infinitely close to the integration path. For simplicity, assume that $a(\xi)$ has a simple pole at the origin: this case corresponds to the problem of Dynamic fracture mechanics considered later. Otherwise the function $a(\xi)$ can be multiplied by a rational function in order to obtain a simple pole at the origin.

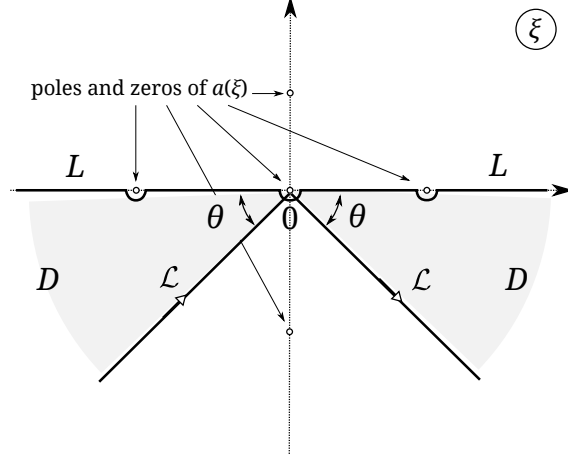


Figure 6.2: The integration paths L and \mathcal{L} on the complex plane

6.1.1 Auxiliary Wiener–Hopf factorization.

Since there are only finitely many poles and zeros of the function $a(\xi)$ in the four quadrants of the complex plane \mathbb{C} , there is an angle $\theta \in (0, \pi/2)$ such that $a(\xi)$ is analytic and non-zero in the union of two sectors (see Figure 6.2)

$$D(\theta) = \{\xi : -\theta - \varepsilon < \arg \xi < 0\} \cup \{\xi : -\pi < \arg \xi < -\pi + \theta + \varepsilon\}$$

for a small positive value ε . Let \mathcal{L}_1 and \mathcal{L}_2 be two rays with a common endpoint at the origin

$$\mathcal{L}_1(\theta) = \{re^{-i\theta} : r > 0\}, \quad \mathcal{L}_2(\theta) = \{re^{i(\theta-\pi)} : r > 0\}$$

Hereafter, whenever it is important to emphasize the dependence of D , \mathcal{L}_1 , and \mathcal{L}_2 on the parameter θ , they are written with θ as their argument, otherwise the argument is dropped.

In order to obtain the representation (6.1), construct an auxiliary Wiener–Hopf factorization of $a(\xi)$ on the union $\mathcal{L} = \mathcal{L}_1 \cup \mathcal{L}_2$. Since the function $a(\xi)$ is analytic in D , it is Hölder continuous [41] on \mathcal{L} and its Wiener–Hopf factorization is given by

$$a_{\theta}^{\pm}(\xi) = \exp \left\{ \frac{1}{2\pi i} \int_{\mathcal{L}} \frac{\ln a(t)}{t - \xi} dt \right\}, \quad \xi \in \mathbb{C} \setminus \mathcal{L} \quad (6.2)$$

where the direction of the path integration is chosen so that $\operatorname{Re}\{\mathcal{L}\}$ is increasing. However, the integral in (6.2) has a logarithmic singularity at infinity due to $\ln a(t)$ may approach

different limits as $t \rightarrow \infty$ along \mathcal{L}_1 and along \mathcal{L}_2 . Hence, it is computationally beneficial to rewrite the functions $a_\theta^+(\xi)$ and $a_\theta^-(\xi)$ as follows.

Let A_1 and A_2 be the limits of $a(\xi)$ as $\xi \rightarrow \infty$ along \mathcal{L}_1 and \mathcal{L}_2 respectively,

$$A_1 = \lim_{r \rightarrow +\infty} a(re^{-i\theta}), \quad A_2 = \lim_{r \rightarrow +\infty} a(re^{i(\theta-\pi)}) \quad (6.3)$$

Represent the function $a(\xi)$ as the product

$$a(\xi) = k(\xi) a^*(\xi), \quad k(\xi) = \gamma \frac{\sinh \pi(\xi + iq)}{\sinh \pi \xi} \quad (6.4)$$

and choose the parameters γ and q so that the function $k(\xi)$ would have the behavior of $a(\xi)$ at infinity. It is easy to check that the values

$$\gamma = \sqrt{A_1 A_2}, \quad q = \frac{1}{2\pi i} \ln \frac{A_1}{A_2}$$

with a correct choice of branches of the square root and the logarithm above, provide

$$A_1 = \lim_{r \rightarrow +\infty} k(re^{-i\theta}), \quad A_2 = \lim_{r \rightarrow +\infty} k(re^{i(\theta-\pi)}) \quad (6.5)$$

In the representation (6.4), the function $k(\xi)$ can be factorized explicitly as a product and ratio of Γ -functions, while the Wiener–Hopf factorization of $a^*(\xi)$ on \mathcal{L} can be obtained with Cauchy integrals of a better convergence due to $a^*(\xi)$ being a Hölder function and $\ln a^*(\xi) \rightarrow 0$ as $\xi \rightarrow \infty$, $\xi \in \mathcal{L}$. Hence,

$$\begin{aligned} a_\theta^+(\xi) &= k^+(\xi) \exp \left\{ \frac{1}{2\pi i} \int_{\mathcal{L}(\theta)} \frac{\ln a^*(t)}{t - \xi} dt \right\} \\ a_\theta^-(\xi) &= k^-(\xi) \exp \left\{ \frac{1}{2\pi i} \int_{\mathcal{L}(\theta)} \frac{\ln a^*(t)}{t - \xi} dt \right\} \\ k^+(\xi) &= \gamma \frac{(\xi + iq)\Gamma(1 - i\xi)}{\Gamma(1 - i\xi + q)}, \quad k^-(\xi) = \frac{\xi\Gamma(1 + i\xi - q)}{\Gamma(1 + i\xi)} \end{aligned} \quad (6.6)$$

where $a_\theta^+(\xi)$ is analytic and non-zero in $\mathbb{C}^+ \cup L \cup D(\theta)$ and $a_\theta^-(\xi)$ is analytic and non-zero in $\mathbb{C}^- \setminus D(\theta)$. The identity

$$\sinh(\xi) = \pi\xi / [\Gamma(1 + i\xi)\Gamma(1 - i\xi)] \quad (6.7)$$

and the Sokhotsky–Plemelj formulas [62, 41] imply the Wiener–Hopf factorization $a(\xi) = a_\theta^+(\xi)/a_\theta^-(\xi)$ for $\xi \in \mathcal{L}(\theta)$.

6.1.2 Transform of the integration path

Notice that for $\theta = 0$, the functions $a^\pm = a_0^\pm(\xi)$ would give the required Wiener–Hopf factorization (6.1) if the integrals in (6.6) existed. Moreover, to find relation between the integral over $\mathcal{L}(0)$ and over $\mathcal{L}(\theta)$, one would use Cauchy’s theorem and derive the identities

$$\begin{aligned} a^+(\xi) &= k^+(\xi) \exp \left\{ \frac{1}{2\pi i} \int_{\mathcal{L}(\theta)} \frac{\ln a^*(t)}{t - \xi} dt \right\}, \quad \xi \in \mathbb{C}^+ \\ a^-(\xi) &= \begin{cases} \frac{k^-(\xi)}{a^*(\xi)} \exp \left\{ \frac{1}{2\pi i} \int_{\mathcal{L}(\theta)} \frac{\ln a^*(t)}{t - \xi} dt \right\}, & \xi \in D \\ k^-(\xi) \exp \left\{ \frac{1}{2\pi i} \int_{\mathcal{L}(\theta)} \frac{\ln a^*(t)}{t - \xi} dt \right\}, & \xi \in \mathbb{C}^- \setminus D \end{cases} \end{aligned} \quad (6.8)$$

Notice again that the identities (6.8) can be derived under the assumption of existence of the integrals in (6.6). Since the integrals do not exist for the class of functions considered here, the identities (6.8) cannot be taken for granted. Instead, it is possible to use (6.8) as the definition of the functions $a^\pm(\xi)$ and to prove that they provide the requited Wiener–Hopf factorization on L .

Thus, define the functions $a^\pm(\xi)$ by the formulas (6.8). First show that in spite of its piecewise definition, the function $a^-(\xi)$ is analytic in \mathbb{C}^- . Fix a point $\xi \in \mathcal{L}(\theta)$, $\xi \neq 0$. If $\zeta \rightarrow \xi$ from above of $\mathcal{L}(\theta)$ (that is, $\zeta \in D$), then the Sokhotski–Plemelj formulas imply

$$\lim_{\zeta \rightarrow \xi} a^-(\zeta) = \frac{k^-(\xi)}{a^*(\xi)} \exp \left\{ \frac{1}{2} \ln a^*(\xi) \right\}, \quad (\zeta \in D) \quad (6.9)$$

Similarly, if $\zeta \rightarrow \xi$ from below of $\mathcal{L}(\theta)$ (that is, $\zeta \in \mathbb{C}^- \setminus D$), then

$$\lim_{\zeta \rightarrow \xi} a^-(\zeta) = k^-(\xi) \exp \left\{ -\frac{1}{2} \ln a^*(\xi) \right\}, \quad (\zeta \in \mathbb{C}^- \setminus D) \quad (6.10)$$

Thus, the limits above at the point ξ are equal as long as the branches of $\ln a^*(\xi)$, $\xi \in \mathcal{L}(\theta)$ are the same in the both formulas (6.9) and (6.10). Since ξ is an arbitrary non-zero point of $\mathcal{L}(\theta)$ and $\ln a^*(\xi)$ is Hölder continuous on $\mathcal{L}(\theta)$, the formula (6.8) defines a function $a^-(\xi)$, which is analytic in D and $\mathbb{C}^- \setminus D$, continuous on $\mathcal{L}(\theta)$, and, therefore, analytic in \mathbb{C}^- due to uniqueness of the analytic continuation.

Now, show that the function $a^\pm(\xi)$ is indeed the Wiener–Hopf factorization of $a(\xi)$ on L ; that is, that they satisfy the equality (6.1). Notice that the function $a^+(\xi)$ can be analytically continued onto $\mathbb{C}^+ \cup L \cup D$, thus is defined and continuous on $L \setminus \{0\}$ (behavior near the origin $\xi = 0$ will be considered later). The function $a^-(\xi)$ is analytic in \mathbb{C}^- and having singularities on the real axis \mathbb{R} , which are zeros of $a^*(\xi)$. Since the curve L passes around under those singularities, the function $a^-(\xi)$ is defined and continuous on L . Therefore, for any point $\xi \in L$, that is not the origin, the formulas (6.8) yield the equality (6.1).

The case when ξ is the origin, should be treated separately since $\xi = 0$ lies on the integration path and is the vertex of the angle $\mathcal{L}(\theta)$. The Sokhotski–Plemelj formulas for a polygonal line [41] imply

$$\begin{aligned} a^+(0) &= i\gamma q \frac{[a^*(0)]^{\frac{1}{2} - \frac{\theta}{\pi}}}{\Gamma(1+q)} \exp \left\{ \frac{1}{2\pi i} p.v. \int_{\mathcal{L}(\theta)} \ln a^*(t) \frac{dt}{t} \right\} \\ a^-(\xi) &\sim \xi \frac{\Gamma(1-q)}{[a^*(0)]^{\frac{1}{2} + \frac{\theta}{\pi}}} \exp \left\{ \frac{1}{2\pi i} p.v. \int_{\mathcal{L}(\theta)} \ln a^*(t) \frac{dt}{t} \right\}, \quad \xi \rightarrow 0 \end{aligned}$$

where $a^-(\xi)$ is the continuation of the function $a^-(\xi)$ defined by (6.8) onto a neighborhood of $\xi = 0$. Thus

$$\frac{a^+(\xi)}{a^-(\xi)} \sim i\gamma q \frac{a^*(0)}{\Gamma(1+q)\Gamma(1-q)} \frac{1}{\xi}, \quad \xi \rightarrow 0 \quad (6.11)$$

Using the representation (6.4) of the function $a(\xi)$ and the identity (6.7), it is easy to see that the right-hand side of (6.11) is the first term of the expansion of $a(\xi)$ near the origin. Thus, $a^+(\xi)/a^-(\xi) \sim a(\xi)$ as $\xi \rightarrow 0$, and the functions $a^\pm(\xi)$ defined by (6.8) is the Wiener–Hopf factorization of the function $a(\xi)$ on L .

Notice that in spite of the function $a(\xi)$ having an infinitely many poles and zeros on the real axis \mathbb{R} and no limit as $\xi \rightarrow \pm\infty$, the formulas (6.8) provide the Wiener–Hopf factorization of $a(\xi)$ almost everywhere on \mathbb{R} and the integrals in (6.8) are understood in the usual sense. Moreover, the parameter θ can be chosen from the range of possible values so that to provide the best convergence of the integrals.

6.2 Symmetric Crack in an Infinite Strip

The Wiener–Hopf technique is applicable to many problems in physics and engineering. In order to demonstrate the technique described above, consider a problem of Dynamic fracture mechanics on an intersonic steady–state crack propagation in a strip: the intersonic speed of a crack and its propagation in a strip provide an example of an equation with a function–coefficient of the class considered in Section 6.1.

6.2.1 Inter-sonic symmetric steady-state crack propagation

An elastic, isotropic, homogeneous medium under the plane–strain condition is characterized by elastic modulus μ , shear wave speed c_s , and longitudinal wave speed c_l and has the shape of an infinite strip of width $2d$, that occupies the region $S = \{(x_1, x_2) : x_1 \in \mathbb{R}, x_2 \in (-d, d)\}$ in \mathbb{R}^2 . Through the middle of the strip, a stable propagation of a crack at the constant speed v is assumed (see Figure 6.1). Introduce a coordinate system moving together with the crack so that the crack tip stays at the origin for any time t , while the crack faces lie on the negative real semi-axis. The faces are subject to a shear traction,

$$\begin{aligned}\sigma_{12}(x_1, 0^\pm) &= \pm\sigma_0(x_1), & -\infty < x_1 < 0 \\ \sigma_{22}(x_1, 0^\pm) &= 0,\end{aligned}\tag{6.12}$$

where the superscripts “+” and “−” denote the upper and the lower faces of the crack, respectively. For simplicity, it is assumed that σ_0 is an L_2 -function with compact support on \mathbb{R}_- , although a bigger class can be considered. The borders of the strip are traction-free,

$$\sigma_{12}(x_1, \pm d) = \sigma_{22}(x_1, \pm d) = 0, \quad -\infty < x_1 < \infty\tag{6.13}$$

The stress and displacement components in an elastic solid are expressed through two displacement potentials ϕ and ψ [39],

$$\begin{aligned}\frac{1}{\mu}\sigma_{12} &= 2\frac{\partial^2\phi}{\partial x_1\partial x_2} - \frac{\partial^2\psi}{\partial x_1^2} + \frac{\partial^2\psi}{\partial x_2^2} \\ \frac{1}{\mu}\sigma_{22} &= \left(\frac{c_l^2}{c_s^2} - 2\right)\frac{\partial^2\phi}{\partial x_1^2} + \frac{c_l^2}{c_s^2}\frac{\partial^2\phi}{\partial x_2^2} - 2\frac{\partial^2\psi}{\partial x_1\partial x_2} \\ u_1 &= \frac{\partial\phi}{\partial x_1} + \frac{\partial\psi}{\partial x_2}, \quad u_2 = \frac{\partial\phi}{\partial x_2} - \frac{\partial\psi}{\partial x_1}\end{aligned}\tag{6.14}$$

and the potentials satisfy the wave equations (in the moving coordinate system)

$$\alpha^2 \frac{\partial^2 \phi}{\partial x_1^2} + \frac{\partial^2 \phi}{\partial x_2^2} = 0, \quad -\beta^2 \frac{\partial^2 \psi}{\partial x_1^2} + \frac{\partial^2 \psi}{\partial x_2^2} = 0, \quad (x_1, x_2) \in S \setminus \mathbb{R}_- \quad (6.15)$$

where $\alpha = \sqrt{1 - v^2/c_l^2}$ and $\beta = \sqrt{v^2/c_s^2 - 1}$ are positive constants in the case of the inter-sonic steady-state propagation $c_s < v < c_l$.

Because the crack lies on an axis of the strip symmetry, components of the displacement satisfy the conditions $u_1(x_1, -x_2) = -u_1(x_1, x_2)$ and $u_2(x_1, -x_2) = u_2(x_1, x_2)$, which implies

$$u_1(x_1, 0) = 0, \quad x_1 > 0 \quad (6.16)$$

Thus, it suffices to consider only the upper half of the strip with the additional assumption that the u_1 -component vanishes in front of the crack.

Applying the Fourier transform (hereafter, the hat “ \wedge ” denotes the Fourier transform of a function)

$$\hat{f}(\xi, x_2) = \int_{-\infty}^{\infty} f(x_1, x_2) e^{i\xi x_1} dx_1 \quad (6.17)$$

to the wave equations (6.15) reduces them to ordinary differential equations in x_2 -variable, whose solutions are

$$\begin{aligned} \hat{\phi}(\xi, x_2) &= C_1(\xi) \cosh(\alpha \xi x_2) + C_2(\xi) \sinh(\alpha \xi x_2), \\ \hat{\psi}(\xi, x_2) &= D_1(\xi) \cos(\beta \xi x_2) + i D_2(\xi) \sin(\beta \xi x_2), \end{aligned} \quad 0 < x_2 < d \quad (6.18)$$

where the coefficients C_1 , C_2 , D_1 , and D_2 can be found from the Fourier transforms of the boundary conditions (6.12), (6.13), and the first two of the relations (6.14). After algebraic calculations, one derives

$$\begin{aligned} C_1(\xi) &= -\frac{\beta}{\Delta(\xi)} [R \sinh(\alpha + i\beta)\xi d + \bar{R} \sinh(\alpha - i\beta)\xi d] \frac{\hat{\sigma}_{12}(\xi, 0)}{\mu \xi^2} \\ C_2(\xi) &= \frac{2\beta}{\Delta(\xi)} \left[R \sinh^2 \frac{\alpha + i\beta}{2} \xi d + \bar{R} \sinh^2 \frac{\alpha - i\beta}{2} \xi d \right] \frac{\hat{\sigma}_{12}(\xi, 0)}{\mu \xi^2} \\ D_1(\xi) &= \frac{1 - \beta^2}{\Delta(\xi)} \left[R \sinh^2 \frac{\alpha + i\beta}{2} \xi d - \bar{R} \sinh^2 \frac{\alpha - i\beta}{2} \xi d \right] \frac{\hat{\sigma}_{12}(\xi, 0)}{\mu \xi^2} \\ D_2(\xi) &= -\frac{1 - \beta^2}{2\Delta(\xi)} [R \sinh(\alpha + i\beta)\xi d + \bar{R} \sinh(\alpha - i\beta)\xi d] \frac{\hat{\sigma}_{12}(\xi, 0)}{\mu \xi^2} \end{aligned} \quad (6.19)$$

where

$$\Delta(\xi) = R^2 \sinh^2 \frac{\alpha + i\beta}{2} \xi d - \bar{R}^2 \sinh^2 \frac{\alpha - i\beta}{2} \xi d, \quad R = (1 - \beta^2)^2 - 4i\alpha\beta$$

In (6.19), the function $\hat{\sigma}_{12}(\xi, 0)$ is unknown, and it is to be determined by the Wiener–Hopf technique. Introduce the function representing the Fourier transform of the strain component $\varepsilon_{11} = \partial u_1 / \partial x_1$ on the line $x_2 = 0$,

$$E^-(\xi) := \hat{\varepsilon}_{11}(\xi, 0) = \int_{-\infty}^0 \varepsilon_{11}(x_1, 0) e^{i\xi x_1} dx_1 \quad (6.20)$$

where the integral is taken over the negative part of the real axis $x_2 = 0$ since $\varepsilon_{11}(x_1, 0) = 0$ for $x_1 > 0$ due to the condition (6.16). The function $E^-(\xi)$ is analytic in the lower half-plane $\{\xi : \text{Im}(\xi) < 0\}$ and decays at infinity, provided that $\varepsilon_{11}(x_1, 0)$ is integrable on \mathbb{R}_- . For negative values of x_1 , the stress component $\sigma_{12}(x_1, 0)$ is equal to $\sigma_0(x_1)$; that is

$$\hat{\sigma}_{12}(\xi, 0) = \Sigma^+(\xi) + \hat{\sigma}_0(\xi), \quad \Sigma^+(\xi) = \int_0^\infty \sigma_{12}(x_1, 0) e^{i\xi x_1} dx_1 \quad (6.21)$$

The unknown function $\Sigma^+(\xi)$ is analytic in the upper half plane $\{\xi : \text{Im}(\xi) > 0\}$, provided that $\sigma_{12}(x_1, 0)$ is an integrable function on \mathbb{R}_+ . The last two relations in (6.14) along with (6.18), (6.19) yield the equation

$$E^-(\xi) = a(\xi)[\Sigma^+(\xi) + \hat{\sigma}_0(\xi)], \quad \xi \in L \quad (6.22)$$

$$a(\xi) = \frac{\beta(1 + \beta^2)}{\mu\Delta(\xi)} [R \sinh(\alpha + i\beta)\xi d + \bar{R} \sinh(\alpha - i\beta)\xi d]$$

where the curve L mostly coincides with the real axis \mathbb{R} and passes around under the poles and zeros of $a(\xi)$ (see Figure 6.2). Notice that the choice of L is somewhat arbitrary: the curve L can pass around each of the poles and zeros of $a(\xi)$ either above or below, which would change the index [62] of $a(\xi)$ and the Wiener–Hopf factors. However, in order to utilize the technique described in Section 6.1, one needs the curve L passing around below the poles and zeros of $a(\xi)$. Notice also that with a few changes, the technique can be applicable if L passes around above the poles and zeros of $a(\xi)$.

Thus, the problem of intersonic steady-state propagation of the semi-infinite crack in a strip is reduced to the Riemann-Hilbert problem of finding two L_2 -functions $\Sigma^+(\xi)$ and $E^-(\xi)$ so that $\Sigma^+(\xi)$ is analytic in \mathbb{C}^+ , E^- is analytic in \mathbb{C}^- , and they both are continuous on the contour L and satisfy the boundary condition (6.22) on L .

6.2.2 Solution of the Riemann-Hilbert problem

Considering the function $a(\xi)$ defined in (6.22) on the complex plane \mathbb{C} , we conclude that it is meromorphic on the complex plane \mathbb{C} with infinitely many simple poles on the real and imaginary axes, that cannot be expressed in radicals. Thus, its Wiener-Hopf factorization can be obtained by (6.8) and (6.4) with the parameters

$$\gamma = \frac{2\beta(1 + \beta^2)}{\mu|R|}, \quad q = \frac{1}{\pi} \tan^{-1} \frac{4\alpha\beta}{(1 - \beta^2)^2}$$

The following solution follows the standard 3-steps procedure described in Section 2.1.2. In the boundary condition (6.22), replace the function $a(\xi)$ by its Wiener-Hopf factorization and multiply the condition by $a^-(\xi)$. Then the equation (6.22) takes the form

$$a^-(\xi)E^-(\xi) = a^+(\xi)\Sigma^+(\xi) - a^+(\xi)\hat{\sigma}_0(\xi), \quad \xi \in L \quad (6.23)$$

In order to find $E^-(\xi)$ and $\Sigma^+(\xi)$ satisfying (6.23), one needs to represent the function $a^+(\xi)\hat{\sigma}_0(\xi)$ as a difference of a function analytic in \mathbb{C}^+ and a function analytic in \mathbb{C}^- . Similar to the justification that (6.8) is the Wiener-Hopf factorization of $a(\xi)$ on L , it can be shown that $a^+(\xi)\hat{\sigma}_0(\xi) = \Psi^+(\xi) - \Psi^-(\xi)$ on L where

$$\begin{aligned} \Psi^+(\xi) &= \frac{1}{2\pi i} \int_{\mathcal{L}(\theta_1)} \frac{a^+(t)\hat{\sigma}_0(t)}{t - \xi} dt, \quad \xi \in \mathbb{C}^+ \\ \Psi^-(\xi) &= \begin{cases} -a^-(\xi)\hat{\sigma}_0(\xi) + \frac{1}{2\pi i} \int_{\mathcal{L}(\theta_1)} \frac{a^+(t)\hat{\sigma}_0(t)}{t - \xi} dt, & \xi \in D \\ \frac{1}{2\pi i} \int_{\mathcal{L}(\theta_1)} \frac{a^+(t)\hat{\sigma}_0(t)}{t - \xi} dt, & \xi \in \mathbb{C}^- \setminus D \end{cases} \end{aligned}$$

Notice that although the product $a^+(\xi)\hat{\sigma}_0(\xi)$ has no singularities on the real axis \mathbb{R} , the angle $\mathcal{L}(\theta_1)$ was used as an integration path, which significantly improves convergence of the

integrals above. The parameter θ_1 can be chosen arbitrary such that $0 < \theta_1 \leq \theta$. Notice that the function $a^+(\xi)$ is defined only on \mathbb{C}^+ in (6.8). Here, $a^+(\xi)$ for $\xi \in \mathcal{L}(\theta_1)$ is understood as its analytic continuation from \mathbb{C}^+ onto $\mathbb{C}^+ \cup L \cup D$, which is given by the same formula (6.8). In the case $\theta_1 = \theta$, the values $a^+(\xi)$ are understood as the limit for $\zeta \rightarrow \xi$ from $\mathbb{C}^+ \cup L \cup D$. Replacing $a^+(\xi)\hat{\sigma}_0(\xi)$ in the equation (6.23) by the difference $\Psi^+(\xi) - \Psi^-(\xi)$ yields

$$a^-(\xi)E^-(\xi) - \Psi^-(\xi) = a^+(\xi)\Sigma^+(\xi) - \Psi^+(\xi), \quad \xi \in L \quad (6.24)$$

Define the auxiliary function

$$R(\xi) = \begin{cases} a^+(\xi)\Sigma^+(\xi) - \Psi(\xi), & \xi \in \mathbb{C}^+ \\ a^-(\xi)E^-(\xi) - \Psi(\xi), & \xi \in \mathbb{C}^- \end{cases} \quad (6.25)$$

It is analytic in \mathbb{C}^+ and \mathbb{C}^- , while it is continuous across L due to the equality (6.24). Hence, R is an entire function on the complex plane \mathbb{C} . In order to determine the function, notice that

$$\begin{aligned} k^+(\xi) &\sim i\gamma(-i\xi)^{1-q}, \quad \hat{\sigma}_{12}^+(\xi) = O(|\xi|^{-\frac{1}{2}}), \quad \text{Im}(\xi) \rightarrow \infty \\ k^-(\xi) &\sim -i(i\xi)^{1-q}, \quad \hat{\varepsilon}_{11}^+(\xi) = O(|\xi|^{-\frac{1}{2}}), \quad \text{Im}(\xi) \rightarrow -\infty \end{aligned} \quad (6.26)$$

while the exponent terms in (6.8) approach unity, and $\Psi^\pm(\xi)$ vanishes at infinity. From the behavior (6.26), the definition (6.25), and the factorization (6.8), it follows that $R(\xi) = O(|\xi|^{\frac{1}{2}-q})$, $0 < q < 1/2$. Hence, $R(\xi)$ is identically equal to a constant for all $\xi \in \mathbb{C}$. To determine the constant, notice that $E^-(\xi)$ should be regular at the origin, while $a^-(\xi)$ vanishes at $\xi = 0$. Therefore, $R(\xi) \equiv R(0) = -\Psi^-(0)$. From (6.25), one derives the solution of (6.22)

$$\begin{aligned} \Sigma^+(\xi) &= [\Psi(\xi) - \Psi^-(0)]/a^+(\xi), \quad \xi \in \mathbb{C}^+ \\ E^-(\xi) &= [\Psi(\xi) - \Psi^-(0)]/a^-(\xi), \quad \xi \in \mathbb{C}^- \end{aligned} \quad (6.27)$$

6.2.3 Behavior of the solution near the crack tip

From the formulas (6.26), (6.27), and the identity [80]

$$\lim_{x_1 \rightarrow 0^+} \frac{\Gamma(1-q)}{x_1^{-q}} \sigma_{12}(x_1, 0) = \lim_{\text{Im}(\xi) \rightarrow +\infty} (-i\xi)^{1-q} \Sigma^+(\xi) \quad (6.28)$$

it immediately follows that the stress component $\sigma_{12}(x_1, 0)$ has a power singularity at the origin,

$$\sigma_{12}(x_1, 0) \sim \frac{K}{\sqrt{2\pi}x_1^q}, \quad x_1 \rightarrow 0^+, \quad K = \frac{i\sqrt{2\pi}}{\gamma} \frac{\Psi^-(0)}{\Gamma(1-q)} \quad (6.29)$$

Since the possible value of the parameter q for the problem are those from the interval $(0, 1/2)$ whenever $v \neq \sqrt{2}c_2$, the crack-tip energy rate [39] vanishes, which means the crack does not propagate and the physical model should be considered as being incorrect. A correct model of the crack propagation is introduced in [24]: a cohesive zone of length l is imposed behind the crack tip so that the stress component $\sigma_{12}(x_1, 0)$ is prescribed on the interval $(0, l)$,

$$\sigma_{12}(x_1) = -\sigma_c H(x_1 + l), \quad x_1 < 0 \quad (6.30)$$

where the shear cohesive stress σ_c is depended on the strip material, and H is the unit step function.

Assume that a pair of concentrated shear forces is applied to the crack faces at the points $(-x_0, 0^\pm)$ as shown on Figure 6.1, then the resulting stress field is a sum of two solutions corresponding to the boundary condition (6.30) and the boundary condition

$$\sigma_{12}(x_1) = \sigma_* \delta(x_1 + x_0), \quad x_1 < 0 \quad (6.31)$$

where δ is the Dirac delta function and $x_0 > l$.

In order to determine length l of the cohesive zone, consider the near-tip behavior of the two solutions of the problem: the first is for the boundary condition (6.31) and the second is for the boundary condition (6.30). The behavior is given by the formula (6.29), where the only term depending on the boundary conditions is $\Psi^-(0)$. According to the cohesive zone model, the sum of two solutions should be regular at the crack tip, thus the formula (6.29) implies that the equation

$$\Psi_1^-(0) + \Psi_2^-(0) = 0 \quad (6.32)$$

where the value $\Psi_1^-(0)$ corresponds to the solution of the problem with the boundary condition (6.31), while the value $\Psi_2^-(0)$ corresponds to the solution of the problem with the

boundary condition (6.30). Thus, the length l is determined from the equation (6.32). The length l and energy release rate [39]

$$G = 2\sigma_c \int_0^{-l} \frac{\partial u_1}{\partial x_1} dx_1 = \frac{\sigma_c}{\pi i} \int_L E^-(\xi) \frac{1 - e^{il\xi}}{\xi} d\xi$$

for different values of the parameters σ_* , σ_c , x_0 , and d were estimated numerically and shown on Figure 6.3 and Figure 6.4.

6.3 Lattice Model of a Fracture in a Composite Infinite Strip

In this chapter, we will consider the problem of a crack propagation in a strip. The strip consists of two different materials with the interface line between two materials, parallel to the edges of the strip. The crack propagates along the interface with a constant velocity. One edge of the strip is fixed while a uniform displacement is assumed on the other edge. Anti-plane deformations of the strip are considered. This problem is similar to the one solved

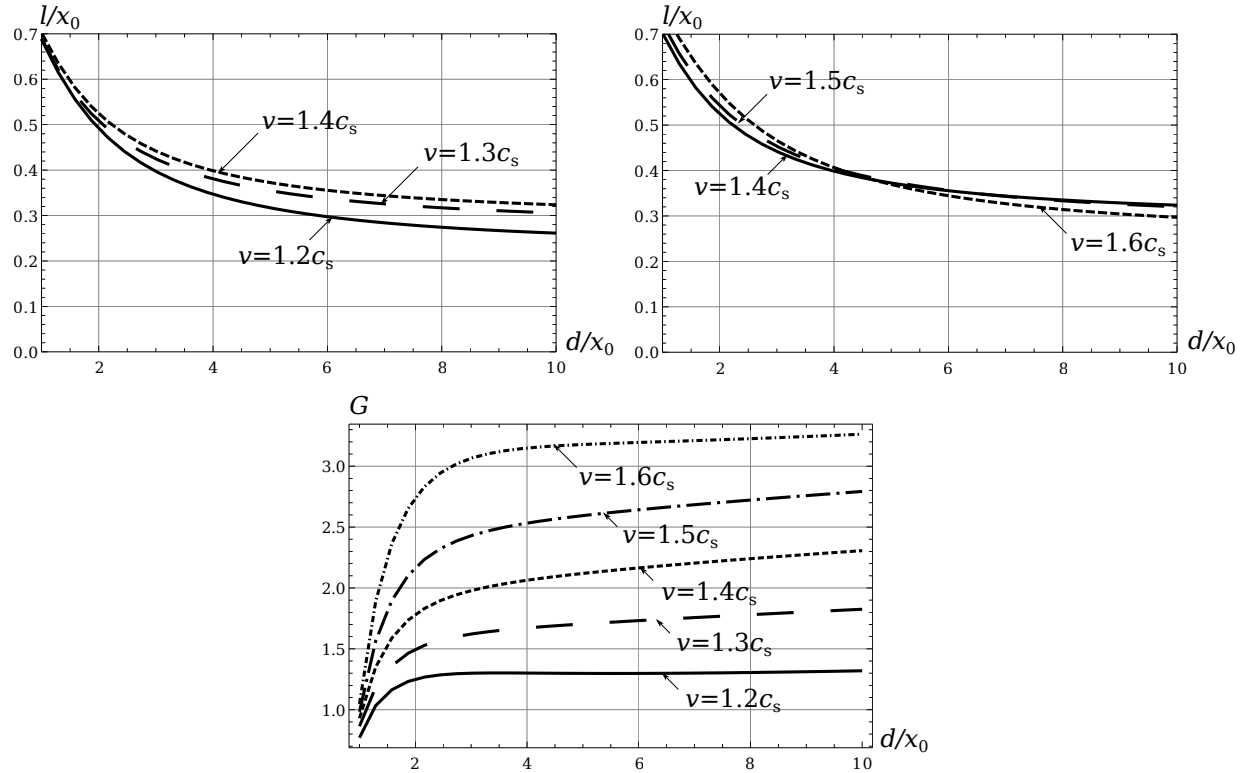


Figure 6.3: The length l and the energy release rate G versus the half-width d of the strip for various speeds v of the crack propagation (for the case $\sigma_* = \sigma_c$ and $\nu = 1/3$)

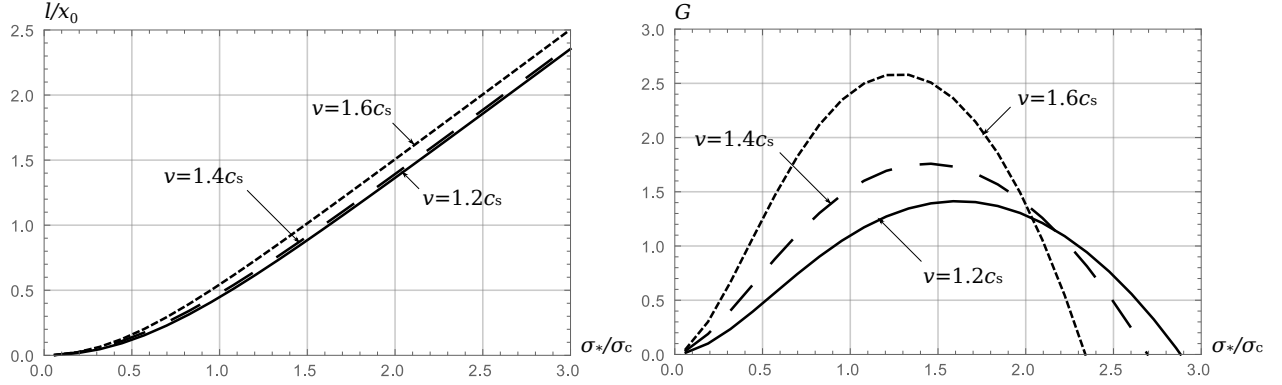


Figure 6.4: The length l and the energy release rate G versus the ratio σ_*/σ_c for various speeds v of the crack propagation (for the case $d = x_0/2$ and $\nu = 1/3$)

in [37, 57], except the current problem is not symmetric, so it is reduced to a system of two Riemann–Hilbert problems.

6.3.1 Fracture in a composite infinite strip

Let us consider a problem of a crack propagation in a composite infinite strip. The crack is modeled as the unit square lattice of mass points so that the first $N_1 + 1$ layers of the points constitute the first material and the other $N_2 + 1$ layers of the points constitute the second material (see Figure 6.5). The mass points of mass m_1 and mass m_2 are connected by zero-mass bonds of stiffness k_1 and k_2 respectively. It is assumed that a bond can be stretched until its deformation reaches a critical value resulting to a bond break. Thus, a sequence of broken bonds forms a crack propagating along the interface between the materials under the loading applied to the strip edges.

Let $u_{n,m}$ be anti-plane displacement of the point (n, m) . Then the balance of forces acting on the interior mass point at the coordinate (n, m) of the upper material yields the equation

$$\begin{aligned}
 m_1 \ddot{u}_{n,m} = & -b_1 \dot{u}_{n,m} + k_1(u_{n,m+1} - 2u_{n,m} + u_{n,m-1}) \\
 & + k_1(u_{n+1,m} - 2u_{n,m} + u_{n-1,m}) \\
 n = & 1, \dots, N_1 - 1, \quad m = 0, \pm 1, \dots
 \end{aligned} \tag{6.33}$$

where b_1 is the coefficient of Stokes dissipation. The steady-state deformation is assumed; that is, after the substitution $x = m - vt$, the balance equation does not depend on time t .

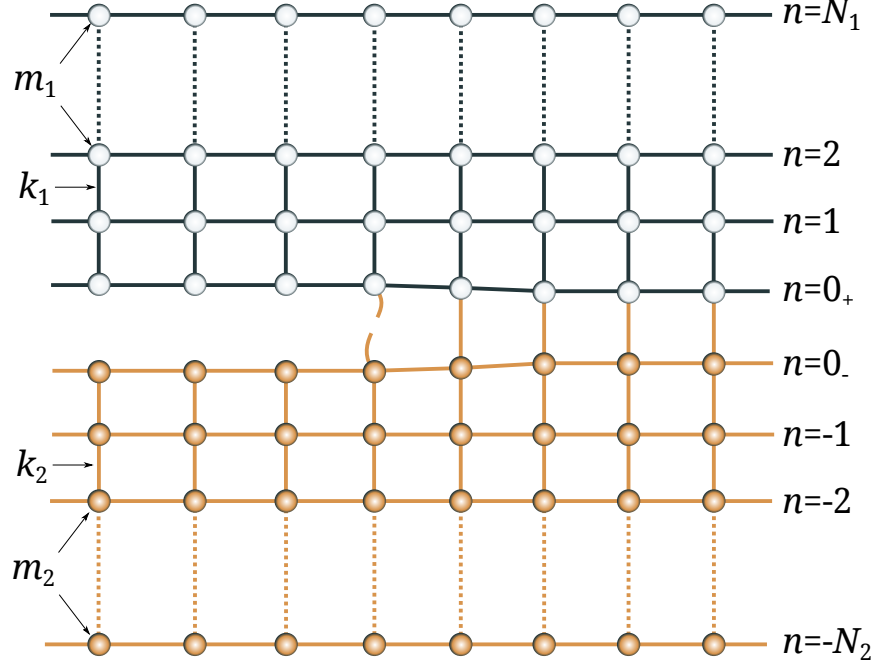


Figure 6.5: Lattice model of a composite infinite strip

Denote

$$u_{n,m}(t) = U_n(m - vt)$$

and apply the Fourier transform

$$\hat{U}_n(\xi) = \int_{-\infty}^{\infty} U_n(x) e^{ix\xi} dx$$

so that the balance equation (6.33) yields

$$\hat{U}_{n+1}(\xi) - \Delta_1(\xi) \hat{U}_n(\xi) + \hat{U}_{n-1}(\xi) = 0, \quad n = 1, \dots, N_1 - 1, \quad \xi \in \mathbb{R}$$

$$\Delta_1(\xi) = 4 - 2 \cos \xi - \frac{m_1}{k_1} v^2 \xi^2 + i \frac{b_1}{k_1} v \xi$$

Solution to the equation above is sought in the form $\lambda^n(\xi)$. After substitution $\hat{U}_n = \lambda^n$, one derives the quadratic equation $\lambda^2 - \Delta_1 \lambda + 1 = 0$, and its solution is

$$\lambda_{1,2} = \frac{1}{2} \Delta_1 \pm \frac{1}{2} \sqrt{\Delta_1^2 - 4}$$

Hereafter, the argument ξ of the functions $\lambda_{1,2}$, Δ_1 , and others is sometimes dropped in order to improve readability. The general solution of the equation has the form

$$\hat{U}_n(\xi) = C_1(\xi) \lambda_1^n(\xi) + C_2(\xi) \lambda_2^n(\xi), \quad \xi \in \mathbb{R}$$

The functions C_1 and C_2 can be chosen to express the derived solution in terms of the values \hat{U}_n on the layers $n = 0_+$ and $n = N_1$. Therefore,

$$\hat{U}_n = \frac{\lambda_2^n \lambda_1^{N_1} - \lambda_1^n \lambda_2^{N_1}}{\lambda_1^{N_1} - \lambda_2^{N_1}} \hat{U}_{0_+} + \frac{\lambda_1^n - \lambda_2^n}{\lambda_1^{N_1} - \lambda_2^{N_1}} \hat{U}_{N_1}, \quad n = 0_+, \dots, N_1 \quad (6.34)$$

In the similar manner, the solution of the force balance equations for the interior points of the lower material is derived,

$$\hat{U}_n = \frac{\mu_1^n \mu_2^{-N_2} - \mu_2^n \mu_1^{-N_2}}{\mu_2^{-N_2} - \mu_1^{-N_2}} \hat{U}_{0_-} + \frac{\mu_2^n - \mu_1^n}{\mu_2^{-N_2} - \mu_1^{-N_2}} \hat{U}_{-N_2}, \quad n = -N_2, \dots, 0_- \quad (6.35)$$

where

$$\mu_{1,2} = \frac{1}{2} \Delta_2 \pm \frac{1}{2} \sqrt{\Delta_2^2 - 4}, \quad \Delta_2(\xi) = 4 - 2 \cos \xi - \frac{m_2}{k_2} v^2 \xi^2 + i \frac{b_2}{k_2} v \xi$$

For mass points on the interface, the force balance equations are different due to participating of points and bond with different masses and stiffness respectively, and due to bond snapping,

$$\begin{aligned} m_1 \ddot{u}_{0_+,m} &= k_1(u_{0_+,m+1} - 2u_{0_+,m} + u_{0_+,m-1}) + k_1(u_{1,m} - u_{0_+,m}) \\ &\quad - k_2(u_{0_+,m} - u_{0_-,m}) H(u_f - |u_{0_+,m} - u_{0_-,m}|) \\ m_2 \ddot{u}_{0_-,m} &= k_2(u_{0_-,m+1} - 2u_{0_-,m} + u_{0_-,m-1}) - k_2(u_{0_-,m} - u_{-1,m}) \\ &\quad + k_2(u_{0_+,m} - u_{0_-,m}) H(u_f - |u_{0_+,m} - u_{0_-,m}|) \\ m &= 0, \pm 1, \dots \end{aligned}$$

where H is the Heaviside step function and u_f critical separation resulting to a bond snap.

Assume that the crack lies on the part of the interface corresponding to negative values of $x = m - vt$. After applying the Fourier transform, one derives the equations

$$\begin{aligned} -\frac{\mu_1}{k_1} v^2 \xi^2 \hat{U}_{0_+} &= (2 \cos \xi - 3) \hat{U}_{0_+} + \hat{U}_1 - \frac{k_2}{k_1} (\hat{U}_{0_+}^+ - \hat{U}_{0_-}^+) \\ -\frac{\mu_2}{k_2} v^2 \xi^2 \hat{U}_{0_-} &= (2 \cos \xi - 3) \hat{U}_{0_-} + \hat{U}_{-1} + (\hat{U}_{0_+}^+ - \hat{U}_{0_-}^+) \end{aligned} \quad \xi \in \mathbb{R} \quad (6.36)$$

Hereafter, the super indices “+” and “-” stand for the parts of the Fourier transforms \hat{U}_{0_\pm} defined by

$$\hat{U}_{0_\pm}^+(\xi) = \int_0^\infty U_{0_\pm}(x) e^{ix\xi} dx, \quad \hat{U}_{0_\pm}^-(\xi) = \int_{-\infty}^0 U_{0_\pm}(x) e^{ix\xi} dx$$

so that $\hat{U}_{0\pm}^+(\xi)$ is analytic in the upper half-plane $\mathbb{C}^+ = \{\xi : \text{Im } \xi > 0\}$ and $\hat{U}_{0\pm}^-(\xi)$ analytic in the lower half-plane $\mathbb{C}^- = \{\xi : \text{Im } \xi < 0\}$. Substituting the functions \hat{U}_1 and \hat{U}_{-1} determined from the relations (6.34) and (6.35) into the equation (6.36), one derives relations between $\hat{U}_{0\pm}^\pm$, which can be written in the vector form as follows

$$AU^+ + U^- = B \quad \text{on } \mathbb{R} \quad (6.37)$$

where

$$U^\pm = \begin{pmatrix} \hat{U}_{0+}^\pm \\ \hat{U}_{0-}^\pm \end{pmatrix}, \quad A = \begin{pmatrix} 1 + k\phi_1 & -k\phi_1 \\ -\phi_2 & 1 + \phi_2 \end{pmatrix}, \quad B = \begin{pmatrix} \psi_1 \hat{U}_{N_1} \\ \psi_2 \hat{U}_{-N_2} \end{pmatrix}$$

$$\phi_1 = \frac{\lambda_1^{N_1} - \lambda_2^{N_1}}{\lambda_1^{N_1}(\lambda_1 - 1) - \lambda_2^{N_1}(\lambda_2 - 1)}, \quad \phi_2 = \frac{\mu_1^{N_2} - \mu_2^{N_2}}{\mu_1^{N_2}(\mu_1 - 1) - \mu_2^{N_2}(\mu_2 - 1)}, \quad k = \frac{k_2}{k_1}$$

$$\psi_1 = \frac{\lambda_1 - \lambda_2}{\lambda_1^{N_1}(\lambda_1 - 1) - \lambda_2^{N_1}(\lambda_2 - 1)}, \quad \psi_2 = \frac{\mu_1 - \mu_2}{\mu_1^{N_2}(\mu_1 - 1) - \mu_2^{N_2}(\mu_2 - 1)}$$

Notice that if the upper and lower materials are identical, then $k = 1$, $N_1 = N_2$, $\phi_1 = \phi_2$, and $\psi_1 = \psi_2$. The matrix A and the vector B should be replaced in (6.37) by

$$A_0 = \begin{pmatrix} 1 + \phi_1 & -\phi_1 \\ -\phi_1 & 1 + \phi_1 \end{pmatrix}, \quad B_0 = \begin{pmatrix} \psi_1 \hat{U}_{N_1} \\ \psi_1 \hat{U}_{-N_1} \end{pmatrix} \quad (6.38)$$

Thus, in this case, the solution of the problem with symmetric loading is symmetric itself in the sense that $\hat{U}_{0+}^\pm = \hat{U}_{0-}^\pm$, as expected.

Relation (6.37) can be considered as a boundary condition on the real axis \mathbb{R} of the vector Riemann–Hilbert problem with respect to the vectors U^\pm with components of the vector U^+ analytic in the upper half-plane \mathbb{C}^+ and vanishing at infinity, and components of the vector U^- analytic in the lower half-plane \mathbb{C}^- and vanishing at infinity.

The total index $\kappa = \frac{1}{2\pi}[\arg \det A]_{\mathbb{R}}$ of the Riemann–Hilbert problem (6.37) is equal to zero. Since the matrix coefficient A becomes symmetric (see formula (6.38)) in the case $k = 1$ and $N_1 = N_2$, the corresponding partial indexes κ_1 and κ_2 should be equal to each other. Therefore, $\kappa_1 = \kappa_2 = 0$ due to the fact that $\kappa_1 + \kappa_2 = \kappa = 0$. In more general case of the Riemann–Hilbert problem (6.37), we make a suggestion that $\kappa_1 = \kappa_2 = 0$ as well,

although this suggestion requires a proper justification that goes beyond the scope of this dissertation. However, if $\kappa_1 = 0$ and $\kappa_2 = 0$, then the solution of the problem is unique and stable [42].

6.3.2 Solution of the Riemann-Hilbert problem

The solution of the Riemann-Hilbert problem will be found using a variation of the Wiener-Hopf technique for vector problems. First, apply the LDU-factorization to the matrix A as follows: $A = T_1^{-1}DT_2$, where T_1 is a lower triangular matrix, T_2 is an upper triangular matrix, and D is diagonal,

$$T_1 = \begin{pmatrix} 1 & 0 \\ \phi_2/(1+k\phi_1) & 1 \end{pmatrix}, \quad T_2 = \begin{pmatrix} 1 & -k\phi_1/(1+k\phi_1) \\ 0 & 1 \end{pmatrix}$$

$$D = \begin{pmatrix} 1+k\phi_1 & 0 \\ 0 & (1+k\phi_1+\phi_2)/(1+k\phi_1) \end{pmatrix}$$

The triangular form of the matrices T_1 and T_2 is crucial and will play an important role in derivation of the solution later. Since the matrix D is diagonal with components continuous on the real axis \mathbb{R} and approaching the unity at infinity, its Wiener-Hopf factorization can be found as follows

$$D = [D^-]^{-1}D^+ \quad \text{on } \mathbb{R}$$

where

$$D^\pm(\xi) = \exp \begin{pmatrix} \frac{1}{2\pi i} \int_{\mathbb{R}} \ln\{1+k\phi_1(\tau)\} \frac{d\tau}{\tau-\xi} & 0 \\ 0 & \frac{1}{2\pi i} \int_{\mathbb{R}} \ln \frac{1+k\phi_1(\tau)+\phi_2(\tau)}{1+k\phi_1(\tau)} \frac{d\tau}{\tau-\xi} \end{pmatrix}$$

After applying the LDU-factorization and Wiener-Hopf factorization, and multiplying by D^-T_1 , the equation (6.37) takes the form

$$D^+T_2\hat{U}^+ + D^-T_1\hat{U}^- = D^-T_1B \quad \text{on } \mathbb{R}$$

Assume that the upper edge of the strip is fixed and the lower edge of the strip is subjected to a uniform displacement $-U_2$. In this case, $\hat{U}_{N_1} = 0$, $\hat{U}_{-N_2} = -2\alpha/(\xi^2 + \alpha^2)U_2$, and

$$D^-T_1B = -U_2 \frac{2\alpha}{\xi^2 + \alpha^2} \psi_2 D_2^- \begin{pmatrix} 0 \\ 1 \end{pmatrix}$$

where α is arbitrary small positive number, and the limit $\alpha \rightarrow 0^+$ will be taken later. For α being arbitrary small, the factor $2\alpha/(\xi^2 + \alpha^2)$ acts as the delta function. Therefore, ψ_2 and D_2^- can be replaced by their values at the origin $\psi_2(0)$ and $D_2^-(0)$. Since

$$\frac{2\alpha}{\xi^2 + \alpha^2} = \frac{i}{\xi + i\alpha} - \frac{i}{\xi - i\alpha}$$

the representation $D^-T_1B = \Psi^+ - \Psi^-$ is valid for

$$\Psi^\pm = \begin{pmatrix} 0 \\ \Psi_2^\pm \end{pmatrix}, \quad \Psi_2^\pm(\zeta) = -\frac{i}{\zeta \pm i\alpha} U_2 \psi_2(0) D_2^-(0)$$

Thus, the condition (6.37) of the Riemann–Hilbert problem can be rewritten as follows

$$D^-T_1\hat{U}^- + \Psi^- = \Psi^+ - D^+T_2\hat{U}^+ \quad \text{on } \mathbb{R}$$

Consider the vector-function

$$R = \begin{cases} \Psi^+ - D^+T_2U^+ & \text{in } \mathbb{C}^+ \\ D^-T_1U^- + \Psi^- & \text{in } \mathbb{C}^- \end{cases} \quad (6.39)$$

Notice that in the case of a scalar Riemann–Hilbert problem, the factors T_1 and T_2 are absent, and, since Ψ^+ , D^+ , U^+ are analytic in the upper half-plane \mathbb{C}^+ , while Ψ^- , D^- , U^- are analytic in the lower half-plane \mathbb{C}^- , the auxiliary function R is continuous across the real axis \mathbb{R} and, therefore, analytic in the whole complex plane, which allows to uniquely determine R using Liouville's theorem. Here, because of presence of T_1 and T_2 , the process of determination of the vector R is more elaborate but it follows the same pattern.

First, find all poles of the vector R . Its first component,

$$R_1 = \begin{cases} -X_1^+ \hat{U}_{0+}^+ + \frac{k\phi_1}{1+k\phi_1} X_1^+ \hat{U}_{0-}^+ & \text{in } \mathbb{C}^+ \\ X_1^- \hat{U}_{0+}^- & \text{in } \mathbb{C}^- \end{cases} \quad (6.40)$$

vanishes at infinity and is analytic everywhere but simple poles ξ_j^+ in \mathbb{C}^+ , which are the zeros of $1 + k\phi_1$, with the corresponding residues $X_1^+(\xi_j^+)\hat{U}_{0-}^+(\xi_j^+)\text{res}_{\xi_j^+} \frac{k\phi_1}{1+k\phi_1}$. Therefore, Mittag-Leffler's theorem implies

$$R_1(\xi) = \sum_{j=1}^{\infty} X_1^+(\xi_j^+)\hat{U}_{0-}^+(\xi_j^+)\text{res}_{\xi_j^+} \frac{k\phi_1}{1+k\phi_1} \cdot \frac{1}{\xi - \xi_j^+} \quad (6.41)$$

The second component of R ,

$$R_2 = \begin{cases} \Psi_2^+ - X_2^+\hat{U}_{0-}^+ & \text{in } \mathbb{C}^+ \\ \frac{\phi_2}{1+k\phi_1}X_2^-\hat{U}_{0+}^- + X_2^-\hat{U}_{0-}^- + \Psi_2^- & \text{in } \mathbb{C}^- \end{cases} \quad (6.42)$$

vanishes at infinity and analytic everywhere but simple poles ξ_j^- in \mathbb{C}^- , which are the poles of ϕ_2 and zeros of $1 + k\phi_1$. Therefore,

$$R_2(\xi) = \sum_{j=1}^{\infty} X_2^-(\xi_j^-)\hat{U}_{0+}^-(\xi_j^-)\text{res}_{\xi_j^-} \frac{\phi_2}{1+k\phi_1} \cdot \frac{1}{\xi - \xi_j^-} \quad (6.43)$$

Notice that the poles of the functions R_1 and R_2 are all different. In fact, all poles of R_1 are in the upper half-plane \mathbb{C}_1 while all poles of R_2 are in the lower half-plane \mathbb{C}^- . This fact is due to the triangular form of the matrices T_1 and T_2 and was chosen on purpose.

The representations (6.41) and (6.43) contain the values $\hat{U}_{0-}^+(\xi_j^+)$ and $\hat{U}_{0+}^-(\xi_j^-)$, which are yet to be determined. To find $\hat{U}_{0-}^+(\xi_j^+)$ and $\hat{U}_{0+}^-(\xi_j^-)$, evaluate the function R_1 at the points ξ_i^- , $i = 1, 2, \dots$, using the definitions (6.40) and (6.41),

$$R_1(\xi_i^-) = X_1^-(\xi_i^-)\hat{U}_{0+}^-(\xi_i^-) = \sum_{j=1}^{\infty} X_1^+(\xi_j^+)\hat{U}_{0-}^+(\xi_j^+)\text{res}_{\xi_j^+} \frac{k\phi_1}{1+k\phi_1} \cdot \frac{1}{\xi_i^- - \xi_j^+}$$

Likewise, evaluate the function R_2 at the points ξ_i^+ , $i = 1, 2, \dots$, using the definitions (6.42) and (6.43),

$$R_2(\xi_i^+) = \Psi_2(\xi_i^+) - X_2^+(\xi_i^+)\hat{U}_{0-}^+(\xi_i^+) = \sum_{j=1}^{\infty} X_2^-(\xi_j^-)\hat{U}_{0+}^-(\xi_j^-)\text{res}_{\xi_j^-} \frac{\phi_2}{1+k\phi_1} \cdot \frac{1}{\xi_i^+ - \xi_j^-}$$

Since the sets of poles ξ_i^+ and ξ_i^- ($i = 1, 2, \dots$) are disjoint, the factors $1/(\xi_i^\pm - \xi_j^\pm)$ are bounded and the sums are convergent. Moreover, the equalities above form an infinite system of linear equations with respect to $\hat{U}_{0-}^+(\xi_j^+)$ and $\hat{U}_{0+}^-(\xi_j^-)$ admitting a unique solution.

After the solution of the system is found, components of the vector R are determined by (6.41) and (6.43), while the vectors U^\pm can be found from (6.39) as follows

$$U^+ = [D^+T_2]^{-1}(\Psi^+ - R), \quad U^- = [D^-T_1]^{-1}(R - \Psi^-) \quad (6.44)$$

6.3.3 Analysis of the solution

On Figure 6.6, values of the displacement $U_{0+}(x)$ on the upper interface layer and of the displacement $U_{0-}(x)$ on the lower interface layer are showed for $x = m - vt$. For the values far ahead of of crack ($x \gg 0$), the displacements correspond to those of anti-plane deformation of the strip without a crack. Near the origin ($x = 0$), the separation starts increasing until it reaches the critical values u_f , which results to a bond snap. After the snapping, the upper mass points tend to reach the equilibrium displacement $U_{0+}(x) = 0$ ($x \ll 0$), while the lower mass points tend to reach the displacement $U_{0-}(x) = -1$ ($x \ll 0$).

In order to study stability of the crack [], consider relation between the crack velocity v and the external loading U_2 . It is assumed that the crack propagates when the difference $\delta_m = u_{0+,m} - u_{0-,m}$ reaches a critical value u_f at the tip of the crack ($m = 0$). The value δ_0 is given by the formula

$$\lim_{x \rightarrow 0^-} [U_{0+}(x) - U_{0-}(x)] = \delta_0$$

where the limit values of $U_{0\pm}(x)$ as $x \rightarrow 0^-$ are determined from the Fourier transform $\hat{U}_{0\pm}^-(\xi)$, which in turn are given by (6.44),

$$\begin{aligned} U_{0+}(x) &= \frac{1}{2\pi} \int_{-\infty}^{\infty} \frac{R_1(\xi)}{D_1^-(\xi)} e^{-ix\xi} d\xi \\ U_{0-}(x) &= \frac{1}{2\pi} \int_{-\infty}^{\infty} \frac{R_2(\xi) - \Psi_2^-(\xi)}{D_2^-(\xi)} e^{-ix\xi} d\xi \\ &\quad - \frac{1}{2\pi} \int_{-\infty}^{\infty} \frac{\phi_2(\xi)}{1 + k\phi_1(\xi)} \frac{R_1(\xi)}{D_1^-(\xi)} e^{-ix\xi} d\xi \end{aligned}$$

Notice that the first two integrands behave like $1/\xi$ at infinity. Therefore, the inverse Fourier transform have jump discontinuities at the origin. In particular, since $R_1(\xi) \sim \rho_1/\xi$, $R_2(\xi) \sim \rho_2/\xi$, and $\Psi_2(\xi) \sim -iU_2\psi_2(0)D_2^-(0)/\xi$ as $\xi \rightarrow \pm\infty$, the functions U_{0+} and U_{0-} have jumps

$$-i\rho_1 \quad \text{and} \quad -i\rho_2 + U_2\psi_2(0)D_2^-(0)$$

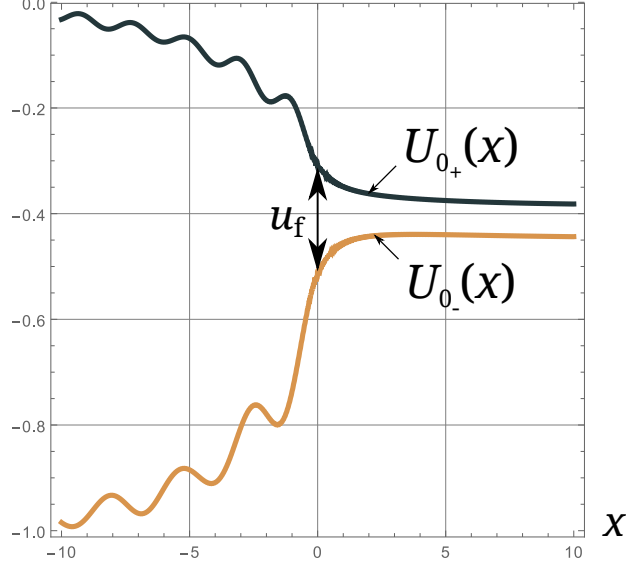


Figure 6.6: Anti-plane separation between the upper interface layer $n = 0_+$ and the lower interface layer $n = 0_-$ for parameters $U_2 = 1$, $c_2 = \frac{5}{6}c_1$, $v = \frac{4}{6}c_1$, $u_f \approx 0.2$, $N_1 = N_2 = 5$, $b_1 = b_2 = 0.01$, where $c_j = \sqrt{\frac{k_j}{m_j}}$, $j = 1, 2$, are the shear wave speeds for the upper and lower material.

respectively. On the other hand, the functions $U_{0\pm}(x)$ are equal to zero for positive values of x . Therefore,

$$\lim_{x \rightarrow 0^-} U_{0+}(x) = i\rho_1, \quad \lim_{x \rightarrow 0^-} U_{0-}(x) = i\rho_2 - U_2\psi_2(0)D_2^-(0)$$

Hence, for the crack to propagate, the solution must satisfy the following condition

$$u_f = \delta_0 = i(\rho_1 - \rho_2) + U_2\psi_2(0)D_2^-(0)$$

Since ρ_1 , ρ_2 , and $D_2^-(0)$ depends on velocity v , the expression above relates velocity v of the crack propagation, the critical separation u_f , and the external loading U_2 .

One can simplify the relation above, using the energy balance. Consider displacements $u_{n,\infty}$ far on the right of the strip. Solving the equation of one-dimensional force balance for $u_{n,\infty}$, one derives

$$u_{n,\infty} = \begin{cases} -U_2 \frac{k(N_1 - n)}{1 + kN_1 + N_2}, & 0_+ \leq n \leq N_1 \\ -U_2 \frac{1 + kN_1 - n}{1 + kN_1 + N_2}, & -N_2 \leq n \leq 0_- \end{cases}$$

The elastic potential energy of one stretched bond is given by $k(\delta u)^2/2$ where k is stiffness and δu the distance stretched. Therefore the elastic potential energy far on the right of the strip is the following

$$E_{right} = \frac{1}{2}k_2 \frac{U_2^2}{1 + kN_1 + N_2}$$

The elastic potential energy far on the left of the strip is zero. Thus, all potential energy E_{right} is to be spent on breaking the bond at the tip of the crack,

$$E_{break} = \frac{1}{2}k_2 u_f^2$$

The energy balance implies

$$\frac{1}{2}k_2 u_f^2 \leq \frac{1}{2}k_2 \frac{U_2^2}{1 + kN_1 + N_2}$$

Therefore $u_f = \delta_0 \leq U_2/\sqrt{1 + kN_1 + N_2}$.

Define a dimensionless parameter

$$\Delta = \frac{U_2}{\delta_0 \sqrt{1 + kN_1 + N_2}}$$

so that Δ is proportional to the external loading U_2 and the crack propagates if $\Delta \geq 1$.

Figure 6.7 shows the relation between the crack velocity v and the parameter Δ for the case $c_2 = \frac{5}{6}c_1$, where $c_j = \sqrt{\frac{k_j}{m_j}}$, $j = 1, 2$, are the shear wave speeds of the two materials.

As it was shown in [57], [37], when v is less then about half of the limiting speed c_1 , the crack does not propagate. When v changes from $c_1/2$ to c_2 , the crack propagation is stable; that is, the crack propagates along the interface between the materials. The case when the crack velocity v lies between the two limiting speed,

$$c_1 < v < c_2$$

is of special interest and is shown on the picture on the right (Figure 6.7). One can distinguish three regimes of the crack propagation: when v is close to c_2 , the crack propagates along the interface; when v is somewhat in the middle between c_1 and c_2 , the steady-state crack propagation is unphysical (increase in the loading Δ results to decrease of the velocity v); when

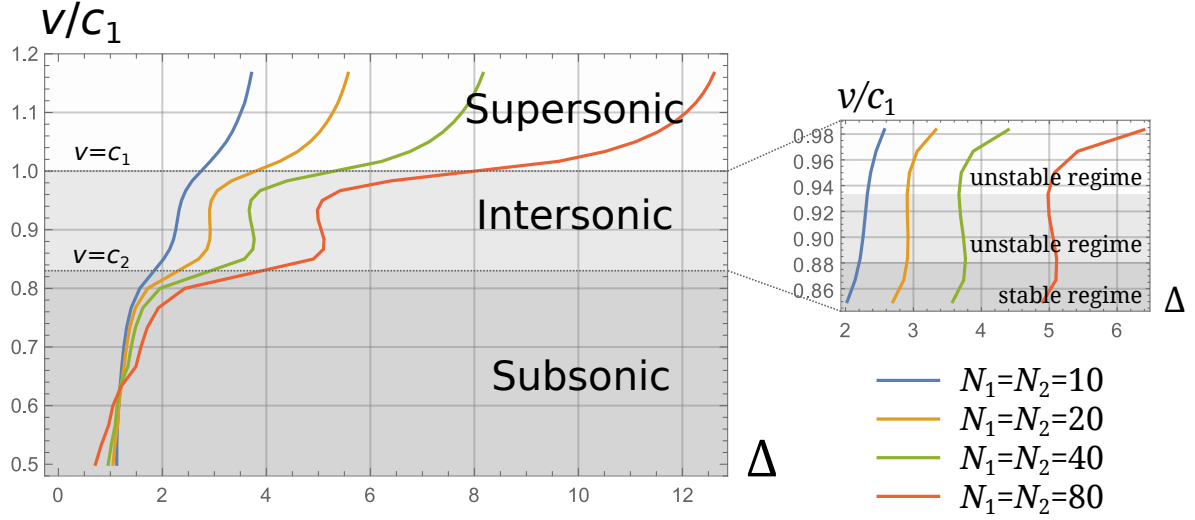


Figure 6.7: Relation between the crack velocity v and the dimensionless parameter Δ for different numbers of the layers N_1 and N_2 .

v is close to the limiting speed c_1 , the crack propagation is unstable due to crack branching. The case of branching can be observed by evaluating the relative displacements between neighbor mass points on the upper and lower interface layers: if the relative displacements on the lower interface layer exceed the critical separation u_f , then the crack propagates not only along the interface but towards the interior of the second material as well. Thus, crack branching occurs in this case.

Chapter 7

Summary and Conclusions

In the dissertation, the Riemann–Hilbert formalism was used to derive solution for several problems from the field of Dynamic Fracture Mechanics. Many problems on crack propagation in an unbounded plane have been solved using the Riemann–Hilbert problem, which allows for finding analytical closed-form solution suitable for studying of fracture phenomena. However, many of the problems on crack propagation in domains with a boundary (e.g. a half-plane or a strip) require much more sophisticated techniques for solving the corresponding Riemann–Hilbert problems. In the dissertation, we considered several of such problems.

The vector Riemann–Hilbert problems considered here do not admit an analytical solution in the closed form (to the author’s knowledge) and, thus, have been solved approximately using numerical techniques. However, analytical methods have been applied in order to improve both convergence and applicability of the numerical techniques. With that in mind, the technique of a partial Wiener–Hopf factorization was proposed and applied in two cases of a vector Riemann–Hilbert problem.

In Chapter 4, we have analyzed a two-dimensional steady-state problem on propagation of a semi-infinite crack in a half-plane. The crack is subjected to normal and tangential loads applied to its faces, and it propagates at speed v along the half-plane boundary free of traction. The boundary of the half-plane breaks the symmetry of the problem, and, in contrast to the problem for a plane, the modes I and II are coupled. We have deduced an order-2 vector Riemann–Hilbert problem associated with the model. The coefficient is a Hermitian matrix which cannot be factorized in a closed form. We have reduced the problem to a system of two singular integral equations with respect to the derivatives of

the displacement jumps. The method of orthogonal polynomials has been employed for its solution. The unknown functions have been expanded in terms of the orthonormal Jacobi polynomials. The coefficients of the expansions have been determined from an infinite system of linear algebraic equations of the second kind.

We have derived formulas for the stress intensity factors K_I and K_{II} and the weight functions $W_{I,I}$, $W_{I,II}$, $W_{II,I}$ and $W_{II,II}$. By determining the energy δU released when the crack extends to a small distance, we applied the Griffith criterion and established that the crack starts propagating when $H \geq \mu T$, where

$$H = \frac{\sqrt{1 - (v/c_l)^2} K_I^2 + \sqrt{1 - (v/c_s)^2} K_{II}^2}{4(c_s/v)^2 R(v)},$$

$R(v)$ is the Rayleigh function, c_s , c_l are the shear and longitudinal waves speeds, μ is the shear modulus, and T is the Griffith material constant. We have computed the stress intensity factors, the weight functions, and the function H for different v/c_R and δ (c_R is the Rayleigh speed, and δ is the distance between the half-plane boundary and the crack). It has been found that H grows to infinity when the distance δ between the crack and the half-plane boundary decreases while the crack speed does not vary. The function H monotonically decreases as δ grows. When the distance δ is fixed, H , as a function of v/c_R , attains its minimum in the interval $(0, 1)$ and grows as v/c_R approaches the points 0 and 1.

In Chapter 5, we have derived the fundamental solution and the weight functions of the transient two-dimensional problem on a semi-infinite crack propagating at constant speed parallel to the boundary of a half-plane. The boundary of the half-plane is free of traction, while the crack faces are subjected to general time-independent loading. We have reduced the boundary-value problem to a vector Riemann–Hilbert problem on the real axis. We have split the matrix coefficient into a discontinuous diagonal matrix and a continuous matrix, factorized the discontinuous part and rewritten the vector Riemann–Hilbert problem as a system of two convolution equations on the segment $-\infty < x < 0$. For numerical purposes, it was recast as a system of two Fredholm integral equations on the segment $(-1, 1)$. We

have derived the Laplace transforms of the stress intensity factors and the weight functions in terms of the solution of the convolution equations at the point $x = 0$. The Laplace transform has been inverted numerically. To improve the convergence, we have applied the Euler summation method for alternating series. We have obtained numerical results for the stress intensity factors for the case when concentrated loads are applied to the crack faces (at time $t = 0$ at the crack tip). This model problem generates four weight functions $W_{i,j}$, $i, j = I, II$. It has been discovered that during a certain initial period of time, $0 < t < 2t_l$, the off-diagonal weight functions $W_{i,j}$, $i \neq j$, approximately equal zero, and the diagonal functions almost coincide with the ones for the case of the whole plane. For time $t > 2t_l$, the boundary effects play a significant role, and, in general, all the four weight functions do not vanish and are different from the corresponding functions associated with the whole plane. It has also been found that the dimensionless functions $w_{i,i}(0, t) = \sqrt{\frac{1}{2}\pi V t} W_{i,i}(0, t)$ ($i = I, II$) tend to 1 and 0 as v/c_R tends to 0 and 1, respectively (v is the crack speed and c_R is the Rayleigh speed), while $w_{i,j}$ ($i \neq j$) vanish when v/c_R approach both points, 0 and 1. We have found that w_{ij} are not monotonic functions of v/c_R and attain their local maximum in the interval $(0, v/c_R)$. As the distance δ from the crack to the boundary decreases, all the functions w_{ij} grow. We emphasize that apart from small δ our numerical method is stable for all parameters δ .

Based on the Freund approximate algorithm [39] for the problem on a semi-infinite crack propagated at a nonuniform rate in the whole plane, we have developed a procedure for the case when the crack propagates also at prescribed variable sub-Rayleigh speed in a half-plane parallel to the boundary and when the boundary effects are significant. The implementation of the method requires solving a system of Volterra convolution equations whose kernels are the associated weight functions, not a single Abel integral equation as in the whole plane case. The system of Volterra equations also admits a closed-form solution. However, in the case of a half-plane, there is no analog of the remarkable formula for the Mode I stress

intensity factors $K_I(l(t), V_k) = k(V_k)K_I(l(t), 0)$ in any interval $t_k < t < t_{k+1}$ derived for the whole plane [39]. There is another difference between the whole plane and half-plane solutions. The displacement jumps though the crack line $x_2 = 0$ have to vanish on the segments $l_i < x_1 < v_{i-1}t$, $i = 1, \dots, k$. This property was analytically proved in [39] for the sub-Rayleigh regime and in [46] in the transonic regime. For the half-plane problem, this condition needs to be verified numerically for each Problem P_i ($i = 0, 1, \dots, k-1$) during the implementation of the procedure.

To compute the stress intensity factors at time t , $2t_l < t_k < t < t_{k+1}$, for the crack in a half-plane, one needs to derive the weight functions for all intermediate speeds v_i . We have shown that initially, before the longitudinal wave reflected from the boundary strikes the crack and when the weight functions coincide with those for the whole plane, the relatively simple Freund's algorithm works. At the same time, the solution is still different since it relies on the static solution on a cracked half-plane, not the whole plane with the crack. When the first longitudinal wave reflected from the half-plane boundary reaches the crack surface moving at speed $v(t) < c_R$, the boundary substantially affects the weight functions. To determine the stress intensity factors at the crack tip at some time $t \in (t_k, t_{k+1})$, consequently, one may employ the procedure presented that requires solving the same transient problem for different constant speeds v_i ($i = 0, 1, \dots, k$) and a system of Volterra equations to determine at each step the loads need to be negated to make possible for the crack to advance.

As for the speeds v_j ($j = 0, 1, \dots$) themselves, they have been determined by applying the dynamic Griffith criterion and solving a certain transcendental equation associated with each step of the algorithm.

In Chapter 6, we have constructed Wiener–Hopf factorization of one class of functions, those with countably many singular points on the contour of a Riemann–Hilbert problem, which make them difficult to applying numerical techniques. We have deformed the integration contour to bypass the singular points and showed that the solution of the new

Riemann–Hilbert problem can be used to find a closed-form solution of the original one. The main advantage of this approach is that, without recourse to the Cauchy integral, the solution has been expressed in terms of integrals of exponentially vanishing functions, which are easy to compute. An application of the technique to the problem on propagation of a symmetric crack in a strip has been given in Section.

Also, we have considered a crack propagating in a strip along the interface between two elastic materials. Under the assumption of anti-plane deformation, the lattice model of the materials has been accepted. The lattice model allows for a better description of behavior of stress and deformation fields near the crack tip: specifically, for supersonic speeds of a crack propagation under anti-plane deformation, the continuum fracture mechanics results to a zero energy release rate around the crack tip, which yields to the conclusion that such propagation is impossible. In order to construct a feasible mathematical model of the phenomena, the cohesive zone model (see Section 6.2) and the lattice model (see, for instance, [74]) were proposed. It is interesting to note that even in the case of anti-plane deformation, the lattice model yields a vector Riemann-Hilbert problem. A similar situation is in the anti-plane strain problem of micropolar elasticity [10] when two out three modes are coupled, and the necessity of solving a vector Riemann-Hilbert problem arises. The solution of the Riemann–Hilbert problem was derived using the partial Wiener–Hopf factorization technique proposed in Section 2.3.3.

References

- [1] J. Abate and W. Whitt, *Numerical inversion of Laplace transforms of probability distributions*, ORSA J. Comput. **7**, 1995, pp. 36–43.
- [2] I.D. Abrahams, *Radiation and scattering of waves on an elastic half-space; a non-commutative matrix Wiener-Hopf problem*, J. Mech. Phys. Solids, **44**, no. 12, 1996, pp. 2125–2154.
- [3] I.D. Abrahams, *On the solution of Wiener-Hopf problems involving noncommutative matrix kernel decompositions*, SIAM J. Appl. Math., **57**, no. 2, 1997, pp. 541–567.
- [4] I.D. Abrahams, *The application of Padé approximations to Wiener-Hopf factorization*, IMA J. Appl. Math., **65**, no. 3, 2000, pp. 257–281.
- [5] I.D. Abrahams and J.B. Lawrie, *On the factorization of a class of Wiener-Hopf kernels*, IMA J. Appl. Math., **55**, no. 1, 1995, pp. 35–47.
- [6] M. Abramowitz and I.A. Stegun, *Handbook of mathematical functions*, Washington: Dover Publications, 1965.
- [7] D.V. Anosov and A.A. Bolibruch, *The Riemann-Hilbert problem*, Aspects of Mathematics, E22, Braunschweig: Friedr. Vieweg and Sohn, 1994.
- [8] Y.A. Antipov, *Subsonic semi-infinite crack with a finite friction zone in a bimaterial*, J. Mech. Phys. Solids, **57**, 2009, pp. 1934–1957.
- [9] Y.A. Antipov *A symmetric Riemann-Hilbert problem for order-4 vectors in diffraction theory*, Quart. J. Mech. Appl. Math., **63**, 2010, pp. 349–373.
- [10] Y.A. Antipov, *Weight functions of a crack in a two-dimensional micropolar solid*, Quart. J. Mech. Appl. Math., **65**, 2012, pp. 239–271.
- [11] Y.A. Antipov and N.G. Moiseyev, *Exact solution of the plane problem for a composite plane with a cut across the boundary between two media*, J. Appl. Math. Mech., **55**, 1991, pp. 531–539.
- [12] Y.A. Antipov, O. Obrezanova, and J.R. Willis, *A fracture criterion of “Barenblatt” type for a transonic shear crack*, Math. Mech. of Solids, **9**, 2004, pp. 271–283.
- [13] Y.A. Antipov and V.V. Silvestrov, *Factorization on a Riemann surface in scattering theory*, Quart. J. Mech. Appl. Math., **55**, 2002, 607–654.
- [14] Y.A. Antipov and V.V. Silvestrov, *Second-order functional-difference equations. I. Method of the Riemann-Hilbert problem on Riemann surfaces*, Quart. J. Mech. Appl. Math., **57**, no. 2, 2004, pp. 245–265.

- [15] Y.A. Antipov and V.V. Silvestrov, *Second-order functional-difference equations. II. Scattering from a right-angled conductive wedge for E-polarization*, Quart. J. Mech. Appl. Math., **57**, no. 2, 2004, pp. 267–313.
- [16] Y.A. Antipov and V.V. Silvestrov, *Method of Riemann surfaces in the study of supercavitating flow around two hydrofoils in a channel*, Phys. D, **235**, no. 1-2, 2007, pp. 72–81.
- [17] Y.A. Antipov and A.V. Smirnov, *Subsonic propagation of a crack parallel to the boundary of a half-plane*, Math. Mech. Solids, **18**, no. 2, 2013, pp. 153–167.
- [18] Y.A. Antipov and A.V. Smirnov, *Fundamental solution and the weight functions of the transient problem on a semi-infinite crack propagating in a half-plane*, ZAMM Z. Angew. Math. Mech., 2016, pp. 1–19.
- [19] Y.A. Antipov and J.R. Willis, *Transient loading of a rapidly-advancing Mode-II crack in a viscoelastic medium*, Mech. Materials, **35**, 2003, pp. 415–431.
- [20] G. B. Arfken and H. J. Weber, *Mathematical methods for physicists*, Academic Press, Inc., San Diego, CA, 1995.
- [21] G.D. Birkhoff, *Singular points of ordinary linear differential equations*, Trans. Amer. Math. Soc., **10**, 1909, pp. 436–470.
- [22] G.D. Birkhoff, *A simplified treatment of the regular singular point*, Trans. Amer. Math. Soc., **11**, 1910, pp. 199–202.
- [23] B.V. Bojarski, *On the stability of the Hilbert problem for an unknown vector*, Soobšč. Akad. Nauk Gruz. SSR, **25**, 1958, 391–398.
- [24] K.B. Broberg, *Cracks and fracture*, San Diego: Academic Press, 1999.
- [25] H.F. Bueckner, *A novel principle for the computation of stress intensity factors*, Zeit. Angew. Math. Mech., **50**, 1970, pp. 529–546.
- [26] T. Carleman, *Sur la résolution de certaines équations intégrales*, Archiv för matematik astronomi och fysik, **16**, no. 26, 1932.
- [27] J.F. Carlson and A.E. Heins, *The reflection of an electromagnetic plane wave by an infinite set of plates, I*, Quart. Appl. Math., **4**, 1947, pp. 313–329.
- [28] J.F. Carlson and A.E. Heins, *The reflection of an electromagnetic plane wave by an infinite set of plates, II*, Quart. Appl. Math., **5**, 1947, pp. 82–88.
- [29] G.N. Chebotarev, *On closed-form solution of the Riemann problem for a system of $2n$ functions* (Russian), Kazan. Gos. Univ. Uchen. Zap., **116**, no. 4, 1956, pp. 31–58 .
- [30] E.T. Copson, *On an integral equation arising in the theory of diffraction*, Quart. J. Math., **17**, 1946, pp. 19–34.

- [31] J.W. Craggs, *On the propagation of a crack in an elastic-brittle material*, J. Mech. Phys. Solids, **8**, 1960, pp. 66–75.
- [32] V.G. Daniele, *On the factorization of Wiener-Hopf matrices in problems solvable with Hurd's method*, IEEE Trans. Antennas and Propagation, **26**, no. 4, 1978, pp. 614–616.
- [33] M.L. Dow and D. Elliott, *The numerical solution of singular integral equations over $(-1, 1)$* , SIAM J. Numer. Anal., **16**, no. 1, 1979, pp. 115–134.
- [34] D. Elliott, *The classical collocation method for singular integral equations*, SIAM J. Numer. Anal., **19**, no. 4, 1982, pp. 816–832.
- [35] F. Erdogan and G.D. Gupta, *On the numerical solution of singular integral equations*, Quart. Appl. Math., **29**, 1971/72, pp. 525–534.
- [36] H.M. Farkas and I. Kra, *Riemann surfaces*, Springer-Verlag, New York-Berlin, **71**, 1980.
- [37] L. Fineberg and M. Marder, *Instability in Dynamic Fracture*, Physics Reports, **313**, 1999, pp. 1–108.
- [38] L.B. Freund, *Crack propagation in an elastic solid subjected to general loading – I. Constant rate of extension*, J. Mech. Phys. Solids **20**, 1972, 129–140.
- [39] L.B. Freund, *Dynamic fracture mechanics*, Cambridge University Press, Cambridge, 1990.
- [40] F.D. Gakhov, *On the Riemann boundary problem*, Matem. sborn., **2**, 1937, pp. 673–683.
- [41] F.D. Gakhov, *Boundary value problems*, Pergamon Press, Oxford-New York-Paris; Addison-Wesley Publishing Co., Inc., Reading, Mass.-London, 1966.
- [42] I.C. Gohberg and M.G. Kreĭn, *On the stability of a system of partial indices of the Hilbert problem for several unknown functions* (Russian), Dokl. AN SSSR, **119**, pp. 854–857.
- [43] D. Hilbert, *Über eine anwendung der integralgleichungen auf ein problem der funktionentheorie*, Verhandl. des. III Internat. Mathematiker Kongresses, Heidelberg, pp. 233–240.
- [44] D. Hilbert, *Grundzüge einer allgemeinen Theorie der linearen Integralgleichungen*, Dritter Abschnitt, Leipzig-Berlin, 1924.
- [45] Y. Huang and H. Gao, *Intersonic crack propagation - Part I: The fundamental solution*, J. Appl. Mech., **68**, 2001, 169–175.
- [46] Y. Huang and H. Gao, *Intersonic crack propagation - Part II: Suddenly stopping crack*, J. Appl. Mech., **69**, 2002, 76–80.
- [47] R.A. Hurd, *The Wiener-Hopf Hilbert method for diffraction problems*, Canad. J. Phys., **54**, 1976, pp. 775–780.

- [48] G.R. Irwin, *Analysis of stresses and strains near the end of a crack traversing a plate*, J. Appl. Mech., **24**, 1957, pp. 361–164.
- [49] D.S. Jones, *A simplifying technique in the solution of a class of diffraction problems*, Quart. J. Math., **3**, 1952, pp. 189–196.
- [50] D.S. Jones, *Commutative Wiener-Hopf factorization of a matrix*, Proc. Roy. Soc. Lond. A, **393**, 1984, pp. 185–192.
- [51] D.S. Jones, *Factorization of a Wiener-Hopf matrix*, IMA J. Appl. Math., **32**, 1984, pp. 211–220.
- [52] A.A. Khrapkov, *Certain cases of the elastic equilibrium of an infinite wedge with a non-symmetric notch at the vertex, subjected to concentrated forces* (Russian), Appl. Math. Mech., **35**, 1971, pp. 625–637.
- [53] A.A. Khrapkov, *Closed form solutions of problems on the elastic equilibrium of an infinite wedge with nonsymmetric notch at the apex* (Russian), Appl. Math. Mech., (35), 1971, pp. 1009–1016.
- [54] L.D. Landau and E.M. Lifshitz, *Theory of elasticity*, Pergamon Press, London-Paris-Frankfurt; Addison-Wesley Publishing Co., Inc., Reading, Mass., 1959.
- [55] H. Levine and J. Schwinger, *On the radiation of sound from and unflanged circular pipe*, Phys. Rev., **73**, 1948, pp. 383–406.
- [56] G.S. Litvinchuk and I.M. Spitkovskii, *Factorization of Measurable Matrix Functions*, Math. Research, Akademie, Berlin, **37**, 1987.
- [57] M. Marder M. and S. Gross, *Origin of Crack Tip Instabilities*, J. Mech. Phys. Solids, **43**, No 1, 1995, pp. 1–48.
- [58] V.V. Morozov, *On commutative matrices* (Russian), Uchen. Zap. Karel Ped. Inst. Ser. Fiz.-Mat. Nauk, **9**, 1952.
- [59] N.G. Moiseev, *Factorization of matrix functions of special form*, Soviet Math. Dokl., **39**, 1989, pp. 264–267.
- [60] N.G. Moiseyev and G.Y. Popov, *Exact solution of the problem of bending of a semi-infinite plate completely bonded to an elastic half-space* (Russian), Izv. AN SSSR, Solid Mechanics. **25**, 1990, 113–125.
- [61] N.I. Muskhelishvili, *Singular integral equations*, Dover Publications, Inc., New York, 1953.
- [62] B. Noble, *Methods based on the Wiener-Hopf technique for the solution of partial differential equations*, Pergamon Press, New York-London-Paris-Los Angeles, 1958.
- [63] S. Olver, *A general framework for solving Riemann-Hilbert problems numerically*, Numer. Math., **122**, no. 2, 2012, pp. 305–340.

- [64] V.Z. Parton and P.I. Perlin, *Integral Equations in Elasticity*, Mir, Moscow, 1982.
- [65] J. Plemelj, *Ein ergänzungssatz zur Cauchyschen integralderstellung analytischer funktionen*, Monatshefte für Math. and Phys., **19**, 1908, pp. 205–210.
- [66] J. Plemelj, *Riemanmsche funktionenscharen mit gegebener monodromiegruppe*, Monatshefte für Math. and Phys., **19**, 1908, pp. 211–245.
- [67] J. Plemelj, *Problems in the sense of Riemann and Klein*, Wiley, New York, 1964.
- [68] A.D. Rawlins and W.E. Williams, *Matrix Wiener-Hopf Factorization*, Quart. J. Mech. Appl. Math., **34**, 1981, pp. 1–8.
- [69] A.J. Rosakis, et al., *Intersonic crack propagation in bimaterial systems*, J. Mech. Phys. Solids, **46**, np. 10, 1998, pp. 1789–1813.
- [70] V.V. Silvestrov and A.V. Smirnov, *The Prandtl integrodifferential equation and the contact problem for a piecewise homogeneous plate*, J. Appl. Math. Mech., **74**, no. 6, 2010, pp. 679–691.
- [71] B. Shawyer and B. Watson, *Borel's Methods of Summability: Theory and Applications*, Oxford UP, 1994.
- [72] P.N. Shivakumar and J.J. Williams, *An iterative method with truncation for infinite linear systems*, J. Comput. Appl. Math., **24**, no. 1-2, 1988, pp. 199–207.
- [73] L.I. Slepyan, *Models and Phenomena in Fracture Mechanics*, Springer, Berlin, 2002.
- [74] L.I. Slepyan, *On discrete models in fracture mechanics*, Mech. Solids, **45**, no. 6, 2010, pp. 803–814.
- [75] I.M. Spitkovsky, *Generalized factorization of matrix-functions and the Riemann boundary value problem with infinite partial indices*, Dokl. Akad. Nauk SSSR, **286**, no. 3, 1986, pp. 559–562.
- [76] G. Szegő, *Orthogonal Polynomials*, American Mathematical Society, New York, 1939.
- [77] E.C. Titchmarsh, *Introduction to the theory of Fourier integrals*, Chelsea Publishing Co., New York, 1986.
- [78] F.G. Tricomi, *Integral equations*, Interscience Publishers, Inc., New York; Interscience Publishers Ltd., London, 1957.
- [79] F. Ursell, *Infinite systems of equations. The effect of truncation*, Quart. J. Mech. Appl. Math., **49**, no. 2, 1996, pp. 217–233.
- [80] B. van der Pol and H. Bremmer, *Operational calculus*, Chelsea Publishing Co., New York, 1987.
- [81] N.P. Vekua, *Systems of Singular Integral Equations*, Noordhoff, Groningen, 1967.

- [82] B.H. Veitch and I.D. Abrahams, *On the commutative factorization of $n \times n$ matrix Wiener-Hopf kernels with distinct eigenvalues*, Proc. Roy. Soc. Lond. A, **463**, 2007, pp. 613–639.
- [83] N. Wiener and E. Hopf, *Über eine classes singulärer integralgleichungen*, Sitz. Berliner Akad. Wiss., 1931, pp. 696–706.
- [84] W.E. Williams, *Recognition of some readily Wiener-Hopf factorizable matrices*, IMA J. Appl. Math., **32**, 1984, pp. 367–378.
- [85] J.R. Willis, *A comparison of the fracture criteria of Griffith and Barenblatt*, J. Mech. Phys. Solids, **15**, 1967, pp. 151–162.
- [86] A.N. Zlatin and A.A. Khrapkov, *A semi-infinite crack that is parallel to the boundary of an elastic half-plane* (Russian), Dokl. Akad. Nauk SSSR, **291**, no. 4, 1986, pp. 810–813.
- [87] È.I. Zverovič, *Boundary value problems in the theory of analytic functions in Hölder classes on Riemann surfaces* (Russian), Uspehi Mat. Nauk, **26**, no 1(157), 1971, pp. 113–179.

Vita

Aleksandr Smirnov was born in 1982, in Cheboksary, Russia. He finished his undergraduate studies at I.N. Ulianov Chuvash State University July 2008. He earned a candidate of sciences in Physics and Mathematics degree from the I. Yakovlev Chuvash State Pedagogical University in July 2011. In August 2011 he came to Louisiana State University to pursue graduate studies in mathematics. He earned a master of science degree in mathematics from Louisiana State University in May 2013. He is currently a candidate for the degree of Doctor of Philosophy in mathematics, which will be awarded in May 2016.